Integrative Modelling of Glucocorticoid Induced Apoptosis with a Systems Biology Approach

A thesis submitted to the University of Manchester for the

degree of Doctor of Philosophy in the Faculty of Life Sciences

2012

Daphne Wei-Chen Chen

Table of Contents

List of Abbreviations

ABL	abelson
ACTR	activator of the thyroid and retinoic acid receptor
ACTH	adrenocorticotropic hormone
AF-1	activation function-1
AF-2	activation function-2
AIB1	amplified in breast cancer 1
AF-1/2	activation function 1/ 2
ALL	acute lymphoblastic leukaemia
AP-1	activating protein 1
AR	androgen receptor
ARC	activated recruited factor
ATM	ataxia telangiectasia mutated
ATR	ataxia telangiectasia and Rad-3 related
AVP	vasopressin
BAD	Bcl-2 antagonist of cell death
BAK	Bcl-2 antagonist killer 1
BAX	Bcl-2 associated x protein
BCL-2	B-cell lymphoma-2
Bcl-X_L	Bcl-2 related gene, long isoform
BCR	breakpoint cluster region
β-gal	Beta galactosidase
BH	Bcl-2 homology
bHLH	basic Helix-Loop-Helix
BID	Bcl-2 interacting domain death agonist
BIM	Bcl-2 interacting mediator of cell death
BMF	Bcl-2 modifying factor
BMPRII	bone morphogenetic protein receptor, type II
BRG-1	brahma related gene-1
CARM1	coactivator-associated arginine methyltransferase 1
CBP	CREB binding protein
CDK	cyclin dependent kinase
ChIP	chromatin immunoprecipitation
ChIP-Seq	chromatin immunoprecipitation sequencing

CREB	cyclic-AMP response element binding protein
CRH	corticotropin-releasing hormone
CTD	C-terminal domain
DBD	DNA binding domain
Dex	dexamethasone
DIABLO	direct IAP-bind protein with low pi
DISC	death-inducing signalling complex
DMEM	Dulbecco's modified eagle medium
DNA	deoxyribonucleic acid
dNTPs	deoxyribonucleotide triphosphate
DRIP	vitamin D receptor interacting protein
ER	estrogen receptor
ERE	estrogen response element
ERG	Ets Related Gene
FADD	FAS-associated death domain
FBS	foetal bovine serum
GCs	glucocorticoids
GO	gene ontology
GR	glucocorticoid receptor
GRE	glucocorticoid response element
GRIP1	glucocorticoid receptor-interacting protein 1
GSK3	glycogen synthase kinase 3
GTFs	general transcription factors
HAT	histone acetyl transferase
HDAC	histone deacetylase
HDM2	human double minute 2
HRE	hormone response element
HSF1	heat shock factor 1
HSP	heat shock protein
IAP	inhibitor of apoptosis protein
JNK	c-Jun N terminal kinase
LBD	ligand binding domain
LcoR	ligand dependet corepressor
MAPK	mitogen activated protein kinase
mRNA	messenger ribonucleic acid

NCoA	nuclear receptor coactivator
NCoR	nuclear hormone receptor corepressor
NFκB	nuclear factor κB
NID	nuclear receptor interacting domain
NR	nuclear hormone receptors
NRE	nuclear hormone response element
NuRD	nucleosome remodeling and deacetylase
ODEs	ordinary differential equations
PBS	phosphate buffered saline
P/CAF	p300/ CBP associated factor
p/CIP	p300/CBP cointegrator associated protein
PCR	polymerase chain reaction
POMC	proopiomelanocortin gene
PPAR	peroxisome proliferator-activated receptor
PP5	protein phosphatase 5
PR	progesterone receptor
qRT-PCR	quantitative real time polymerase chain reaction
RAC3	receptor-associated co-activator 3
RAR	retinoic acid receptor
RIP-140	receptor interacting protein 140
RNA	ribonucleic acid
RPL19	ribosomal protein l19
Rpm	revolutions per minute
RUNX	runt-related transcription factor
SDPR	serum deprivation response
SDS PAGE	sodium dodecyl sulphate poly-acrylamide gel electrophoresis
SGK	serum and glucocorticoid induced kinase
SMRT	silencing mediator of thyroid and retinoid receptor
SRA	steroid receptor RNA activator
SRC-1	steroid receptor co-activator 1
STAT	signal transducers and activators of transcription
STEM	short time expression miner
SUMO	small ubiquitin related modifier
SVM	support vector machine

SWI/ SNF	switch/ sucrose non-fermentable
TAFs	TATA-box binding protein associated factors
TAT3	tyrosine amino transferase
TBP	TATA-box binding protein
TGF-α	transforming growth factor-α
TNF	tumour necrosis factor
TNFR	tumour necrosis factor receptor
TPA	12-O-tetradecanoylphorbol-13-acetate
TPR	tetratricopeptide motif
TR	thyroid hormone receptor
TRAP	thyroid receptor associated proteins
TRE	TPA DNA response element
TSG101	tumour susceptibility gene 101
UPP	ubiquitin proteasome pathway
VDR	vitamin D receptor
VEGF	vascular endothelial growth factor
WT	wild type

List of Tables

List of Figures

Word count: 60,154

Abstract

Glucocorticoids (GCs) have an important role in anti-inflammation, apoptosis and immunomodulatory activity. GCs exert their effect by binding to their receptor, glucocorticoid receptor (GR), which subsequently triggers receptor dimerisation, nuclear translocation and eventually causes impact on transcriptional activity. Such regulatory mechanism is complex as it is not only controlled at the transcription level, but also at the post translational level with other contributing factors such as protein stability and cofactor recruitment. Glucocorticoids are commonly used as part of the chemotherapeutical protocols for lymphoid malignancies and have been successfully implicated in treating childhood acute lymphoblastic leukaemia (ALL). Nevertheless, resistance and side effects such as muscle atrophy and osteoporosis still occur frequently.

With the advance in high-throughput technology, vast amount of data on various scales, including genomics, proteomics, and metabolomics make the molecular study of cancer more complicated. The rise of systems biology helps the scientist to address this problem with the use of computation. Although the concept and the approach may vary depending on the research fields, the ultimate goal remains the same which is to create a comprehensive understanding of biological processes and to forecast outcome.

The goal of this body of work is to better understand glucocorticoid induced apoptosis in acute lymphoblastic leukaemia by adopting a systems biology approach. As the Bcl-2 family, particularly Bim is known to be a key determinant of GC-induced apoptosis, we investigated the molecular mechanism of GC induction of Bim. By adopting ordinary differential equation modelling approach, we were able to make prediction and investigate details of Bim regulation by GCs. Further to this, we carried out an integrated microarray analysis in various ALL to study GC resistance and identified crucial candidate gene c-Jun as a regulator of Bim and Erg as a determinant for GC resistance. These results allowed us to refine our models and enabled more answers to be addressed.

In conclusion, our findings not only suggest potential regulatory mechanisms for determining GC sensitivity, they also aid us to find potential biomarkers for determining GC resistance. More importantly, this study represents a successful example for utilising systems biology to study the genetic complexity in cancer.

Short Abstract

The overall project is to study the underlying mechanism in glucocorticoid (dexamethasone) treatment in acute lymphoblastic leukaemia (ALL). The thesis is structured into several chapters. **Chapter 1** reviews the literature on the molecular mechanism to GR resistance, and the approaches already adopted to study this topic. Chapter 2 to 4 describe the research project undertaken to study GR resistance in ALL. **Chapter 2** describes how we study GR regulation of several key Bcl-2 members by building kinetic models based on ordinary differential equations. To gain a global view on GR resistance in ALL and to extend the previously established models, the study in **Chapter 3** describes timecourse microarray analysis in various types of ALL and clinical data that was used to correlate the findings. By taking the models and the findings from Chapter 2 and 3, in **Chapter 4** we are able to further extend the models and make new predictions. In **Chapters 5 and 6** we discuss our approach, the overall success and limitations of our models and findings, possible experiments and suggestions are also discussed for future improvements.

Declaration

No portion of the work referred to in this thesis has been submitted in support of an application for another degree or qualification at this or any other university or institute of learning. The author conducted the experiments, prepared and analysed the data and wrote the papers presented in this thesis.

Copyright Statement

Acknowledgements

I am extremely grateful to my supervisors, Dr. Marija Krstic-Demonacos and Dr. Jean-Marc Schwartz for their constant support during this research and their guidance while preparing the manuscripts for Chapter 2 to Chapter 4. I would like to thank Dr. Constantinos Demonacos for his invaluable advice, James Lynch for his help with setting up the experiments to the work in Chapter 2, Dr. Vaskar Saha and Ji-Zhong for providing clinical microarray data as seen in Chapter 3, and my advisor Dr. David Robertson for his excellent guidance. Thank you so much to the past and present members in Jean-Marc's, Marija's and Costas's lab. I am indebted to my sisters Cindy and Tiffany, the rest of my beloved family and friends for their support in many ways and I am extremely thankful for it. I would also like to mention a few friends of mine; Natalie who sadly is no longer with us, may you rest in peace, Karishma, Diana, Kelly (Eunju), Rahna, Del and Kazz for their companionship, Tracy and Gregg, thank you for being there for me and listening. Finally, I would like to take this opportunity to give a warmest thanks to my parents and grandparents for their confidence, patience and support for all these years; I wouldn't have come this far if it wasn't for you.

1 CHAPTER 1: Introduction

This chapter reviews the literature on the molecular mechanism to GR resistance, the work and the approach that has already been done related to this topic.

1.1 Glucocorticoids (GCs)

Glucocorticoids (GCs) are steroids that are produced by the adrenal cortex in humans. In general, adrenal steroids hormones fall into 3 classes, including mineralocorticoids, androgens and glucocorticoids, which exist as cortisol in the human body. Glucocorticoids have an important molecular function in binding to glucocorticoid receptor thereby maintaining homeostasis in response to stress (1, 2).

Due to their ability to influence virtually all of the cells in the body, synthetic glucocorticoid agonists and antagonists are used for the treatments of many diseases. They are similar to natural corticosteroids, but with minor changes to optimise therapeutic potential, making them become more stable and minimizing unwanted side effects. For example, prednisone, triamcinolone acetonide and dexamethasone are all agonistic to glucocorticoid receptor and are commonly used. The strength of their receptor activation varies, with dexamethasone being one of the most potent steroids, and widely used as diagnostic and therapeutic tools in several inflammatory and autoimmune disorders such as leukaemia (3, 4). A typical example of a glucocorticoid receptor antagonist is RU486, which is also well known as the “abortion pill” by antagonising progesterone. So far, information about RU486 is limited, but studies suggest RU486 is significant in dissociating preserved anti-inflammatory activity from possible side effects (5).

1.1.1 Structure

The major source of glucocorticoids in humans is cortisol. Cortisol is synthesised from cholesterol in the adrenal glands. Like all other steroids, cortisol has a biochemical structure with a 4-hydrocarbon ring skeleton structure, but with a slight difference which results to its functional specificity. Cortisol is a hydrophobic molecule that is able to move between plasma membrane and cytoplasm (6). Around 90% of the serum cortisol is bound to specific protein carriers such as corticosteroid binding globulin protein (CBG) and serum albumin, which in turn speeds up the transportation of this steroid around the blood. Cortisone is an inactive precursor

of active cortisol, and it is only in the presence of isoenzyme 11β-hydroxysteroid dehydrogenase (11β-HSD1 and 11β-HSD2) that these two forms of steroid can be interconverted (Fig. 1.1) (1, 7). In addition, the expression of this enzyme varies in tissues, hence leading to cell, tissue and organ specific glucocorticoid induced response (8).

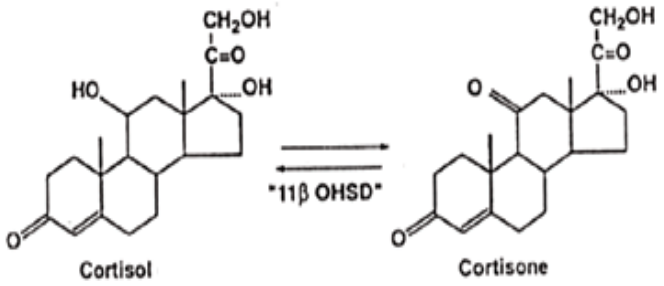

Figure 1.1 Cortisol and cortisone interconversion.

Cortisol is an active form of glucocorticoid in humans which can be converted to the inactive cortisone by isoenzyme 11β- hydroxysteroid dehydrogenase (adapted from (9)).

1.1.2 Physiological role of glucocorticoids

Glucocorticoids are named for their carbohydrate regulating activities, and are essential to the maintenance of homeostasis in response to either physical or emotional stress (10). Apart from regulating metabolism, they are also known to be important in the maintenance of blood pressure, central nervous system, development and programmed cell death (1, 8). They play a crucial role in the regulation of immune and inflammatory responses hence are frequently used as anti-inflammatory and immunosuppressive drugs. In addition, due to their pro-apoptotic function, glucocorticoids have been applied in cancer treatment including Hodgkin's lymphoma, acute lymphoblastic leukaemia (ALL), and multiple myeloma (11-13). Having mentioned their ability to induce cell death, glucocorticoids can also support cell survival in some cases, such as erythroblasts, neutrophils and several nonhaematologic tissues (14).

In humans, cortisol is released from the adrenal cortex under the control of hypothalamic-pituitary adrenal axis (HPA) (Fig. 1.2). Initially, the hypothalamus responds to stress and releases corticotropin-releasing hormone (CRH) and vasopressin (AVP). These hormones then travel to the anterior pituitary gland, stimulate adrenocorticotropic hormone (ACTH) production and eventually trigger adrenal cortex to release cortisol and other steroids. Cortisol level is regulated by cortisol itself as it acts as a negative inhibitor of CRH in a circadian pattern (15).

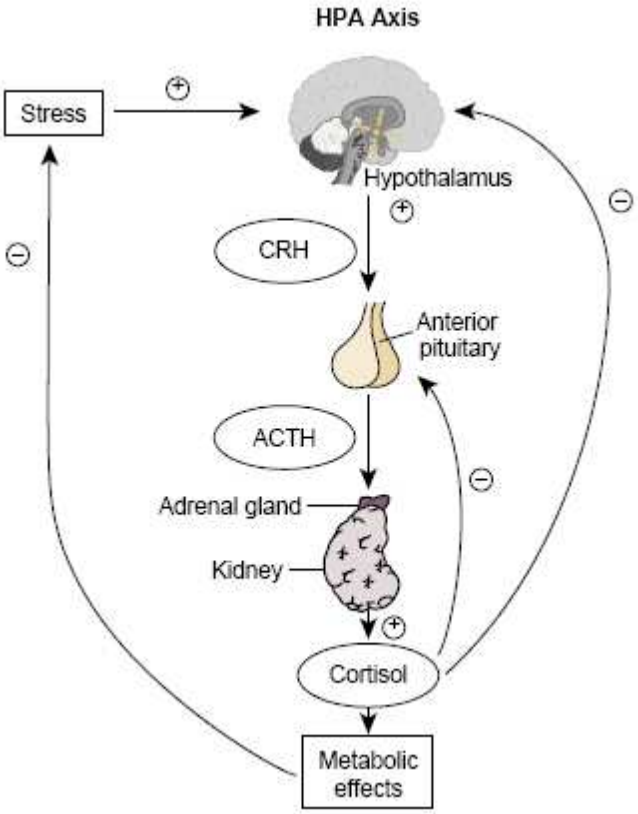

Figure 1.2 Schematic representation of the HPA axis

In response to stress, the hypothalamus secretes corticotrophin-releasing hormone (CRH) and stimulates the anterior pituitary gland to release adrenocorticotropic hormone (ACTH). ACTH then activates the production of cortisol from adrenal gland. Negative feedback is produced by cortisol acting as a negative inhibitor on the anterior pituitary gland and hypothalamus (adapted from (1))

1.1.3 Risks of treatment with glucocorticoids side effects

Glucocorticoids in a pharmacological dosage are commonly used as prescribed drugs for therapeutic purpose. However, long term use of the glucocorticoids can cause many side effects. Glucocorticoids overdose can lead to Cushing's syndrome, which has symptoms such as endocrine disorder including fat redistribution, rapid weight gain, muscle wasting, thinning of skin, osteoporosis and many other impaired functions (1, 16). Another glucocorticoid related disease is Addison's disease, which is caused by the adrenal gland not producing a sufficient amount of glucocorticoids in the body. In contrast to Cushing's syndrome, symptoms of Addison's are not as obvious and take time to develop. Common signs for this disorder include muscle weakness, weight loss, vomiting, diarrhoea, headache and sweating (16).

The benefits of using glucocorticoids for therapeutic purposes have been established for over 50 years. Drugs such as prednisolone, hydrocortisone and dexamethasone, which are derived based on the structure of cortisol, were developed for various treatments including inflammatory diseases, skin disorders, leukaemia and the prevention of rejection during organ transplant (17). However, long term treatment of glucocorticoids may result in cancer cells such as leukaemia cells to become resistant to glucocorticoid evoked apoptosis.

1.1.4 Acute Lymphoblastic Leukaemia (ALL)

Leukaemia refers to a type of blood or bone marrow cancer which is characterised by the abnormal growth of immature white blood cells called blasts. It is mainly classified as four main categories clinically, either being acute (fast disease development) or chronic (slower disease development), or by the type of affected white blood cells i.e. lymphoid or myeloid. Acute lymphoblastic leukaemia (ALL) is one of the commonest forms of malignancy characterised by the presence of immature lymphoid cells, and affects mostly children (17-19). ALL is derived from both B- or T- lymphoid progenitors and often diagnosis requires further classification that is based on many subcategories. These include phenotype, genetic features or risk of relapse, which involves a stringent assessment of the blast count in either the peripheral blood or in the bone marrow of patients after early treatment (20).

Depending on the mentioned factors, the therapy for the ALL treatment varies. In most ALL the initial therapy (also called the remission-induction therapy) consists of administration of a cocktail of drugs including glucocorticoid (prednisone, prednisolone or dexamethasone), vincristine and either asparaginase or anthracycline (21, 22). Comparing the various synthetic glucocorticoids, dexamethasone appeared to be more effective due to its longer half-life and better penetration into the central nervous system (20). In addition, fuelled by the evolution of genomic technologies, molecular target therapy holds a great deal of promises towards personalised therapy and reduces toxic effect. For instance, imatinib is a drug that has been used to treat Philadelphia chromosome-positive (Ph^+) ALL, where ALL patients express a genotype of chromosomal translocation at t (9;22). Such chromosomal translocation results in the BCR (breakpoint cluster region) gene at chromosome 22 fusion with the ABL (Abelson) gene and leads to the production of tyrosine kinase protein BCR-ABL thereby promoting uncontrolled cell proliferation (23). Imatinib can inhibit the BCR-ABL protein by binding to its ATP binding site and further locking it in its inactive conformation (23). However, resistance can still arise suggesting the need for more investigation towards successful ALL therapy.

1.2 The Glucocorticoid Receptor (GR)

Glucocorticoid response is activated via binding to their two receptors, glucocorticoid receptor (GR, also known as NR3C1 in the nomenclature) and mineralocorticoid receptor (MR or NR3C2). These receptors belong to the steroid nuclear receptor family and are widely conserved in different species, along with many other members which include progesterone, androgen and mineralcorticoid (24). The steroid nuclear receptor family, together with nuclear receptor families such as the retinoid X receptor (RXR) heterodimers and the dimeric and monomeric orphan receptors families, are grouped into a superfamily namely the nuclear receptor superfamily. All nuclear receptors share a common structure, that is, a conserved DNA binding domain (DBD), a ligand binding domain (LBD) with variable N- and C- terminal and a hinge region. So far, there have been over 150 different members being identified across various species, due to the increasing numbers of the discovery, members are usually being further divided into either the steroid or thyroid/retinoid/vitamin D (or non-steroid) family (25). Alternatively it can be divided into different classes based on their dimerisation and DNA binding properties, for instance GR belongs to class III nuclear receptor (25).

Overall, these nuclear receptors are potent transcription factors that can activate transcription upon ligand binding. The MR is only expressed in the distal renal tubule and specific tissues or cells such as the brain. It has a high affinity (K_d approximately 0.5-2nM) for glucocorticoids such as cortisol, corticosterone, and aldosterone which is a form of mineralocorticoid. Due to its high binding affinity and location specificity, the MR has a function in maintaining sodium-retaining balance in the colon and sweat glands (26). It also plays an important role in the feedback regulation of HPA axis by acting on the central nervous system (CNS) (1, 2). In comparison with the MR, the GR has a lower affinity (K_d for cortisol approximately 10-20nM) and does not have a restricted expression. It is found in blood and most of the human organs and tissues, particularly in the lungs, spleen, brain and liver. The GR related responses of cells in these regions not only depend on the presence of the GR but also its concentration and the proportion to the glucocorticoids. The GR is mainly responsible for mediating the observed biological effects when glucocorticoid levels rise as a response to stress (27).

1.2.1 Expression of human glucocorticoid receptor gene

Human glucocorticoid receptor gene (hGR) is located on chromosome 5, at the locus 5q31-32 and comprises of 9 exons over 140 kb nucleotides. The protein coding sequence of hGR is made up by exon 2-9, with exon 1 and 9 being the 5’ and 3’ untranslated regions. 3 promoter

regions in exon 1 are thought to be important for glucocorticoid receptor gene regulation (Fig. 1.3). None of these promoters contain typical core promoters such as TATA box or CCAAT motif. Instead, they all contain an array of binding sites for various proteins such as AP-1, AP-2, SP-1, Yin Yang 1 (YY1) and NF-κB (27). A putative interferon regulatory region and a sequence resembling glucocorticoid response element were also found further upstream in exon 1 (8). This variety of transcription factors binding sites may explain the observation of GR being constitutively expressed under different physiological conditions. Alternative splicing of hGR produces several isoforms, with hGRα and hGRβ being the most abundant (28). These two isoforms both contain identical exon 1-8 (up to 727 amino acids) and it is the divergence beyond exon 9 that confers the difference in their functions. The classical hGRα protein has a molecular weight of 94kDa and consists of 777 amino acids. It is expressed in most human tissues and cells and is a ligand dependent transcriptional factor. In comparison with hGRα, very little information has been published on hGRβ. hGRβ protein has a molecular weight of 90 kDa and consists of 742 amino acids. It is expressed in a unique set of human tissues and cells but with a much lower concentration compared with hGRα (28). So far, there is no evidence on whether hGRβ binds to glucocorticoids. However, it was found that hGRβ inhibits hGRα in cell culture and may be correlated with glucocorticoid resistance (28).

1.2.2 GR Protein Structure

Being the first cloned and sequenced nuclear receptor member, GR consists of several functional and structural domains in a modular form (29). These are the N-terminal (NTD), DNA binding domain (DBD), hinge region, ligand binding domain (LBD) and C-terminal (Fig. 1.3). The NTD consists of 420 amino acids and is highly variable among different forms of the GR (30). NTD contains a ligand independent domain called AF-1 (activation function 1) spanning from amino acid 77-262 (31, 32), which is able to interact with GR cofactors and pre-initiation factors such as TFIID and TBP thereby maximizing transcriptional activation (Fig.1.3) (8). Apart from being hormone independent, AF-1 also contains residues that are target for post translational modifications such as phosphorylation, sumoylation or ubiquitination (33, 34). In the human GR, AF-1 contains phosphorylated residues S203, S211 and S226. S211 and S226 are thought to be particularly important in GR related transcription as they were found to be targeted by major kinases cyclin-dependent kinase (CDK) and mitogen activated protein kinase (MAPK) families respectively (35).

The DBD (between amino acid 421-488) is the most conserved region within the nuclear receptor superfamily (2, 5). It consists of highly conserved amino acid sequences along with two characteristic zinc fingers which target specific DNA (Fig. 1.3). This domain plays a major part in dimerisation, nuclear translocation, and the interaction with the GR response elements in the target gene which eventually induces transactivation (35).

The DBD is not the only domain that has the ability to induce protein dimerisation, the LBD (between amino acid 527-777) is known for its dimerisation function and its selective binding ability (36). The LBD is located near the C-terminus, joined with the DBD by a hinge region. It contains a dimerisation surface as well as AF-2 (Activation Function 2) which is an AF-1 like but smaller transactivation domain spanning across amino acid 727-763 (37). In contrast to AF-1, AF-2 is ligand dependent and forms contact with a number of coregulators. Its structure is the reason for LBD being ligand and cofactor specific. The LBD is composed of α-helices and β-sheets that form a hydrophobic pocket which can bind to a number of cofactors and leads to a stabilising structure. Furthermore, unlike other steroid nuclear hormone receptors, the GR:LBD has an additional charged pocket which is thought to be crucial in its selectivity of cofactors binding (37).

The C-terminal helix (helix-12) is important to AF-2 function as it determines which coactivator or corepresser to bind with (5, 38). When GR is bound with agonists such as dexamethasone, helix-12 changes from an “open” position to one closed over the bound ligand which subsequently presents a favourable surface for coactivators to bind with. In comparison with GR agonists, antagonists such as RU486 prevent helix-12 to close properly over the bound ligand. This is because antagonists tend to have side chains which are too long to be contained within the binding cavities. As a consequence, different receptor surfaces are created to interact with corepressors and prevent coactivator interactions (5, 37). The LBD structure is essential as GR is a ligand dependent transcriptional factor. Changes in the LBD affect many GR activities such as heat shock protein interaction, nuclear translocation and interaction with other transcriptional proteins (Fig. 1.3) (39, 40).

Nuclear translocation is also dependent on the two nuclear localisation sequences, namely NL1 and NL2, located next to the DBD and LBD. In comparison with the poorly defined NL2, NL1 is found between residues 479-506 and is known to play a major role in shuttling GR in and out of the nucleus by the interaction with the importin family of proteins (5, 39, 40).

A.

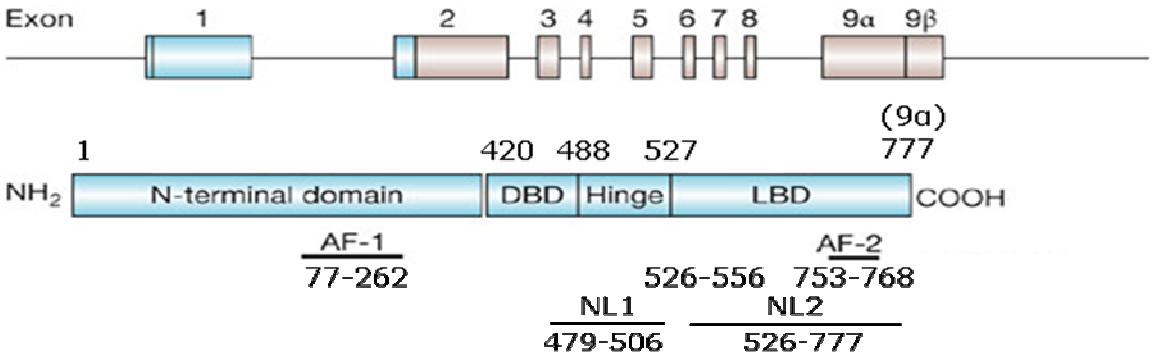

B.

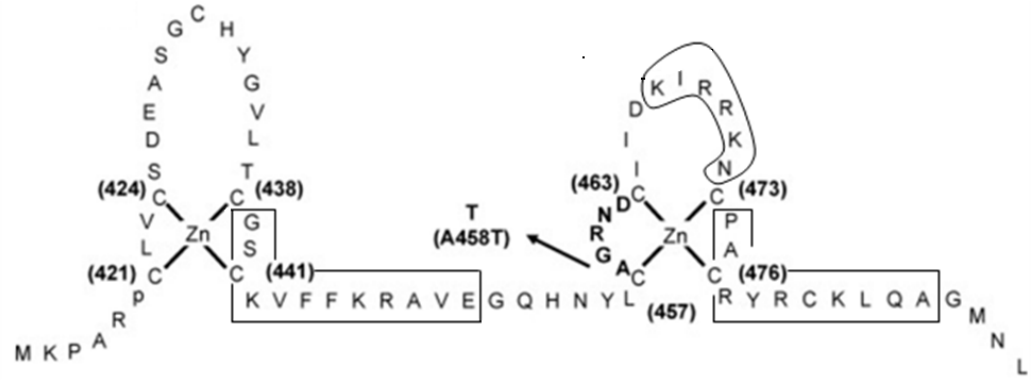

C.

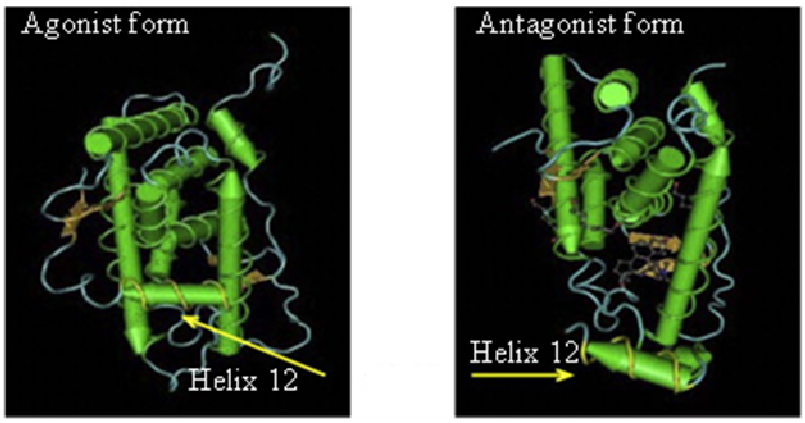

Figure 1.3 The human glucocorticoid receptor structure. (A) Schematic representation of GR structure

The receptor is encoded by nine exons. The protein coding regions are in exon 2-9. Alternative splicing at exon 9 produces two abundant isoforms, hGRα and hGRβ. The glucocorticoid receptor consists of a common nuclear receptor structure, N-terminal, DBD and LBD which are

joined by a hinge region and C-terminus. The most variable N-terminal domain is highly immunogenic and contains activation function domain (AF-1) which is responsible for enhancing transcriptional activation and phosphorylation of GR (adapted from (41)). **(B) The schematic structure of zinc fingers in the DBD.** The DBD locates in the central part of the amino acids sequence (single letter codes). It is composed of two α-helices (boxed sequences) along with two highly conserved zinc fingers. This domain plays an important role in dimerisation, nuclear translocation and transactivation in GR (33, 42). **(C) The crystal structure of LBD.** The crystal structure of LBD consists of 12 α helices (including the ligand-dependent activation function, AF-2 coactivator helix) and 4 small β strands which form a three layer, helical domain. The AF-2, depending on the position of the C-terminal helix (helix-12), undergoes conformational changes when binds to ligand and enables specific interactions with coregulatory proteins.

1.2.3 Mode of action of GR

The classic mode of action for steroid hormones such as glucocorticoids is through direct activation or repression of genes. The three key activities in triggering glucocorticoid response include ligand binding, nuclear translocation and DNA binding.

In the absence of glucocorticoids, GR resides in the cytoplasm forming a stabilised heter-oligomeric complex with heat shock proteins 90, 70, 50, immunophilins and several other co-chaperone molecules such as p23 (43). Upon ligand binding, the receptor complex undergoes a conformational change which causes GR to dissociate from the complex. This allows GR to dimerise and translocate to the nucleus and bind with the glucocorticoid response element of the target gene which subsequently induces either activation or repression (Fig. 1.4) (2).

Other than through direct DNA binding, GR also activates or represses genes through interacting with various transcription factors and cofactors. GR consists of AF-1, a hormone independent domain in its N-terminal, and a ligand dependent domain AF-2 in its LBD region. These two domains allow GR to interact with other transcription factors in several ways. For instance, GR can bind with transcription factors adjacent to the binding sites in a tethering manner, which is referred as the glucocorticoid responsive unit (GRU). The composition of GRU is diverse and is tissue specific. Through this mechanism, GR interacts with a selection of transcription factors such as nuclear factor κB (NFκB) and activator protein complex 1 (AP-1) in the GRU and integrates multiple signals into a much greater glucocorticoid response than direct binding with GRE (2). Upon binding to the GRU, association with cofactors may occur through

interaction with the activation function domains in GR. This can lead to either a negative or a positive effect on the transcription machinery, depending on the binding sites and the cofactors. The exact mechanism for termination of glucocorticoid response is not fully understood, previous studies suggest that GR is able to regulate itself via protein degradation through the ubiquitin-proteasome pathway and through self binding to its own promoter (44).

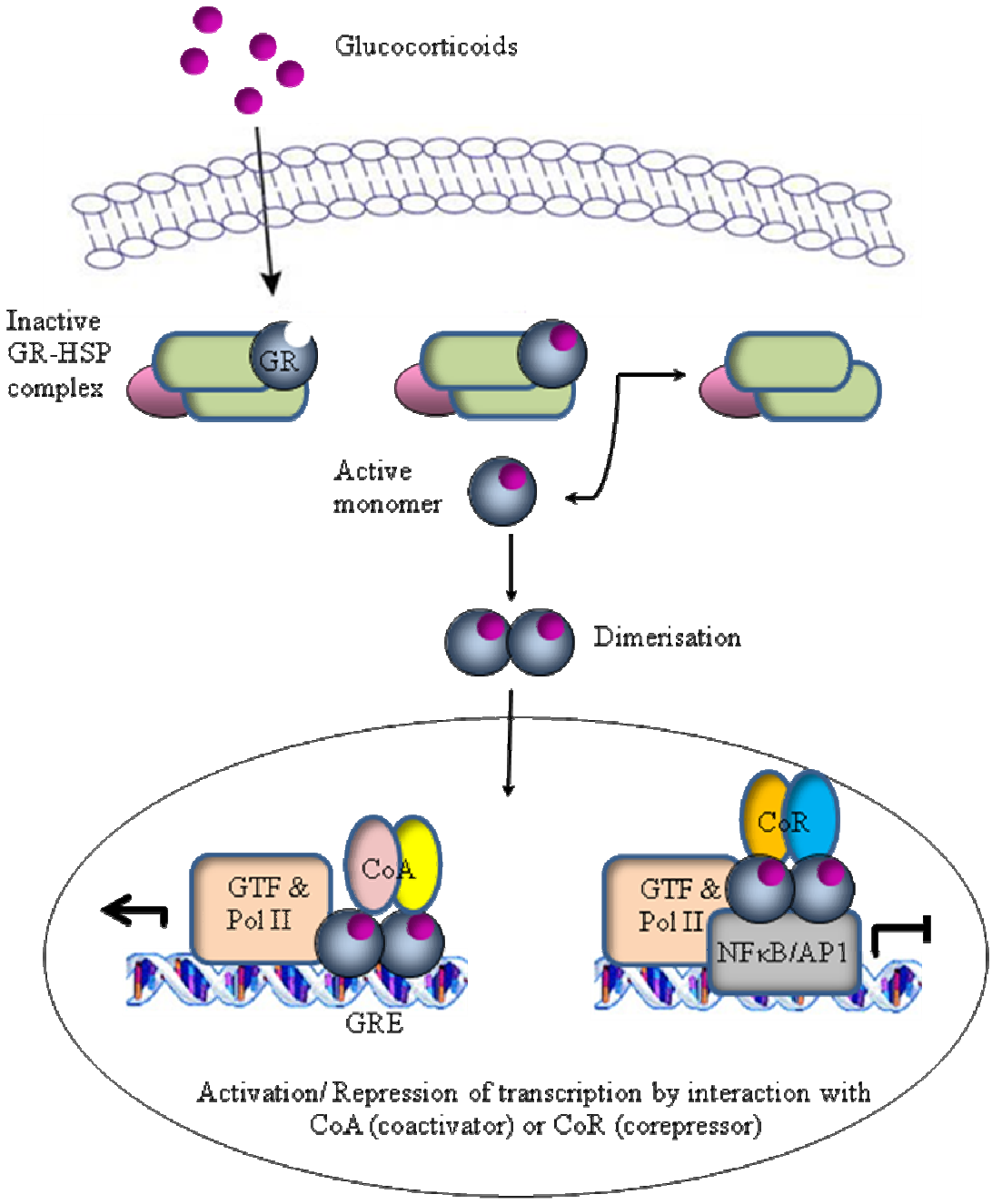

Figure 1.4 Mechanisms of glucocorticoid receptor action

Once glucocorticoid diffuses through the cell membrane, it activates GR and causes the inactive cytoplasmic heat shock protein (HSP) complex to release GR. This causes GR to

dimerise and translocate to the nucleus to bind with glucocorticoid responsive elements (GREs) of the target gene. This in turns either activates or represses gene transcription depending on the recruitment of cofactors (CoA and CoR) and the interaction with the basal transcription machinery (GTFs and Pol II). The activated GR can bind with transcription factors such as nuclear factor κB (NFκB) and activator protein complex (AP-1), if they are bound with their own target DNA element, they can inhibit transcription through recruitment of corepressors.

1.3 GR: the transcription factor

1.3.1 General transcription

Gene expression is regulated by many processes which include RNA transcription, transport, degradation and post translational modification. Transcription is one of the major regulatory mechanisms, it is a process carried out by copying genetic information from DNA into a RNA sequence by enzyme RNA polymerases. Under a tightly controlled process the RNA has an important role in acting as a template in protein synthesis during translation. RNA polymerase II (pol II) is a particularly important enzyme for synthesising messenger RNA (mRNA), small nuclear ribonucleic acid (snRNA) and microRNA through initiating transcription. This requires binding of RNA pol II to the promoter, which is typically a short A/T rich sequence around 30 base pairs upstream from the transcription start site. Such binding motif is named the TATA box which was also the first characterised eukaryotic core promoter (45). Eukaryotic RNA pol II itself cannot recognise the promoter, it relies on the recruitment of the TATA binding protein (TBP) complex, which contains a number of TBP associated factors (TAFs) including one of the general basal transcription factor TFIID. TFIID binds to the TATA box via the TBP complex and recruits other general basal transcription factors (TFIIA, TFIIB, TFIID, TFIIE, TFIIF and TFIIH) which are also important in aiding transcription initiation (46, 47). Once transcription begins, it continues downstream from the transcription start site, through elongation and eventually terminates. Apart from binding with the promoter region, transcription can also be regulated by the interaction between transcriptional factor and the enhancer region. In comparison with the promoter, enhancer is more transcription factor selective and can be located upstream or downstream from the TSS, within the non-coding section of gene- the introns or even on different chromosomes. When transcriptional activator such as GR or activator protein 1 (AP-1) is bound with the enhancer, a protein complex named the mediator is able to transduce signals by forming contact with general transcription factors and RNA pol II at the promoter (Fig. 1.5) (47).

Glucocorticoid receptor is able to control gene transcription through the interaction with either the promoter or the enhancer region of responsive genes (48). These regulatory regions are categorised into four groups, the simple glucocorticoid response element (GRE) and the glucocorticoid half site (GRE1/2s), which are involved in activation of gene expression. For gene repression, there is the negative glucocorticoid response element (nGRE). Furthermore, there is the tethering GRE which is involved in both negative and positive gene regulations (Fig. 1.6). Apart from nuclear translocation and intracellular interactions, the function of GR is also affected by various post translational modifications and the cofactors that are recruited.

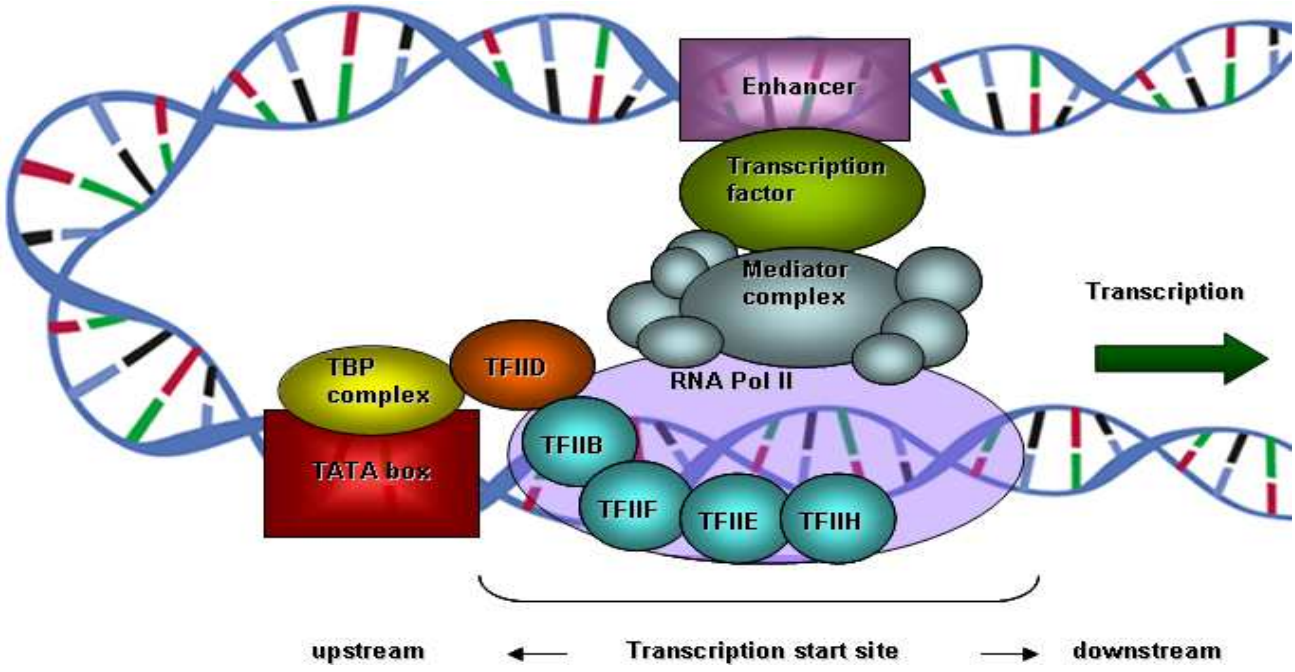

Figure 1.5 Model of general transcription

Initiation of transcription requires RNA polymerase II to form contact with the TATA box by recruiting the general transcription factors. TFIID binds to the TATA box via the TBP complex and subsequently recruits TFIIB, TFIIF, TFIIE and TFIIH. Transcription factor such as GR can aid transcription by binding to the enhancer region (upstream from the transcription start site) and the mediator complex thereby forming contact with the basal transcriptional machinery.

1.3.2 Transactivation

The simplest way for transcriptional activation is the direct binding of GR to the positive glucocorticoid response element (GRE) with a previously identified consensus sequence 5'-GGTACAnnnTGTTCT-3', also called the simple GRE (Fig. 1.6) (2, 49). All GREs have the

same imperfect palindrome structure which is composed of two half site sequences with a three base pair spacer in between (49). Due to this spatial structure, dimerisation of GR is crucial as it requires two monomers to bind with two half sites via GR:DBD. Such binding sites are referred as the simple GREs. Although they share substantial similarities with the consensus GREs, individual GREs can still differ according to their positions, number of copies, distance from their transcription start sites and their sequences. In a study of A549 human lung cells, GR direct targets such as glucocorticoid induced leucine zipper (GILZ) and human inhibitor of apoptosis (HIAP) were identified. Strong correlations were found between glucocorticoid response, GRE architecture, along with GR occupancy and core GR binding sites, which suggest that these factors may be the determinants for inducing glucocorticoid response (2, 50).

Native GREs usually exist as a part of "composite elements", which are comprised of GR binding sites and multiple regulatory factors such as enhancer binding proteins (C/EBPs) and hepatocyte nuclear factor 4 (HNF4) (2, 50). The glucocorticoid induction level is usually higher in this case as the glucocorticoid response is not only dependent on the binding of the GRE, but also on the interaction with these proteins. Occasionally, GR binds with the DNA as a monomer rather than a dimer to a sequence which is called the GRE half site (GRE 1/2s) (51, 52). Unlike simple GRE, GRE1/2s generally requires either additional transcription factors or multiple copies to mediate glucocorticoid response due to their low binding affinities to GR.

Once GR is bound with these regulatory regions in the target gene, it recruits coactivators which falls into a few major categories based on their mode of action, for example the nucleosome remodellrs, the chromatin modifiers and those that interact with the basal transcription machinery (32, 33).

Once GR is bound at a positive GRE, be it simple or composite, it recruits coactivators which tend to fall into three major categories based on their method of action; nucleosome remodellers, chromatin modifiers and those which interact with the general transcription factors.

1.3.3 Transrepression

Repression of gene transcription is achieved by direct binding to negative GRE or interaction with DNA-bound transcription factor in the regulatory complex. nGRE have a similar recognition sequence to GRE. However, due to its highly variable consensus sequence (ATYACnnTnTGATCn), nGRE mediates transcriptional repression rather than activation (2). This mode of action is proposed in proopiomelanocortin (POMC) gene, where GR interacts with

DNA both as a homodimer and a monodimer. As nGRE on its own is not sufficient for transrepression, GR also interacts with other transcription factors that are located close to the POMC promoter region thereby hinders the interactions between TATA binding protein and RNA polymerase II (53, 54).

Besides direct binding to nGRE, repression of transcription can also occur at tethering GRE, where GR binds with certain nuclear bound transcription factors such as AP-1, NFκB, and enhancer binding proteins (C/EBPs) (55, 56). In inflammatory genes, there is no nGRE being identified and it is thought that inflammatory response is induced via GR acting on pro-inflammatory protein such as NFκB and AP-1. NFκB is a heterodimer that usually consists of two monomeric proteins, P50 and p65. Like nuclear hormone receptor, NFκB is usually associated with the cytoplasmic inhibitor protein IκBα in an inactive state. NFκB is activated by a number of extracellular stimuli including cytokines (e.g. tumour necrosis factor (TNF) and interleukin-1 (IL-1)) and viral infections (e.g. Tax protein from human T cell leukaemia virus) (55, 56). These extracellular signals activate IκB kinases (IKKs), which in turn cause IκBα degradation through ubiquitin-proteasome pathway and dissociate with NFκB. Once NFκB is free from association with IκBα, it translocates to the nucleus and bind to the response elements of the pro-inflammatory genes (55, 56).

Glucocorticoids can also trigger the anti-inflammatory response through interacting with NFκB. The exact mechanism for this is not fully understood, but it has been proposed that GR inhibits p65-induced transcription by interfering with several activities such as histone acetylation, which is controlled by histone acetyltransferase (HATs) and histone deacetylases (HDACs), and RNA polymerase II phosphorylation (57, 58). High concentration of dexamethasone is able to induce constant HDACs expression which leads to deacetylation of histones and subsequently represses target genes (57).

GR represses AP-1 activity in a very similar way to the NFκB. AP-1 is usually a heterodimer protein that consists of members such as Jun, Fos, activating transcription factor (ATF) and Maf families. In particular, the interaction between GR and c-Jun is thought to be the key for gene transcription and that the composition of AP-1 plays a critical role in the direction of gene regulation. GR is able to repress or activate the phosphorylation of mitogen-activated protein kinases (MAPK) such as c-Jun N-terminal kinase (JNK) thereby affecting gene transcription negatively or positively (2, 59). Although there is a great deal of similarity between NFκB and AP-1 regulation, each of these mechanisms is still very different depending on the promoter,

receptor and cell type. Several models were proposed for GR-mediated repression between AP-1 and NFκB signalling, including direct binding of GR to AP-1 and NFκB to prevent binding to their response elements, competition between GR and these proteins for binding to their overlapping response elements and for binding with cofactors such as CBP (2, 59).

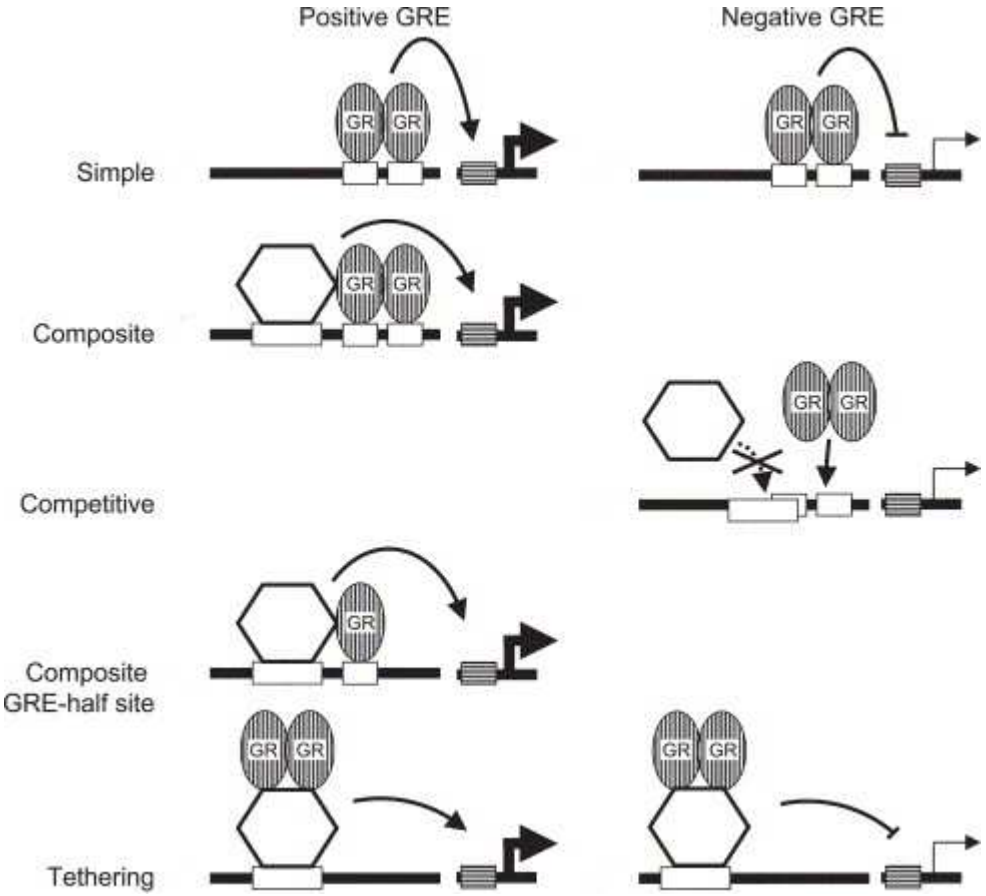

Figure 1.6 Mechanisms of GR interactions with regulatory elements

GREs are distinguished as simple, composite and tethering GRE. There are four binding sites for GR, which include simple positive GRE, GRE-half site (transactivation), nGRE (transrepression) and tethering GRE (can be either negative or positive regulations). Transcription is also affected by the competition with other transcription factors such as AP-1 and NFκB (adapted from (2)).

1.4 Post translational modifications

Apart from cellular localisation and molecular interaction, nuclear receptor response is also regulated by various post translational modifications such as phosphorylation, sumoylation,

ubiquitination, acetylation and methylation. Different isoforms of nuclear receptors may result in various levels of translational regulation, which lead to various degrees of signalling and ultimately affect processes such as tissue and cellular distribution, protein-protein interactions, transcription and protein turnover.

Among different types of post translational modifications, the study of phosphorylation in GR function has attracted the most interest. GR is a phosphoprotein and human GR contains 5 phosphorylated residues in its N terminal domain (AF-1), which are amino acids serine 113 (S113), S141, S203, S211 and S226 (8, 60). In particular, S211 and S226 are thought to be significantly important to transcriptional regulation. Phosphorylation is controlled by a group of enzymes named kinases, and these include mitogen activated protein kinase (MAPK), cyclin-dependent kinase (CDK), and glycogen synthetase kinase-3 (GSK-3). These kinases carry out their effects by recognising the phosphorylation sites in their target proteins and by adding a phosphate molecule to the amino acid. Analysis of hGR phosphorylation sites indicated that a p38 MAPK phosphorylates GR at S211 in lymphoid cells and that such phosphorylation correlates with GR transactivation (8, 60). It was further shown that in the presence of glucocorticoids, the GR phosphorylated at S211 translocates from cytoplasm to nucleus. However, phosphorylation may also affect gene transcription negatively depending on the phosphorylation site (61, 62). For instance, it has been shown that GR phosphorylation at S226 by JNK leads to a repression of GR transcriptional activity (8, 63). Additional research also proposed that phosphorylation may be linked to many other processes. These include ligand binding, nuclear translocation, receptor hormone binding, interaction with general transcription factors, receptor dimerisation and protein stability (44, 64). However, the exact mechanism is unclear and further research is needed to determine molecular details.

Other post translational modifications also affect gene transcription in various ways. Ubiquitin proteasome pathway is controlled by a large group of different proteins such as ubiquitin-activating enzymes (UBAs), E2 ubiquitin-conjugating enzymes (UBCs), and E3 ubiquitin-ligase enzymes and that GR was thought to be a target for ubiquitination (64). Furthermore, a small ubiquitin-related modifier 1 (SUMO) is responsible for targeting proteins that are also implicated in gene regulation i.e. transcription factors, coregulators and chromatin remodellers (65). It triggers sumoylation which is involved in mediating protein stability, localisation and the transcriptional regulation (61). It is thought that JNK dependent GR phosphorylation may be linked to sumoylation thereby affecting its target gene transcription (8). Others such as acetylation and methylation of coregulators can also affect transcription through chromatin

remodelling thereby altering gene transcription. GR recruitment with HDAC2 has been shown to have an inhibitory effect on interleukin-1β induced histone H4 acetylation (49). The diverse post translational modifications are reversible and are closely related to GR functions. Together this indicates that GR signalling should be an integration of multiple processes rather than a single input (66).

1.5 GR cofactors

Cofactors are recruited to interact with DNA-bound receptors and support either transactivation or transrepression. DNA is packaged into chromatin in a compact structure and these cofactors can regulate transcription through altering the chromatin architecture or forming direct contact with the transcriptional machinery. The recruitment of cofactor proteins are promoter and cell specific, they are divided into two groups, coactivators and corepressors. Most of the coregulators function as large protein complexes and possess various activities which contribute to the chromatin structure alterations. For instance, a complex with coactivators that consist of histone acetyltransferases (HAT) is able to modify chromatin and thus induce transactivation. Some of these complexes may also consist of proteins with other functions such as ATP dependent chromatin remodelling, histone arginine methyltransferases activity, RNA processing and mediating interactions with the transcriptional machinery. In contrast, corepressor complexes usually contain HDACs which are able to reverse HAT activities. Occasionally, some complexes may contain proteins that are able to recruit additional corepressors through ligand binding (Fig. 1.7) (66).

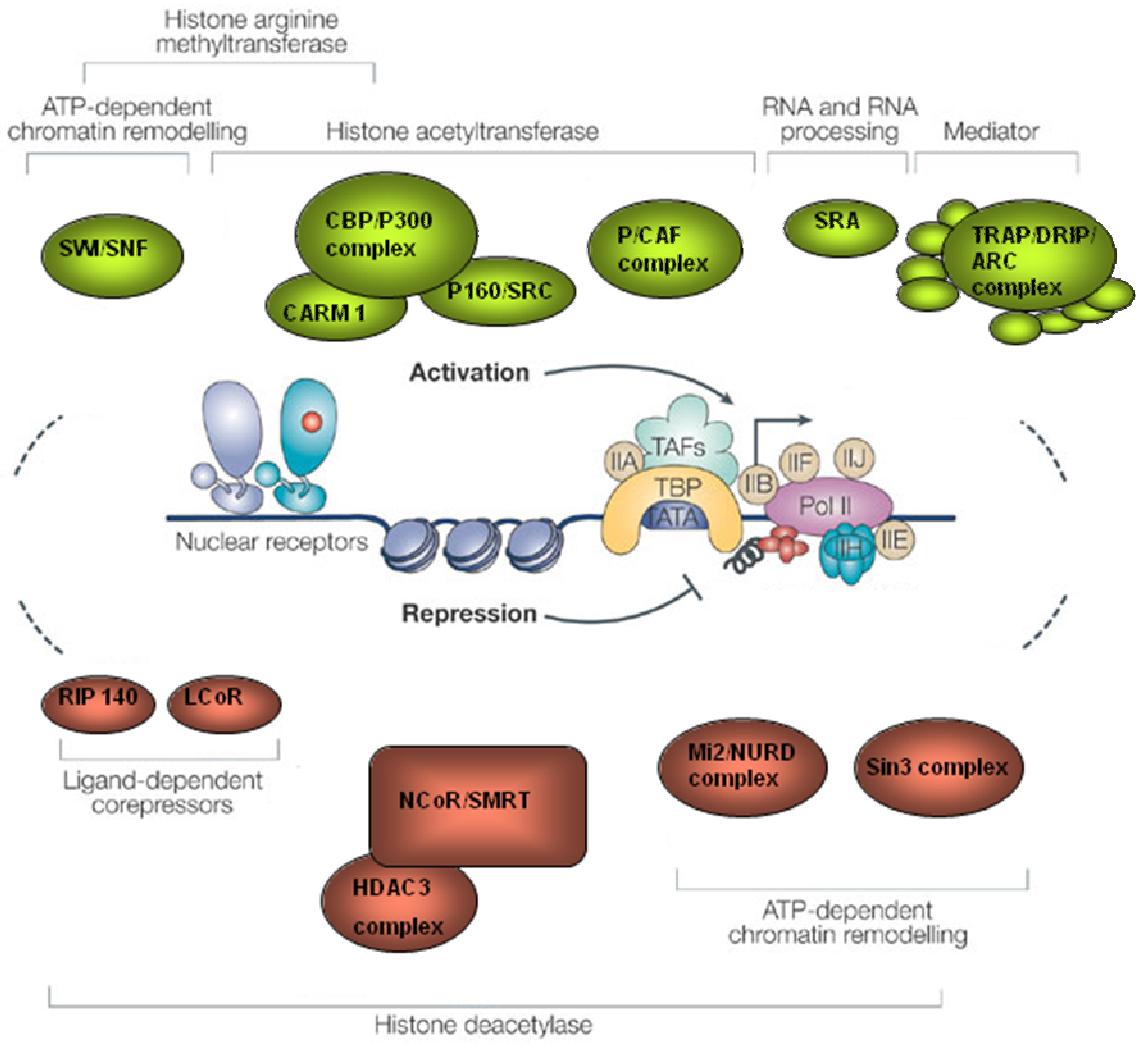

Figure 1.7 Coregulators in nuclear receptor transcription

Transcription regulation requires numerous coregulatory protein complexes that contain coactivators and corepressors with various functions and enzyme activities. Coactivators (green) aid transactivation through various functions which include ATP-dependent chromatin remodelling, histone acetyltransferases activity, RNA processing and acting as a mediator in RNA polymerase (Pol II) interaction. In contrast, the corepressor contains function such as histone deacetylase which packages chromatin in to a “closed” position to prevent the transcription factor binding and subsequently represses transcription. Furthermore, some of corepressor is able to recruit general corepressors upon ligand binding and enhance transrepression. IIA, IIB, IIE, IIF, IIH, IIJ, general transcription factors (adapted from (67)).

1.5.1 Coactivators

- ***Histone acetyltransferases (HATs)***

Many GR coactivators are known to possess histone acetyltransferases activity. DNA is packaged into chromosomal material which is called the chromatin. Each chromatin is in a compressed structure which consists of nucleosomes, which acts as a unit of DNA packaging that contains around 146 base pairs of DNA wrapping a protein histone octamer core made by two of the histone molecules, such as H2A, H2B, H3 and H4 (68, 69). Each nucleosome is linked by one molecule of histone 1 (H1). HAT is an enzyme that catalyses acetyl group transfer to lysine residues in histones N-terminal tail within chromatin thereby disrupting its positive charge. This reduces the affinity between histones and the negatively charged DNA phosphate backbone, which in turns facilitates chromatin into an "open" structure to allow DNA to become more accessible for transcription factors thus increasing transcription activity (68, 69). Such acetylation is identified in coactivator complexes such as p160/SRC, CBP/P300, and P/CAF.

P160/SRC (steroid receptor coactivator) is a group of proteins that binds with nuclear receptor in a ligand dependent manner. So far, there are three classes of p160 protein being identified according to their sequences which include SRC1 (NcoA-1), SRC2 (GRIP1/ TIF2 /NcoA-1) and SRC3 (pCIP/ACTR/AIB1/TRAM) (70-72). These proteins are able to activate transcription by interacting with the LBD of GR via their unique "LXXLL" motifs (where L is leucine and X is any amino acid) in a receptor specific manner. Although p160 is not HAT proteins, the major role of p160 proteins seems to be to recruit other HAT proteins to the coactivator complex, for instance, SRC1 has been reported to recruit HATs such as P/CAF, CBP, P300 or histones methyltransferases (HMTs) such as CARM1 (73, 74). SRC family are well known coactivators however, some of the members such as SRC2 (GRIP1/ TIF2 /NcoA-1) may also have a role in repressing gene transcription. Functional analysis has shown that GRIP1 contains a repression domain that interacts with GR at NFκB tethering GRE in the IL-8 gene and AP-1 tethering GRE in the collagenase-3 gene (75).

CBP (CREB-binding protein) and P300 (E1A binding protein p300) are closely related proteins. They play an important role in gene activation and in overcoming chromatin mediated repression (76). Apart from being HATs, CBP/p300 complex also act as a scaffold protein to recruit other coactivators such as p160s. It also forms direct contact with RNA pol II via TBP and TFIIB to facilitate GR mediated gene transcription (73). CBP/p300 complex

interacts with numerous nuclear receptors and transcriptional factors (i.e. p53, CREB), either through direct contact with AF-1 in the nuclear receptor, or indirect interaction with other coactivators (70, 77). Occasionally, CBP and p300 may function differently or even act as a corepressor in a cell specific mode. In the case of mouse Schwann cells, p300 inhibits GR transcription whereas CBP does not have any functional effect (78).

Different HATs may have different preferences for histones, for instance, P/CAF exhibits a preference for H3 over the other primary target H4. Like CBP/p300, P/CAF can interact directly with nuclear receptors and also recruit other coactivators such as p/300/CBP, SRC-1 and SRC-3. In addition, P/CAF is able to form a complex with other cofactors such as TAFs (TATA box binding protein associated factors) thereby forming a direct contact with RNA polymerase II core machinery (79, 80).

- ***Histone methyltransferases (HMTs)***

Similar to acetyltransferases, histones methyltransferases (HMTs) can also target histones such as H3 and H4 and cause transactivation or transrepression. Members of HMTs are categorised into three groups. These include the H3 lysine 9 (H3-K9)-specific HMTs such as Suv39HI and G9a, which are responsible for gene repression and silencing, the H3 lysine 4 (H3-K4)-specific HMTs i.e. Set9 and the protein arginine methyltransferases (PRMTs) such as PRMT1 and coactivator associated arginine methyltransferases (CARM1/RPMT4), are both found to be involved in activating transcription (81).

- ***Chromatin remodellers***

Activation or repression of transcription requires rearrangement of chromatin from a condensed “closed” structure to an “open” form for general transcription factors to access. Promoter bound GR is known to recruit chromatin remodellers which are either responsible for covalent histone modification such as HATs or catalysing the nucleosomal repositioning on DNA in an ATP-dependent manner through protein complex such as SWI/SNF.

SWI and SNF were firstly identified in yeast, biomolecular study has shown that GR can target SWI/SNF complex to hydrolyse ATP. This in turn disrupts the binding affinity between histones and DNA thereby regulating genes for mating type switching (82). A homologous complex of SWI2/SNF2 in yeast was identified in mammals named brahma (brm)/ brahma-related gene 1 (brg-1). It has been reported that human brm/brg-1 interacts

with GR in a ligand dependent fashion and subsequently supports transcriptional activation (83).

- ***Mediator***

GR can form contact with general transcription factors and RNA pol II, either through interaction with P/CAF complex which contains TAF, or through mediator complex such as DRIP/TRAP/ARC. The yeast two hybrid studies have shown that DRIP150, which is a member of DRIP complex, enhances GR:AF-1 mediated transactivation. In addition, it was also shown that DRIP150 interacts with another member DRIP205, which binds with AF-2 of GR in a hormone dependent manner. The results suggest that DRIP150 and DRIP205 activate GR in a synergistic manner and are possibly involved in coordinating AF-1 and AF-2 functions (84). DRIP150 is also proposed to inhibit transcription as DRIP150 was found in a human corepressor complex named NAT (84, 85).

- ***Other coactivators***

Apart from the coactivators mentioned previously, there are still many coactivators involved in GR signalling via different processes and interactions. Such as the E3 ubiquitin-protein ligase (E6-AP and RPF-1), which catalyses protein degradation and coactivates GR transcription in a ligand dependent mode. In addition, there are selective coactivators such as the steroid receptor RNA activator (SRA), which is present in the SRC-1 complex and interacts with AF-1 of the steroid receptors to enhance transcription (68, 80).

1.5.2 Corepressors

- ***Histone deactelylases (HDACs)***

As mentioned previously, acetylation neutralises the positive charge on histones and weakens the binding affinity between the histones and DNA to activate transcription. HDACs induce opposite effect in comparison with HATs, they repress gene transcription by removing the acetyl groups from lysine. This increases the positive charge of histones and facilitates histones binding to DNA thereby preventing transcription. There are three classes of HDACs in humans being identified so far. Although it is known that they are involved in transcription repression, however, the exact picture is still unclear. Class I (HDAC1, HDAC2, HDAC3) such as HDAC3 is able to direct interact with and activate NCoR and SMRT which further recruits other HDACs 4, 5 and 7. HDAC1 and HDAC2 were found to

interact with the mammalian protein Sin3 which subsequently recruit NCoR and SMRT. How these corepressors mediate Sin3 repression is not fully understood (86, 87). Class II HDACs (HDAC4, HDAC5, HDAC6 and HDAC7) have also been demonstrated to interact with NCoR and SMRT in Sin3. However, only class I HDACs were identified in SMRT/NCoR in human cells or *Xenopus* oocytes (88, 89). Other repressor proteins such as RIP140 (receptor protein interacting 140) and LCoR (ligand dependent repressor) have been shown to interact with the nuclear receptors including GR via their LBD thereby reducing transcriptional activity, Besides the direct interaction between corepressors and the nuclear receptors, class I or class II HDAC complex such as Mi-2/NURD can also affect nuclear receptor dependent transcription by targeting chromatin modification via their histone interacting protein i.e. RbAP46/48, the snf 2 related ATPase Mi-2, and methyl-DNA binding proteins i.e. MBD2 and MeCP1, thereby preventing chromatins become accessible for transactivation (81, 90).

Another class of nuclear receptor cofactors, NCoR and SMRT are the first two related corepressors that were found to interact with unliganded nuclear receptors such as thyroid hormone receptor (TR) and retinoic acid receptor (RAR) (91, 92). It was found that this interaction is mediated by a conserved amino acid helix motif, CoRNR box, of consensus sequence LXXI/HIXXXI/L (where L is leucine and I is isoleucine, H is histidine and X is any amino acid residue) (93). As NCoR and SMRT can also recruit other corepressors via their repression domain, it is thought that NCoR and SMRT create a connection between the corepressors and nuclear receptors. Post translational modifications of the nuclear receptors, such as phosphorylation, acetylation, methylation, ubiquitination and sumoylation provide a further level of regulation of the nuclear hormone receptors (Krstic-Demonacos and Demonacos, 2001). These modifications link steroid receptor signalling to other signalling pathways and create a context dependent level of regulation of transcriptional activity.PTMs provide reversible switches for the activity and stability of co-regulators and link their action to cell signalling pathways.

1.6 GC induced apoptosis and resistance

1.6.1 GC resistance

Glucocorticoid resistance is a rare, familial and sporadic condition characterised by the reduced response to GC in the target tissues or cells which is called primary generalized GC resistance. This in turns leads to the activation of the hypothalamic pituitary axis which results

the increasing of plasma cortisol concentrations, which is a sign of Cushion diseases (94). In cancers such as acute lymphoblastic leukaemia and osteosarcoma, the most common GC resisatnce occurs when the cells bypass GC induced apoptosis. The molecular basis of such condition can be due to either the loss of GR function or a lower GR expression. For instance, GR downregulation may be ascribed to GR promoter activity influenced by transcription factors such as AP-1 or Ets proteins. On the other hand, GR function may be impaired due to mutation thereby altering GR transcriptional regulation (95). The molecular study of GC sensitivity has revealed many candidate GR target genes that are critical in regulating apoptosis, including the components of apoptotic machinery such as the B cell lymphoma 2 family (Bcl-2) (96, 97).

1.6.2 GC induced apoptosis: extrinsic and intrinsic pathways

Apoptosis is a cell defense mechanism which serves to remove excess, damaged or infected cells in organisms. It is a form of cell death programme that is mediated by caspases, which are essential proteases in tissue homeostasis. There are two apoptotic signalling pathways established so far, the intrinsic pathway and the extrinsic pathway.

The extrinsic pathway is initiated by ligand mediated activation and the death receptor. For instance, the pro-inflammatory cytokine tumour necrosis factor (TNF) can bind to its death receptor tumour necrosis factor receptor (TNFR) which spans the plasma membrane and causes conformational changes thereby recruiting adapter molecules like FADD to form a protein complex, termed the death-inducing signalling complex (DISC). The protein complex results in the activation of the initiator caspase 8, which leads to the cleavage of the downstream effector caspases such as caspase 3 and subsequently induces apoptosis (Fig. 1.8) (98, 99).

The intrinsic pathway is a classic apoptosis pathway, where the Bcl-2 family regulates apoptosis in response to intracellular stress. The intrinsic pathway is closely associated with the permeabilisation of the mitochondria for activation of caspase 9. Such permeabilisation, also called the mitochondrial outer membrane potential (MOMP), is regulated by the Bcl-2 family and the cell fate is determined by the balance between the expression of the pro- and anti-apoptotic Bcl-2 family members (43). Depending on the individual Bcl-2 family members' functions, they either permit the release of apoptogenic factors within the mitochondria (i.e. cytochrome c, Smac/DIABLO, Omi) into the cytosol, or keep them sequestered. Once cytochrome c has escaped into the cytosol, it initiates the assembly of apoptosome complex comprising of Apaf-1 and caspase 9. This in turn activates caspase 3 and 7 and induces apoptosis (Fig. 1.8) (100). For instance, upon cytotoxic signals, pro-apoptotic proteins such as Bad and

Bim are phosphorylated by protein kinases PKA and Akt. This causes the other pro-apoptotic member Bax to translocate to the mitochondria and form a complex with another pro-apoptotic Bcl-2 family member Bak, which is inserted into the mitochondrial outer membrane. The activated Bak/Bax can form a mitochondrial apoptosis-induced channel and mediate the release of cytochrome c which then activates apoptosome and a series of downstream caspases to trigger apoptosis. In contrast, the anti-apoptotic Bcl-2 would block the release of cytochrome c, possibly by inhibiting Bax /Bak (101).

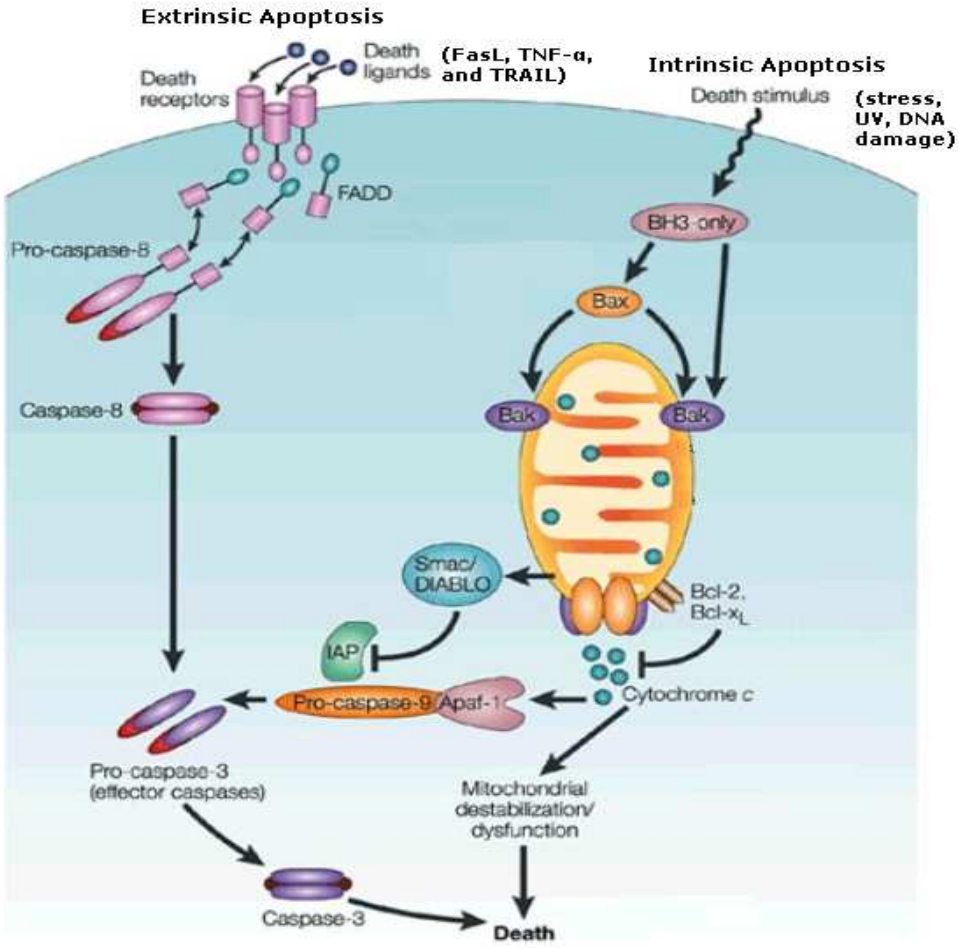

Figure 1.8 Apoptotic signalling pathways

There are two forms of signalling pathway, the intrinsic stress pathway is mediated by the Bcl-2 family under condition such as stress, UV irradiation or DNA damage. The Bcl-2 family induces mitochondrial outer membrane potential (MOMP) which releases cytochrome c to target Apaf-1 thereby facilitating caspases to execute apoptosis. Such signalling pathway can be repressed by inhibitor of apoptotic proteins (IAP), which is controlled by

mitochondrial protein Diablo/Smac. The extrinsic death receptor pathway is triggered by signals such as FasL, TNF-α, and TRAIL from other cells, which activate death receptors and recruit caspases through the adaptor protein FAS-associated death domain (FADD) (adapted from (102)).

1.7 Mechanism of GR induced apoptosis

Chemotherapeutic drugs such as glucocorticoid have been widely used for the treatment of cancer such as lymphoid malignancy due to their ability to facilitate MOMP to induce apoptosis. Several mechanisms currently stand for GR induced intrinsic apoptosis, for instance, the ligand activated GR may directly binds to its target genes which have an apoptotic function i.e. the Bcl-2 family members. Alternatively, GR may bind to the nGRE in the proinflammatory genes such as AP-1 or other anti-apoptotic genes thereby inhibiting its transcription. Other theories also exist including reduction in GR expression or where apoptosis occurs as a result of GC inhibitory effect on cell cycle progression (103).

1.7.1 The Bcl-2 family: the pro- and anti-survival members

Bcl-2 (B-cell lymphoma 2) is an integral membrane protein (25kDa) encoded by the bcl-2 gene (104, 105). This gene was first identified in human B-cell lymphoma and is considered to be a central regulator in prolonging cell survival by inhibiting apoptosis. There are approximately 25 members in this family sharing at least one of four conserved Bcl-2 homology (BH) domains, which determine their functions. It is therefore logical that the Bcl-2 family members are characterised by the presence of these four distinct sequence motifs (Fig. 1.9). Generally, members with all four domains are pro-survival proteins, whereas proteins with BH1-3 or BH3-only tend to be pro-apoptotic. The Bcl-2 family consists of the anti-apoptotic proteins Bcl-2, Bcl-X_L, Mc1-1, A1 and Bcl-W, or pro-apoptotic proteins, such as the Bax and the BH3-only families (Fig. 1.9) (106). Overall, the Bcl-2 family can be divided into 3 groups according to their functional structures; the pro-survival members, Bax and BH3-only molecules.

Bcl-2 is an anti-apoptotic protein that is found in all types of cells. In comparison, Bcl-2 homologues such as Bcl-X_L and Bcl-W become associated with intracellular membranes only in the presence of cytotoxic signals. The majority of these proteins are initially localised in the cytosol, but have the ability to translocate in response to death signals due to their functional hydrophobic carboxyl-terminal domain, which is formed by the residues of BH1, BH2, and BH3. It allows Bcl-2 to undergo a conformational change and target the cytoplasmic face of the

mitochondrial outer membrane, endoplasmic reticulum membrane and nuclear envelope and eventually trigger apoptosis (107). As with the other two more divergent members, Mc1-1 and A1, currently not much information has been published but it has been proposed that they have a much weaker pro-survival activity in cells. Although the mechanism is poorly understood, it is known that the Bcl-2 members have the ability to form homo- or heterodimers with each other, which suggests the potential of mediating the balance between the pro- and anti apoptotic proteins.

The BH3 domain is thought to be the critical domain for triggering apoptosis. So far, all Bcl-2 members that contain only BH3 domain are pro-apoptotic. BH3 itself is critical for mediating apoptotic response, therefore BH3 only molecules are usually categorised as a group on its own, these include Bid, Bad, Bik, Bim, Bmf, Puma, Noxa, Hrk/DP5 in mammals and Eg11 from *C.elegans* (108).

Other studies have shown that the BH4 domain of anti-apoptotic members such as Bcl-2 and Bcl-X_L form a direct contact with the C terminus of Apaf-1. This prevents caspase-9 to associate with Apaf-1 which indicates the possibilities of alternative mechanism (109, 110). In addition, the cytochrome c/Apaf-1/caspase9 pathway may not be the only signalling apoptotic pathway as cells lacking Apaf-1 or cytochrome c can still undergo apoptosis (111). It was also shown that dexamethasone induced apoptosis by activating caspase 9 without involving cytochrome c and Apaf-1 interaction (112).

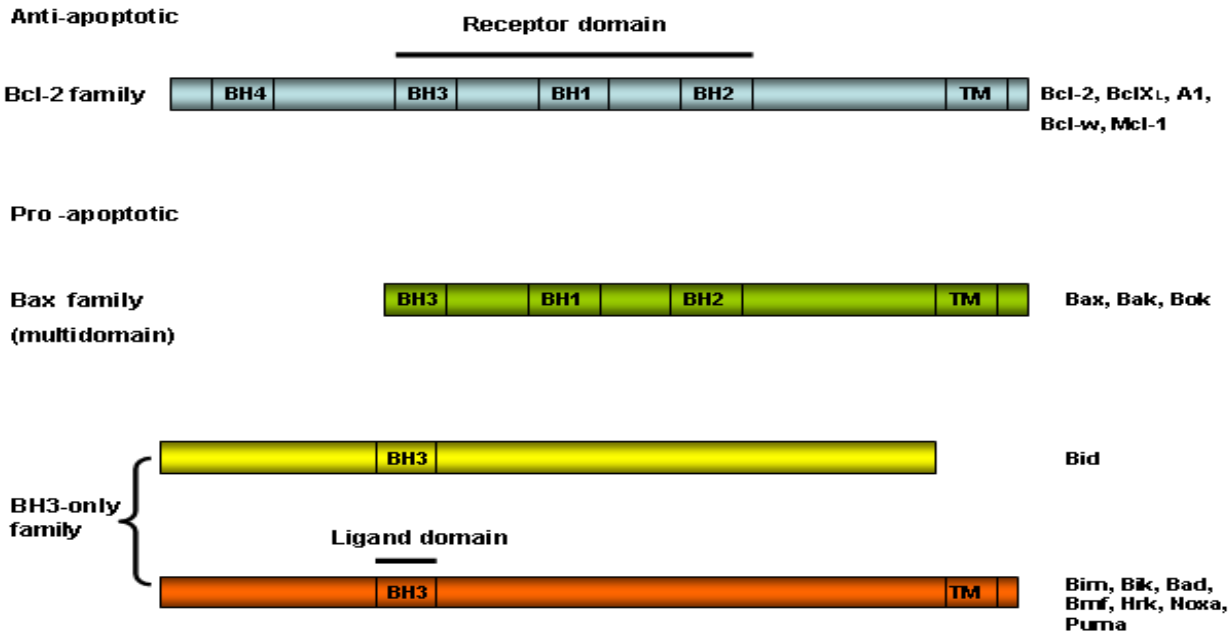

Figure 1.9 Members of the Bcl-2 family

1.7.2 Three Bcl-2 subfamilies have been identified according to their structure domains. These include the pro-survival Bcl-2 family and the two pro-apoptotic families i.e. the Bax family and the BH3-only family. Apart from A1 and several BH3-only proteins, most members have a carboxyl-hydrophobic region (TM) which is considered to aid association with the intracellular membrane. Bcl-2 and Bax families are antiapoptotic channel-forming Bcl-2 proteins with at least three BH domains (BH1-3) and a transmembrane anchor sequence. They are believed to be anchored on the mitochondria membrane, whereas the BH3-only family acts as "ligands" that form dimerisation with these channel-forming Bcl-2 "receptors" thereby regulating apoptosis. Post translational regulation of the Bcl-2 family in apoptosis

- ***Dimerisation, Phosphorylation, Sequestration and Proteolytic cleavage***

Bcl-2 family can be regulated transcriptionally during different stress conditions and by various post translational modifications. The Bcl-2 family can exert their functions either independently or synergistically with other members via dimerisation. It was reported that Bax has the ability to either homo-dimerise to promote cell death or to interact with its inhibitor, Bcl-2 via its BH3 domain and abolish the function of Bax itself (113). The yeast two hybrid study revealed several possible interactions among the Bcl-2 family. These

include (i) Bcl-2 with Bcl-2, (ii) Bcl-2 with Bcl-X_L, (iii) Bcl-2 with Bcl-X_S, (iv) Bcl-2 with Mcl-1, (v) Bcl-X_L with Bcl-X_L, (vi) Bcl-X_L with Mcl-1 and (ix) Bax with Mcl-1. Details of such interactions have not been elucidated, it was suggested that these interactions may be either direct or indirect, which requires additional bridging proteins (114).

Phosphorylation is particularly important in regulating BH3-only molecules such as Bad, which is phosphorylated at serine sites S112 and S116. Phosphorylated Bad is usually sequestered by a 14-3-3 molecule in the cytosol and is unable to carry out its pro-apoptotic function (Fig. 1.10). Upon death signal i.e. growth factor deprivation, survival promoting kinases such as Akt and PKA become inhibited. This causes the inactive Bad to be dephosphorylated and to interact with Bcl-2 and Bcl-X_L which eventually leads to activation of caspases (115).

Alternative splicing in Bim results in three isoforms including Bim_{EL}, Bim_L, and Bim_S. In healthy cells, Bim remains inactive and is held by the microtubule associated dynein motor complexes. In response to the death stimuli, Bim dissociates from microtubules and translocates to the mitochondria, where it interacts with Bcl-2 and Bcl-X_L and eventually promotes cell death. Exposure to certain apoptotic signals such as taxol can amplify the release of Bim from the dynein light chain 1 and enhance apoptosis. It is known that Bim is a key executer for apoptosis induction in many cell types such as lymphocytes (108, 116).

Bmf is another BH3 only protein that functions in a very similar way. Bmf is usually sequestered by binding with the dynein light chain 2 that is associated with actin cytoskeleton in the healthy cells (117). Certain stimulus such as loss of cell attachment (anoikis) causes Bmf to translocate and bind with Bcl-2 during apoptosis(118).

Another critical BH3 protein is Bid, which is thought to promote cell death through activation of Bax and Bak and inactivation of anti-apoptotic members. BH3 domain in inactive Bid is usually buried due to its protein structure. The activation of Bid requires the exposure of BH3 domain which is induced by the cleavage in its amino-terminal region. Bid can be cleaved by caspase 8 which is induced by death ligands in the extrinsic apoptosis. Alternatively, it can be cleaved by caspase 3 or granenzyme B which are involved in the intrinsic apoptosis. Proteolytic cleavage of Bid results in the production of tBid which targets mitochondria and subsequently induces apoptosis. It is thought that proteolytic cleavage in Bcl-2 and Bcl-X_L can also cause the exposure of BH3 domain and convert their functions from anti-apoptotic to pro-apoptotic (119, 120).

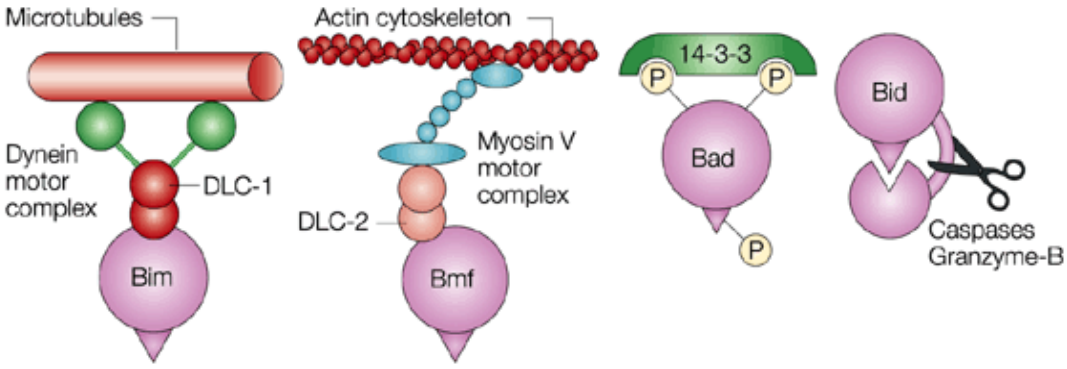

Figure 1.10 Post translational regulations of BH3 only proteins

In healthy cells, Bim and Bmf are sequestered by dynein light chains (DLCs) associated with microtubules or actin cytoskeleton respectively. Upon certain death signals, BH3 Bcl-2 members such as Bim and Bmf are released and interact with Bcl-2 and their homologues during apoptosis. Phosphorylated Bad requires kinases such as Akt and PKA to induce dephosphorylation and activate Bad. Activation of Bid requires proteolytic cleavage by caspases or granenzyme-B to releases Bid and induces apoptosis (adapted from(117)).

1.7.3 GR: Transcriptional regulator of the Bcl-2 family

In response to the apoptotic stimuli, the Bcl-2 proteins are transcriptionally regulated by certain cytokines, transcriptional factors and several post translational modifications as mentioned. The level of Bcl-2 transcription is important in cell death regulation, each Bcl-2 member responds differently depending on death signals and cell types. Pro-apoptotic members generally remain transcriptionally silent in healthy cells unless death signals are introduced (121). Regulation of the Bcl-2 transcription is dependent on many processes and factors. These include protein degradation and transcription factors such as p53. Bax and BH3-only proteins such as Puma and Noxa are thought to be the potential transcription targets for p53 (122-124).

For years GCs are known to invoke apoptosis and are regularly used in treatments of acute lymphoblastic leukaemia and related malignancies (97). In some cases, cells may fail to respond to GCs, the exact reason is unclear but there are many speculations with genetic alterations being one of the many possible reasons (125). The detail on how GCs regulate apoptotic signalling is not fully understood, it is thought that GCs induce cell death by either directly regulating apoptosis associated genes or by acting as an apoptotic stimuli which perturbs gene network and

causes cellular distress. Previous studies have demonstrated that glucocorticoid regulates apoptotic signalling pathways differently depending on the cell types, cell cycling states and extracellular supporting factors (126).

Several cell signalling pathways have been identified in lymphoid cells and are thought to be important in apoptosis. These include the MAPK pathway, the cAMP/PKA pathway, the hedgehog pathway (Hh), the mTOR system and the c-Myc system. Many of these signalling events rely on either the transcription, or the post translational modifications that are involved in enzyme activities (127). In particular, the Bcl-2 family mediated apoptosis is thought to be one of the crucial apoptosis signalling pathways. As mentioned, GCs might induce cell death by regulation of apoptotic genes or via perturbation of gene networks. In both cases, it is thought that Bcl-2 members can either act as direct targets of GCs, or as sensors to detect harmful GC effects (128).

Affymetrix studies in lymphoblasts of patients (adults and children) with primary ALL indicated that BH3-only molecules, in particular Bim and Bmf are induced after GC treatment (97). There are also other reported Bcl-2 regulations affected by GC such as the induction of Bmf and Puma mRNA in thymocytes, and Bcl-2 and Bcl-X_L protein repressions in children with ALL, which suggest the importance of Bcl-2 rheostat in GC response (97, 129). The full picture of Bcl-2 rheostat influencing GC sensitivity is not yet fully understood. Several possible regulations have been considered. These include primary induction, delayed primary induction, and secondary response. Primary gene control is the most straight forward mechanism. The ligand activated receptor binds directly to DNA and affects transcription either negatively or positively. Details of delayed primary induction are unclear; it is thought that the process requires chromatin modifications and protein complex formations between GR and various proteins. In comparison with these two mechanisms which are direct and do not require *de novo* protein synthesis, secondary mechanism is indirect and requires the production of the protein induced by GR that then controls downstream regulatory target genes (Fig. 1.11) (127).

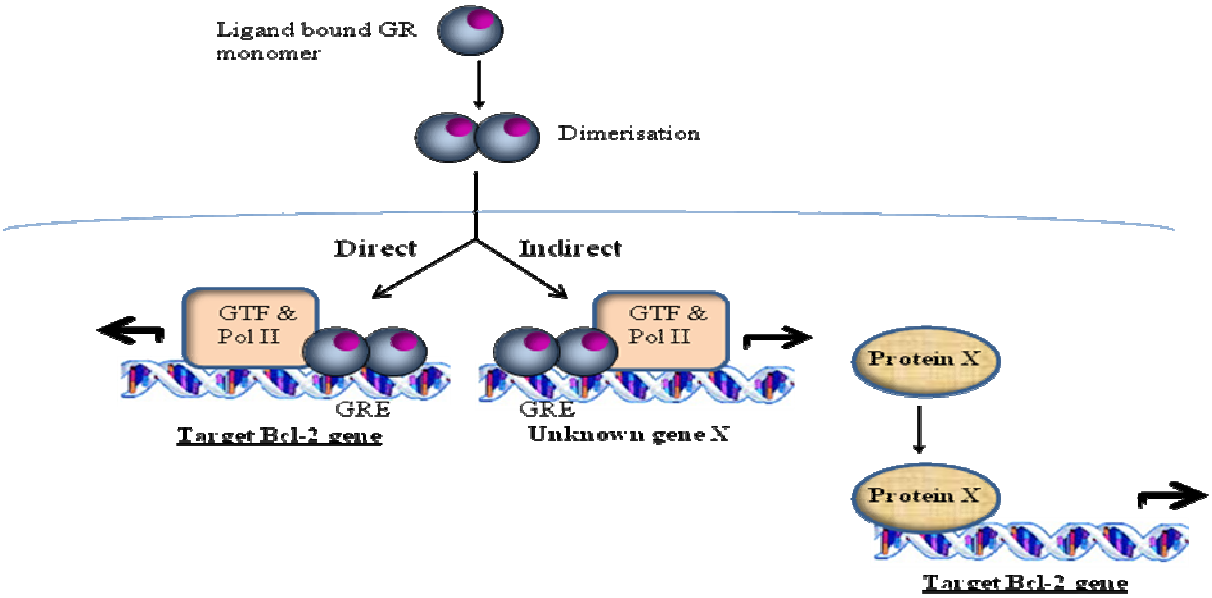

Figure 1.11 Schematic diagram of possible transcriptional regulation by GR

Transcription upon binding of ligand activated receptor to GREs can be categorised into the direct and indirect mechanisms. In the direct mechanism, ligand activated receptor activates regulatory genes by direct binding to its promoter regions. In contrast, the indirect mechanism is a two step transcription and requires protein synthesis which is essential in activating the second set of regulatory genes.

1.7.4 Bcl-X_L

Bcl-X_L is a direct target of GR, which is one of the two major isoforms of Bcl-X (130). The two isoforms were identified in human and mice, which include the anti-apoptotic Bcl-X_L and the pro-apoptotic Bcl-X_s. The larger isoform Bcl-X_L shares a high homology with Bcl-2, Bcl-X_L is composed of 233 amino acids and contains highly conserved BH1 and BH2 domains (131). It is widely expressed in tissues containing long-lived-post-mitotic cells such as the adult brain. Unlike Bcl-X_L which has a functionality of inhibiting apoptosis, Bcl-X_s has an opposite effect of promoting apoptosis. Bcl-X_s encodes a protein which is short of a 63 amino acid corresponding with to BH1 and BH2 domains (132). Strong expression of Bcl-X_s can be found in cells undergoing a high rate of turnover, for instance, lymphocytes during the development (131).

The Bcl-X_L gene was found to be dominantly expressed in embryonic and postnatal organs, including lymphoid tissue (133). As a result, Bcl-X_L is thought to be a perfect candidate to study the regulation of apoptosis in haematological malignancies. Primary and secondary resistance

can be caused by long term treatment of ionization radiation, chemotherapeutic agents, and multi-drug treatment which leads to elevation of Bcl-X_L transcription and promote cell survival (108, 134, 135).

Primer extension analysis has identified multiple transcription initiation sites in the Bcl-X gene (136). It is thought that each of these sites is used differentially depending on the cell type and differentiation state, and possibly contributes to the level of transcriptional regulation (137). At this stage the Bcl-X_L regulation is poorly understood, a number of transcription factors has been identified to be directly regulating the Bcl-X gene, including STAT, Rel/NFκB, Sp1, AP-1 Oct-1, Ets, and GATA-1 (136). Furthermore, recent investigations indicated that GR is related to the repression of Bcl-X_L in dexamethasone treated lymphoid cells by direct binding to the P4 promoter of the Bcl-X gene (138, 139).

1.7.5 Bim

Bim is a potent apoptotic BH3-only member. It has many isoforms including Bim_{EL}, Bim_L and Bim_S. Bim_S is known as the most potent pro-apoptotic member in most cells, for instance, in GC sensitive cells such as CEM-C7-14 (125, 140). There are two possible interactions for Bim to induce apoptosis, Bim can either bind to Bcl-2 members such as Mcl-1 to inactivate their anti-apoptotic properties, or induce oligomerisation of Bax and trigger caspases mediated apoptosis (97, 108). Compared with what was found in the GC sensitive ALL- CEM-C7-14, there was no reported Bim induction in the GC resistant ALL cell line (CEM-C1-15) and was found to be weakly induced in the lung cancer A549 cells, which emphasises the importance of cell specific regulation (97).

The transcriptional regulation of Bim seems to be rather complex. So far, no GREs were identified in the promoter of Bim and different modes of regulation have been reported possibly due to its cell specific property. It was shown that growth factor withdrawal can lead to the induction of Bim in various neuronal and hematopoietic cell types (141, 142). In particular, only Bim_{EL} was found to be notably up-regulated in nerve growth factor deprived neurons (NGF) (143). This finding suggests that an additional level of regulation of pre-mRNA splicing may occur in addition to transcriptional induction. It was further shown that Bim upregulation is achieved via c-Jun N-terminal kinase (JNK) activation in NGF deprived neurons, but by the forehead transcription factor FKHR-L1 in hematopoietic cells (118, 142, 143). It is important to note that the gene regulating profile is also stimulus dependent, previous studies indicated that cytokine (IL-3) stimulated hematopoietic cells down-regulate Bim via activation of two major

RAS pathways, Raf/mitogen activated kinase (MAPK) pathway and the phosphatidylinositol 3' kinases (PI3K) (144). To this point, the relationship between dexamethasone and Bim transcription is poorly understood. Microarray analysis and pre- treatment with the protein synthesis inhibitor cycloheximide (CHX) revealed that Bim is not only induced by dexamethasone in lymphoid cells, it is also an indirect target of GR (96, 116, 145-147).

1.7.6 Bmf

Bmf, along with Bim is believed to be located on the cytoskeleton to sense any intracellular changes. In comparison with Bim, Bmf is a much weaker pro-apoptotic member and cannot induce apoptosis alone. It is thought that Bmf may induce apoptosis via inhibiting pro-survival member Bcl-2, Bcl-X or Bcl-W, which subsequently release pro-apoptotic member Bak from being associated with Bcl-X_L (97). Bmf mRNA has been identified in various cell lines, which include B- and T-lymphoid cells, myeloid, and in mouse embryos at all developmental stages (118). Abundant protein expression was found in many mouse organs such as pancreas, liver, kidney and hematopoietic tissues (118). The expression of Bmf was also dependent on the culture condition, for instance, EGF withdrawal in human mammary epithelial cells causes an induction of Bmf but not upon serum withdrawal or UV irradiation (148). Two signalling pathways that are related to epithelial tumourgenesis, the ERK and AKT pathways were thought to be linked to the matrix-mediated Bmf transcriptional regulation (148).

Functionality studies revealed that other than Bmf (also referred as Bmf-I), additional spliced isoforms Bmf-II and Bmf-III were found in human B-chronic lymphocytic leukaemia cells (149). In contrast to Bmf-I, Bmf-II and Bmf-III do not have the BH3 domain and do not function as pro-apoptotic proteins. Different protein and mRNA expression were observed in each spliced variants, which suggests that the events of transcriptional activation and alternative splicing are crucial in Bmf expression. It is noteworthy that other than these two mechanisms, post translational regulation of Bmf is also important for the Bmf apoptotic activity (149).

Microarray studies have shown that Bim and Bmf were dominantly expressed in acute lymphoblastic leukaemia (97). However, the physical interaction between Bmf and GR is uncertain. Previous studies indicated that CHX did not affect HDAC inhibitors induced Bmf transcripts in adenocarcinoma cells, which suggests that Bmf mRNA induction does not require protein synthesis (150). Together with these findings, it is highly likely that GR may be a direct target of Bmf.

1.8 The AP-1 complex: Jun and Fos

AP-1 (activator protein 1) is a family of heterodimeric proteins that contains a number of leucine zipper proteins which consists of the basic region that is required for recognition of its AP-1 binding site, the TPA (12-O-tetradecanoylphorbol-13-acetate) DNA response element (TRE) (151). The AP-1 complex is composed of members including Jun (c-Jun, JunB, JunD), Fos (c-Fos, FosB, Fra1 and Fra2), CREB/ATF families. It has been reported that AP-1 regulates various cellular processes such as cellular growth, differentiation and death. Amongst various AP-1 subunits, c-Jun is thought to be the most important transcriptional activator, with its activity sometimes being antagonised by JunB. It is thought that the composition of AP-1, particularly regarding c-Jun homodimer and c-Jun:c-Fos complex, play an important role on determining GR functions (152-154).

1.8.1 Jun

The Jun protein family consists of members of basic leucine zipper proteins that act as the components of AP-1 complex. The Jun proteins are able to dimerise with other AP-1 subunits such as the Fos proteins or the CREB/ATF proteins, in some cases the Jun family may bind to others proteins, for instance Ets protein PU.1 and GATA protein GATA1 possess a dimerisation motif that can form interaction with c-Jun.

The c-Jun gene is located on chromosome 1, at locus p31-32 in human, which was originally isolated from avian sarcoma virus 17 in 1987 as a homolog of the retroviral oncogene v-Jun (155). c-Jun protein is composed of 334 amino acids with 3 well conserved domains that are found among the Jun and Fos family. These are the leucine zipper domain, the basic region and the transactivation domain (Figure. 1.12). It is an intronless protein and immediate early gene that responds to various environmental stresses. c-Jun dimerisation is important in many cellular functions including embryonic development, cell proliferation, tumourgenesis and apoptosis (156-158). Such dimerisation is critical for DNA binding (159) and also aids the nuclear translocation (160), it is thought that c-Jun preferably dimerises with the c-Fos proteins as c-Fos cannot form a homodimer itself (161).

c-Jun expression is regulated at various levels; c-Jun contains two binding sites at its enhancer regions, including one that has been reported to mediate c-Jun positive autoregulation (162). On the other hand, post translational modification such as phosphorylation is thought to be crucial in c-Jun regulation. Phosphorylation by JNK activates c-Jun transcription by

phosphorylation at serines 63 and 73 in the transactivation domain of c-Jun. In addition, dephosphorylation of c-Jun also contributes to c-Jun activation. For instance, it was shown that glycogen synthase kinase 3 (GSK3) phosphorylates c-Jun at threonine 239 and serine 249 which prevents binding of c-Jun to DNA (163). Other MAPK pathway such as p38 is also thought to play a role in c-Jun phosphorylation at serine 63 and 73 and causes c-Jun induction (164).

Other Jun proteins such as JunB and JunD have also been reported to play a role in tumourgenesis. For instance, in contrast to c-Jun which activates its own transcription and collagenase by binding to the TRE site at the promoter regions of these genes, JunB in fact inhibits the activation of these promoters (165). Other Jun family members such as JunD also has been implicated to have a growth suppressing role, where Weitzman et al. have found increased proliferation in JunD deficient fibroblasts (166). In comparison with c-Jun, the functions of JunB and JunD are less understood.

1.8.2 Fos

Similar to Jun, Fos is also an immediate early proto oncogene with rapid transcriptional activation when stimulated by mitogenic factors and is involved in cellular processes such as proliferation, differentiation and apoptosis. Among the Fos protein family only c-Fos and FosB contain transactivation domains whereas others such as Fra1 and Fra2 do not (161). The gene encoding human c-Fos is located on chromosome 14 at region q21-31 (167). c-Fos protein contains 381 amino acids and is usually expressed at low or undetectable levels in most cell types in a tightly controlled manner (Figure 1.12). Upon external stimuli such as growth factors or cytokines, c-Fos expression is induced and regulates various biological processes. Fos protein requires dimerisation in order to bind to DNA, however unlike Jun protein, Fos cannot form homodimer and require heterodimerisation with other proteins such as Jun proteins.

The regulatory c-Fos promoter activity is controlled via the presence of various *cis* inducible elements. For instance, c-Fos contains a *cis* inducible enhancer that can be recognised by the STAT transcription transcription factors which are regulated by ERKs (168). The regulation of c-Fos is also controlled by the post translational modification such as phosphorylation. It has been reported that p38 MAPKs phosphorylated c-Fos at threonines 232, 325, and 331 and at serine 374 when exposed to UV (169). However, transcriptional activation would require more than one of the indicated phosphorylations.

FosB behaves similarly to c-Fos, where FosB expression is also induced by the exposure to serum and mitogens and is able to form complex with c-Jun and JunB in vitro in NIH3T3 mouse fibroblast cells (170). Other Fos proteins such as Fra1 and Fra2 were later shown to also be involved in embryo development and were able to bind with Jun proteins during cell cycle (171).

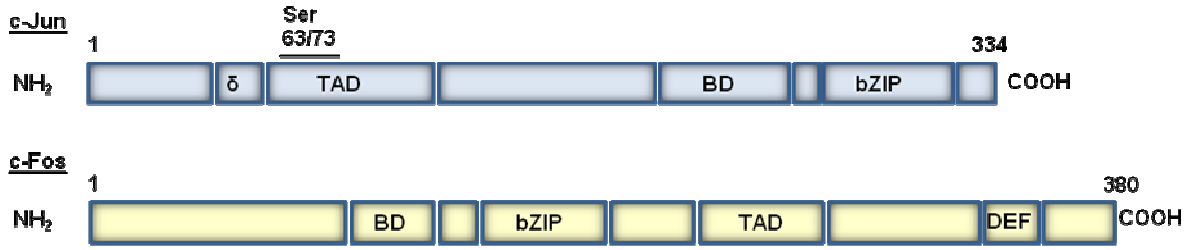

Figure 1.12 Structure of Jun and Fos protein

The three conserved domains of Jun and Fos are shown; Leucine zipper (bZIP) is important in dimerisation, basic domain for DNA binding (BD), transactivation domains (TAD) for transactivation (172). Both Jun and Fos protein are regulated by kinases. In c-Jun, JNK binds to the δ domain thereby phosphorylates serine residues at position 63 and 73 in the transactivation domain. Whereas c-Fos protein contains the DEF domain which is targeted by ERK (172).

1.8.3 Crosstalk between AP-1 and GR

As mentioned, AP-1 interacts with GR at multiple levels by functioning as a competitor for coactivators (see 1.3.3.Transrepression). Typically, AP-1 appears to be a tumour promoter and is downregulated when treated with GCs. Several studies have demonstrated additional levels of crosstalk between AP-1 and GR other than simply competing for interaction with transcription factors such as CREB binding proteins (CBP) or binding to target genes (152, 154). For instance, GR function is determined by the composition of AP-1, Diamond et al. have shown that c-Jun homodimer causes GC dependent stimulation in the mouse proliferin gene, in contrast, c-Fos and c-Jun heterodimer have the opposite effect (153).

In addition, the GR function is context dependent, it is also controlled by the type of hormone response element on the target gene, cellular levels and composition of AP-1 and cell types. It has been previously shown that GC represses collagenase-3 gene by modulating AP-1 binding to the target response element Col3A. Such binding was however, not identified in collagenase-1 gene in the same cell (173). Pearce et al. have shown that different GR and AP-1

DNA binding mechanisms occur depending on the distance between the respective response elements (154). GR has a synergetic effect with AP-1 when GRE and the AP-1 site are separated at least 26 basepairs (bps), whereas GR represses AP-1 complex c-Jun-c-Fos but not c-Jun homodimer when the two sites are around 14-18 bps apart (154). Another possible mechanism is that GC controls AP-1 transcriptional activity via regulation of JNK pathway. As JNK phosphorylation is critical to Jun and Fos transcription and it has been demonstrated that GC causes 50% reduction in JNK activity (174). This suggests GR may modulate Jun and Fos at a post translational modification level, however it is unclear whether such effect can account for the dramatic repression of AP-1 target genes such as collagenase (175). A recent study has demonstrated that such JNK inhibition controlled by GC was greater in the nucleus in comparison with the cytoplasm and that this was not based on the physical interaction between GR and JNK, suggesting an additional level of controlling mechanism to GC modulating JNK activity (176).

A recent report highlights the role of AP-1 on GR binding to target genes by facilitating chromatin accessibility (177). Genome-wide analysis showed that AP-1 occupancy prior to GC treatment is important in acting as a pioneering factor which mediates the chromatin to an "open" state for GR recruitment. The mechanisms may be differentiated by the GR binding mechanisms either being composite or non-composite and may require additional transcription factor involvement such as the Ets protein family. A study revealed the possible AP-1 and Ets proteins cooperating mechanisms in regulating Plau gene transcription in a Ras/MAPK signalling dependent manner (178). Taken together, these findings suggest that GR and AP-1 crosstalk is controlled on multiple levels and each factor results in alteration of the GR transcriptional properties.

1.9 The Ets proteins: Erg and its relevance to GR in ALL

The Ets proteins are a group of 28 transcription factors that are categorised into 12 subfamilies, these are Elf , Elg, Erg, Erf, Ese, Ets, Pdef, Pea3, Er71, Spi, Tcf and Tel (184) (Table 1-1). The protein structure is characterised by the conserved Ets DNA binding domain consisting of around 85 amino acids; this region recognises the consensus Ets binding sequence (GGAA/T) (179). A few proteins such as Ets1 and Erg also contain the PNT domain which is important for protein-protein interaction. It was also found that other Ets proteins contain other functional regions. For example, some proteins such as the Elg subfamily GABPα may contain the OST domain, which plays a role in recruiting cofactors. Ets proteins have been found to be

associated with various biological processes such as cellular proliferation, differentiation, haematopoiesis and apoptosis (179). Although Ets proteins are structurally related, they are functionally diverged, thus allowing them to regulate their target genes both positively and negatively. In addition, many Ets factors are involved in chromosomal translocation which is related to cancer development. Ews-Erg and Ews-Fli1 are the two common fusion proteins found in Ewing's sarcoma, which is a type of cancer that often occurs in bone and soft tissues (178, 180).

It has been well established that Ets transcription is regulated by phosphorylation via mitogen-activated protein kinases (MAPK) such as Erk, JNK and p38 in an Ets family dependent manner. For instance, the Pea3 subfamily proteins Er81and Erm are phosphorylated by the Erk signalling cascade whereas Spi family member SpiB is phosphorylated by both Erk and JNK (179). In addition, the status of phosphorylation and the selection of Ets subfamily may have a role in regulating Ets target genes. A chromatin immunoprecipitation sequencing (ChIP-Seq) study in prostate cells identified Ets and AP-1 synergistically regulate their target gene Plau in a MAPK signalling depending manner (181).

In acute lymphoblastic leukaemia, a high level of Erg expression was found to associate with leukaemia progression (182, 183). Ets proteins have been implicated in both positive and negative GR transcriptional modulation. ChIP assay showed that both GR and Spi subfamily member Pu.1 are recruited to the GR promoter in human myeloma IM-9 B cells, which in turns represses GR regulation (184). Such effect is cell type dependent, as Pu.1 recruitment was not found in T-ALL CEM-C7-14 cells, instead, another transcription factor c-Myb was found recruited to the GR promoter and positively regulated GR autoregulation.

Ets	Mammalian family members
Spi	Spi1 (Pu.1), SpiB, SpiC
Pea3	Etv4 (Pea3/E1AF), Etv5 (Erm), Etv1 (Er81)
Er71	Etv2 (Er71)
Erf	Erf (Pe2), Etv3 (Pe1)
Elf	Elf1, Elf2 (Nerf), Elf4 (Mef)
Tcf	Elf1, Elf4 (Sap1), Elk3 (Net/Sap2)
Ets	Ets1, Ets2
Pdef	Spdef (Pdef/Pse)
Erg	Erg, Fli1, Fev
Ese	Elf3 (Ese1/Esx), Elf5 (Ese2), Ese3 (Ehf)
Elg	Gabpα
Tel	Etv6 (Tel), Etv7 (Tel2)

Table 1-1 The human Ets protein family

The table illustrates 12 Ets subfamilies and their members, Ets proteins are defined with their well conserved Ets binding domain, with some proteins exhibiting variation in their protein structures, for example, Ets, Pdef, Erg, Ese, Elg and Tel all consist of an extra protein-protein interaction PNT domain.

1.10 Systems Biology: The integrated approach to study gene network

Due to the advance in high throughput technology, scientists have designed novel approaches to analyse large sets of data from various sources. For this reason, systems biology has become a popular concept, in which it symbolises the understanding of biology at the system level. Systems biology can be described as a cycle, starting from the selection of biological data obtained through laboratory based research and the creation of the models. The models represent a set of computable assumptions, which need to be tested against the established experimental facts; models showing consistency with the established findings will become the studied subject and the generated hypotheses would be tested experimentally. In contrast, the inconsistent models will either be rejected or modified. Once the consistent models are tested against the "wet" lab experiment, improvement of models can be made to further generate new hypotheses. The approaches for systems biology in general can be divided between being bottom-up or top-down. Bottom-up systems biology starts with the molecular properties to construct models to

predict systemic properties followed by experimental validation and model refinement. In contrast, top-down systems biology is systemic-data driven. It starts with experimental data to discover or refine pre-existing models that describe the measured data successfully. In this way, previously unidentified interactions, mechanisms and molecules can be identified. Contemporary bottom-up systems biology often considers kinetic models whereas top-down systems biology predominantly focuses on regulatory models to analyze data. Regardless of which approach is adopted, the integration of experimental data and modelling are essential, and the selection of approaches and tools vary depending on the question one seek to address (185).

1.10.1 Microarray, clustering and the identification of biomarkers

Since the invention of polymerase chain reaction (186) and the initiation of the human genome project in the 1990s (187), the field of molecular biology has entered an "omics" era. Microarray has become one of the most popular "omic" approaches in experimental molecular biology, such techniques allow us to study the entire genome under various environments. This breakthrough technology in turn furthered our understanding towards various biological events such as identifying subtypes of disease, predicting disease progression and assigning novel functions to genes.

The core principle of microarray technology is the hybridisation between two strands of DNA; the mRNAs of interest are first extracted, reverse transcribed to generate their complementary DNAs (cDNAs). The cDNAs are then labelled with fluorescent dye such as Cy3-dUTP and Cy5-dUTP followed by incubation with the chip where they hybridise to the spot which contains the immobilised complementary target DNA (188). Such microarray is referred to as spotted cDNA microarray; there are many other types of microarrays such as the Affymetrix GeneChip sharing the same basic principle but slightly different experimental design. Different to spotted cDNA microarray, Affymetrix utilises the photolithographic synthesis strategy which uses light to build sequence of probes that can specifically match the target RNA; more information about the design of Affymetrix can be found in (Figure 1.13).

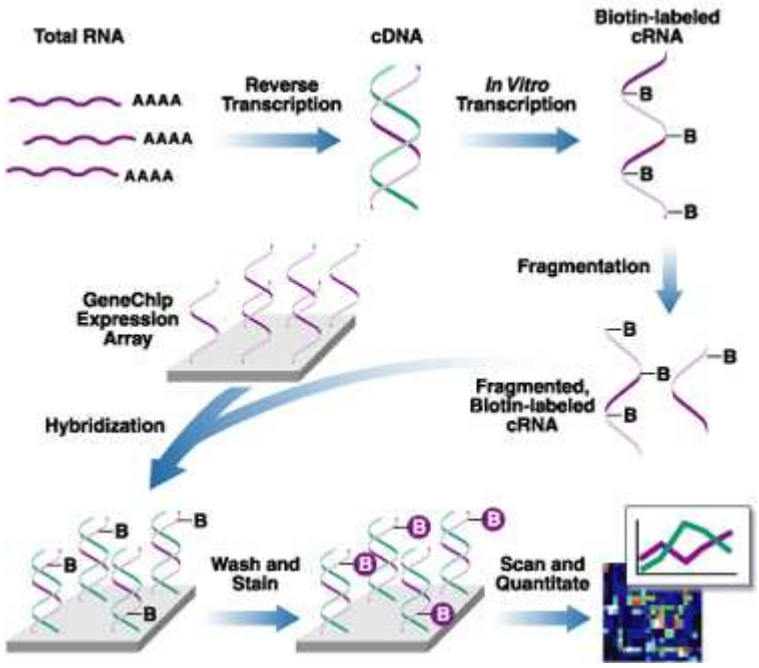

Figure 1.13 Schematic diagram of Affymetrix microarray experiment

The total RNA is first extracted from the subject of study, then being reversed transcribed to cDNA and undergoes in vitro transcription to generate cRNA. The cRNA is labelled with the coenzyme biotin and is further fragmented. The fragmentated cRNA hybridises with its complementary probes, which were generated via photolithography, and the unmatched cRNA is then washed off. Finally, the array is scanned with a laser and the information is read and quantified by the computer (adapted from German Cancer Research Centre http://www.dkfz.de/gpcf/24.html).

In order to transform the raw microarray data into interpretable results, several levels of analysis need to be performed. The procedure starts with the initial quality check of the arrays and the elimination of any potential outliers, followed by normalisation, classification of genes into groups and assessment of biological functions. For gene group classification, clustering analysis is a method that is commonly used in order to identify gene expression patterns. Currently there are many different clustering techniques and algorithms; clustering can be either divisive or agglomerative, which refers to breaking down or building up clusters. Alternatively, clustering can be supervised or unsupervised, depending on whether a “reference” gene is used as a guide to perform clustering (189). Base on the question one would like to address, the choice of the clustering technique may vary. For instance, a clustering tool such as short time expression miner (STEM) (190, 191) is specifically used for clustering short timecourse gene expression data (190). This is achieved by assigning genes to a series of pre-defined kinetic profile

individually and each gene kinetic profile is grouped into clusters. The significance of the profiles is estimated from the number of member genes. Gene ontology analysis is also implemented in the software for further functional analysis. The authors have shown that STEM is a more robust algorithm in comparison with other time series data analysis algorithms such as k-means and CAGED when selecting the gene expression kinetics from a pool of noisy data.

Microarray clustering has been widely used for identifying biomarkers. It has for example been applied in primary lymphocytes, where they adapted a supervised clustering method, support vector machine (SVM) based clustering algorithm to identify bone morphogenetic protein receptor, type II (BMPRII) as a key gene for determining GC sensitivity (192). SVM is a type of clustering that is commonly used for disease classification; it is able to group the genes that belong together by taking the training data information into account (188). Such approach has also been used in acute lymphoblastic leukaemia, where authors identified common genetic defect in ETV6 and RUNX1 genes amongst various ALL subtypes (193). So far, there is a limited amount of data on studying the gene expression kinetics in acute lymphoblastic leukaemia.

1.10.2 Overview: Gene network modelling

The inference of genetic regulation networks is an important aim in the field of systems biology. Modern technologies allow more accurate, time efficient, high-throughput integrative analyses of DNA, RNA, proteins and metabolites in biological systems. As a result, post genomic research requires the use of simulation and analysis tools to gain understanding of the dynamic and temporal characteristics of complex pathways (194). One of the most common approaches is to reconstruct the interaction network in the organism and to analyse this network. This involves mapping the individual biomolecules and observing all the possible interactions. Once a biological network is built, it allows the individual branches of the network to be analysed further. A detailed network should contain all the relevant interactions and the associated parameters (195).

As mentioned, bottom-up and top-down approaches are commonly used in gene expression modelling. In gene signalling network, the first approach is knowledge based and focuses on one or few genes, referred as the “bottom-up” approach. Such models should include all the details such as transcription, translation, mRNA degradation, protein activity, RNA processing and RNA localisation (194). However, the downside of this approach is that the kinetic parameters are often difficult to obtain. Alternatively, there is also the “top-down” approach, where the

models can be built from DNA arrays as it allows thousands of genes to be analysed simultaneously. The gene expression profiles and patterns permit the search for their interactions and relations with one another which may eventually lead to deducing their functional correlations (196). So far, the biggest challenge is to deduce the function in relation to each gene. Various modelling methods have been developed, which include Boolean networks, differential equation descriptions and Bayesian networks (Fig. 1.14) (197).

A Boolean network is a simplified representation of gene expression dynamics. This approach consists in modelling species by two discrete states, on (1) and off (0), depending on various regulatory processes and conditions. Such models are also named as the "logical" or the "binary" approach. It enables the control of the dynamic by assigning a switch to each gene, however, it is restrained in computing discrete dynamics only (198).

Biological processes can be described mathematically by sets of ordinary differential equations. Mathematical formulations may vary depending on the type of bimolecular interactions. For instance, a standard Michaelis-Menten equation is used to describe enzyme catalysed reaction whereas mass action equation is used for complex-bindings (Equation 1) (194). Mass action kinetics is used for describing the dynamics of all reactants and products in a chemical reaction, where the reaction rate is directly proportional to the reactant concentration. Mass action kinetics is commonly used and has previously been successfully implicated in glucocorticoid receptor transduction models (199).

For a mass action reaction with two substrates (S_1 and S_2) and two products (P_1 and P_2), obeying first-order kinetics like:

$$S_1 + S_2 \xrightarrow{k} P_1 + P2$$

The reaction rate is described by the following ordinary differential equation (ODE):

$$\mathbf{-\frac{d[S_1]}{dt} = -\frac{d[S_2]}{dt} = +\frac{d[P_1]}{dt} + \frac{d[P_2]}{dt} = \mathit{k}\,[S_1]\,[S_2]} \quad \textbf{(Equation 1)}$$

Where *k* is the net rate or the kinetic constant, the reaction rate is proportional to the concentration of each of the reactants S_1 and S_2. d[ ]/dt represents the rate equation that expresses the change of either S_1 or S2 over time due to transcription, translation or other individual processes. Such reaction is commonly known as bimolecular reaction.

ODE models are commonly used to describe the rate of change in species concentrations in a continuous time frame. Many simulation softwares have been developed to model biological systems by ordinary differential equations (ODE). One of the advantages of this approach is to take detailed knowledge about individual interactions in gene regulation into consideration (198). However, obtaining the kinetic constants is often a major problem.

An alternative method is Bayesian networks (also known as Bayesian belief networks or belief networks), which are forms of probabilistic graphical models. A Bayesian network consists of two major components, the nodes, which represent variables i.e. genes, and the arcs which represent statistical dependence relations among the variables (200). Bayesian networks are one of the most promising tools to be used in gene analysis because their probabilistic nature is much more tolerant to the noise inherent in microarray measurements. In most cases, it is a discrete model that can explain the probabilistic relationships between the variables. Such approach offers a natural way for selecting the most suitable sub-graph from the complete network for data analysis. There are a few advantages including using the scoring metric to avoid over-fitting data and handle the uncertainties of data via prior distributions. Bayesian networks, however, have a few prominent disadvantages. This network is only useful if the prior knowledge is reliable and it is not practical for dealing with large numbers and combinations of variables, which highlights the difficulties for utilising Bayesian network for scaling realistically sized network (194, 200).

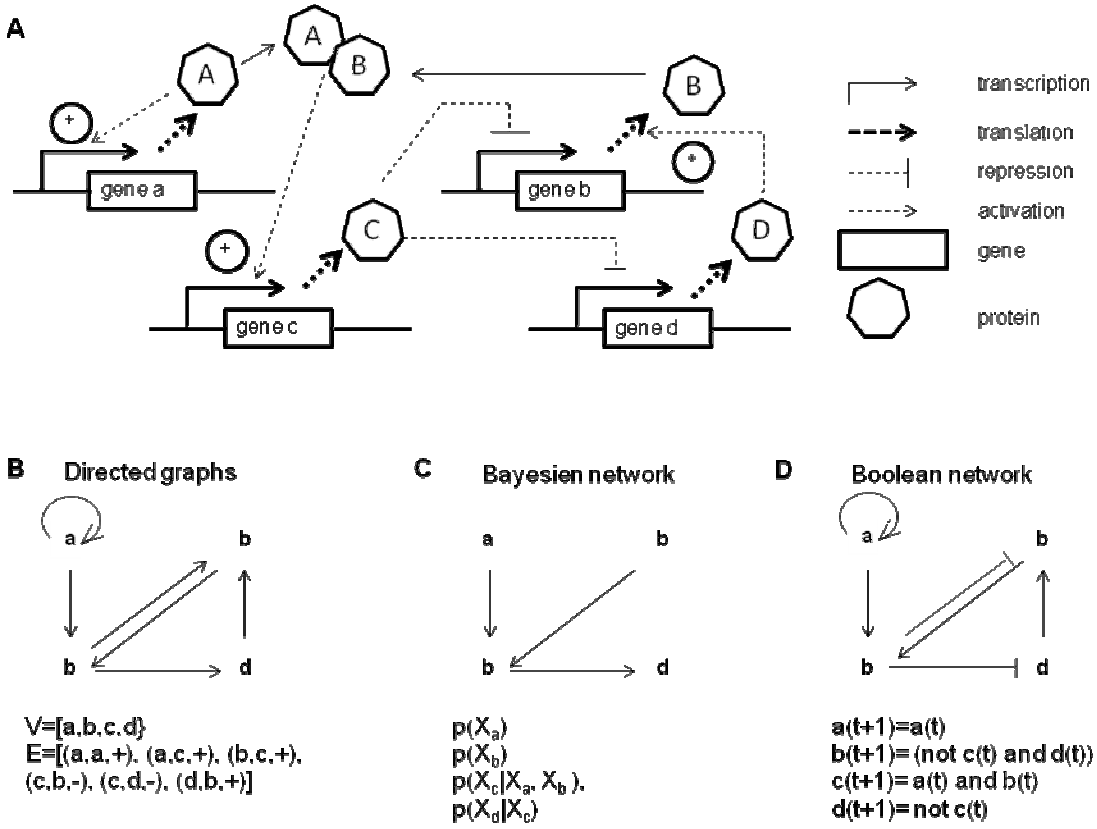

Figure 1.14 Gene regulatory network representations

(A) Dependencies of translation of genes a-d and their transcriptions in relation to proteins A-D. **(B)** Directed graphs indicate all the connectivity. However, they are not suitable for dynamic predictions. **(C)** Bayesian networks are based on representation of a direct acyclic graph and certain interactions are neglected (inhibition of b by c, activation of b by d). **(D)** Boolean networks show all the logic control relations in gene network (adapted from (194)).

1.10.3 Systems biology approach and the kinetic modelling of GR

Many researchers have made contributions towards understanding signalling pathways in organisms from a systematic point of view. Small scale models can direct towards specific problems and focus on drug development and treatment scheduling (201). A classic example for this is the development of Hoffmann's *in-silico* model based on a simple IκB-NFκB signalling pathway (202). This model has inspired many other studies and was later on adapted in Sung's model, where they discovered more knowledge about the drug treatment schedules and an alternative drug target in NFκB signalling (203, 204). In contrast, large scale modelling can address a variety of problems, including predicting system behaviour, gaining understanding towards the molecular mechanism and helping designing experiments and interpreting results

(205). An example for this is Jusko's model focusing on GR regulation (199, 206). Jusko and co-workers used a variety of techniques for modelling corticosteroid genomics in rat liver. These include the construction of schematic diagrams to describe the molecular interactions in response to corticosteroid treatments, possible receptor dynamics, microarray and cluster analyses (199). This work reveals the effect of corticosteroids on a set of functional gene regulations and also generates new hypotheses regarding the understanding of corticosteroid receptor regulated mechanisms (199).

As previously mentioned, the selections of the experimental and bioinformatics approaches are important when studying a particular biological issue or to test the new generated hypotheses from the models. Miller and co-workers have identified a set of genes which may be involved in GC induced apoptosis (207). Diverse techniques were used for analysing GC signalling pathway, including quantitative real-time polymerase chain reaction, microarray, spotfire statistical software and ingenuity pathway analysis software. Various types of cell (leukaemia cells and thymocytes) were used for functional gene identification and significance analysis of genes in inducing GC sensitivity. Several genes (BCL2L11/Bim, DDIT4, DSCR1, TXNIP, NFKBIA, and TSC22D3/DSIPI/GILZ) were found in both human leukaemia cells and thymocytes, which indicate that a fundamental network is involved in GC-dependent apoptosis (207). In addition, signalling networks in GC sensitive CEM cells have shown that genes that are associated with the repression of MYC and the induction of NR3C1 (the GR) may be the determinants of promoting GC apoptosis in leukaemia cells (207).

Taken together, these findings emphasise the importance of modelling different biological processes with diverse approaches. For instance, gene regulatory networks are often analysed by Boolean logic assignment. In comparison, proteins are usually characterised by a static view of putative interactions therefore the yeast two hybrid or chromatin immunoprecipitation techniques are commonly used. In metabolic networks, various techniques are used to determine catalysing enzymes, their metabolic fluxes and intrinsic modes of regulations, one of the many techniques including using carbon-13 isotopic labelling for carbon flux measurements. Currently a major challenge for systems biology is to integrate all these techniques in order to create comprehensive models of biological systems.

1.10.4 Modelling and Parameter Estimation tools

It has become increasingly popular to use SBML-compliant software to model and analyse biological systems. The System Biology Markup Language (SBML) is a free and open XML

based format for describing models in many areas of computational biology. These include cell signalling pathways, metabolic pathways, and gene regulation (194). Many contemporary studies demonstrated the importance of modelling biological systems by integrating scientific knowledge, mathematical theories, computing techniques and experimental data to produce a predictive model. SBML is a format that represents entire computational models and allows them to be exchanged by different software. By supporting SBML as an input and output format, various software tools for kinetic modelling and parameter estimation can be utilised without recoding, which in turns reduces the possibility of errors in translation and assures a common starting point for analyses and simulations (208).

Currently, there are large numbers of tools that support SBML and most of them are stand alone and platform specific. Regarding the kinetic simulation, the number of modelling tools has increased significantly in the field of systems biology. For instance, CellDesigner is a tool for modelling the structure and dynamics of gene regulatory and biochemical networks. It consists of a few important features, which cover construction of network topology, detailed description of reactants, integration with other SBML software and connection with databases (209). The only downside is that it does not include a list of standard kinetic laws and requires manual input of kinetic formulations. Other tools such as COPASI are also widely used for analysing biochemical network. In comparison with CellDesigner, COPASI has the advantage of generating reaction equations automatically, however, it becomes less user-friendly when working with integrative systems (i.e. gene expression network with various GC chemical reaction and GR translocation) (210).

The determination of kinetic parameters is important in building a realistic model. Several SBML-compliant tools have been developed to estimate parameters from experimental data. Some modelling software tools such as COPASI also support parameter estimations, however the process for parameter estimation can be complex (211). SBML-PET is a more straightforward parameter estimation tool that deals with many events such as constraints for parameters, measurement errors and data normalisation. An advantageous key feature of SBML-PET is that it also allows information to be exchanged with other SBML simulation software (212).

1.11 Hypothesis and Aims

Despite intensive research efforts, GC-induced death of white blood cells is still not fully understood. Many patients suffering from leukaemia are either resistant or develop secondary

resistance to dexamethasone treatment. A major question is how GR regulates the transcription of so many genes thereby deciding cellular fate. There is a critical need for building a biologically realistic model that can quantitatively and qualitatively connect GC-related cell death on various scales and compartment levels. A realistic model for GC-induced apoptosis needs to include all the possible interactions and regulations. Unfortunately there are numerous events that may be involved in GC-induced apoptosis and the relevant mechanisms are still unclear. Since the Bcl-2 family is a group of apoptotic genes that is crucial in mediating intrinsic apoptosis and its members were found to be associated with GC sensitivity, this project will be focusing on building models for glucocorticoid controlled Bcl-2 genes in order to study GC resistance.

The purpose of this work is to construct models based on the kinetic descriptions of several important Bcl-2 members (i.e. Bim, Bmf and Bcl-X_L), particularly the potent pro-apoptotic Bcl-2 member Bim and GR, and to be further extended to represent GC sensitivity in ALL. Any findings would be important to understanding GR function, including indentifying novel regulatory mechanisms in GR induced apoptosis, or to help the discovery of alternative drug targets.

In order to build the models, several specific aims are defined as follows:

- Measurement of gene expression and protein levels of GR targets over time.
- Determine kinetic parameters from the experimental data and build ODE models of individual genes.
- Investigate GC sensitivity on a larger scale by analysing timecourse microarray data, enabling us to construct more detailed models.
- Construct an integrated model of GR-induced apoptotic gene expression to extract more information and derive new hypotheses.
- Test the model validity by various experimental approaches which include the use of potential drug inhibitors.

By constructing the models, we hope that more useful information will be extracted which includes:

- Identify the similarity and difference of Bcl-2 gene expression patterns in different cell types in response to GCs.
- A better understanding of GR regulated apoptosis mechanisms.

- Identify unknown genes and signalling pathways determining GC resistance.
- More knowledge on the transcriptional regulation of Bcl-2 family genes.

1.12 References

1. Buckingham JC. Glucocorticoids: Exemplars of multi-tasking. *British Journal of Pharmacology* 2006; **147:** S258-S268.

2. Schoneveld OJ, Gaemers IC, Lamers WH. Mechanisms of glucocorticoid signalling. *Biochimica et Biophysica Acta (BBA) - Gene Structure and Expression* 2004; **1680:** 114-128.

3. Pui C-H, Cheng C, Leung W, Rai SN, Rivera GK, Sandlund JT *et al*. Extended follow-up of long-term survivors of childhood acute lymphoblastic leukemia. *N Engl J Med* 2003; **349:** 640-649.

4. Gómez-Almaguer D, González-Llano O, Jorge M, Jaime-Pérez JC, Galindo C. Dexamethasone in the treatment of meningeal leukemia. *American journal of hematology* 1995; **49:** 353-354.

5. McMaster A, Ray DW. Drug insight: Selective agonists and antagonists of the glucocorticoid receptor. *Nat Clin Pract End Met* 2008; **4:** 91-101.

6. Burris TP, McCabe ERB (eds) *Nuclear receptors and genetic disease*. Academic Press, 2001. pp.409.

7. Tomlinson JW, Walker EA, Bujalska IJ, Draper N, Lavery GG, Cooper MS *et al*. 11beta-hydroxysteroid dehydrogenase type 1: A tissue-specific regulator of glucocorticoid response. *Endocr Rev.* 2004; **25:** 831-866.

8. Duma D, Jewell CM, Cidlowski JA. Multiple glucocorticoid receptor isoforms and mechanisms of post-translational modification. *J Steroid Biochem Mol Biol.* 2006; **102:** 11-21.

9. Palermo M, Quinkler M, Stewart PM. Apparent mineralocorticoid excess syndrome: An overview. *Arq Bras Endocrinol Metab* 2004; **5:** 687-96.

10. Sapolsky RM, Romero LM, Munck AU. How do glucocorticoids influence stress responses? Integrating permissive, suppressive, stimulatory, and preparative actions. *Endocr Rev* 2000; **21:** 55-89.

11. Wessely O, Deiner EM, Beug H, von Lindern M. The glucocorticoid receptor is a key regulator of the decision between self-renewal and differentiation in erythroid progenitors. *EMBO J.* 1997; **16:** 267-280.

12. Liles WC, Dale DC, Klebanoff SJ. Glucocorticoids inhibit apoptosis of human neutrophils. *Blood* 1995; **86:** 3181-3188.

13. Barnes PJ. Anti-inflammatory actions of glucocorticoids : Molecular mechanisms. *Clinical Science (London)* 1998; **94:** 557-572.

14. Felig P, Baxter JD, Broadus AE, Frohman LA (eds) *Endocrinology and metabolism*. McGraw-Hill, Inc, 1987. pp.1855.

15. Hiller-Sturmhöfel S, Andrzej B. The endocrine system: An overview. *Alcohol Health & Research World* 1998; **22:** 153-164.

16. Ten S, New M, Maclaren N. Addison's disease 2001. *J. Clin. Endocrinol. Metab.* 2001; **86:** 2909-2922.

17. Pui C-H, Robison LL, Look AT. Acute lymphoblastic leukaemia. *The Lancet* 2008; **371:** 1030-1043.

18. Mullighan CG, Zhang J, Kasper LH, Lerach S, Payne-Turner D, Phillips LA *et al*. Crebbp mutations in relapsed acute lymphoblastic leukaemia. *Nature* 2011; **471:** 235–239.

19. Basso G, Veltroni M, Valsecchi MG, Dworzak MN, Ratei R, Silvestri D *et al*. Risk of relapse of childhood acute lymphoblastic leukemia is predicted by flow cytometric measurement of residual disease on day 15 bone marrow. *Journal of Clinical Oncology* 2009; **27:** 5168-5174.

20. Pui C-H, Evans WE. Treatment of acute lymphoblastic leukemia. *New England Journal of Medicine* 2006; **354:** 166-178.

21. Mitchell CD, Richards SM, Kinsey SE, Lilleyman J, Vora A, Eden TOB *et al*. Benefit of dexamethasone compared with prednisolone for childhood acute lymphoblastic leukaemia: Results of the UK medical research council ALL97 randomized trial. *British Journal of Haematology* 2005; **129:** 734-745.

22. Bostrom BC, Sensel MR, Sather HN, Gaynon PS, La MK, Johnston K *et al*. Dexamethasone versus prednisone and daily oral versus weekly intravenous mercaptopurine for patients with standard-risk acute lymphoblastic leukemia: A report from the children's cancer group. *Blood* 2003; **101:** 3809-3817.

23. Gambacorti-Passerini CB, Gunby RH, Piazza R, Galietta A, Rostagno R, Scapozza L. Molecular mechanisms of resistance to imatinib in philadelphia-chromosome-positive leukaemias. *The Lancet Oncology* 2003; **4:** 75-85.

24. Mangelsdorf DJ, Thummel C, Beato M, Herrlich P, Schütz G, Umesono K *et al*. The nuclear receptor superfamily: The second decade. *Cell* 1995; **83:** 835-839.

25. Laudet V. Evolution of the nuclear receptor superfamily: Early diversification from an ancestral orphan receptor. *Journal of Molecular Endocrinology* 1997; **19:** 207-226.

26. de Kloet ER, Reul JMHM, Sutanto W. Corticosteroids and the brain. *J Steroid Biochem Mol Biol.* 1990; **37:** 387-394.

27. Breslin MB, Geng C-D, Vedeckis WV. Multiple promoters exist in the human GR gene, one of which is activated by glucocorticoids. *Mol. Endocrinol.* 2001; **15:** 1381-1395.

28. Lu NZ, Cidlowski JA. The origin and functions of multiple human glucocorticoid receptor isoforms. *Ann N Y Acad Sci.* 2004; **1024:** 102-123.

29. Hollenberg SM, Weinberger C, Ong ES, Cerelli G, Oro A, Lebo R *et al*. Primary structure and expression of a functional human glucocorticoid receptor cDNA. *Nature* 1985; **318:** 635-41.

30. McEwan IJ, Wright AP, Dahlman-Wright K, Carlstedt-Duke J, Gustafsson JA. Direct interaction of the Tau 1 transactivation domain of the human glucocorticoid receptor with the basal transcriptional machinery. *Molecular and Cellular Biology* 1993; **13:** 399-407.

31. Hahn S. Structure(?) and function of acidic transcription activators. *Cell* 1993; **72:** 481-483.

32. Ford J, McEwan IJ, Wright APH, Gustafsson J-A. Involvement of the transcription factor iid protein complex in gene activation by the N-terminal transactivation domain of the glucocorticoid receptor in vitro. *Mol. Endocrinol.* 1997; **11:** 1467-1475.

33. Kumar R, Thompson EB. Gene regulation by the glucocorticoid receptor: Structure: Function relationship. *J Steroid Biochem Mol Biol.* 2005; **94:** 383-394.

34. Ismaili N, Garabedian MJ. Modulation of glucocorticoid receptor function via phosphorylation. *Ann N Y Acad Sci.* 2004; **1024:** 86-101.

35. Schaaf MJM, Cidlowski JA. Molecular mechanisms of glucocorticoid action and resistance. *J Steroid Biochem Mol Biol.* 2002; **83:** 37-48.

36. McEwan IJ, Wright AP, Gustafsson JA. Mechanism of gene expression by the glucocorticoid receptor: Role of protein-protein interactions. *Bioessays* 1997; **19:** 153-160.

37. Bledsoe RK, Montana VG, Stanley TB, Delves CJ, Apolito CJ, McKee DD *et al*. Crystal structure of the glucocorticoid receptor ligand binding domain reveals a novel mode of receptor dimerization and coactivator recognition. *Cell* 2002; **110:** 93-105.

38. Brzozowski AM, Pike ACW, Dauter Z, Hubbard RE, Bonn T, Engstrom O *et al*. Molecular basis of agonism and antagonism in the oestrogen receptor. *Nature* 1997; **389:** 753-758.

39. Picard D, Yamamoto KR. Two signals mediate hormone-dependent nuclear localization of the glucocorticoid receptor. *Embo J* 1987; **6:** 3333-3340.

40. Freedman ND, Yamamoto KR. Importin 7 and importin alpha/importin beta are nuclear import receptors for the glucocorticoid receptor. *Mol Biol Cell* 2004; **15:** 2276-2286.

41. Nicolaides NC, Galata Z, Kino T, Chrousos GP, Charmandari E. The human glucocorticoid receptor: Molecular basis of biologic function. *Steroids* 2010; **75:** 1-12.

42. Pratt WB, Toft DO. Regulation of signaling protein function and trafficking by the hsp90/hsp70-based chaperone machinery. *Experimental Biology and Medicine* 2003; **228:** 111-133.

43. Schmidt S, Rainer J, Ploner C, Presul E, Riml S, Kofler R. Glucocorticoid-induced apoptosis and glucocorticoid resistance: Molecular mechanisms and clinical relevance. *Cell Death & Differ* 2004; **11:** S45-S55.

44. Wallace AD, Cidlowski JA. Proteasome-mediated glucocorticoid receptor degradation restricts transcriptional signaling by glucocorticoids. *J. Biol. Chem.* 2001; **276:** 42714-42721.

45. Orphanides G, Reinberg D. A unified theory of gene expression. *Cell* 2002; **108:** 439-451.

46. Orphanides G, Lagrange T, Reinberg D. The general transcription factors of rna polymerase ii. *Genes & Dev.* 1996; **10:** 2657-2683.

47. Thomas MC, Chiang CM. The general transcription machinery and general cofactors. *Crit Rev Biochem Mol Biol.* 2006; **41:** 105-178.

48. Yudt MR, Cidlowski JA. The glucocorticoid receptor: Coding a diversity of proteins and responses through a single gene. *Molecular Endocrinology* 2002; **16:** 1719-1726.

49. Nordeen SK, B.J. S, Kuhnel B, Hutchison CA. Structural determinants of a glucocorticoid receptor recognition element. *Mol. Endocrinol.* 1990; **4:** 1866-1873.

50. So AY-L, Chaivorapol C, Bolton EC, Li H, Yamamoto KR. Determinants of cell- and gene-specific transcriptional regulation by the glucocorticoid receptor. *PLoS Genetics* 2007; **3:** e94.

51. Aumais JP, Lee HS, Degannes C, Horsford J, White JH. Function of directly repeated half-sites as response elements for steroid hormone receptors. *J. Biol. Chem.* 1996; **271:** 12568-12577.

52. Segard-Maurel I, Rajkowski K, Jibard N, Schweizer-Groyer G, Baulieu E-E, Cadepond F. Glucocorticosteroid receptor dimerization investigated by analysis of receptor binding to glucocorticosteroid responsive elements using a monomer−dimer equilibrium model. *Biochemistry* 1996; **35:** 1634-1642.

53. Newton R, Holden NS. Separating transrepression and transactivation: A distressing divorce for the glucocorticoid receptor? *Mol Pharmacol* 2007; **72:** 799-809.

54. Drouin J, SunY L , Chamberland M, Gauthier Y, De Léan A, Nemer M *et al*. Novel glucocorticoid receptor complex with DNA element of the hormone-repressed pomc gene. *EMBO J.* 1993; **12. :** 145–156.

55. Hayashi R, Wada H, Ito K, Adcock IM. Effects of glucocorticoids on gene transcription. *European Journal of Pharmacology* 2004; **500:** 51-62.

56. De Bosscher K, Vanden Berghe W, Haegeman G. The interplay between the glucocorticoid receptor and nuclear factor-kappaB or activator protein-1: Molecular mechanisms for gene repression. *Endocr Rev.* 2003; **24:** 488-522.

57. Ito K, Jazrawi E, Cosio B, Barnes PJ, Adcock IM. P65-activated histone acetyltransferase activity is repressed by glucocorticoids. Mifepristone fails to recruit HDAC2 to the p65-HAT complex. *J. Biol. Chem.* 2001; **276:** 30208-30215.

58. Nissen RM, Yamamoto KR. The glucocorticoid receptor inhibits NFkappaB by interfering with serine-2 phosphorylation of the RNA polymerase II carboxy-terminal domain. *Genes & Dev.* 2000; **14:** 2314-2329.

59. Kamei Y, Xu L, Heinzel T, Torchia J, Kurokawa R, Gloss B *et al*. A CBP integrator complex mediates transcriptional activation and AP-1 inhibition by nuclear receptors. *Cell* 1996; **85:** 403-414.

60. Wang Z, Frederick J, Garabedian MJ. Deciphering the phosphorylation "Code" Of the glucocorticoid receptor in vivo. *J. Biol. Chem.* 2002; **277:** 26573-26580.

61. Davies L, Karthikeyan N, Lynch JT, Sial E-A, Gkourtsa A, Demonacos C *et al*. Cross talk of signaling pathways in the regulation of the glucocorticoid receptor function. *Mol. Endocrinol.* 2008; **22:** 1331-1344.

62. Lynch J, Rajendran R, Xenaki G, Berrou I, Demonacos C, Krstic-Demonacos M. The role of glucocorticoid receptor phosphorylation in Mcl-1 and Noxa gene expression. *Molecular Cancer* 2010; **9:** 38.

63. Weigel NL. Steroid hormone receptors and their regulation by phosphorylation. *BiochemJ* 1996; **319:** 657-667.

64. Kinyamu HK, Chen J, Archer TK. Linking the ubiquitin-proteasome pathway to chromatin remodeling/modification by nuclear receptors. *Mol. Endocrinol.* 2005; **34:** 281-297.

65. Le Drean Y, Mincheneau N, Le Goff P, Michel D. Potentiation of glucocorticoid receptor transcriptional activity by sumoylation. *Endocrinology* 2002; **143:** 3482-3489.

66. Nawata H, Okabe T, Yanase T, Nomura M. Mechanism of action and resistance to glucocorticoid and selective glucocorticoid receptor modulator to overcome glucocorticoid-related adverse effects. *Clin Exp Allergy Rev* 2008; **8:** 53-56.

67. Perissi V, Rosenfeld MG. Controlling nuclear receptors: The circular logic of cofactor cycles. *Nat Rev Mol Cell Biol* 2005; **6:** 542-554.

68. McKenna NJ, Lanz RB, O'Malley BW. Nuclear receptor coregulators: Cellular and molecular biology. *Endocr Rev.* 1999; **20:** 321-344.

69. Roth SY, Denu JM, Allis CD. Histone acetyltransferases. *Ann Rev Biochem* 2001; **70:** 81-120.

70. Lee JW, Lee YC, Na SY, Jung DJ, Lee SK. Transcriptional coregulators of the nuclear receptor superfamily: Coactivators and corepressors. *Cell. Mol. Life Sci.* 2001; **58:** 289-297.

71. Hong H, Kohli K, Garabedian MJ, Stallcup MR. Grip1, a transcriptional coactivator for the AF-2 transactivation domain of steroid, thyroid, retinoid, and vitamin d receptors. *Mol. Cell. Biol.* 1997; **17:** 2735-2744.

72. Torchia J, Rose DW, Inostroza J, Kamei Y, Westin S, Glass CK *et al*. The transcriptional co-activator P/CIP binds CBP and mediates nuclear-receptor function. *Nature* 1997; **387:** 677-684.

73. Jenkins BD, Pullen CB, Darimont BD. Novel glucocorticoid receptor coactivator effector mechanisms. *Trends in Endocrinology and Metabolism* 2001; **12:** 122-126.

74. Sousa AR, Lane SJ, Cidlowski JA, Staynov DZ, Lee TH. Glucocorticoid resistance in asthma is associated with elevated in vivo expression of the glucocorticoid receptor beta-isoform. *J. Allergy and Clinical Immunology* 2000; **105:** 943-950.

75. Rogatsky I, Luecke HF, Leitman DC, Yamamoto KR. Alternate surfaces of transcriptional coregulator Grip1 function in different glucocorticoid receptor activation and repression contexts. *PNAS* 2002; **99:** 16701-16706.

76. Kraus WL, Kadonaga JT. P300 and estrogen receptor cooperatively activate transcription via differential enhancement of initiation and reinitiation. *Genes & Dev.* 1998; **12:** 331-342.

77. Glass CK, Rosenfeld MG. The coregulator exchange in transcriptional functions of nuclear receptors. *Genes & Dev.* 2000; **14:** 121-141.

78. Fonte C, Grenier J, Trousson A, Chauchereau A, Lahuna O, Baulieu E-E *et al*. Involvement of beta-catenin and unusual behavior of CBP and p300 in glucocorticosteroid signaling in schwann cells. *PNAS* 2005; **102:** 14260-14265.

79. Ogryzko VV, Kotani T, Zhang X, Schiltz RL, Howard T, Yang X-J *et al*. Histone-like TAFs within the PCAF histone acetylase complex. *Cell* 1998; **94:** 35-44.

80. Lanz RB, McKenna NJ, Onate SA, Albrecht U, Wong J, Tsai SY *et al*. A steroid receptor coactivator, SRA, functions as an RNA and is present in an SRC-1 complex. *Cell* 1999; **97:** 17-27.

81. Kraus WL, Wong J. Nuclear receptor-dependent transcription with chromatin: Is it all about enzymes?. *FEBS journal* 2002; **269:** 2275-2283.

82. Yoshinaga SK, Peterson CL, Herskowitz I, Yamamoto KR. Roles of SWI1, SWI 2, and SWI 3 proteins for transcriptional enhancement by steroid receptors. *Science* 1992; **258:** 1598-1604.

83. Muchardt C, Yaniv M. A human homologue of saccharomyces cerevisiae SNF2/SWI2 and drosophila brm genes potentiates transcriptional activation by the glucocorticoid receptor. *EMBO J.* 1999; **12:** 4279-4290.

84. Hittelman A, Burakov D, Iñiguez-Lluhí J, Freedman L, Garabedian M. Differential regulation of glucocorticoid receptor transcriptional activation via AF-1-associated proteins. *EMBO J.* 1999; **18:** 5380-5388.

85. Sun X, Zhang Y, Cho H, Rickert P, Lees E, Lane W *et al*. NAT, a human complex containing SRB polypeptides that functions as a negative regulator of activated transcription. *Molecular Cell* 1998; **2:** 213-222.

86. Heinzel T, Lavinsky RM, Mullen T-M, Soderstrom M, Laherty CD, Torchia J *et al*. A complex containing N-CoR, mSIN3 and histone deacetylase mediates transcriptional repression. *Nature* 1997; **387:** 43-48.

87. Nagy L, Kao H-Y, Chakravarti D, Lin RJ, Hassig CA, Ayer DE *et al*. Nuclear receptor repression mediated by a complex containing SMRT, mSIN3A, and histone deacetylase. *Cell* 1997; **89:** 373-380.

88. Huang EY, Zhang J, Miska EA, Guenther MG, Kouzarides T, Lazar MA. Nuclear receptor corepressors partner with class ii histone deacetylases in a SIN3-independent repression pathway. *Genes & Dev.* 2000; **14:** 45-54.

89. Jones PL, Sachs LM, Rouse N, Wade PA, Shi Y-B. Multiple N-CoR complexes contain distinct histone deacetylases. *J. Biol. Chem.* 2001; **276:** 8807-8811.

90. Urnov FD, Yee J, Sachs L, Collingwood TN, Bauer A, Beug H *et al*. Targeting of N-CoR and histone deacetylase 3 by the oncoprotein v-ErbA yields a chromatin infrastructure-dependent transcriptional repression pathway. *EMBO J.* 2000; **19:** 4074-4090.

91. Chen JD, Evans RM. A transcriptional co-repressor that interacts with nuclear hormone receptors. *Nature* 1995; **377:** 454-457.

92. Perissi V, Staszewski LM, McInerney EM, Kurokawa R, Krones A, Rose DW *et al*. Molecular determinants of nuclear receptor-corepressor interaction. *Genes & Dev.* 1999; **13:** 3198-3208.

93. Hu X, Lazar MA. The CoRNR motif controls the recruitment of corepressors by nuclear hormone receptors. *Nature* 1999; **402:** 93-96.

94. DeRijk RH, Schaaf M, de Kloet ER. Glucocorticoid receptor variants: Clinical implications. *The Journal of Steroid Biochemistry and Molecular Biology* 2002; **81:** 103-122.

95. Schlossmacher G, Stevens A, White A. Glucocorticoid receptor-mediated apoptosis: Mechanisms of resistance in cancer cells. *Journal of Endocrinology* 2011; **211:** 17-25.

96. Wang Z, Malone MH, He H, McColl KS, Distelhorst CW. Microarray analysis uncovers the induction of the proapoptotic BH3-only protein bim in multiple models of glucocorticoid-induced apoptosis. *J. Biol. Chem.* 2003; **278:** 23861 - 23867.

97. Ploner C, Rainer J, Niederegger H, Eduardoff M, Villunger A, Geley S *et al*. The Bcl2 rheostat in glucocorticoid-induced apoptosis of acute lymphoblastic leukemia. *Leukemia* 2007; **22:** 370-377.

98. Ashkenazi A. Targeting death and decoy receptors of the tumour-necrosis factor superfamily. *Nat Rev Cancer* 2002; **2:** 420-430.

99. Herold M, McPherson K, Reichardt H. Glucocorticoids in T cell apoptosis and function. *Cellular and Molecular Life Sciences* 2006; **63:** 60-72.

100. Adrain C, Martin S. Cell biology: Double knockout blow for caspases. *Science* 2006; **311:** 785-786.

101. Dejean LM, Martinez-Caballero S, Manon S, Kinnally KW. Regulation of the mitochondrial apoptosis-induced channel, MAC, by Bcl-2 family proteins. *Biochimica et Biophysica Acta (BBA) - Molecular Basis of Disease* 2006; **1762:** 191-201.

102. Tilly JL. Commuting the death sentence: How oocytes strive to survive. *Nat Rev Mol Cell Biol* 2001; **2:** 838-848.

103. Greenstein S, Ghias K, Krett NL, Rosen ST. Mechanisms of glucocorticoid-mediated apoptosis in hematological malignancies. *Clinical Cancer Research* 2002; **8:** 1681-1694.

104. Chen-Levy Z, Nourse J, Cleary ML. The Bcl-2 candidate proto-oncogene product is a 24-kilodalton integral-membrane protein highly expressed in lymphoid cell lines and lymphomas carrying the t(14;18) translocation. *Mol. Cell. Biol.* 1989; **9:** 701-710.

105. Nguyen M, Millar DG, Yong VW, Korsmeyer SJ, Shore GC. Targeting of Bcl-2 to the mitochondrial outer membrane by a COOH- terminal signal anchor sequence. *J. Biol. Chem* 1993; **268:** 25265-25268.

106. Adams JM, Cory S. The Bcl-2 protein family: Arbiters of cell survival. *Science* 1998; **281:** 1322-1326.

107. Burlacu A. Regulation of apoptosis by Bcl-2 family proteins. *J Cell Mol Med.* 2003; **7:** 249-257.

108. Chan SL, Yu VC. Proteins of the Bcl-2 family in apoptosis signalling: From mechanistic insights to therapeutic opportunities. *Clin Exp Pharmacol Physiol.* 2004; **31:** 119-128.

109. Huang DC, M AJ, S C. The conserved N-terminal BH4 domain of Bcl-2 homologues is essential for inhibition of apoptosis and interaction with ced-4. *EMBO J.* 1998; **17:** 1029-1039.

110. Pan G, O'Rourke K, Dixit VM. Caspase-9, Bcl-X_L, and Apaf-1 form a ternary complex. *J. Biol. Chem.* 1998; **273:** 5841-5845.

111. Marsden VS, O'Connor L, O'Reilly LA, Silke J, Metcalf D, Ekert PG *et al*. Apoptosis initiated by Bcl-2-regulated caspase activation independently of the cytochrome c/Apaf-1/caspase-9 apoptosome. *Nature* 2002; **419:** 634-637.

112. Chauhan D, Rosen S, Reed JC, Kharbanda S, Anderson KC. Apaf-1/cytochrome-c independent and SMAC-dependent induction of apotosis in multiple myeloma (mm) cells. *J. Biol. Chem* 2001**:** C100074200.

113. Oltval ZN, Milliman CL, Korsmeyer SJ. Bcl-2 heterodimerizes in vivo with a conserved homolog, Bax, that accelerates programed cell death. *Cell* 1993; **74:** 609-619.

114. Sato T, Hanada M, Bodrug S, Irie S, Iwama N, Boise LH *et al*. Interactions among members of the Bcl-2 protein family analyzed with a yeast two-hybrid system. *PNAS* 1994; **91:** 9238–9242.

115. Klumpp S, Krieglstein J. Serine/threonine protein phosphatases in apoptosis. *Curr Opin Pharmacol.* 2002; **2:** 458-462.

116. Bouillet P, Metcalf D, Huang DC, Tarlinton DM, Kay TW, Kontgen F *et al*. Proapoptotic Bcl-2 relative Bim required for certain apoptotic responses, leukocyte homeostasis, and to preclude autoimmunity. *Science* 1999; **286:** 1735 - 1738.

117. Cory S, Adams JM. The bcl2 family: Regulators of the cellular life-or-death switch. *Nat Rev Cancer* 2002; **2:** 647-656.

118. Puthalakath H, Villunger A, O'Reilly LA, Beaumont JG, Coultas L, Cheney RE *et al*. Bmf: A proapoptotic BH3-only protein regulated by interaction with the myosin V actin motor complex, activated by anoikis. *Science* 2001; **293:** 1829 - 1832.

119. Cheng EHY, Kirsch DG, Clem RJ, Ravi R, Kastan MB, Bedi A *et al*. Conversion of Bcl-2 to a Bax-like death effector by caspases. *Science* 1997; **278:** 1966-1968.

120. Clem RJ, Cheng EHY, Karp CL, Kirsch DG, Ueno K, Takahashi A *et al*. Modulation of cell death by Bcl-X_L through caspase interaction. *PNAS* 1998; **95:** 554-559.

121. Inohara N, Ding L, Chen S, Núñez G. Harakiri, a novel regulator of cell death, encodes a protein that activates apoptosis and interacts selectively with survival-promoting proteins Bcl-2 and Bcl-x(l). *EMBO J.* 1997; **16:** 1686-1694.

122. Miyashita T, Reed JC. Tumor suppressor p53 is a direct transcriptional activator of the human Bax gene. *Cell* 1995; **80:** 293-299.

123. Nakano K, Vousden KH. Puma, a novel proapoptotic gene, is induced by p53. *Molecular Cell* 2001; **7:** 683-694.

124. Oda E, Ohki R, Murasawa H, Nemoto J, Shibue T, Yamashita T *et al*. Noxa, a BH3-only member of the Bcl-2 family and candidate mediator of p53-induced apoptosis. *Science* 2000; **288:** 1053-1058.

125. Thompson EB, Johnson BH. Regulation of a distinctive set of genes in glucocorticoid-evoked apoptosis in CEM human lymphoid cells. *Recent Progress in Hormone Research* 2003; **58:** 175 - 197.

126. Harmon JM, Norman MR, Fowlkes BJ, Thompson EB. Dexamethasone induces irreversible G1 arrest and death of a human lymphoid cell line. *J Cell Physio*l 1979; 98: 267−278

127. Thompson EB. Stepping stones in the path of glucocorticoid-driven apoptosis of lymphoid cells. *Acta Biochim Biophys Sin.* 2008; **40:** 595-600.

128. Almawi WY, Melemedjian OK, Jaoude MMA. On the link between Bcl-2 family proteins and glucocorticoid-induced apoptosis. *J. Leukocyte Biology* 2004; **76:** 7-14.

129. Casale F, Addeo R, D'Angelo V, Indolfi P, Poggi V, Morgera C *et al*. Determination of the in vivo effects of prednisone on Bcl-2 family protein expression in childhood acute lymphoblastic leukemia. *Int. J Oncol.* 2003 **22:** 123-128.

130. Gascoyne DM, Kypta RM, Vivanco MdM. Glucocorticoids inhibit apoptosis during fibrosarcoma development by transcriptionally activating Bcl-xl* *J. Biol. Chem* 2003; **278:** 18022-18029,.

131. Yang E, Korsmeyer SJ. Molecular thenatopsis: A discourse on the Bcl2 family and cell death. *Blood* 1996; **88:** 386-401.

132. Xerri L, Parc P, Brousset P, Schlaifer D, Hassoun J, Reed JC *et al*. Predominant expression of the long isoform of Bcl-x (Bcl-xl) in human lymphomas. *Br J Haematol.* 1996; **92:** 900-906.

133. González-García M, Pérez-Ballestero R, Ding L, Duan L, Boise L, Thompson C *et al*. Bcl-xl is the major Bcl-x mRNA form expressed during murine development and its product localizes to mitochondria *Development* 1994; **120:** 3033-3042.

134. Zhan Q, Alamo I, Yu K, Boise L, Cherney B, Tosato G *et al*. The apoptosis-associated gamma-ray response of Bcl-x(l) depends on normal p53 function. *Oncogene* 1996; **13:** 2287-2293.

135. Tu Y, Steven R, Feng-hao X, Fleishman A, Jeremy T, Jeffrey W *et al*. Bcl-x expression in multiple myeloma: Possible indicator of chemoresistance. *Cancer Res.* 1998 **58:** 256-262.

136. Grillot DA, Gonzalez-Garcia M, Ekhterae D, Duan L, Inohara N, Ohta S *et al*. Genomic organization, promoter region analysis, and chromosome localization of the mouse Bcl-x gene. *J Immunol* 1997; **158:** 4750-4757.

137. Grad J, Zeng X, Boise L. Regulation of Bcl-xl: A little bit of this and a little bit of STAT. *Curr Opin Oncol.* 2000; **12:** 543-549.

138. Rocha-Viegas L, Vicent GP, Barañao JL, Beato M, Pecci A. Steroid hormones induce Bcl-x gene expression through direct activation of distal promoter P4 *J. Biol. Chem* 2004; **279:** 9831-9839.

139. Rocha-Viegas L, Vicent GP, Barañao JL, Beato M, Pecci A. Glucocorticoids repress Bcl-x expression in lymphoid cells by recruiting STAT5b to the P4 promoter *J. Biol. Chem.* 2006; **281:** 33959-33970.

140. Strasser A. The role of BH3-only proteins in the immune system. *Nat Rev Immunol* 2005; **5:** 189-200.

141. Putcha GV, Moulder KL, Golden JP, Bouillet P, Adams JA, Strasser A *et al*. Induction of bim, a proapoptotic BH3-only Bcl-2 family member, is critical for neuronal apoptosis. *Neuron* 2001; **29:** 615-628.

142. Dijkers PF, Medema RH, Lammers J-WJ, Koenderman L, Coffer PJ. Expression of the pro-apoptotic Bcl-2 family member Bim is regulated by the forkhead transcription factor FKHR-l1. *Current Biology* 2000; **10:** 1201-1204.

143. Whitfield J, Neame SJ, Paquet L, Bernard O, Ham J. Dominant-negative c-Jun promotes neuronal survival by reducing Bim expression and inhibiting mitochondrial cytochrome c release. *Neuron* 2001; **29:** 629-643.

144. Shinjyo T, Kuribara R, Inukai T, Hosoi H, Kinoshita T, Miyajima A *et al*. Downregulation of bim, a proapoptotic relative of Bcl-2, is a pivotal step in cytokine-initiated survival signaling in murine hematopoietic progenitors. *Mol. Cell. Biol.* 2001; **21:** 854-864

145. Medh RD, Webb MS, Miller AL, Johnson BH, Fofanov Y, Li T *et al*. Gene expression profile of human lymphoid CEM cells sensitive and resistant to glucocorticoid-evoked apoptosis. *Genomics.* 2003; **81:** 543 - 555.

146. Abrams MT, Robertson NM, Yoon K, Wickstrom E. Inhibition of glucocorticoid-induced apoptosis by targeting the major splice variants of Bim mRNA with small interfering RNA and short hairpin RNA. *J. Biol. Chem* 2004; **279:** 55809 - 55817.

147. Zhang L, Insel PA. The pro-apoptotic protein bim is a convergence point for Camp/protein kinase A- and glucocorticoid-promoted apoptosis of lymphoid cells. *J. Biol. Chem* 2004; **279:** 20858 - 20865.

148. Schmelzle T, Mailleux AA, Overholtzer M, Carroll JS, Solimini NL, Lightcap ES *et al*. Functional role and oncogene-regulated expression of the BH3-only factor Bmf in mammary epithelial anoikis and morphogenesis. *PNAS* 2007; **104:** 3787-3792.

149. Morales AA, Olsson A, Celsing F, Osterborg A, Jondal M, Osorio LM. Expression and transcriptional regulation of functionally distinct Bmf isoforms in B-chronic lymphocytic leukemia cells. *Leukemia* 2004; **18:** 41-47.

150. Zhang Y, Adachi M, Kawamura R, Imai K. Bmf is a possible mediator in histone deacetylase inhibitors FK228 and CBHA-induced apoptosis. *Cell Death & Differ* 2005; **13:** 129-140.

151. Decesare D, Vallone D, Caracciolo A, Sassonecorsi P, Nerlov C, Verde P. Heterodimerization of c-Jun with Atf-2 and c-Fos is required for positive and negative regulation of the human urokinase enhancer. *Oncogene* 1995; **11:** 365-376.

152. Jonat C, Rahmsdorf HJ, Park K-K, Cato ACB, Gebel S, Ponta H *et al*. Antitumor promotion and antiinflammation: Down-modulation of AP-1 (fos/jun) activity by glucocorticoid hormone. *Cell* 1990; **62:** 1189-1204.

153. Diamond MI, Miner JN, S.K. Y, Yamamoto KR. Transcription factor interactions: Selectors of positive or negative regulation from a single DNA element. *Science* 1990; **249:** 1266-1272.

154. Pearce D, Matsui W, Miner JN, Yamamoto KR. Glucocorticoid receptor transcriptional activity determined by spacing of receptor and nonreceptor DNA sites. *Journal of Biological Chemistry* 1998; **273:** 30081-30085.

155. Maki Y, Bos TJ, Davis C, Starbuck M, Vogt PK. Avian sarcoma virus 17 carries the Jun oncogene. *Proc Natl Acad Sci U S A.* 1987; **84:** 2848–2852.

156. Hilberg F, Aguzzi A, Howells N, Wagner EF. c-Jun is essential for normal mouse development and hepatogenesis. *Nature* 1993; **365:** 179-181.

157. Vogt PK. Jun, the oncoprotein. *Oncogene* 2001; **20:** 2365-2377.

158. Ham J, Eilers A, Whitfield J, Neame SJ, Shah B. c-Jun and the transcriptional control of neuronal apoptosis. *Biochemical Pharmacology* 2000; **60:** 1015-1021.

159. Chida K, Nagamori S, Kuroki T. Nuclear translocation of Fos is stimulated by interaction with jun through the leucine zipper. *Cellular and Molecular Life Sciences* 1999; **55:** 297-302.

160. Smeal T, Angel P, Meek J, Karin M. Different requirements for formation of Jun: Jun and Jun: Fos complexes. *Genes & Development* 1989; **3:** 2091-2100.

161. Shaulian E, Karin M. AP-1 as a regulator of cell life and death. *Nat Cell Biol* 2002; **4:** E131-E136.

162. Angel P, Hattori K, Smeal T, Karin M. The jun proto-oncogene is positively autoregulated by its product, Jun/AP-1. *Cell* 1988; **55:** 875-885.

163. Boyle WJ, Smeal T, Defize LHK, Angel P, Woodgett JR, Karin M *et al*. Activation of protein kinase c decreases phosphorylation of c-jun at sites that negatively regulate its DNA-binding activity. *Cell* 1991; **64:** 573-584.

164. Wadgaonkar R, Pierce JW, Somnay K, Damico RL, Crow MT, Collins T *et al*. Regulation of c-Jun N-terminal kinase and p38 kinase pathways in endothelial cells. *American Journal of Respiratory Cell and Molecular Biology* 2004; **31:** 423-431.

165. Chiu R, Angel P, Karin M. Jun-B differs in its biological properties from, and is a negative regulator of, c-Jun. *Cell* 1989; **59:** 979-986.

166. Weitzman JB, Fiette L, Matsuo K, Yaniv M. JunD protects cells from p53-dependent senescence and apoptosis. *Molecular Cell* 2000; **6:** 1109-1119.

167. Barker PE, Rabin M, Watson M, Breg WR, Ruddle FH, Verma IM. Human c-Fos oncogene mapped within chromosomal region 14q21---q31. *Proceedings of the National Academy of Sciences of the United States of America* 1984; **81:** 5826-5830.

168. Wyke AW, Lang A, Frame MC. Uncoupling of the pathways which link MAP kinase to c-Fos transcription and AP-1 in response to growth stimuli. *Cellular Signalling* 1996; **8:** 131-139.

169. Tanos T, Marinissen MJ, Leskow FC, Hochbaum D, Martinetto H, Gutkind JS *et al*. Phosphorylation of c-Fos by members of the p38 mapk family. *Journal of Biological Chemistry* 2005; **280:** 18842-18852.

170. Zerial M, Toschi L, Ryseck RP, Schuermann M, Müller R, Bravo R. The product of a novel growth factor activated gene, Fos B, interacts with jun proteins enhancing their DNA binding activity. *EMBO J.* 1989; **8:** 805-813.

171. Kovary K, Bravo R. Existence of different fos/jun complexes during the G0-to-G1 transition and during exponential growth in mouse fibroblasts: Differential role of Fos proteins. *Mol Cell Biol.* 1992; **12:** 5015-5023.

172. Hess J, Angel P, Schorpp-Kistner M. AP-1 subunits: Quarrel and harmony among siblings. *Journal of Cell Science* 2004; **117:** 5965-5973.

173. Rogatsky I, Zarember KA, Yamamoto KR. Factor recruitment and Tif2/Grip1 corepressor activity at a collagenase-3 response element that mediates regulation by phorbol esters and hormones. *EMBO J* 2001; **20:** 6071-6083.

174. Caelles C, González-Sancho JM, Muñoz A. Nuclear hormone receptor antagonism with AP-1 by inhibition of the JNK pathway. *Genes & Development* 1997; **11:** 3351-3364.

175. Karin M, Chang L. AP-1--glucocorticoid receptor crosstalk taken to a higher level. *Journal of Endocrinology* 2001; **169:** 447-451.

176. González MV, Jiménez B, Berciano MT, González-Sancho JM, Caelles C, Lafarga M *et al*. Glucocorticoids antagonize AP-1 by inhibiting the activation/phosphorylation of JNK without affecting its subcellular distribution. *The Journal of Cell Biology* 2000; **150:** 1199-1208.

177. Biddie Simon C, John S, Sabo Pete J, Thurman Robert E, Johnson Thomas A, Schiltz RL *et al*. Transcription factor AP1 potentiates chromatin accessibility and glucocorticoid receptor binding. *Molecular Cell* 2011; **43:** 145-155.

178. Hollenhorst PC, McIntosh LP, Graves BJ. Genomic and biochemical insights into the specificity of Ets transcription factors. *Annual Review of Biochemistry* 2011; **80:** 437-471.

179. Hsu T, Trojanowska M, Watson DK. Ets proteins in biological control and cancer. *J Cell Biochem.* 2004; **91:** 896-903.

180. Giovannini M, Biegel JA, Serra M, Wang JY, Wei YH, Nycum L *et al*. Ews-Erg and Ews-Fli1 fusion transcripts in Ewing's sarcoma and primitive neuroectodermal tumors with variant translocations. *J Clin Invest.* 1994; **94:** 489-496.

181. Hollenhorst PC, Ferris MW, Hull MA, Chae H, Kim S, Graves BJ. Oncogenic Ets proteins mimic activated Ras/MAPK signaling in prostate cells. *Genes & Development* 2011; **25:** 2147-2157.

182. Thoms JAI, Birger Y, Foster S, Knezevic K, Kirschenbaum Y, Chandrakanthan V *et al*. Erg promotes T-acute lymphoblastic leukemia and is transcriptionally regulated in leukemic cells by a stem cell enhancer. *Blood* 2011; **117:** 7079-7089.

183. Tsuzuki S, Taguchi O, Seto M. Promotion and maintenance of leukemia by Erg. *Blood* 2011; **117:** 3858-3868.

184. Geng C-D, Vedeckis WV. c-Myb and members of the c-Ets family of transcription factors act as molecular switches to mediate opposite steroid regulation of the human glucocorticoid receptor 1A promoter. *J. Biol. Chem.* 2005; **280:** 43264-43271.

185. Kitano H. Systems biology: A brief overview. *Science* 2002; **295:** 1662-1664.

186. Mullis K, Faloona F, Scharf S, Saiki R, Horn G, Erlich H. Specific enzymatic amplification of DNA in vitro: The polymerase chain reaction. *Cold Spring Harb. Symp. Quant. Biol.* 1986; **51:** 263-273.

187. Venter JC, Adams MD, Myers EW, Li PW, Mural RJ, Sutton GG *et al*. The sequence of the human genome. *Science* 2001; **291:** 1304-1351.

188. Quackenbush J. Computational analysis of microarray data. *Nat Rev Genet* 2001; **2:** 418-427.

189. Murphy D. Gene expression studies using microarrays: Principles, problems, and prospects. *Advances in Physiology Education* 2002; **26:** 256-270.

190. Ernst J, Nau GJ, Bar-Joseph Z. Clustering short time series gene expression data. *Bioinformatics* 2005; **21:** i159-i168.

191. Ernst J, Bar-Joseph Z. STEM: A tool for the analysis of short time series gene expression data. *BMC Bioinformatics* 2006; **7:** 191.

192. Donn R, Berry A, Stevens A, Farrow S, Betts J, Stevens R *et al*. Use of gene expression profiling to identify a novel glucocorticoid sensitivity determining gene, BMPRII. *The FASEB Journal* 2007; **21:** 402-414.

193. van Delft FW, Bellotti T, Luo Z, Jones LK, Patel N, Yiannikouris O *et al*. Prospective gene expression analysis accurately subtypes acute leukaemia in children and establishes a commonality between hyperdiploidy and t(12;21) in acute lymphoblastic leukaemia. *British Journal of Haematology* 2005; **130:** 26-35.

194. Klipp E, Herwig R, Kowald A, Wierling C, Lehrach H *Systems biology in practice. Concepts, implementation, and application*, 1st edn. WILEY-VCH Verlag GmbH & Co. KGaA: Berlin, 2005. pp.

195. Kitano H. International alliances for quantitative modeling in systems biology. *Mol Syst Biol.* 2005; **1:** 1-2.

196. Styczynski MP, Stephanopoulos G. Overview of computational methods for the inference of gene regulatory networks. *Computers & Chemical Engineering* 2005; **29:** 519-534.

197. Hasty J, McMillen D, Isaacs F, Collins JJ. Computational studies of gene regulatory networks: In numero molecular biology. *Nat Rev Genet* 2001; **2:** 268-279.

198. Babu SCV, Song EJ, Yoo YS. Modeling and simulation in signal transduction pathways: A systems biology approach. *Biochimie* 2006; **88:** 277-283.

199. Jin JY, Almon RR, DuBois DC, Jusko WJ. Modeling of corticosteroid pharmacogenomics in rat liver using gene microarrays. *J Pharmacol Exp Ther* 2003; **307:** 93-109.

200. Friedman N, Linial M, Nachman I, Pe'er D. Using bayesian networks to analyze expression data. *J Comput Biol.* 2000; **7:** 601-620.

201. Rajasethupathy P, Vayttaden SJ, Bhalla US. Systems modeling: A pathway to drug discovery. *Current Opinion in Chemical Biology* 2005; **9:** 400-406.

202. Hoffmann A, Levchenko A, Scott ML, Baltimore D. The Ikappa B-NF-kappa B signaling module: Temporal control and selective gene activation. *Science* 2002; **298:** 1241-1245.

203. Sung M-H, Simon R. In silico simulation of inhibitor drug effects on nuclear factor-kappaB pathway dynamics. *Mol Pharmacol* 2004; **66:** 70-75.

204. Sung M-H, Bagain L, Chen Z, Karpova T, Yang X, Silvin C *et al*. Dynamic effect of bortezomib on nuclear factor-kappaB activity and gene expression in tumor cells. *Mol Pharmacol* 2008; **74:** 1215-1222.

205. Musante CJ, Lewis AK, Hall K. Small- and large-scale biosimulation applied to drug discovery and development. *Drug Discovery Today* 2002; **7:** s192-s196.

206. Yao Z, Hoffman EP, Ghimbovschi S, DuBois DC, Almon RR, Jusko WJ. Mathematical modeling of corticosteroid pharmacogenomics in rat muscle following acute and chronic methylprednisolone dosing. *Molecular Pharmaceutics* 2008; **5:** 328-339.

207. Miller A, Komak S, Webb MS, Leiter E, Thompson EB. Gene expression profiling of leukemic cells and primary thymocytes predicts a signature for apoptotic sensitivity to glucocorticoids. *Cancer Cell Int.* 2007; **7:** 18.

208. Hucka M, Finney A, Bornstein BJ, Keating SM, Shapiro BE, Matthews J *et al*. Evolving a lingua franca and associated software infrastructure for computational systems biology: The systems biology markup language (SBML) project *Syst Biol.* 2004; **1:** 41-53.

209. Funahashi AM, Y.; Jouraku, A.; Morohashi, M.; Kikuchi, N.; Kitano, H. CellDesigner 3.5: A versatile modeling tool for biochemical networks. *Proceedings of the IEEE* 2008; **96:** 1254-1265.

210. Hoops S, Sahle S, Gauges R, Lee C, Pahle J, Simus N *et al*. COPASI— a complex pathway simulator. *Bioinformatics* 2006; **22:** 3067-3074.

211. Dada J, Mendes P, Paton N, Missier P, Hedeler C (2009). Design and architecture of web services for simulation of biochemical systems. *Lecture notes in computer science*. Springer Berlin / Heidelberg. pp 182-195.

212. Zi Z, Klipp E. SBML-PET: A systems biology markup language-based parameter estimation tool. *Epub* 2006; **22:** 2704-2705.

2 CHAPTER 2: Quantitative analysis of glucocorticoid controlled genes

In Chapter 2, we describe how we study GR regulation on several key Bcl-2 members by building kinetic models based on ordinary differential equations. This chapter also appeared in "Chen DW-C, Lynch JT, Demonacos C, Krstic-Demonacos M, Schwartz J-M. (2010) Quantitative analysis and modelling of glucocorticoid controlled gene expression. Pharmacogenomics, **11**:11, 1545-1560" with modifications. All authors contributed extensively to the work presented in this paper; D.W.C. performed the experiments, ran the model, analysed output data and wrote the manuscript; J.T.L. and C.D. designed the experiments; M.K-D. and J-M.S. wrote the paper.

2.1 Abstract

Glucocorticoid hormones are used to induce apoptosis of leukaemia cells through glucocorticoid receptor (GR) signalling. Despite intensive research, the molecular mechanism and the causes of patients developing resistance are not fully understood. It is thought that the Bcl-2 family, which is a group of GR target genes that are responsible for mediating apoptosis, may play an important role in deciding cell fate. Pathway modelling is emerging as a valuable tool in understanding and treating diseases. We measured detailed kinetic pattern of GR effects on its own expression as well as expression of its targets Bcl-X_L, Bim and Bmf and then we constructed kinetic simulation models for hormone-induced GR signalling to obtain further insight into the molecular mechanisms in this pathway. Overall, the models reflected well the observed experimental data. The simulations suggested that Bim was targeted by an unkown gene that was induced between 4-6 hours in the presence of synthetic glucocorticoid dexamethasone. Simulations and experimental results also showed that Bmf induction did not require novel protein synthesis and may possibly be a direct target of GR. These models have demonstrated useful predictive characteristics and represent a novel promising approach towards better understanding of GR function.

2.2 Introduction

Computational modelling is becoming an increasingly powerful and versatile methodology in drug discovery, offering efficient and cost effective alternatives to traditional experimental

approaches (1). The mechanistic details of various biological processes derived from laboratory-based analyses can be captured and embedded in *in silico* models. These have the advantage of integrating vast amounts of data, and information generated from modern post genomic technologies, into comprehensive, quantitative and predictive representations. In addition, modelling brings about a better understanding of both the mechanisms of drug action and the biological basis of the disease. This in turn may be used to discover more effective drugs with fewer side effects and in individualizing and optimizing drug dosage and treatment procedures (2, 3).

The important potential of applying computational modelling to drug action and medical research has been successfully illustrated by recent studies. Hoffmann's model of the NF-κB signalling pathway later led to a better understanding of the mechanisms of action of bortezomib, which is a drug used in multiple myeloma, which targets upstream events in the NF-κB pathway (4). This ligand–receptor model has drawn much attention and inspired studies in cancer, apoptosis and other relevant subjects. A quantitative kinetic model has been created to stratify breast cancer patients for personalized therapy and provided an insight into the development of the resistance to the monoclonal antibody trastuzumab (5). Gilchrist *et al.* adopted a systems approach to model the stimulation of macrophages by the Toll-like receptor (TLR) 4 and predicted that the activating transcription factor 3 is a negative regulator of the TLR-mediated inflammatory response. This integrated approach revealed that through the use of systems biology tools, it is possible to identify novel regulatory mechanisms and new potential drug targets (6).

Glucocorticoids (GCs) are steroid hormones that are widely used for the treatment of numerous diseases including allergies, inflammatory diseases and leukaemia. This is due to their ability to suppress inflammation and induce programmed cell death (apoptosis). Most of the responses induced by GCs are mediated by the intracellular protein GC receptor (GR), which is a member of the nuclear receptor superfamily. GR has been a model factor for ligand-regulated transcriptional control. Upon binding of GCs to the receptor, this complex translocates to the nucleus and binds to target DNA sequences, also known as GC response elements (GREs). The molecular mechanisms governing the GR-mediated transcriptional activation or repression are dependent on the cell type, the sequence of GREs, the recruitment of cofactors and post translational modifications (7–11).

A large number of studies have been devoted to the investigation of GR-regulated apoptosis. Previous reports indicated that a surprisingly small fraction of genes are actually regulated by GR in a similar manner in different cell types, with the majority of genes being controlled selectively in a cell-specific fashion (12). The fact that GR inhibits apoptosis in some mammary epithelial cells, but induces cell death in white blood cells, raises the question of how GR-selective modulation of the expression of genes controlling cellular fate occurs (13, 14). Therefore, further investigation is required to determine the mechanistic details of the pathways involved in GR-regulated apoptosis.

Gene-profiling studies in patients with primary acute lymphoblastic leukaemia (ALL) indicated that a common set of genes are regulated by GCs. These studies highlighted that some of the apoptosis-regulating genes of the B cell lymphoma 2 (Bcl-2) family, and in particular the BH3-only molecules Bim and Bmf, as well as Bcl-X_L, are crucial transcriptional GR targets by direct and/or indirect mechanisms (9, 14–18). It is believed that the Bcl-2 rheostat, which is a ratio between pro- and anti-apoptotic Bcl-2 members, is a major determinant of GR-dependent apoptosis in leukaemia cells, and that the activity of each one of the Bcl-2 family members is controlled in a cell-type- and stimuli-specific manner (19). Bcl-2 family members, depending on their function, are categorized into two distinct groups; the proapoptotic, such as Bim, Bax and Bid, and the antiapoptotic for example Bcl-X_L, Bcl-2 and Mcl-1. The cellular fate is determined by the levels and ratio of free and heterodimerised components of the Bcl-2 family members. Another well-known GR direct target involved in the regulation of inflammation, GILZ, was also markedly induced in human lung A549 and various lymphoid cells treated with synthetic GCs (9, 20). The control of GILZ transcriptional regulation is achieved by GR interaction with its GRE sequences, and potentially accompanied by accessory regulatory regions such as forkhead box class O3 (FoxO3) binding sites (9, 20, 21).

A study has identified 71 direct GR target genes in human lung A549 cells, with 50 genes being positively regulated and 21 genes being negatively regulated at the transcriptional level (9). This study identified genes involved in the control of inflammation, apoptosis, signal transduction and metabolism as well as genes with unknown cellular functions. In addition, thousands of potential GR target genes have been identified with less stringent approaches in other cell types. Nevertheless, quantitative data describing the molecular mechanisms of GR action is still lacking. For instance, the kinetic parameters of GR-controlled gene expression, defined by mathematical approaches, have been described for only a small number of genes and in a limited number of cell types. In order to fully understand and exploit cellular systems

influenced by GR, multidisciplinary approaches are necessary to integrate the existing knowledge in GR biology regarding the role of ligand, GREs and cofactors with mathematical modelling (12, 22).

In this report we built a set of dynamic models of GR-dependent transcription and translation that quantitatively define the response of ALL cells to GC treatment. We used a direct activation mechanism for modelling Bcl-X_L and GILZ gene expression as these have been established as direct GR transcriptional targets. Conversely, Bim was considered an indirect target to model GCs dependent gene expression, whereas both direct and indirect activation were used to model Bmf since the hormone-mediated activation mode of this gene is unknown. We determined detailed kinetic profiles of protein and mRNA expression levels of these direct and indirect GR target genes involved in the regulation of apoptosis, in dexamethasone (Dex; a synthetic GC) responsive and resistant leukaemia cell lines. Using systems biology tools we reconstructed GC-induced gene expression *in silico* and determined the kinetic parameters of the model from experimental data. We then used these models to simulate GR-dependent direct and indirect transcription and tested their predictive potential.

2.3 Material and Methods

2.3.1 Cell culture & treatments

GC responsive leukaemia (CEM-C7-14) and GC resistant leukaemia (CEM-C1-15) cell lines (23) were cultured in RPMI-1640 medium supplemented with 10% foetal bovine serum and 1% penicillin and streptomycin (Cambrex, NJ, USA) and were seeded into 60mm plates for RNA extraction and western blots. Prior to the hormone treatment the media was changed to RPMI-1640 supplemented with 10% charcoal stripped foetal bovine serum (HyClone, UT, USA). Cells were treated with 1µM Dex (Sigma, MO, USA) at indicated time points (for 0, 2, 4, 6, 10, 14, 18 and 22 h). To determine whether Bmf is a direct or indirect target of GCs, cells were treated with 1µM cycloheximide (Sigma) 1 h prior to Dex treatment for the indicated time points.

2.3.2 Immunoblotting

Cells were harvested by centrifugation, followed by two washes with phosphate-buffered saline and lysed in high salt lysis buffer (45mM HEPES pH 7.5, 400mM NaCl, 1mM ethylenediaminetetraacetic acid [EDTA], 10% glycerol, 0.5% NP-40, 1mM DTT, 1mM PMSF, protease inhibitor cocktail including 1µg/ml aprotinin, 1µg/ml leupeptin, 1µg/ml pepstatin, 20mM b-glycerophosphate, 5mM sodium pyrophosphate and 2mM sodium orthovanadate) (11).

Protein concentration was determined by the Bradford assay (Bio-Rad (CA, USA) protein assay), and equal amounts of protein were analyzed by SDS-PAGE, transferred to Immobilon-P membrane (Millipore, MA, USA) and probed with indicated antibodies. Blots were developed with the enhanced chemiluminescence substrate according to manufacturer's instructions (Pierce, IL, USA) and the intensity of the bands was quantified using ImageJ software. ImageJ is a tool which can be used to compare the density or the intensity of the protein bands on the western blot. With the use of the gel analysis option, it generates plot which gives the relative location of each band and banding intensity. The relative protein expression was calculated by normalising the intensity of the samples to the internal control (actin in this case) and to the intital protein expression at time 0 (untreated). This can then be used for the comparison between samples. The antisera against the following proteins were used in the experiments: actin (Abcam, Cambridge, UK), 2F8 was generously provided by Dr Alexis, Bim (Abcam), Bmf (AbD Serotec, Oxford, UK), Bcl-X_L (Cell Signaling, MA, USA), and GILZ (Santa Cruz, CA, USA).

2.3.3 Quantitative real-time PCR

Cells were harvested and the total RNA was extracted using the RNeasy® plus mini kit and QIAshredder (Qiagen, Hilden, Germany), following manufacturer's guidelines. RNA concentration was determined by nanodrop measurements and cDNA was synthesized using the two-step protocol, with anchored oligos (Thermo Scientific, MA, USA) and Reverse-iT™ RTase Blend reverse transcriptase (Bioline, London, UK). Gene-specific cDNA was amplified in 20 µl of master mix containing SYBR® Green (Sigma), Taq DNA polymerase (New England Biolabs, MA, USA), and the reverse and forward primers for quantitative real-time (qRT)-PCR. qRT-PCR was then performed and standard curve analysis was carried out using the Opticon monitor 3.1 software. All values were normalised with RPL-19 control. Primers used were RPL-19 (F: ATGTATCACAGCCTGTACCTG, R: TTCTTGGTCTCTTCCTCCTTG), GR (F: GTTGCTCCCTCTCGCCCTCATTC, R: CTCTTACCCTCTTTCTGTTTCTA), Bim (F: GAGAAGGTAGACAATTGCAG, R: GACAATGTAACGTAACAGTCG), Bmf (F: ATGGAGCCATCTCAGTGTGTG, R: CCCCGTTCCTGTTCTCTTCT), Bcl-X_L (F:GGAGCTGGTGGTTGACTTTC, R: TCACTGAATGCCCGCCGGTAC), GILZ (F: GGACTTCACGTTTCAGTGGACA, R: AATGCGGCCACGGATG).

2.3.4 Statistical analysis

Statistical analysis was carried out with the GraphPad (GraphPad Software, Inc., CA, USA) and SPSS 15.0 software for Windows (SPSS Inc., IL, USA). All protein and mRNA

measurements for multiple time points were compared by the Tukey–Kramer test, which is a statistical test that allows a single-step multiple comparison between means in order to determine which pairs of means have statistically significant differences. The independent two-sample t-test was carried out for Bim and Bmf mRNA expression upon treatment with cycloheximide and Dex; this test was used to compare the mean scores of two groups on a given variable. All differences were considered statistically significant if the p-value was less than 0.05.

2.3.5 Model development

The classic cellular process of GR dynamics has been illustrated in a number of publications (24, 25). Lipophilic GCs pass into the cytoplasm and induce the nuclear localization of GR, which in turn either activates or represses genes in a cell-specific manner. Other transcriptional modes of action have also been identified, for instance, GR may bind with the DNA as a monomer, or it may interact with other transcription factors to elicit the transcriptional response without binding directly to the response element of the target gene (25). As the GR-induced mechanisms are highly complex and target dependent, the effects of GR dimerisation and subcellular compartmentalisation were not taken into consideration. Two cell lines were chosen for determining GC sensitivity in this study; the CEM-C7-14 cells and the CEM-C1-15 cells. These CEM cells are the direct clones of from the patients with acute lymphoblastic leukaemia, with C7 being GC sensitive, C1 being GC resistant. They are used in the experiment due to their long established specific steroid response of the orginial parental clones. For modelling, two separate models were created to represent different possible mechanisms of GR regulation in sensitive CEM-C7-14 cells and in resistant CEM-C1-15 cells: the direct model represents a direct activation of the target, while the indirect model represents an indirect activation via an unknown protein. The models in different cell types differ by the nature of the positive autoregulation of GR. It was found that GR autoinduction is relevant to CEM cell lines and it was believed that the rise in resistance to GCs may be associated with the lack of GR-positive autoregulation (26, 27). Although the exact mechanism for this remains uncertain, previous work has demonstrated that GR is able to regulate its own expression through binding to the half GRE of the hGR 1A promoter in CEM-C7 cells (28). Therefore, we incorporated the GR autoinduction mechanism in CEM-C7-14 cells only. The models were built as sets of ordinary differential equations (ODE) using mass action kinetics, following principles established by Jin *et al.* (22). Our models encompass the reaction kinetics of basal transcription, GR-induced transcription, GR-positive autoregulation, translation and degradation of Bim, Bcl-X_L, Bmf and

GILZ, as well as GR. The parameters used in these models were obtained either directly from experiments, or indirectly via mathematical estimation.

2.3.6 Simulations

The simulations were based on a series of time courses of experimental values of protein and mRNA expression obtained from cells treated with 1μM Dex. All simulations were carried out using the CellDesigner™ software (29, 30). Missing parameters were estimated using the Systems Biology Markup Language-based Parameter Estimation Tool (SBML-PET) (31). The simulation process was divided into two parts; first the initial state (nonstimulated system), and second the system after stimulation by Dex. Without the presence of Dex (at time point 0), a steady state was expected, hence a first set of parameters could be obtained, ensuring that the system remained stable without the addition of Dex. The rates of basal transcription, GR autoregulation and degradation could be obtained in this first stage, thereby decreasing the complexity of parameter estimation in the dynamic stage. The overall simulations were then compared with the experimental datasets, and a least-square residual value (ε) was calculated to determine the overall quality of the fit of the simulation against the experimental data.

$$\varepsilon = \sqrt{\frac{1}{n}\sum_{i=1}^{n}\left(\frac{y_i - Y_i}{Y_i}\right)^2}$$

where ε is the residual, n is the number of experimental data points, y_i are the experimental values and Y_i are the simulated values of the variable under consideration.

2.4 Results

2.4.1 Analysis of GR-mediated gene expression in GC-sensitive cell line CEM-C7-14

In order to obtain detailed kinetic parameters of the GC-mediated regulation of GR target gene expression, we employed western blot and qRT-PCR analysis to monitor GR, Bim, Bcl-X_L, Bmf and GILZ protein and mRNA levels in the GC-sensitive (CEM-C7-14) and -resistant (CEM-C1-15) cells. To closely analyze the effect of GR on its targets, we determined protein and mRNA expression profiles upon treatment of these cells with Dex at time points of 0, 2, 4, 6, 10, 14, 18 and 22 h. The time points were chosen based on previous microarray studies, which indicated that many molecular events, including gene expression and protein synthesis, occur within 24 h of treatment (16, 32). Actin was used as an internal control for the measurements of

protein levels, and RPL-19 as an internal gene known not to be affected by GCs for mRNA levels.

Western blot analysis was carried out in CEM-C7-14 cells treated with 1μM Dex at the indicated time points (Fig. 2.1A). The results showed an induction of protein levels of GR, Bim, Bmf and GILZ, whereas Bcl-X_L protein levels did not change significantly. Overall, GR, Bim, Bmf and GILZ proteins were found to be upregulated upon treatment with hormone for 22 h. No Bim induction was observed in the first 4 h followed by a rapid induction after 6 h. A weaker induction of Bmf was also observed at 14, 18 and 22 h after hormone addition. To obtain statistically significant data, the experiments were repeated four times (Suppl. Fig. 2.1) and all the values of densitometrically quantified bands were normalised to those obtained for actin, which was used as a loading control. Results were plotted as fold of induction over the value acquired for the untreated sample (0 h) (Fig. 2.1B). Statistical analysis of protein quantification based on four sets of experiments demonstrated that there was a significant increase in GR ($p = 1 \times 10^{-8}$), Bim ($p = 5 \times 10^{-12}$), Bmf ($p = 7 \times 10^{-10}$) and GILZ ($p = 0.014$). In comparison with Bim, Bmf protein levels increased more gradually (Fig. 2.1B). GILZ protein levels were found to increase rapidly 6 h after the addition of the hormone and remained at the same level throughout. The average change in Bcl-X_L levels was not statistically significant, although we did detect a downregulation of Bcl-X_L expression in one set of experiments (Suppl. Fig. 2.1A).

To investigate whether these selected GR target proteins (Bim, Bmf, Bcl-X_L and GILZ) were regulated by GR at the transcriptional level, qRT-PCR was performed in three independent experiments to quantify the mRNA levels of each one of them (Figure 2.2). The mRNA levels of GR, Bim, Bmf and GILZ were upregulated following Dex treatment. In particular, Bim mRNA was elevated to greater than twofold and GILZ over 15-fold. The level of Bcl-X_L under the same conditions remained constant. In contrast to GR and Bmf, which both displayed a gradual increase as the hormone incubation time increased, Bim mRNA exhibited a sudden increase between 6 and 10 h after hormone addition ($p = 0.012$), whereas GILZ mRNA expression displayed a strong induction after 6 h of treatment ($p = 0.014$) and became more pronounced throughout (Fig. 2.2). Statistical analysis indicated that a significant induction was found in GR ($p = 0.047$), Bim ($p = 7 \times 10^{-13}$), Bmf ($p = 0.001$) and GILZ ($p = 7 \times 10^{-13}$), in cells treated with hormone for 22 h. There were no significant changes observed for Bcl-X_L in these cells under the experimental conditions used.

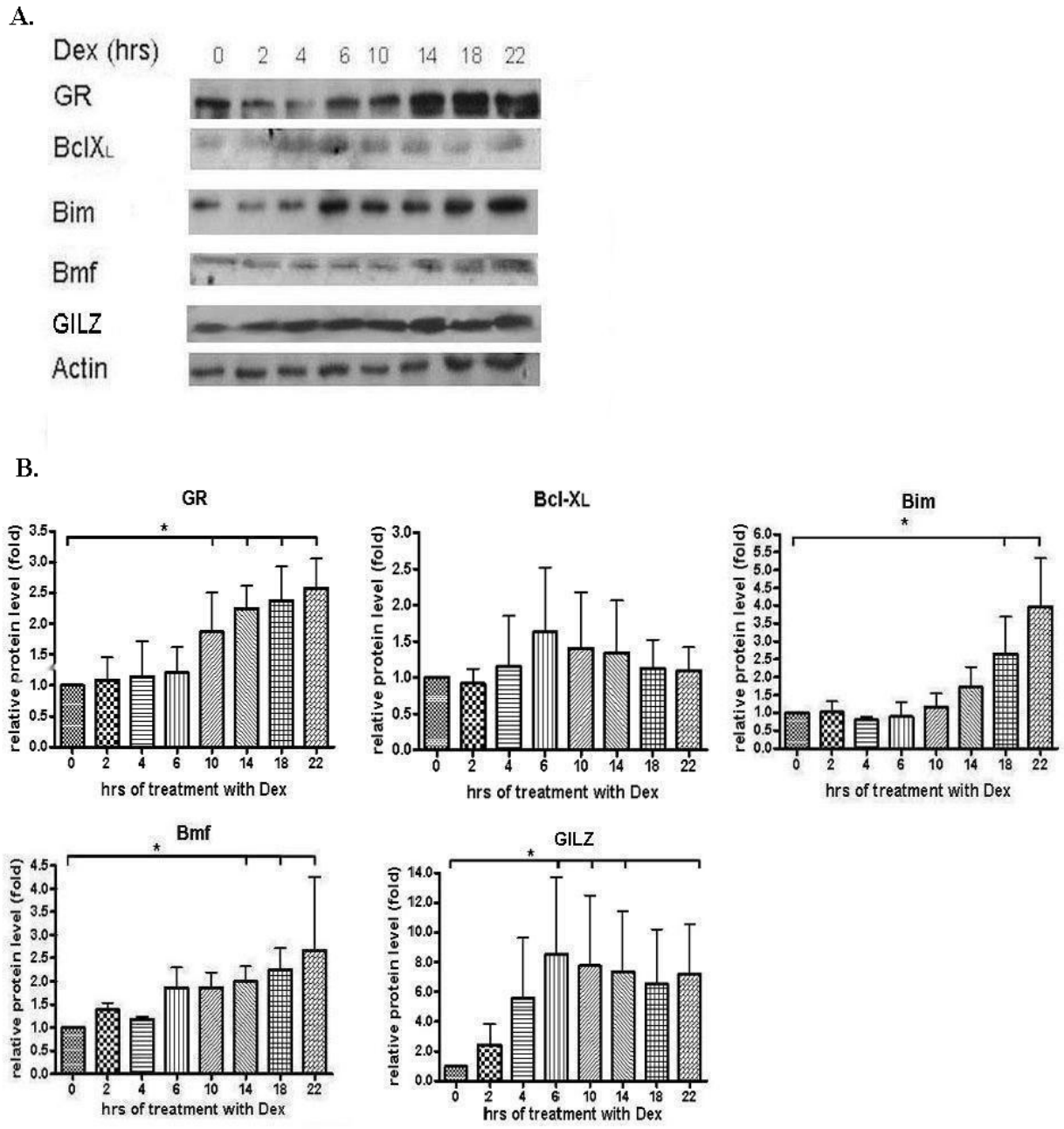

Figure 2.1 Glucocorticoid receptor target gene and protein expression in CEM-C7-14 cells

(A) Western blot analysis of the GR, Bcl-X_L, Bim, Bmf and GILZ protein levels, with actin as a control in CEM-C7-14 cells cultured with 1μM Dex for the indicated times. One representative western blot is shown. **(B)** GR, Bcl-X_L, Bim, Bmf and GILZ protein levels were quantified by ImageJ, normalised to actin and presented as a histogram (see 2.3.2 Immunoblotting). Error bars represent standard deviations of four independent experiments. An asterisk indicates a significant difference of $p < 0.05$.

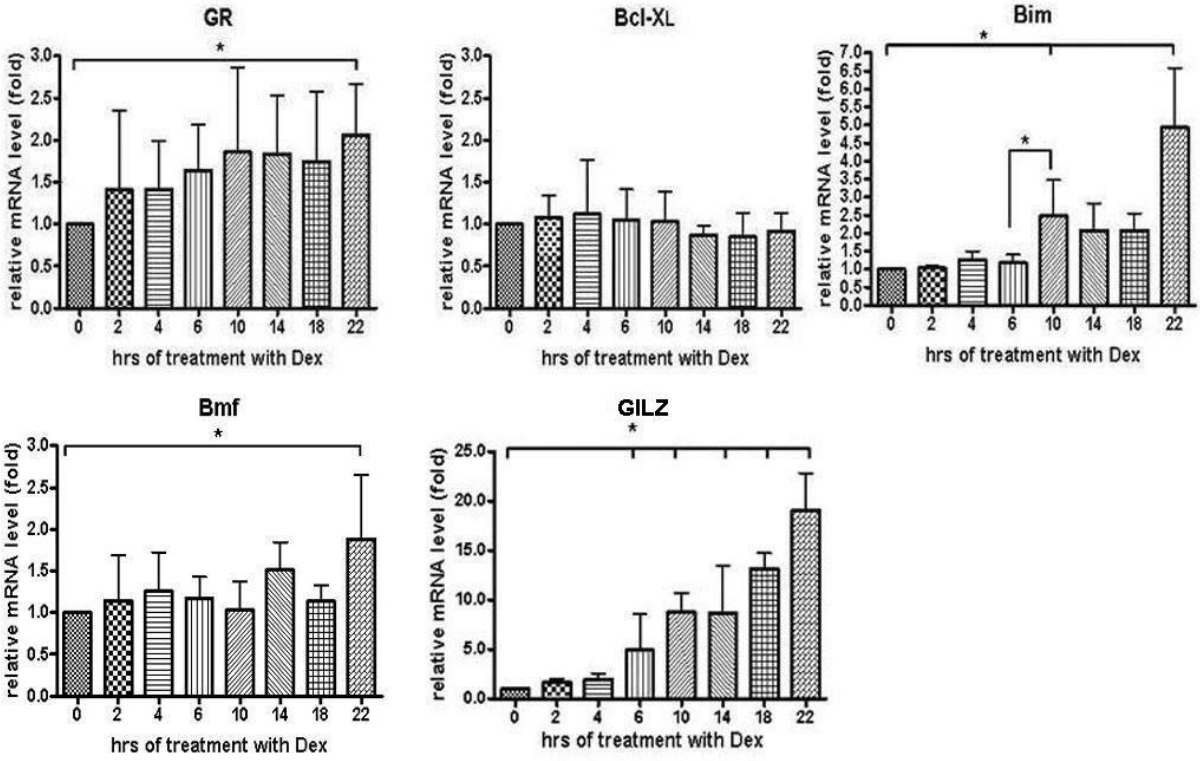

Figure 2.2 Relative mRNA levels of glucocorticoid receptor target genes in CEM-C7-14 cells

CEM-C7-14 cells were treated with 1µM Dex at the indicated time points and the mRNA levels of GR, Bcl-X_L, Bim, Bmf and GILZ (normalised to RPL-19) were determined by quantitative real-time PCR. Error bars represent standard deviations of three independent experiments. An asterisk indicates a significant difference of $p < 0.05$.

2.4.2 Analysis of GR-mediated gene expression in the GC-resistant cell line CEM-C1-15

To investigate the possibility of differential GR-mediated regulation of gene expression of its target genes in the sensitive CEM-C7-14 versus the resistant CEM-C1-15 cells, the protein expression of GR, Bim, Bcl-X_L, Bmf and GILZ was analyzed in CEM-C1-15 cells treated with Dex the same way as described before (Fig. 2.3A). An increase was observed in the GR, Bcl-X_L, Bmf and GILZ protein levels within the first 6 h of hormone treatment (Fig. 2.3A). Statistical analysis of four independent western blot experiments (Suppl. Fig. 2.2) indicated that GR is significantly upregulated after 6 h ($p = 0.007$) followed by a minor downregulation that was not statistically significant, although this observation requires further investigation since the trend was observed in several experiments (Fig. 2.3B & Suppl. Fig. 2.2). In hormone treated cells, the level of Bcl-X_L protein increased upon 2 h of treatment, whereas Bmf was downregulated after 22 h of treatment with the ligand. However, these changes were not statistically significant (Fig. 2.3A). A rapid (4 h of hormone treatment) significant induction was also found in Bmf ($p = 0.032$) and GILZ ($p = 0.001$), but no significant changes after longer hormone treatment were observed in Bmf, Bim, Bcl-X_L (four independent experiments were taken into account for statistical analysis). Significant GILZ protein induction was detected 4 h after treatment and remained at a similar level at all later time points tested ($p = 3 \times 10^{-4}$) (Fig. 2.3B). The qRT-PCR data indicated that the mRNA levels and the protein kinetic profile did not correlate at all time points (Fig. 2.4). GR protein levels were initially upregulated at early time points after hormone addition, and later downregulated, whereas no significant change in the GR mRNA level was identified at these time points. Statistical analysis showed that there was an upregulation of Bcl-X_L mRNA within the 22 h time frame ($p = 0.009$ between 4 and 22 h, $p = 0.01$ between 6 and 22 h). However, no significant overall changes were observed in Bim and Bmf mRNA levels. A strong induction (>20-fold) was seen in the GILZ mRNA expression after 4 h ($p = 1 \times 10^{-5}$), and such pronounced expression remained more or less constant after prolonged hormone treatments. These data, together with those obtained from CEM-C7-14 cells, further emphasize the need of producing a quantitative dynamic model for analyzing hormone-mediated changes in gene expression.

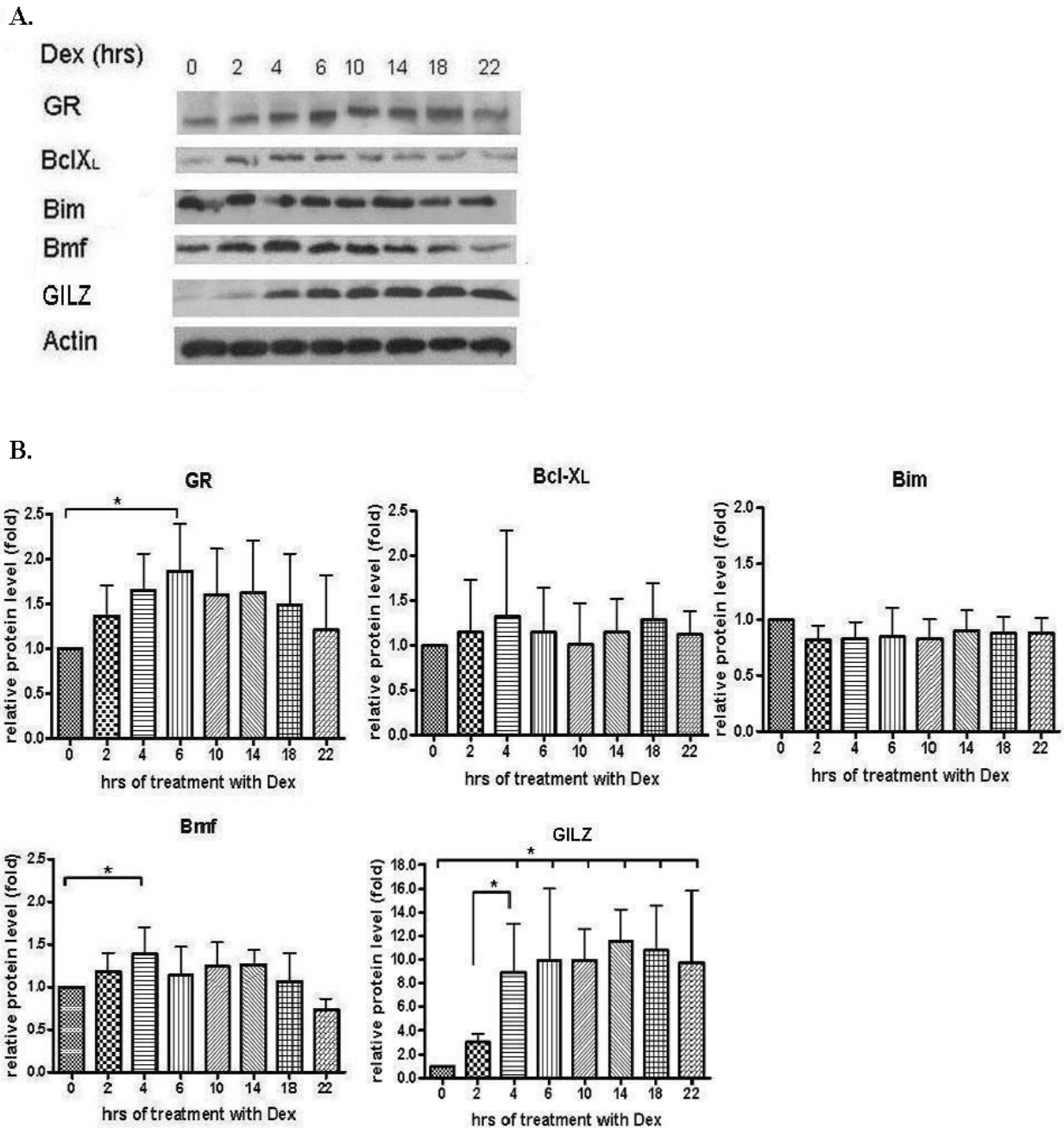

Figure 2.3 Glucocorticoid receptor target gene and protein expression in CEM-C1-15 cells

(A) Western blot analysis of GR, Bcl-X_L, Bim, Bmf and GILZ protein levels with actin as a control. CEM-C1-15 cells were treated with 1μM Dex at indicated time points for 22 h. One representative blot is shown. **(B)** GR, Bcl-X_L, Bim, Bmf and GILZ proteins were quantified by ImageJ and normalised to actin. Error bars represent standard deviations of four independent experiments. An asterisk indicates a significant difference of $p < 0.05$.

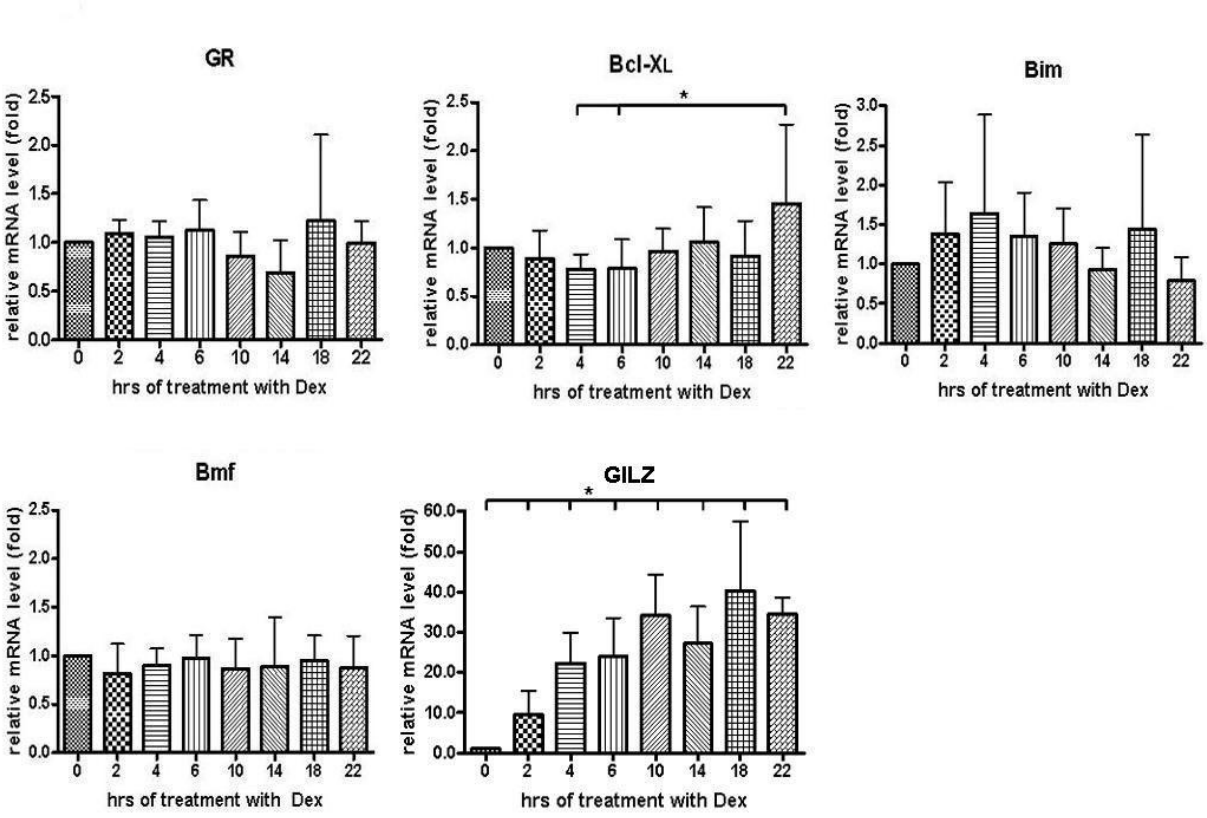

Figure 2.4 Relative mRNA levels of glucocorticoid receptor target genes in CEM-C1-15 cells

Quantitative real-time PCR results of relative mRNA levels of GR, Bcl-X_L, Bim, Bmf and GILZ in CEM-C1-15 cells treated with 1μM Dex at indicated time points and values were normalised to the house keeping gene RPL-19. Error bars represent the standard deviations based on three independent experiments. An asterisk indicates a significant difference of $p < 0.05$.

2.4.3 Model simulations in CEM-C7-14

We built *in silico* models of the GR-dependent direct and indirect transcriptional activation in CEM-C7-14 cells based on a survey of literature regarding the classic cellular process of GR dynamics, which is illustrated in Fig. 2.5A. These models were used to simulate the effect of Dex treatment on GR-induced activation of its target genes, including their transcription,

translation, the degradation of the protein and mRNA and also the GR-mediated regulation of its own expression. Fig. 2.5B represents the direct activation model, while Fig. 2.5C represents the alternative indirect model, where GR induces target genes via regulation of an unknown protein. The ODEs used are presented in Suppl. Table 2.1. Cytoplasmic-nuclear compartmentalization was not considered in these models as a high salt lysis buffer was used to obtain the whole cell extract. Fig. 2.6A shows the experimental data obtained from protein level quantification (squares) together with the simulations (lines). A linear trend of simulation was generated in GR protein expression whereas a nonlinear trend was observed in Bim simulation. The simulation reveals no significant changes in Bcl-X_L, as it maintains a constant level up to 24 h. In this case, the direct activation model was used, and the induction parameter (Bcl-X_L) was set to zero, resulting in the model essentially simulating no induction. The simulation of Bim protein level did not seem to reflect the sharp induction observed after 6 h in the experimental data. In addition, there was a minor difference between direct and indirect simulation of Bmf data, with the direct fitted simulation being closer to the experimental data (with $\varepsilon = 0.1335$ for the direct fit and $\varepsilon = 0.1347$ for the indirect fit). Parameter estimation and simulation for GILZ were based on the first four time points as the induction reached its maximum level and saturated much faster in GILZ compared with the other GR targets, possibly due to the differences in the assembly/disassembly mechanisms of preinitiation complexes (33). Overall, the fit between simulations and experimental data points was good and the model accurately reproduced the datasets, as indicated, with the relatively small and similar residual values ($0.3 > \varepsilon > 0.1$) (Fig. 2.6, least-square residual).

Based on quantification and modelling of protein levels only, we could not confirm whether Bmf fits better with a direct or indirect activation mechanism, despite the fact that the direct simulation showed a better fit. To further investigate this question, simulations with mRNA levels were carried out. Similar behaviours were observed in mRNA simulations, where a linear increasing trend was identified in GR, Bmf (direct model) and GILZ, and a nonlinear trend in Bim (Fig. 2.6B). The significant induction of Bim mRNA levels that was observed between 6 and 10 h was not seen clearly in the simulations. The residual value between experimental data and simulation in GILZ was larger than others ($\varepsilon = 0.2427$), which was expected as expression changes were the largest for GILZ. Both Bmf direct and indirect simulations showed a similar behaviour, with the direct model of Bmf activation showing once again a better fit with the experimental data ($\varepsilon = 0.1399$) than the indirect model ($\varepsilon = 0.1430$).

To test whether Bmf expression was induced directly by Dex in leukemic cells, CEM-C7-14 cells were treated with Dex in the presence and absence of protein synthesis inhibitor cycloheximide, with Bim acting as a positive control for indirect activation by GCs. Inhibition of new protein synthesis by cycloheximide should not affect the Dex-activated induction of GR direct targets, but should block the induction of indirect targets. The experiment was repeated three times and an independent sample t-test was carried out (Fig. 2.7). The results demonstrated that the mRNA level of Bmf was induced in the presence and absence of cycloheximide ($p = 0.0115$ and $p = 0.0092$, respectively), whereas Bim expression appeared to be inhibited. In order to provide further support for the notion that Bmf may be a direct target of GR, we searched for the existence of consensus GREs (ACANNNTGTTNT) (9) within Bmf. Indeed, two consensus GREs were identified; one being 886 bps downstream from the ATG start codon, and the other one located at 4012 bps downstream from the ATG. The finding provides further experimental support for the prediction that Bmf is a direct target. Taken together, both *in silico* generated model and experimental data, suggest that *de novo* protein synthesis is not required for Bmf mRNA induction by GCs and that Bmf may be a direct target for GR.

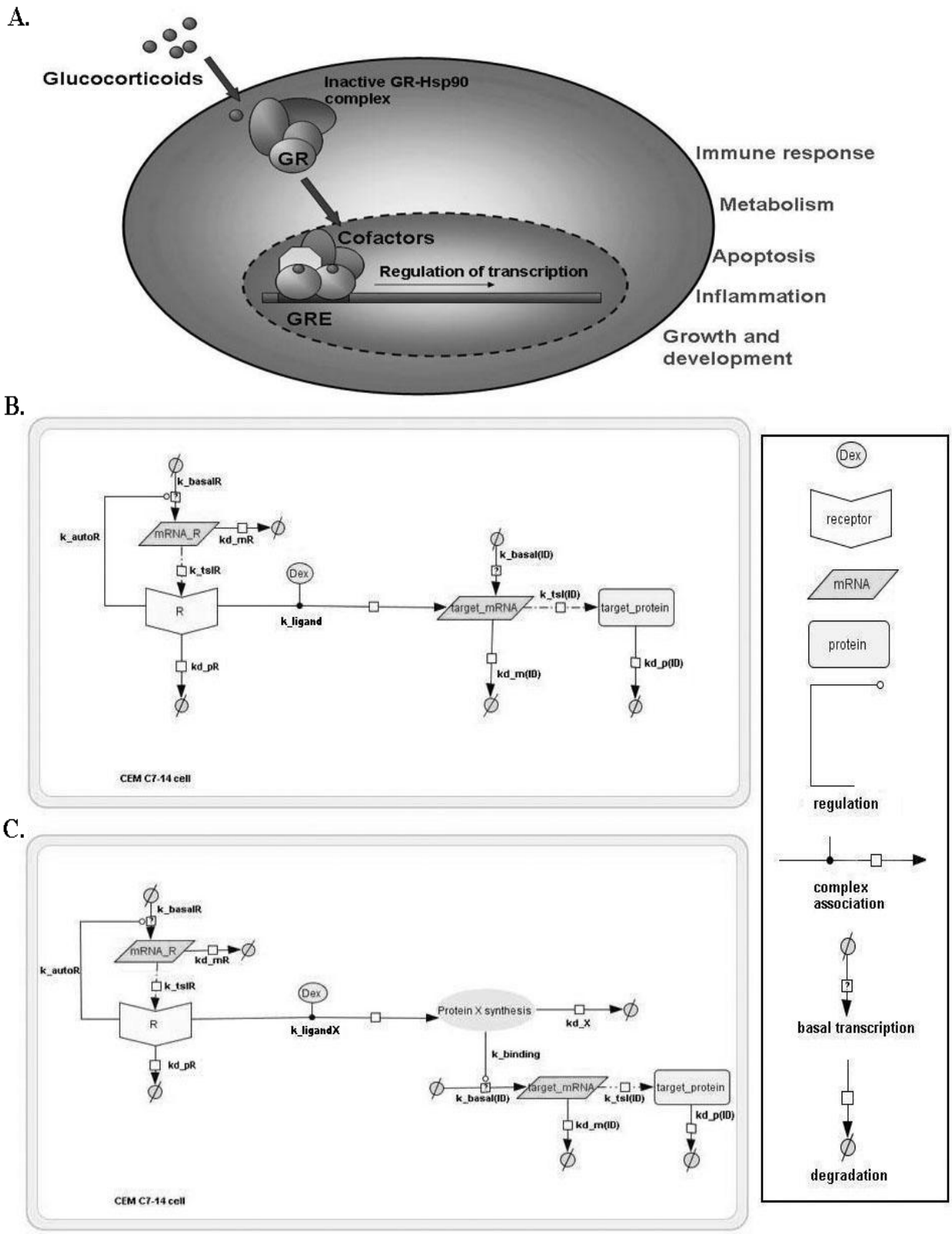

Figure 2.5 Topology of models in CEM-C7-14 cells

(A) GR dynamics. The figure summarizes the basic mechanism of gene regulation controlled by GR. Once the glucocorticoid passes through the cell membrane, it activates GR and

causes the dissociation of the cytoplasmic HSP complex from the GR. This results in GR dimerisation and translocation to the nucleus where it binds to GREs of the target gene or other transcription factors. This in turn either activates or represses gene transcription depending on the target gene, cell type and cofactor interaction. **(B)** Direct model. The model was constructed using CellDesigner™ (Systems Biology Institute, Tokyo, Japan), based on the known molecular mechanisms but without taking the cytoplasmic–nuclear compartmentalization into account. Basal transcription, GR autoregulation, mRNA degradation, protein degradation and binding dynamics are included in the model, and all reactions were modelled by first order mass action kinetics. **(C)** Indirect model. The direct and indirect models only differ by the nature of the interaction between the GR and the mRNA, as in the latter case, an extra step of protein synthesis is required for targeting downstream responsive gene. Kinetic equations describing GR mediated induction of GILZ and the Bcl-2 family are described in detail in Suppl. Table 2.1.

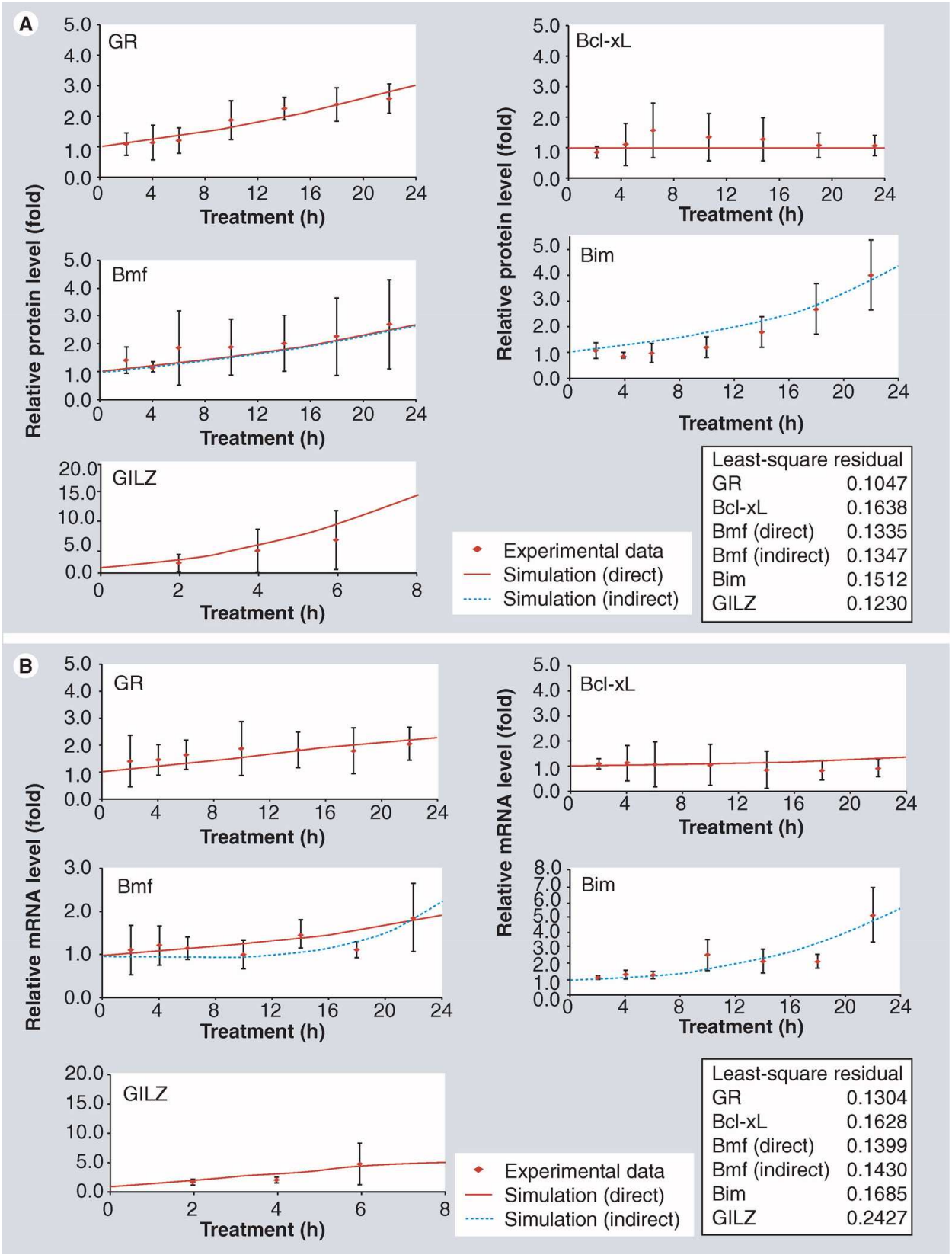

Figure 2.6 Simulations in CEM-C7-14 cells

(A) Protein time course simulations in CEM-C7-14 cells. The expression dynamics were simulated using the CellDesigner™ modelling tool and the parameters were fitted to

experimental data using the Systems Biology Markup Language based Parameter Estimation Tool (SBML-PET). Solid squares are the mean of the normalised protein experimental level and bars are the standard deviations for four sets of experiments. The solid line represents the simulation by the direct model and the dotted line represents the indirect simulation. **(B)** Dynamics of the mRNA expression of the system were simulated via the same process. Solid squares are the mean of the normalised mRNA experimental data and bars are the standard deviations for three sets of experiments. The models as shown revealed the characteristic kinetics of GILZ and the Bcl-2 family members in response to dexamethasone in CEM-C7-14 cells. The residual value was calculated to assess the quality of fit between the simulations and the experimental data.

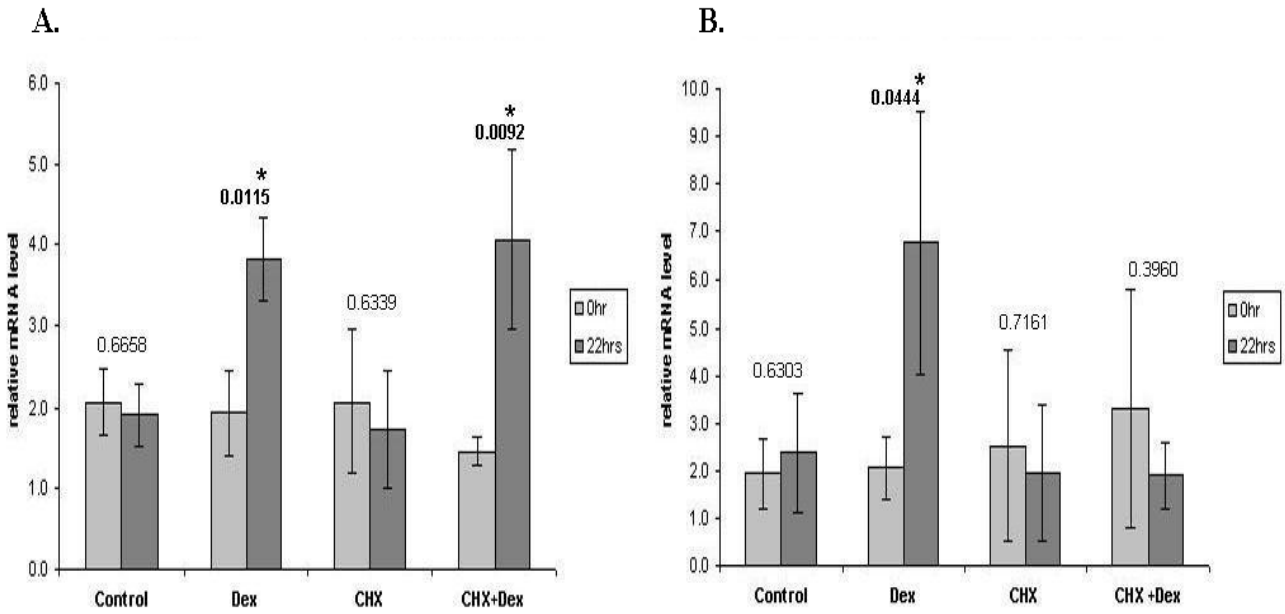

Figure 2.7 Effect of cycloheximide on Bmf induction

(A) Bmf mRNA expression in Dex/CHX treated CEM-C7-14 cells. Quantitative real-timePCR was performed by extracting RNA from CEM-C7-14 cells treated with 1µM Dex for 22 h in the presence or absence of 1µM CHX using Bmf-specific primers. **(B)** Bim mRNA expression in Dex/CHX treated CEM-C7-14 cells. Bim was used as a comparable control in this study. The data was based on three independent experiments. An asterisk indicates a significant difference of $p < 0.05$.

2.4.4 Model simulations in CEM-C1-15

The same modelling approach was employed when simulating gene expression in CEM-C1-15 cells. The direct model was applied to Bcl-X_L and GILZ, the indirect model to Bim and both models to Bmf expression (based on Suppl. Fig. 2.3). GR protein simulation indicated weak hormone-dependent induction, whereas the presence of hormone did not affect Bim and Bmf protein levels in these cells. Interestingly, GILZ protein simulation showed a strong induction (Fig. 2.8A). The GR protein simulation indicated that the observed up- then down-regulation in GR was not significant. As there were no dramatic changes in Bmf expression in CEM-C1-15 cells over 22 h of hormone treatment, in silico models could not distinguish between direct and indirect protein activation ($\varepsilon = 0.1573$ in both models). The simulation of Bcl-X_L protein level indicated a relatively small linear increase after 22 h of Dex treatment. A larger variation in the residual values were observed in the CEM-C1-15 simulations compared with those in CEM-C7-14 ($0.7 > \varepsilon > 0.1$) (Fig. 2.8, least-square residual), and there were not many alterations in the kinetic profiles for most of the genes and proteins besides GILZ. This suggests that experimental data was in better agreement with *in silico* simulations in CEM-C7-14. Together with the protein expression, the mRNA expression time course was monitored. The simulation of Bcl-X_L protein and mRNA levels indicated that transcription does not reflect the level of translation in this case, since Dex treatment resulted in a small increase of protein level, whereas the mRNA level remained constant (Fig. 2.8). The Bmf mRNA simulations using the direct model fitted slightly better in this case ($\varepsilon = 0.1213$ in the direct model and $\varepsilon = 0.1208$ in the indirect model).

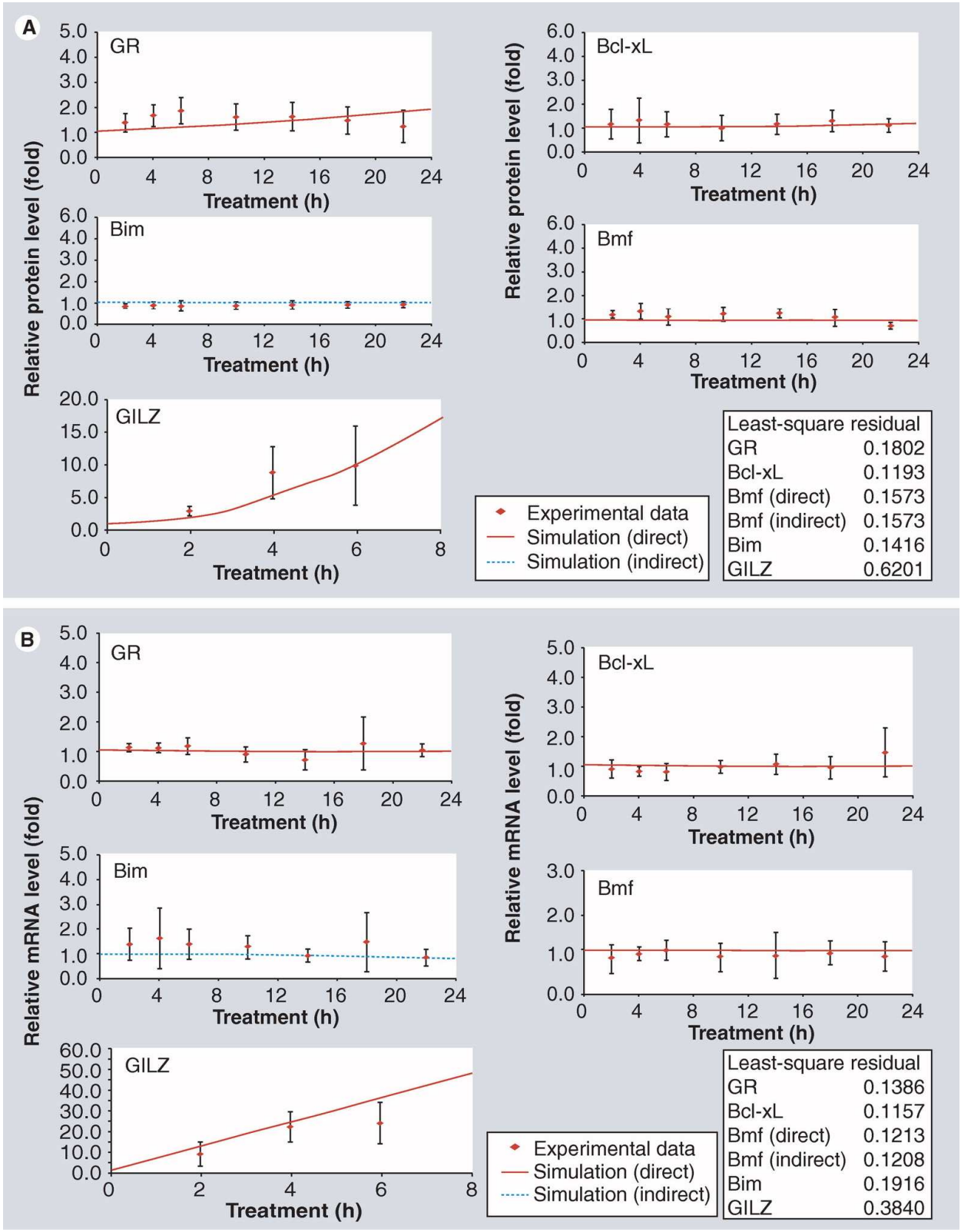

Figure 2.8 Simulations in CEM-C1-15 cells

(A) Protein time course simulation in CEM-C1-15 cells. The same process of simulation was carried out in CEM-C1-15 cells as described in Fig. 2.6. Solid squares are the experimental data and the error bars are standard deviations for four sets of experiments. The residual

value was calculated to assess the quality of the fit between the simulations and the experimental data. **(B)** mRNA time course simulations in CEM-C1-15 cells.

2.5 Discussion

In order to fully understand the complexity of biological processes, a combination of experimentation and computational modelling is required. A qualitative model can trace nonlinear information and predict the behaviour of a system upon perturbations. In comparison, a detailed quantitative model provides new testable insights into the molecular mechanisms that lead to observed phenotypes, enabling us to further explain the failure of certain treatments and identify alternative drug targets (2). Some previous GR kinetic models have adopted a top-down approach to study the molecular mechanisms of gene regulation by the use of microarray analysis to identify target genes responsive to GCs (22, 34). In this study we have adopted a bottom-up approach whereby we determined the detailed kinetic parameters of gene regulation by GCs, focusing on five genes. The purpose of this study was to construct a model that is able to represent the regulation of GR and its targets, such as the Bcl-2 family of proteins with the aim of providing new clues into the mechanisms of this regulation. We hereby present computational models based on ODE that integrate experimental data and a mechanistic representation of GR-mediated gene expression in leukaemia cells. Overall, our models accurately reflect experimental data and yield clues into the understanding of GR effects on its target genes.

In our study, we have determined detailed time courses of Bmf gene and protein induction. We have detected that Bmf mRNA and protein levels were significantly induced in CEM-C7-14 cells after 22 h of hormone treatment, with an oscillatory trend visible in some experimental sets (Fig. 2.1 & 2.2). GR-dependent regulation of Bmf has been reported in other studies of leukaemia (14). In CEM-C7-14 cells, Bim was significantly induced over 22 h, in agreement with previously reported observations (14, 16). A substantial induction of Bim protein and mRNA was observed approximately 6–10 h after the treatment in CEM-C7-14 cells, perhaps due to GR-mediated induction of an unknown protein that activates Bim prior to 6 h of hormone treatment (Fig. 2.1, 2.2 & Suppl. Fig. 2.1). This induction has also been shown in other studies of human ALL, such as CEM-C7H2 cells and several ALL patients (14). This trend, however, was not reflected well in the protein simulation of Bim between 0 and 10 h, implying that better Bim simulation may be carried out by breaking the induction process into two time phases, possibly between 0–6 h and 6–22 h based on the observation of the simulation against the experimental

data (Fig. 2.6). This observation also highlights the importance of performing the analysis with close time points to obtain an accurate simulation.

Bcl-X_L has been reported as a direct target of GR in other cell types (17, 18). However, in our experiments this gene did not show GR-dependent protein induction in CEM-C7-14 cells, and therefore the induction parameter (Bcl-X_L) was set to zero, resulting in the model simulating no induction, which is consistent with previous reports (14, 35). The experimental pattern for GR expression indicated that the GR protein levels and mRNA levels were both upregulated in CEM-C7-14 cells as described before (36). However, we have also observed a difference between the mRNA and protein levels at some time points. For example, GR protein levels rose sharply from 10 to 22 h after Dex treatment, but although a similar trend was observed for the mRNA levels, values varied to a greater extent (Fig. 2.1 & 2.2). Furthermore, GR protein expression in CEM-C1-15 cells was initially induced followed by a minor downregulation during the treatment, whilst no significant changes were detected in the mRNA levels (Fig. 2.3 & 2.4). The process leading from transcription to the production of a protein is complex, and the regulations of mRNA and protein stability have a major impact on this process. Protein levels are dependent on many factors, including not only protein stability, but also the rate of mRNA degradation and synthesis (37). Individual mRNAs and proteins may have their own unique rate of degradation that may change depending on the cell cycle, nutritional needs or during differentiation. For instance, the typical average mRNA half-life in mammalian cells is 24 h, while short-lived mRNA such as c-Fos has a half-life of only 20 min (37, 38). Although GCs regulate gene expression mainly through transcriptional initiation, it is possible that steroid hormones can modulate mRNA stability via post transcriptional regulation (38, 39). For example, it was found that GCs can affect mRNAs such as Cyclin D3 in murine T lymphoma cells, emphasizing the importance of the control of mRNA and protein stability in GR regulation (38, 40).

It has been suggested that GCs regulate GR mRNA stability (38, 41). However, the reported information with regards to GR expression in leukaemia cells is limited, particularly with respect to detailed quantification of GR protein and mRNA levels (42, 43). It has been shown that the amount of GR does not account for the resistance of CEM-C1-15 cells to GCs, which indicates that the quantity of GR does not correlate with the level of gene expression of Bcl-2 family genes and apoptosis (44). GCs regulate GR mRNA levels in a similar way in both sensitive and resistant ALL cells (45). It was thought that the phosphorylation of GR is linked to the accumulated but nonfunctional GR proteins in CEM-C1-15 cells (46). However, other studies

have shown that a significantly lower GR level was found in CEM-C1 cells in comparison with CEM-C7 cell lines (43). In addition, it was found that in CEM-C1 cells, a small induction of GR mRNA level was observed after treatment with Dex for 12 h, though this was not detected at the GR protein level (47). Additional research into GR protein and mRNA stability is required to resolve these discrepancies.

As mentioned in method section (2.3.2 Immunoblotting) both sets of protein and mRNA levels were normalised against not only to the internal control, actin/RPL19, but also to its basal protein or mRNA level at time 0 (untreated). This allows us to compare the induction trends between the CEM-C1-15 cells and CEM-C7-14 cells. Interestingly, the induction of GILZ protein and mRNA expression in CEM-C1-15 cells were found to be clearer than in CEM-C7-14 cells (Fig. 2.1, 2.2, 2.3 & 2.4). Such strong induction was also identified in previous work in both sensitive and resistant CEM cells, which supports the conclusion that the loss of GILZ induction may not contribute to the GR resistance (20). It was believed that GILZ played a crucial role in T lymphocytes by mimicking GC effects and that this could have been correlated with Bcl-X_L, however, the underlying mechanism remains unknown (21). Another interesting fact is that GILZ has been shown to exhibit a high basal expression in many cell types and organs, but the functional significance of this is not known (48).

Microarray studies have shown that Bim and Bmf are dominantly expressed in ALL cells treated with Dex (14). To date, the mechanism of Bmf regulation by GCs is poorly understood. To test whether Dex directly induces Bmf expression, cycloheximide was used to inhibit *de novo* protein synthesis in CEM-C7-14 cells. The simulations in CEM-C7-14 cells suggested that the direct induction model of Bmf fitted better with the time course experimental data than with the indirect model (Fig. 2.6). This results came to our surprise as it is known that models with higher complexity (in this case the indirect model) do in general lead to better fit as the parameter estimation process becomes more flexible. This shows that by dividing the parameter estimation process as two; the system when in its steady state (the unstimulated system) and the system when activated by Dex (as seen in 2.3.6 Simulations), it allows us to resolve the problem of complexed model being more favourable. Furthermore, in accordance with the prediction obtained by simulations, the data indicated that Bmf mRNA induction does not require *de novo* protein synthesis (Fig. 2.7). These findings, together with the fact that the Bmf gene contains several potential GREs downstream of the ATG start codon, support the notion that Bmf fits better with the direct GR activation model and that is a direct GR target. However, this does not exclude the possibility that such binding between GR and the enhancer region of Bmf may

require additional cofactors for Bmf to be induced by GCs. It has for example been reported that acetylation modulates Bmf gene expression in adenocarcinoma cells treated with histone deacetylase inhibitors. Since the presence of GREs has been identified within the regulatory promoter regions of both HDAC2 and Bmf, this indicates that the regulation of Bmf gene expression by Dex is rather complex (49, 50).

In CEM-C1-15 cells, both simulations and experimental data showed that there was not much induction of Bcl-X_L (Fig. 2.8), which is in accordance with previous published observations reporting that there was no induction of Bcl-X_L in primary ALL patients (51, 52). It was thought that other Bcl-2 family members such as Mcl-1 may play a more important role in GC resistance (35, 46). Such findings correlate with our experimental data and simulations, and further confirm the precision of our models.

2.6 Conclusion

In the present study we demonstrate that a small scale ODE model was able to provide useful information and encompass detailed knowledge regarding gene regulatory mechanisms. This model can be used to provide useful predictions and to better understand apoptotic signal transduction pathways. In addition, a potential candidate protein that targets Bim may be induced within first 6 h of Dex treatment in CEM-C7-14 cells. Finally, our results indicated that Bmf is a potential direct target of GR.

This article highlights the need to focus on two aspects in order to gain a better understanding of biological systems in the field of oncology. A short and frequent time frame is able to reveal any anomalous kinetic changes in proteins and genes, and hence provide more insight into signal transduction. A longer time period of simulation would allow us to identify possible oscillation patterns and discover potential feedback mechanisms that are usually associated with such oscillations. One of the challenges we face is the determination of the kinetic constants due to the imprecision of current experimental approaches, and the difficulty of measuring absolute quantitative amounts of mRNAs and proteins. As Klipp *et al*. suggested, the initial model rarely provides a full explanation for the studied objects, and usually leads to more open questions than answers; hence an iterative process of model refinement is essential (53). The present model represents a first step in this iterative process. Additional experiments and improvements will enable us to progress towards a precise understanding of the mechanisms of GR molecular interactions. To improve this model, several aspects may be taken into consideration. These include the determination of the rate of nuclear-cytoplasmic GR shuttling,

cofactors, post translational modifications, protein and mRNA degradation, the inclusion of more GR target genes and the incorporation of the half-life of Dex (between 36 and 54 h) (54). Along with qualitative experimental data, models will provide a better understanding of the molecular basis of GR and its target gene regulation, and will be useful in unravelling the complexity of GR signalling to improve treatments of leukaemia.

2.7 Supplementary data

2.7.1 Supplementary Tables

$$\frac{d[mRNA\_R]}{dt} = k\_basalR - [mRNA\_R]\cdot kd\_mR$$

$$\frac{d[R]}{dt} = [mRNA\_R]\cdot k\_tslR - [R]\cdot kd\_pR \quad \text{..... ....CEM C1-15}$$

$$\frac{d[R]}{dt} = [mRNA\_R]\cdot k\_tslR - [R]\cdot kd\_pR - k\_autoR \quad \text{..... ..... CEM C7-14}$$

$$\frac{d[Bmf\_mRNA]}{dt} = [Dex]\cdot[R]\cdot k\_ligand + k\_basalBmf - kd\_mBmf\cdot[Bmf\_mRNA]$$

$$\frac{d[Bmf\_protein]}{dt} = [Bmf\_mRNA]\cdot k\_tslBmf - kd\_pBmf\cdot[Bmf\_protein]$$

Direct model

$$\frac{d[Bmf\_mRNA]}{dt} = k\_basalBmf - kd\_mBmf + [proteinX\_synthesis]\cdot k\_binding$$

$$\frac{d[Bmf\_protein]}{dt} = k\_tslBmf\cdot[Bmf\_mRNA] - kd\_pBmf\ .$$

Indirect model

$$\frac{d[BclXL\_mRNA]}{dt} = k\_basalBclXL - kd\_mBclXL\cdot[BclXL\_mRNA] + [Dex]\cdot[R]\cdot k\_ıgana$$

$$\frac{d[BclXL\_protein]}{dt} = k\_tslBclXL\cdot[BclXL\_mRNA] - [BclXL\_protein]\cdot kd\_pBclXL$$

$$\frac{d[Bim\_mRNA]}{dt} = k\_basalBim - kd\_mBim + [proteinX\_synthesis]\cdot k\_binding$$

$$\frac{d[Bim\_protein]}{dt} = k\_tslBim\cdot[Bim\_mRNA] - kd\_pBim$$

$$\frac{d[proteinX\_synthesis]}{dt} = [Dex]\cdot[R]\cdot k\_ligandX - kd\_X$$

$$\frac{d[GILZ\_mRNA]}{dt} = k\_basalGILZ - kd\_mGILZ\cdot[GILZ\_mRNA] + [Dex]\cdot[R]\cdot k\_ligand$$

$$\frac{d[GILZ\_protein]}{dt} = k\_tslGILZ\cdot[GILZ\_mRNA] - [GILZ\_protein]\cdot kd\_pGILZ$$

Suppl. Table 2.1 Kinetic equations describing GR mediated induction of GILZ and the Bcl-2 family. This system of ordinary differential equations describes the GR regulatory kinetics

implemented in our models. Here, the kinetics is essentially the same in both cell types apart from the rate of GR protein expression [*R*]. *kd_X* represents the overall degradation; *k_binding* is the regulation between the unknown *proteinX* and the target gene; *k_ligand* and *k_ligandX* are the rates of complex association of dexamethasone and GR in the direct and indirect model respectively; *kd_m* and *kd_p* represent the first order rate constants of the degradation of mRNA and protein respectively. The term *Tsl* denotes translation, *basal* denotes basal transcription, *proteinX* the unknown protein and *R* the glucocorticoid receptor.

2.7.2 Supplementary figures

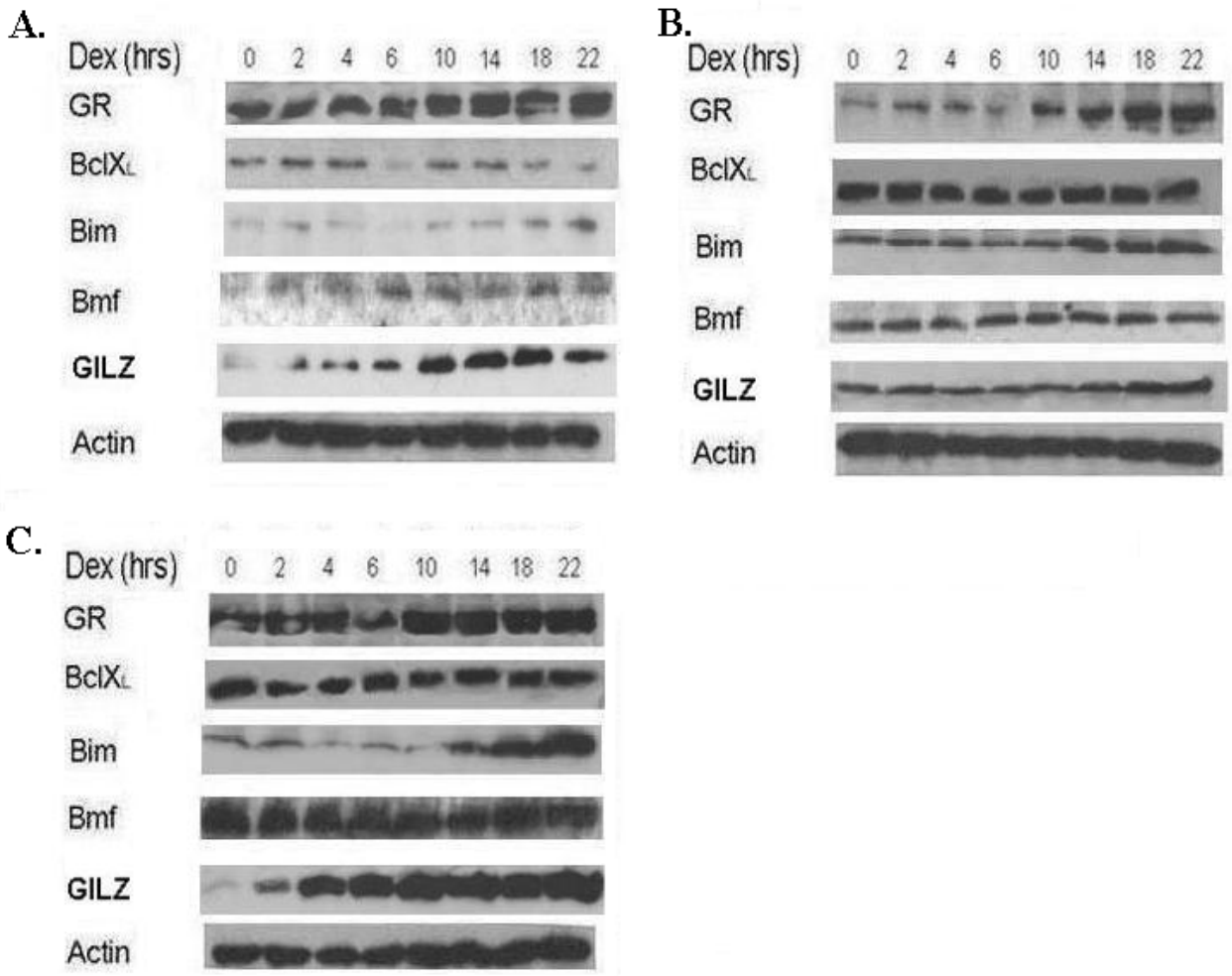

Suppl. Figure 2.1 GR target gene and protein expression in CEM-C7-14 cells

Western blot analysis of the GR, Bcl-X_L, Bim, Bmf and GILZ protein levels, with actin as a control in CEM-C7-14 cells cultured with 1μM dexamethasone (Dex) for indicated time points. A, B and C show independent experiments.

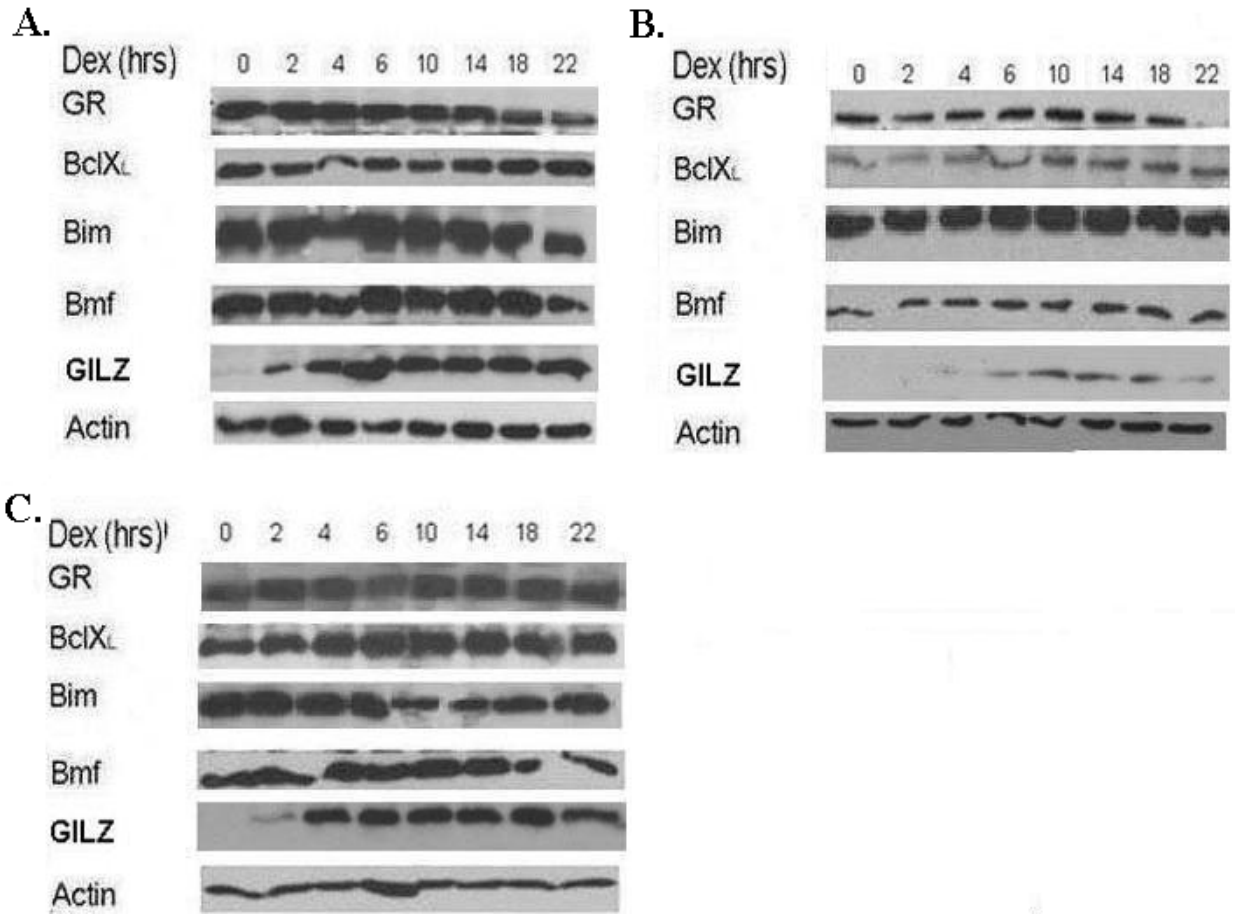

Suppl. Figure 2.2 GR target gene and protein expression in CEM-C1-15 cells

Western blot analysis of the GR, Bcl-X_L, Bim, Bmf and GILZ protein levels, with actin as a control in CEM-C1-15 cells cultured with 1μM dexamethasone (Dex) for indicated time points. A, B and C show independent experiments.

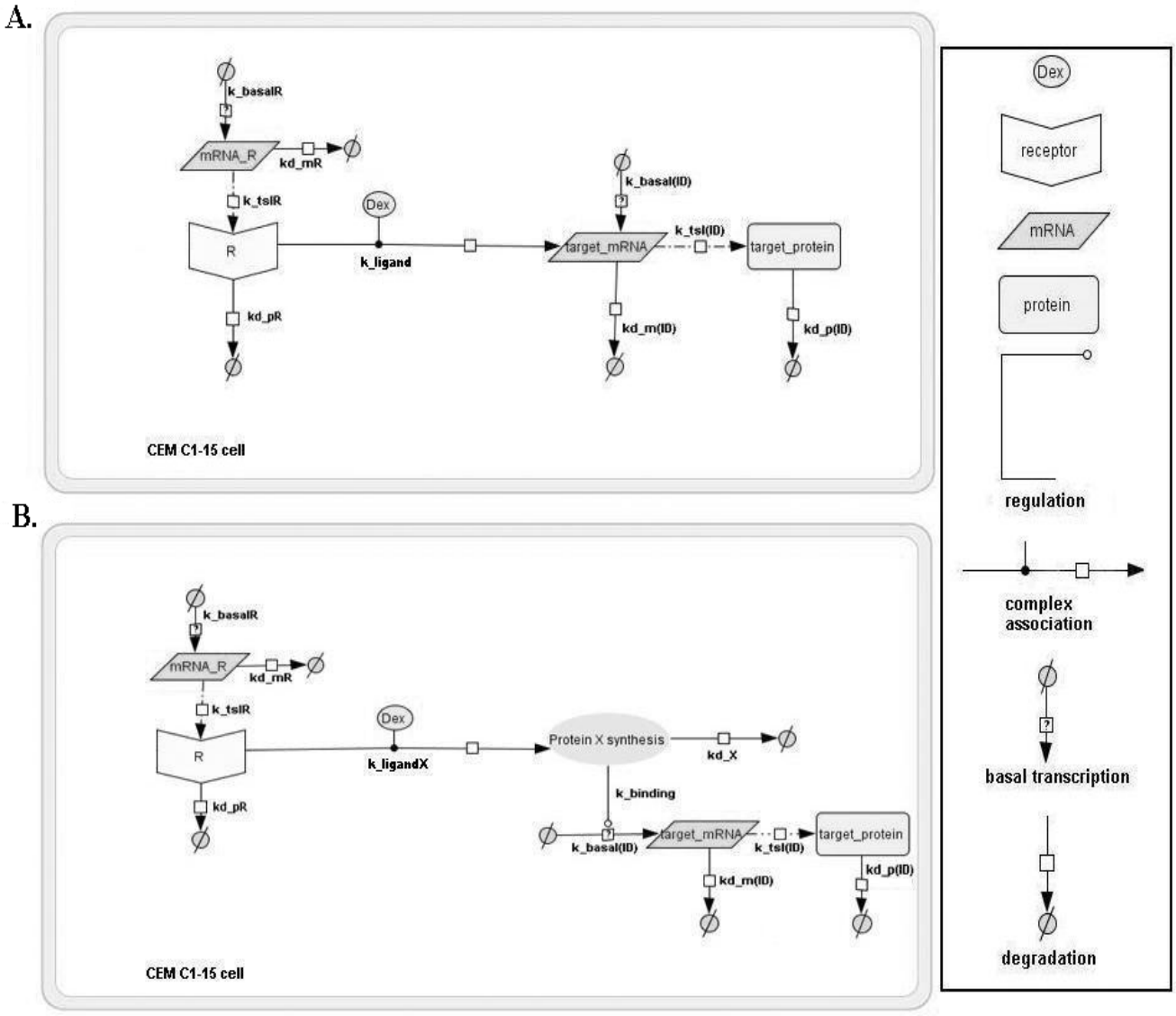

Suppl. Figure 2.3 Topology of models in CEM-C1-15 cells

The direct and the indirect models in CEM-C1-15 are essentially the same as in CEM-C7-14 (Fig. 2.5), differing only by the nature of the regulation of GR. **(A)** Direct model. **(B)** Indirect model. The kinetic equations describing GR mediated induction of GILZ and the Bcl-2 family are described in details in Supplementary table 2.1 *(ID)* in this case represents the identity of the protein or gene.

2.8 References

1. Musante CJ, Lewis AK, Hall K: Small- and large-scale biosimulation applied to drug discovery and development. *Drug Discovery Today.* 2002; 7(20)**:** s192-s196.

2. Rajasethupathy P, Vayttaden SJ, Bhalla US: Systems modelling: a pathway to drug discovery. *Current Opinion in Chemical Biology.* 2005; 9(4)**:** 400-406.

3. Materi W, Wishart DS: Computational systems biology in drug discovery and development: methods and applications. *Drug Discovery Today.* 2007; 12(7-8)**:** 295-303.

4. Hoffmann A, Levchenko A, Scott ML, Baltimore D: The Ikappa B-NF-kappa B signalling module: Temporal control and selective gene activation. *Science.* 2002; 298(5596)**:** 1241-1245.

5. Faratian D, Goltsov A, Lebedeva G, Sorokin A, Moodie S, Mullen P, *et al*: Systems biology reveals new strategies for personalizing cancer medicine and confirms the role of PTEN in resistance to Trastuzumab. *Cancer Res.* 2009; 69**:** 6713-6720.

6. Gilchrist M, Thorsson V, Li B, Rust AG, Korb M, Kennedy K, *et al*: Systems biology approaches identify ATF3 as a negative regulator of Toll-like receptor 4. *Nature.* 2006; 441(7090)**:** 173-178.

7. Yamamoto KR: Steroid receptor regulated transcription of specific genes and gene networks. *Ann Rev Gen.* 1985; 19(1)**:** 209-252.

8. Krstic MD, Rogatsky I, Yamamoto KR, Garabedian MJ: Mitogen-activated and cyclin-dependent protein kinases selectively and differentially modulate transcriptional enhancement by the glucocorticoid receptor. *Mol Cell Biol.* 1997; 17(7)**:** 3947-3954.

9. Wang JC, Derynck MK, Nonaka DF, Khodabakhsh DB, Haqq C, Yamamoto KR: Chromatin immunoprecipitation (ChIP) scanning identifies primary glucocorticoid receptor target genes. *PNAS.* 2004; 101(44)**:** 15603-15608.

10. Lonard DM, O'Malley BW: Nuclear receptor coregulators: Judges, juries, and executioners of cellular regulation. *Molecular Cell.* 2007; 27(5)**:** 691-700.

11. Davies L, Karthikeyan N, Lynch JT, Sial E-A, Gkourtsa A, Demonacos C, *et al*: Cross talk of signaling pathways in the regulation of the glucocorticoid receptor function. *Mol Endocrinol* 2008; 22(6)**:** 1331-1344.

12. So AY-L, Chaivorapol C, Bolton EC, Li H, Yamamoto KR: Determinants of cell- and gene-specific transcriptional regulation by the glucocorticoid receptor. *PLoS Genetics.* 2007; 3(6)**:** e94.

13. Miller A, Komak S, Webb MS, Leiter E, Thompson EB: Gene expression profiling of leukemic cells and primary thymocytes predicts a signature for apoptotic sensitivity to glucocorticoids. *Cancer Cell Int.* 2007; 7(1)**:** 18.

14. Ploner C, Rainer J, Niederegger H, Eduardoff M, Villunger A, Geley S, *et al*: The BCL2 rheostat in glucocorticoid-induced apoptosis of acute lymphoblastic leukemia. *Leukemia.* 2007; 22(2)**:** 370-377.

15. Reddy T, Pauli F, Sprouse R, Neff N, Newberry K, Garabedian M, *et al*: Genomic determination of the glucocorticoid response reveals unexpected mechanisms of gene regulation. *Genome Res.* 2009; 12**:** 2163-2171.

16. Wang Z, Malone MH, He H, McColl KS, Distelhorst CW: Microarray analysis uncovers the induction of the proapoptotic BH3-only protein Bim in multiple models of glucocorticoid-induced apoptosis. *J Biol Chem.* 2003; 278**:** 23861 - 23867.

17. Gascoyne DM, Kypta RM, Vivanco MdM: Glucocorticoids inhibit apoptosis during fibrosarcoma development by transcriptionally activating Bcl-xL* *J Biol Chem.* 2003; 278(20)**:** 18022-18029,.

18. Rocha-Viegas L, Vicent GP, Barañao JL, Beato M, Pecci A: Steroid hormones induce Bcl-X gene expression through direct activation of distal promoter P4 *J Biol Chem.* 2004; 279**:** 9831-9839.

19. Almawi WY, Melemedjian OK, Jaoude MMA: On the link between Bcl-2 family proteins and glucocorticoid-induced apoptosis. *J Leukocyte Biology.* 2004; 76(1)**:** 7-14.

20. Thompson E, Webb M, Miller A, Fofanov Y, Johnson B: Identification of genes leading to glucocorticoid-induced leukemic cell death. *Lipids.* 2004; 39**:** 821 - 825.

21. Ayroldi E, Riccardi C: Glucocorticoid-induced leucine zipper (GILZ): a new important mediator of glucocorticoid action. *FASEB J.* 2009; 23(11)**:** 3649-3658.

22. Jin JY, Almon RR, DuBois DC, Jusko WJ: Modeling of corticosteroid pharmacogenomics in rat Liver using gene microarrays. *J Pharmacol Exp Ther.* 2003; 307(1)**:** 93-109.

23. Thompson EB: Stepping stones in the path of glucocorticoid-driven apoptosis of lymphoid cells. *Acta Biochim Biophys Sin.* 2008; 40(7)**:** 595-600.

24. Schmidt S, Rainer J, Ploner C, Presul E, Riml S, Kofler R: Glucocorticoid-induced apoptosis and glucocorticoid resistance: molecular mechanisms and clinical relevance. *Cell Death & Differ.* 2004; 11(S1)**:** S45-S55.

25. Schoneveld OJ, Gaemers IC, Lamers WH: Mechanisms of glucocorticoid signalling. *Biochimica et Biophysica Acta (BBA) - Gene Structure and Expression.* 2004; 1680(2)**:** 114-128.

26. Ramdas J, Liu W, Harmon JM: Glucocorticoid-induced cell death requires autoinduction of glucocorticoid receptor expression in human leukemic T cells. *Cancer Res.* 1999; 1378-1385.

27. Schmidt S, Irving JAE, Minto L, Matheson E, Nicholson L, Ploner A, *et al*: Glucocorticoid resistance in two key models of acute lymphoblastic leukemia occurs at the level of the glucocorticoid receptor. *FASEB J.* 2006; 20(14)**:** 2600-2602.

28. Geng C-D, Vedeckis WV: c-Myb and members of the c-Ets family of transcription factors act as molecular switches to mediate opposite steroid regulation of the human glucocorticoid receptor 1A promoter. *J Biol Chem.* 2005; 280(52)**:** 43264-43271.

29. Funahashi A, Morohashi M, Kitano H, Tanimura N: CellDesigner: a process diagram editor for gene-regulatory and biochemical networks. *BIOSILICO.* 2003; 1(5)**:** 159-162.

30. Funahashi A, Matsuoka Y, Jouraku A, Morohashi M, Kikuchi N, Kitano H: CellDesigner 3.5: A versatile modeling tool for biochemical networks. *Proceedings of the IEEE.* 2008; 96(8)**:** 1254-1265.

31. Zi Z, Klipp E: SBML-PET: A systems biology markup language-based parameter estimation tool. *Epub.* 2006; 22(21)**:** 2704-2705.

32. Medh RD, Webb MS, Miller AL, Johnson BH, Fofanov Y, Li T, *et al*: Gene expression profile of human lymphoid CEM cells sensitive and resistant to glucocorticoid-evoked apoptosis. *Genomics.* 2003; 81**:** 543 - 555.

33. Samorodnitsky E, Pugh BF: Genome-wide modeling of transcription preinitiation complex disassembly mechanisms using ChIP-chip data. *PLoS Comput Biol.* 2010; 6(4)**:** e1000733.

34. Yao Z, Hoffman EP, Ghimbovschi S, DuBois DC, Almon RR, Jusko WJ: Mathematical modeling of corticosteroid pharmacogenomics in rat muscle following acute and chronic methylprednisolone dosing. *Molecular Pharmaceutics.* 2008; 5(2)**:** 328-339.

35. Wei G, Twomey D, Lamb J, Schlis K, Agarwal J, Stam R, *et al*: Gene expression-based chemical genomics identifies rapamycin as a modulator of MCL1 and glucocorticoid resistance. *Cancer Cell Int.* 2006; 10**:** 331–342.

36. Eisen LP, Elsasser MS, Harmon JM: Positive regulation of the glucocorticoid receptor in human T-cells sensitive to the cytolytic effects of glucocorticoids. *J Biol Chem.* 1988; 263(24)**:** 12044-12048.

37. Hargrove JL, Schmidt FH: The role of mRNA and protein stability in gene expression. *FASEB J.* 1989; 3(12)**:** 2360-2370.

38. Ing NH: Steroid hormones regulate gene expression posttranscriptionally by altering the stabilities of messenger RNAs. *Biology of reproduction.* 2005; 72(6)**:** 1290-1296.

39. Staton JM, Thomson AM, Leedman PJ: Hormonal regulation of mRNA stability and RNA-protein interactions in the pituitary. *J Mol Endocrinol* 2000; 25(1)**:** 17-34.

40. Garcia-Gras EA, Chi P, Thompson EA: Glucocorticoid-mediated destabilization of cyclin D3 mRNA involves RNA-Protein interactions in the 3'-untranslated region of the mRNA*. *J Biol Chem.* 2000; 275(29)**:** 22001-22008.

41. Schaaf MJM, Cidlowski JA: Molecular mechanisms of glucocorticoid action and resistance. *J Steroid Biochem Mol Biol.* 2002; 83(1-5)**:** 37-48.

42. Zawydiwski R, Harmon JM, Thompson EB: Glucocorticoid-resistant human acute lymphoblastic leukemic cell line with functional receptor. *Cancer Res.* 1983; 43(8)**:** 3865-3873.

43. Geley S, Hartmann BL, Hala M, Strasser-Wozak EMC, Kapelari K, Kofler R: Resistance to glucocorticoid-induced apoptosis in human T-cell acute lymphoblastic leukemia CEM-C1 cells is due to insufficient glucocorticoid receptor expression. *Cancer Res.* 1996; 56(21)**:** 5033-5038.

44. Thompson EB, Johnson BH: Regulation of a distinctive set of genes in glucocorticoid-evoked apoptosis in CEM human lymphoid cells. *Recent Progress in Hormone Research.* 2003; 58**:** 175 - 197.

45. Tissing WJE, Meijerink JPP, Brinkhof B, Broekhuis MJC, Menezes RX, den Boer ML, *et al*: Glucocorticoid-induced glucocorticoid-receptor expression and promoter usage is not linked to glucocorticoid resistance in childhood ALL. *Blood.* 2006; 108(3)**:** 1045-1049.

46. Lynch J, Rajendran R, Xenaki G, Berrou I, Demonacos C, Krstic-Demonacos M: The role of glucocorticoid receptor phosphorylation in Mcl-1 and NOXA gene expression. *Molecular Cancer.* 2010; 9(1)**:** 38.

47. Riml S, Schmidt S, Ausserlechner MJ, Geley S, Kofler R: Glucocorticoid receptor heterozygosity combined with lack of receptor auto-induction causes glucocorticoid resistance in Jurkat acute lymphoblastic leukemia cells. *Cell Death Differ.* 2004; 11(S1)**:** S65-S72.

48. Cannarile L, Zollo O, D'Adamio F, Ayroldi E, Marchetti C, Tabilio A, *et al*: Cloning, chromosomal assignment and tissue distribution of human GILZ, a glucocorticoid hormone-induced gene. *Cell Death & Differ.* 2001; 8**:** 201-203.

49. Ito K, Barnes PJ, Adcock IM: Glucocorticoid receptor recruitment of histone deacetylase 2 inhibits interleukin-1beta -induced histone H4 acetylation on lysines 8 and 12. *Mol Cell Biol.* 2000; 20(18)**:** 6891-6903.

50. Zhang Y, Adachi M, Kawamura R, Imai K: Bmf is a possible mediator in histone deacetylase inhibitors FK228 and CBHA-induced apoptosis. *Cell Death & Differ.* 2005; 13(1)**:** 129-140.

51. Holleman A, Cheok MH, den Boer ML, Yang W, Veerman AJP, Kazemier KM, *et al*: Gene-expression patterns in drug-resistant acute lymphoblastic leukemia cells and response to treatment. *N Engl J Med.* 2004; 351(6)**:** 533-542.

52. Laane E, Panaretakis T, Pokrovskaja K, Buentke E, Corcoran M, Soderhall S, *et al*: Dexamethasone-induced apoptosis in acute lymphoblastic leukemia involves differential regulation of Bcl-2 family members. *Haematologica.* 2007; 92(11)**:** 1460-1469.

53. Klipp E, Herwig R, Kowald A, Wierling C, Lehrach H. Systems biology in practice. Concepts, implementation, and application, 1st edn. WILEY-VCH Verlag GmbH & Co. KGaA: Berlin, 2005.

54. Singh H, Singh JR, Dhillon VS, Bali D, Paul H: In vitro and in vivo genetoxicity evaluation of hormonal drugs. II. Dexamethasone. *Mutation Research/Fundamental and Molecular Mechanisms of Mutagenesis.* 1994; 308(1)**:** 89-97.

3 CHAPTER 3: Erg and AP-1 as determinants of glucocorticoid response in acute lymphoblastic leukaemia

To gain a global view on GR resistance in ALL and to extend the previously established models, in **Chapter 3** we perform timecourse microarray analysis in various types of ALL and use experimental and clinical data. This chapter also appeared in "Chen DW-C, Saha V, Liu J-Z, Schwartz J-M and Krstic-Demonacos M. (2012) Erg and AP-1 as determinants of glucocorticoid response in acute lymphoblastic leukemia. Oncogene, doi: 10.1038/onc.2012.321 (In press)" with modfications. In this part of work, D.W.C. prepared the manuscript, conducted data analysis and experiments with contributions from J-M.S. and M.K-D., supervised its analysis and edited the manuscript. S.V. and J-Z L. gathered the microarray data from patients with Philadelphia positive (Ph+) ALL. This section of work was also awarded with the best poster prize from the Childhood Cancer 2012 conference.

3.1 Abstract

Glucocorticoids (GCs) are among the most widely prescribed medications in clinical practice. The beneficial effects of GCs in acute lymphoblastic leukaemia (ALL) are based on their ability to induce apoptosis, but the underlying transcriptional mechanisms remain poorly defined. Computational modelling has enormous potential in the understanding of biological processes such as apoptosis and the discovery of novel regulatory mechanisms. We here present an integrated analysis of gene expression kinetic profiles using microarrays from GC sensitive and resistant ALL cell lines and patients, including newly generated and previously published datasets available from the Gene Expression Omnibus. By applying time series clustering analysis in the sensitive ALL CEM-C7-14 cells, we identified 358 differentially regulated genes that we classified into 15 kinetic profiles. We identified glucocorticoid response element (GRE) sequences in 33 of the upregulated known or potential glucocorticoid receptor (GR) targets. Comparative study of sensitive and resistant ALL showed distinct gene expression patterns and indicated unexpected similarities between sensitivity restored and resistant ALL. We found that AP-1, Erg and GR pathways were differentially regulated in sensitive and resistant ALL. Erg protein levels were substantially higher in CEM-C1-15 resistant cells, c-Jun was significantly induced in sensitive cells, whereas c-Fos was expressed at low levels in both. c-Jun was recruited on the AP-1 site on the Bim promoter whereas a transient Erg occupancy on the GR promoter

was detected. Inhibition of Erg and activation of GR lead to increased apoptosis in both sensitive and resistant ALL. These novel findings significantly advance our understanding of GC sensitivity and can be used to improve therapy of leukaemia.

3.2 Introduction

ALL is the most common type of childhood cancer. GCs are used for the treatment of ALL because of their ability to induce apoptosis in white blood cells whereas in other cell types they have no effect or can increase survival (1). GCs activate GR, which is a transcription factor that upon hormone binding translocates to the nucleus and regulates target gene expression by binding to GREs (2). A better understanding of the mechanism of action of the GCs could identify more potent drugs to prevent resistance development and eliminate side effects, thus facilitating development of better treatment strategies.

GC-induced apoptosis (3) requires Bcl-2 family members and most importantly pro-apoptotic Bim. Bim activates pro-apoptotic Bax through neutralization of pro-survival Bcl-2 like members (3-8). The ability of GCs to selectively induce apoptosis in white blood cells is the main factor contributing to their therapeutic use. The current concept for GC-dependent apoptosis in leukaemia entails the presence of a transcriptionally competent GR (2; 9). In addition, GR auto-induction is specifically observed in some sensitive leukaemia cells, whereas in most epithelial cells GR displays hormone-dependent downregulation of its own mRNA and protein (3; 5; 6; 10; 11). The mechanistic base for this effect is not understood although c-Myb and Ets transcription factors were reported to selectively regulate the GR promoter in different leukaemia cell types (12).

Both activating and repressive functions of the GR have been suggested to play a role in GR mediated apoptosis. One of the major pathways important for GR function is the AP-1 transcription factor composed of the Jun/Fos family of homo and heterodimers. Several levels of control were reported for this crosstalk and both factors were found targeted for phosphorylation by the JNK pathway (13-15). In addition, the interaction between GR, c-Jun and c-Fos is important in determining GR function, as the c-Jun-c-Jun-GR complex causes GC dependent stimulation whereas c-Jun-c-Fos-GR leads to GC dependent repression on the mouse proliferin gene (16). The type of hormone response elements on the target gene, cellular levels of AP-1 and cell types are other major determinants of regulatory factor activities (17). Therefore the outcome of transcriptional regulation through AP-1/GR crosstalk depends on the state of signalling pathways, the response elements and the composition of the protein complexes.

Several studies have successfully used microarray analysis to identify biomarkers or signalling pathways for cancer classification (18; 19). For instance, Segal *et al*. have presented an integrated analysis of microarrays in 22 different types of tumour and identified crucial molecular modules whose activity is coordinated in specific types of tumour (20). A few studies have focused on the analysis of kinetic profiles of gene expression in order to determine the relationship between temporal features of transcriptional control and gene function in relevant signal transduction pathways and cellular processes (21; 22). A microarray study in GC treated T-lymphoblastic cells has shown that approximately 10% of the entire genome is regulated upon GC exposure (23). We have been studying the effect of GCs on the dynamics of downstream targets and were able to construct a basic kinetic model of GR activation (4). The present study of GC induced apoptosis was carried out with the use of microarray time courses in the sensitive ALL cell line CEM-C7-14. In addition, to further understand the genome-wide regulation by GC in ALL, we conducted an integrated analysis of 82 new and previously published arrays (5, 33) derived from ALL patients and cell lines treated for various times with GCs. Together, these analyses indicated a potential functional link between the GR target Bim, AP-1 and the Ets gene family member Erg that has recently been identified as a crucial factor in leukaemia development (24-26). Our results suggest that Erg is expressed markedly in resistant but not in sensitive cells, and that c-Jun is expressed differentially in sensitive versus resistant cell lines. c-Jun is recruited on the AP-1 site in the Bim promoter and Erg is recruited on the GR promoter in a transient fashion in sensitive cells. In contrast, such recruitments were not observed in resistant cells, thus linking c-Jun and Erg to GC resistance in ALL. Finally, we observed increased apoptosis in ALL cells treated with YK-4-279, a functional inhibitor of Erg, Fli1 and Etv1 (27; 28). This approach of studying gene expression kinetics provided a dynamic snapshot of most genes related to GR function and led to identification of a novel mechanism involved in GC resistance that can be a target of future therapies.

3.3 Material and Methods

3.3.1 Cell culture & treatments

GC responsive leukaemia (C7) and GC resistant leukaemia (C1) cell lines (64) were cultured in RPMI-1640 medium supplemented with 10% foetal bovine serum and 1% penicillin and streptomycin (Cambrex, NJ, USA) and were seeded into 60mm plates for RNA extraction. Prior to the hormone treatment the media was changed to RPMI-1640 supplemented with 10% charcoal stripped foetal bovine serum (HyClone, UT, USA). Cells were treated with 1µM Dex (Sigma, MO, USA) at indicated time points (for 0, 2 and 10 h).

3.3.2 RNA extraction

Cells were harvested and the total RNA was extracted using the RNeasy® plus mini kit and QIAshredder (Qiagen), following manufacturer's guidelines and RNA was quantified using a NanoDrop ND-1000 spectrophotometer (NanoDrop Technologies). RNA quality was determined by means of an RNA 6000 NanoAssay on an Agilent 2100 Bioanalyzer.

3.3.3 Microarray and bioinformatics analysis

For each hybridisation, 100ng of total RNA was used in the Affymetrix GeneChip Two-Cycle Target Labeling kit and in the Ambion MEGAscript T7 kit before hybridizing to the GeneChip human genome U133 Plus 2.0 array (Affymetrix) according to manufacturer's instructions. Technical quality control was performed with the dChip software (65). Background correction, normalization, and gene expression analysis were performed using robust multiarray average (RMA) analysis in the Bioconductor software package (66). Differential expression analysis in C7 was performed using routine analytical methods (67). GO mapping, statistical analysis including significance analysis of microarrays (SAM) and Limma t-test, and cluster analysis were performed with the use of the TIGR (The Institute for Genome Research) MultiExperiment Viewer (MeV) program (68) and STEM version 1.3.7 (Carnegie Mellon University) (69). Potential GRE sites were identified using the Transcriptional regulatory element database (TRED) (32) or via text mining tools - The Champion ChiP Transcription Factor Search Portal (CCTSF) from Qiagen SABiosciences's database.

3.3.4 Quantitative real-time polymerase chain reaction

Quantitative real time PCR analysis was performed using the Bio-Rad Chromo4 system (Opticon monitor 3 software version), SensiMix SYBR No-ROX Kit (Bioline), and indicated primer pairs. Relative quantification was performed using standard curves generated for each gene-specific primer pair. Analysis was carried out using the Opticon monitor 3 software as described previously (70). The primers used in this study were: Rpl19: F:ATGTATCACAGCCTGTACCTG; R:TTCTTGGTCTCTTCCTCCTTG; Bim: F: GAGAAGGTAGACAATTGCAG; R:GACAATGTAACGTAACAGTCG; GR: F: GTTGCTCCCTCTCGCCCTCATTC; R: CTCTTACCCTCTTTCTGTTTCTA; c-Jun: F:ACTGCAAAGATGGAAACGAC; R: AAAATGTTTGCAACTGCTGC; c-Fos: F:TCTCTTACTACCACTCACCC; R:TGGAGTGTATCAGTCAGCTC; Erg:

F:CAATCTCGAGCTATGGCCAGCACTATTAAGGAAGC;
R:CAATCCCGGGTTAGTAGTAAGTGCCCAGATGAGAAG.

3.3.5 Immunoblotting analysis

Immunoblotting procedures were as described previously (4). In brief, cells were lysed in HSL buffer (45mM HEPES pH 7.5, 400mM NaCl, 1mM ethylenediaminetetraacetic acid [EDTA], 10% glycerol, 0.5% NP-40, 1mM DTT, 1mM PMSF, protease inhibitor cocktail including 1µg/ml aprotinin, 1µg/ml leupeptin, 1µg/ml pepstatin, 20mM β-glycerophosphate, 5mM sodium pyrophosphate and 2mM sodium orthovanadate). Equal amounts of protein were loaded and resolved by SDS-PAGE, transferred to Immobilon-P membrane (Millipore) using western blot and probed with indicated antibodies. The following antibodies were used: GR (H-300), c-Jun (H79), c-Fos (H-125), Erg (D-3) were purchased from Santa Cruz Biotechnology; Actin and Bim antibodies were purchased from Abcam; Phospho-c-Jun (Ser63) was from Cell Signaling Technology. Blots were developed with the enhanced chemiluminescence substrate according to manufacturer's instructions (Pierce Chemical). The quantification of blots was performed by using the ImageJ software. The relative intensity of c-Jun phosphoisoforms to the total c-Jun was determined by the ratio against the total c-Jun versus actin as seen in Lynch *et al*., 2010 (71).

3.3.6 ChIP Analysis

The procedure for chromatin immnoprecipitation was adapted from (72). Briefly, 5 x 10^7 cells from culture treated with 1µM Dex at indicated time points were cross linked by adding formaldehyde to achieve a final concentration of 1%. Cross-linked chromatin was sonicated to yield a size range from 200 to 1,200 bps (Bioruptor^{TM}, Diagenode) and the debris was removed by centrifugation. The chromatin solution was pre-cleared with protein G beads (Invitrogen) and incubated with the indicated antibodies overnight at 4°C. The used antibodies were non-specific IgG (GE healthcare, Bucks, UK), c-Jun (H79), c-Fos (H-125), Erg (D-3) (Santa Cruz Biotechnology). Following washes and elution, cross-linking was reversed by heating at 65°C for 16 h; DNA was recovered after proteinase K treatment, phenol extraction and ethanol precipitation. Specific sequences in the immunoprecipitates were detected by agarose gel followed by qRT-PCR and the data obtained from qRT-PCR were normalised by the percentage input method **(**Invitrogen). AP-1 binding sites in Bim promoter were identified using the Champion ChiP Transcription Factor Search Portal (Qiagen), the sequences of the primers used were: AP-1 binding site on Bim promoter F: GCAACCTCTCCCAACTTCAG; R:

GCATCACTTGCTGAACCAAA; Erg binding site on GR1A promoter F: CTTGCTCCCTCTCGCCCTCATTC; R: CTCTTACCCTCTTTCTGTTTCTA.

3.3.7 Fluorescence Activated Cell Sorting (FACS) analysis and Annexin V staining

CCRF-CEM cells were plated in six-well plates in RPMI-1640 supplemented with 10% DCC-FBS and incubated overnight. 1µM Dex, 10µM YK-4-279 or 10µM JNK inhibitor (SP600125) were added to the medium and cells were incubated for 48 hours. Apoptosis was assessed using an Annexin V kit (AbD Serotec) according to the instructions of the manufacturer. Briefly, after washing in PBS, cells were resuspended in annexin buffer and incubated with annexin V-FITC for 10 minutes followed by incubation with propidium iodide. All data were acquired on a CyAN ADP flow cytometer and analyzed with the use of Summit software (DakoCytomation).

3.3.8 Description of ALL types used in the analysis

The 63 selected array datasets described in (5; 33) (GEO accession numbers: GSE2677, GSE2842- Suppl. Table 5) were categorized as sensitive, sensitivity restored and resistant ALL including 3 GC-sensitive cell lines, 4 GC-resistant cell lines, 2 GC sensitivity-restored cell lines and 10-child-B-ALL and 3-child-TALL. 14 arrays from Philadelphia positive (Ph+) ALL treated according to the EsPHALL protocol were obtained from Professor Saha. The patients received 8 days of Dex and 1 dose each of anthracycline, vincristine and L-Asparaginase (36). 8 arrays from CEM-C7-14/GC sensitive cell treated with 1µM Dex for 0, 2 and 10 hours were obtained using the core facility in the University of Manchester.

3.3.9 Statistical analysis

All results are reported as mean ± standard deviation (S.D) unless otherwise noted. The Tukey's multiple comparison tests were carried out to analyze western, qRT-PCR, ChIP and Annexin V staining data using SPSS 16.0 (SPSS Statistics).

3.4 Results

3.4.1 Genome-wide identification of GR target time series in CEM-C7-14/ GC sensitive cell lines

Based on our previous study (4), we hypothesised that by identifying different kinetic modes of GR dependent gene expression we could learn more about mechanistic details of the main

determinants of cellular sensitivity to GCs. The CEM-C7-14 cell line sensitive to GC treatment (indicated as C7) was incubated for 0, 2 and 10 hours (h) with synthetic GC dexamethasone (Dex) to identify early and delayed GC response genes (4). Microarray analysis showed altered expression of 2373 genes in total in GC treated cells ($p < 0.05$) (1863 genes after 2 h, 2083 after 10 h). 358 genes were found to have greater than 1.5 fold-change ($p < 0.05$). The short time-series expression miner (STEM) software was used to distinguish between true and random patterns using algorithms specifically designed for clustering and comparing short time series of gene expression data (29). Based on this method, the 358 genes mapped to 15 clusters (Suppl. Table 3.1) with three profiles containing apoptosis related genes (profiles 8, 12, 13) (Fig. 3.1 & Suppl. Table 3.1A & B). There were six profiles that showed gradual repression kinetics (profiles 0-4, 7), while three other profiles showed an oscillatory kinetics (profiles 5, 6, 9). The MYC (c-Myc) gene that is known to be repressed by GC (6) was identified in profile 7, and found to be downregulated at 2 h and 10 h of treatment. Not many genes were repressed in C7 cells treated with Dex for 2 h and most of the downregulation occurred when treated with Dex for 10 h, suggesting that downregulation takes longer than activation. The reason for this phenomenon is unclear, one possible reason is that perhaps upregulating genes are more critical for cells when reacting to the Dex stimulated environment, whilst other potential factors such as the mRNA half life may also contribute to the transcription rate.

There were six profiles with steady activation kinetics; these are profile 8 and 11-15. Profiles 13 and 8 have a more pronounced induction after 2 h whereas profiles 11, 12 and 15 have more linear induction. GR targets such as GR itself, NR3C1, TSC22D3 (Gilz) and NFKBIA (IκBα) displayed such linear kinetics. The distribution of apoptosis related genes in individual profiles was determined using Gene Ontology (GO) mapping via STEM and was indicated below each profile (Fig. 3.1). In five profiles (0, 5, 6, 9, 14, labelled (-)) we were unable to perform GO mapping with STEM as there was no subset of 5 or more genes that belonged to a common GO category at level 3 or below of the GO hierarchy. We also did not identify any apoptotic genes by direct search against the gene ontology. Interestingly, we only identified apoptosis related genes in the GC activating profiles (8, 12, 13). Around a third of the genes were clustered in profile 13, which included 112 genes with a delayed increase in gene expression upon GC treatment (Fig. 3.1 profile 13). Several known GR targets (FKBP5, AKAP13 and ALOX5AP) were also included in this profile. Profile 13 has the highest percentage of apoptosis related genes (17.8%), including BCL2L11 (Bim) and others such as Jun (c-Jun), RUNX2 and DUSP6 (Fig. 3.1 profile 13). Profile 13 also reflects a delayed pattern of GC induced gene expression which correlates with our previous data (4). It has been reported that c-Jun is induced by GCs in

ALL cells and that it targets Bim for activation in neuronal cells (30; 31). These data indicated a potential functional link between the known and crucial GR target Bim and the AP-1 family member c-Jun.

We next examined these 358 genes for the presence of the consensus GRE using the Transcriptional Regulatory Element Database (TRED), 2000 base pairs (bps) up and downstream from the known or predicted transcription start site. We found that in total 33 genes contain the indicated consensus GRE (9; 32) (Suppl. Table 3.1). Out of these, 8 direct GR target genes were previously identified (green) and 25 are potentially novel targets (red). All 33 genes were upregulated by Dex in the GC kinetic profiles 8 and 12-15.

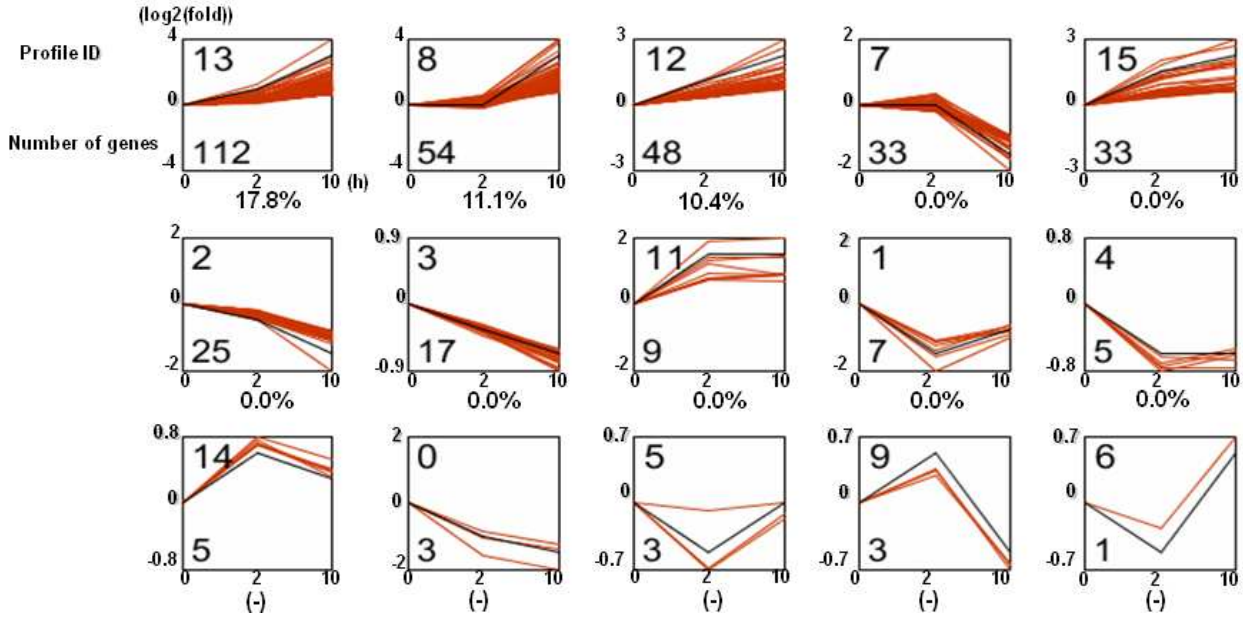

Figure 3.1 STEM clustering of differentially expressed genes in Dex treated C7/GC sensitive cells

Kinetic profiles of significant GC regulated genes ($p < 0.05$, fold-change >1.5) were obtained by microarray analysis in Dex treated C7 cells treated for 0, 2, and 10 h. The x-axis represents time points and the y-axis represents the gene expression ratio. Red lines represent gene expression kinetic profiles of individual genes, the black line represents the reference kinetic profile of each cluster; the percentages represent the number of apoptotic related genes; (-) indicates that no subset of 5 or more genes belong to a common GO category at level 3 (73). Known or potential GREs were identified in 33 genes. Profile 10 does not contain any genes was not included in the figure.

3.4.2 Microarray analysis in GCs treated sensitive and resistant ALL cell lines and patients

To identify potential clinically relevant biomarkers of ALL sensitivity to GCs, we analyzed our microarray data from C7/GC sensitive cells together with data from the Gene Expression Omnibus (GEO) (Suppl. Fig. 3.1 & 3.2) (5; 33). The data include GC sensitive, sensitivity restored and resistant ALL treated with GCs at various times from 0 h up to 24 h (with times between 6-10 h categorized as a single time point) (Suppl. Fig. 3.2). GC sensitivity was restored in resistant CEM-C1^{ratGR} and CEM-C7R1$^{dim\text{-}high}$ cells by over expression of rat GR and human GR^{dim} mutant respectively; the details can be found in supplementary files in (33). In total, 63 arrays from two microarray studies (Affymetrix HGU133 plus 2.0) were combined with our own data obtained from GC treated C7 cells (5 arrays). The data were pre-processed and normalised based on cell subtypes by robust multi-array averaging (RMA) using Bioconductor (34). The log (base 2) of the expression value of genes in each array was calculated via RMA, and the list of significantly altered genes was calculated by significance analysis of microarray (SAM) by grouping ALL data samples according to phenotypes (Table 3-1A & Suppl. Table. 3.2).

Hierarchical clustering was performed to provide a view of the distances between gene expression profiles in different types of ALL. Sensitivity restored ALL were not included in this analysis as the hierarchical clustering showed that the overall genomic profile of sensitivity restored ALL was more similar to resistant than sensitive cells (Suppl. Fig. 3.1). To take the sequential nature of time series data into account, we performed a comparative analysis of two sets of data using STEM (Suppl. Fig. 3.2). We pre-set the number of kinetic profiles (35) in STEM, so as to obtain genes either being linearly up or downregulated by GC to achieve better grouping of gene expression results (Table 3-1A & Suppl. Table 3.2).

An additional 14 arrays were obtained from 10 children with Philadelphia positive (Ph+) ALL treated uniformly. They were categorized as good risk if the marrow had <25% blasts after 8 days of therapy without imatinib and poor risk if the blast count was >25%. During this time they received 8 days of Dex and 1 dose each of anthracycline, vincristine and L-Asparaginase (36). The data was analyzed similarly and the Limma t-test was used to determine significant induction/repression (Table 3-1B & Suppl. Table 3.3).

When the data obtained from the 68 arrays (63 plus 5 arrays as described above) was compared with the 14 arrays obtained from the Ph+ patients, only NFE2, BCL2A1, NCF2 (Ncf2), LGALS3, ERG (Erg) and GBP4 showed a consistent and significant differential

regulation. (Table 3-1, Suppl. Table 3.2 & 3.3). c-Jun was not identified as one of the significantly regulated genes in this case (Table 3-1). In particular, only Ncf2 and Erg had a steady regulatory dynamics, with Erg showing a stronger differential regulation. Ncf2 was upregulated in both sensitive ALL and patients (1.42 log2-fold) and in Ph+ ALL (1.76 log2-fold). Erg was also identified as a significantly differentially regulated gene between sensitive and resistant cell lines ($p < 0.05$, fold-change > 2), as well as between Ph+ ALL patients with good or poor risk. Erg showed a consistent significant repression in both sensitive cell lines (-1.29 log2-fold) and in Ph+ ALL (-2.39 log2-fold) patients with good risk. Such repression was not found in resistant cell lines or in Ph+ ALL patients with bad risk (Suppl. Table 3.2B, Suppl. Table 3.3B). Given the consistency, the magnitude of Erg repression and its role in leukaemia (24), Erg was chosen for further study.

3.4.3 Validation of microarray analysis identifies potential role of the GR/AP-1/Erg in control of the GR and Bim expression

Our microarray analysis pointed towards c-Jun (Fig. 3.1 & Suppl. Table 3.1A) and Erg (Table 3-1) as potential biomarkers of GC response. Direct interactions between Erg, the Jun/Fos complex (also called the AP-1 complex) and various other Ets proteins were shown previously (37). GR auto-regulation in ALL is controlled by Ets family members such as PU.1, c-Ets-1 and c-Ets-2, which downregulate GR auto-induction via a composite hGR1A promoter element in IM-9 B-cells (12). Given the well documented crosstalk between AP-1 and GR pathways (17) and the importance of Erg in leukaemia development (24), we analyzed how these pathways control GR and Bim function since these two genes are major contributors to the GC response. In order to test the predictions of the microarray analysis we determined the protein levels of candidate genes in GC sensitive C7 and GC resistant CEM-C1-15 (indicated as C1) cells treated with GCs (Fig. 3.2 & Suppl. Fig. 3.3). We have detected GC dependent induction of both GR and c-Jun protein levels in C7 but not in C1 cells (Fig. 3.2, lane c-Jun). In contrast, JNK dependent Ser63 phosphorylation that activates c-Jun decreases with hormone treatment in C7 cells (Fig. 3.2A & Suppl. Fig. 3.3, lane p-Jun). In resistant cells the phosphorylation level of c-Jun was generally low with no significant changes in normalised values (Fig. 3.2B and Suppl. Fig. 3.3, lane p-Jun). c-Fos expression was very low and did not change much with GC treatment, whereas the Bim protein level was elevated in sensitive cells treated with Dex but did not change significantly in resistant cells (Fig. 3.2 & Suppl. Fig. 3.3). Importantly, Erg protein levels were markedly higher in C1 cells than in C7 cells (Fig. 3.2 & Suppl. Fig. 3.3-3.4). In C1 cells treated for 24 h with Dex, an upregulation of Erg protein level was found (Suppl. Fig. 3.4).

c-Fos expression was not detected with longer Dex treatment in CEM cells, but was clearly identified in A549 lung cancer cells using the same antibody (Suppl. Fig. 3.4).

To investigate whether the identified changes of protein levels were due to effects on gene expression we determined mRNA levels using qRT-PCR (Fig. 3.3A & B). The results confirmed that Bim, c-Jun and GR were differentially expressed in C7 cells (Fig. 3.3A). mRNA expression levels of Bim and c-Jun were significantly upregulated by >4-fold 10 h after Dex treatment in GC sensitive C7 cells. Similar analysis in Dex treated GC resistant C1 cells indicated an increase in Erg mRNA that was not significant after 10 h of treatment (according to Tukey's test) and a 4-fold significant upregulation in Erg after 24 h treatment, which is much higher than in C7 cells (Fig. 3.3 & Suppl. Fig. 3.4A). Overall, the validation of microarray data pointed to c-Jun and Erg as potentially important biomarkers of GC sensitivity in ALL.

A.

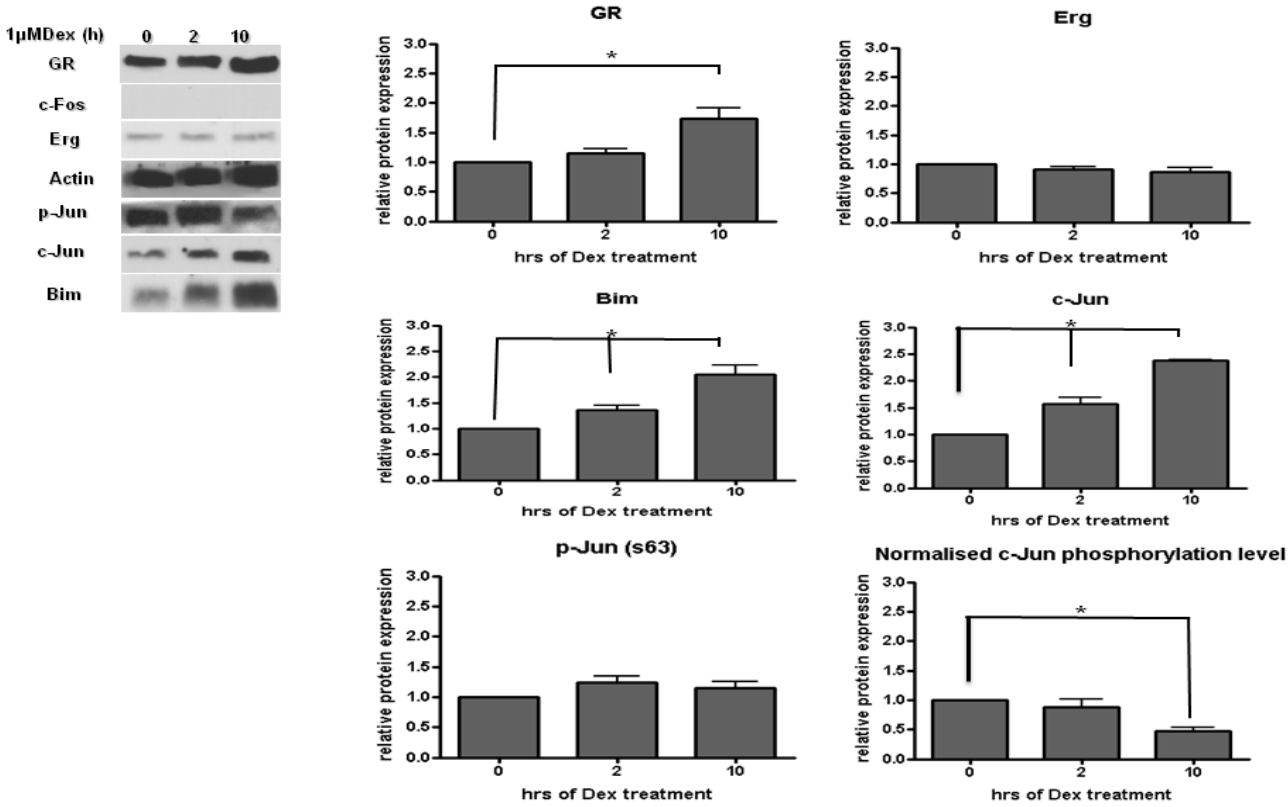

B.

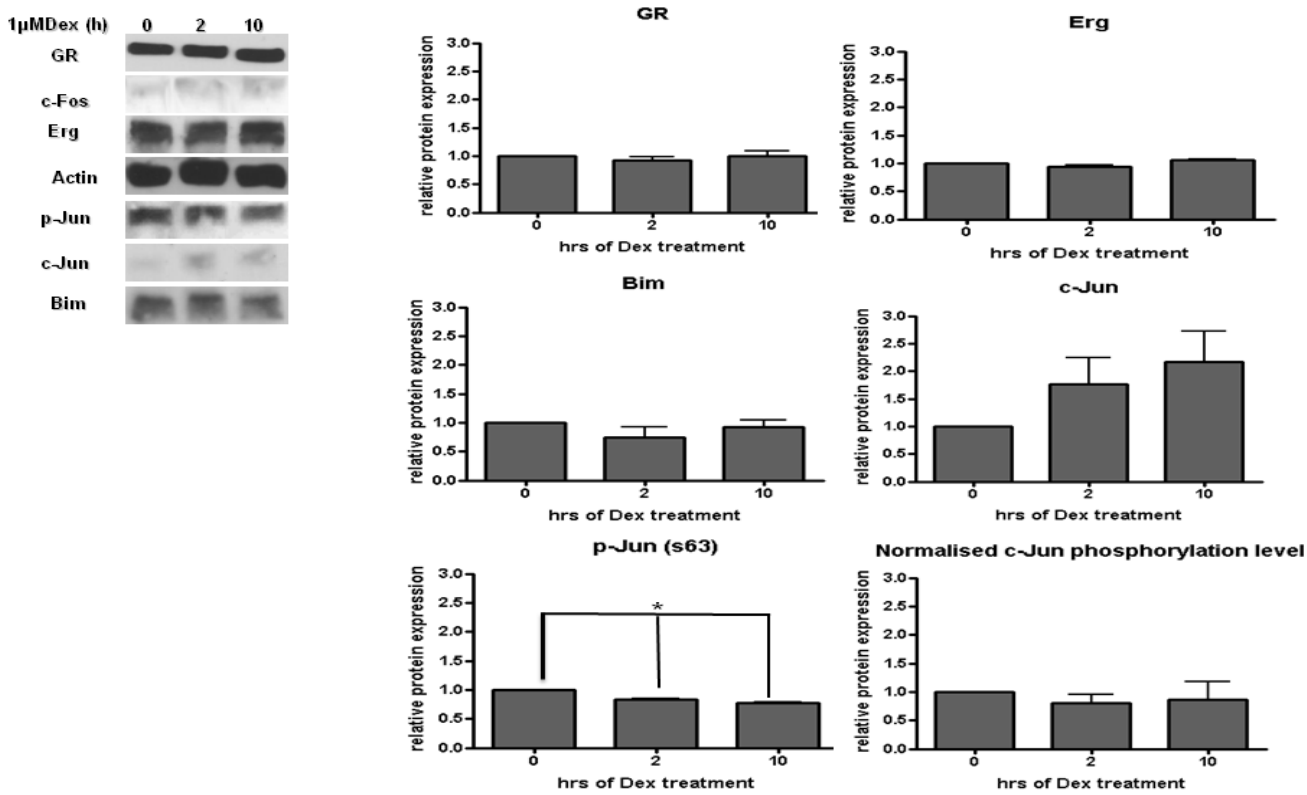

Figure 3.2 Validation of microarray analysis in CEM cells through determination of candidate protein levels

Western blot analysis of GR, c-Fos, Erg, c-Jun, p-Jun (Ser 63) and Bim protein levels, with actin as a control in C7 **(A)** and C1 **(B)** cells cultured with 1μM Dex for the indicated times. Protein levels were quantified by ImageJ, normalised to actin and presented as a histogram. Error bars represent ± standard deviation of three or more independent experiments (additional western blot see Suppl. Fig. 3.3). One representative blot is shown. Asterisk indicates a significant difference at $p < 0.05$.

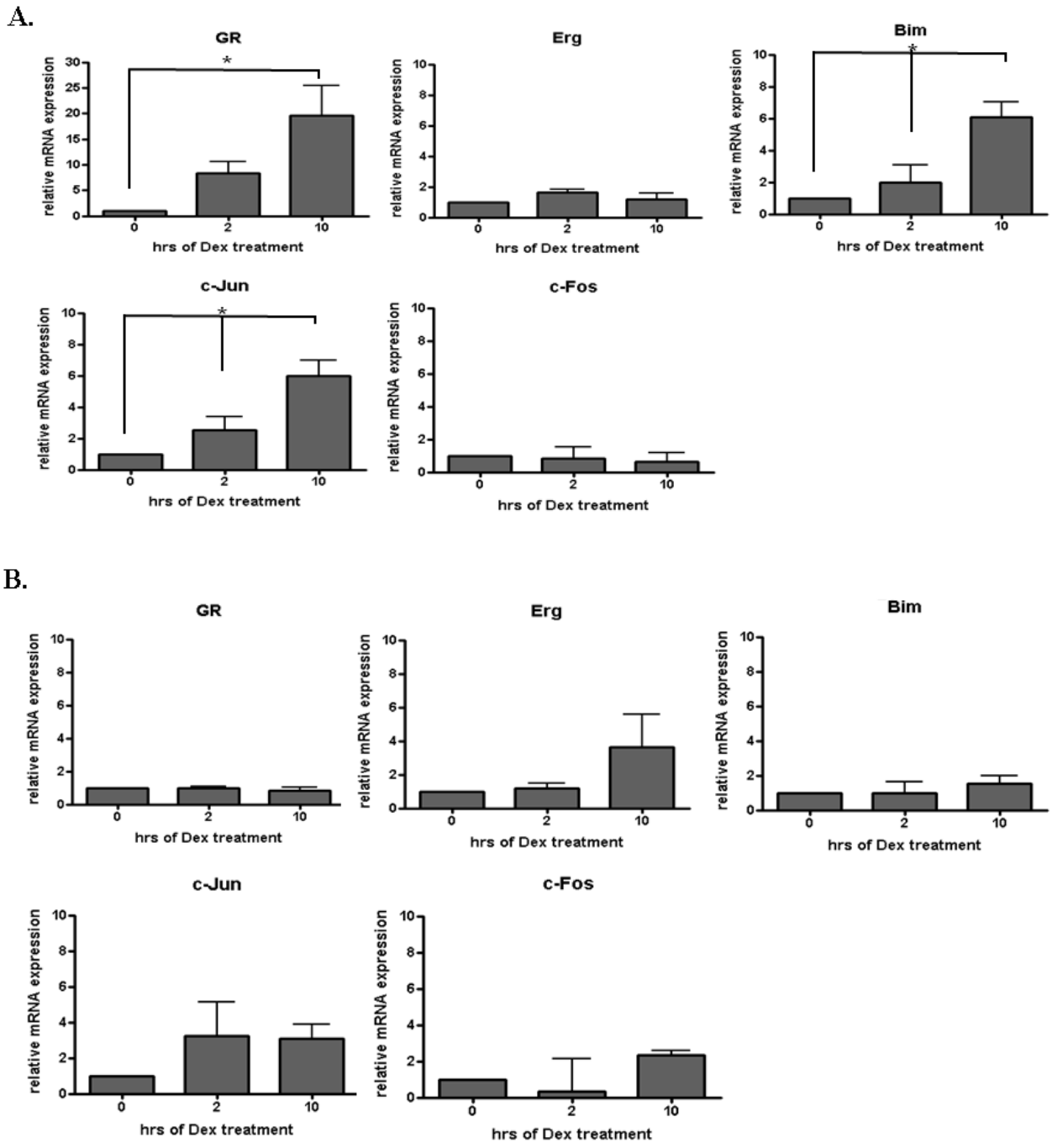

Figure 3.3 Validation of microarray analysis in CEM cells through determination of candidate mRNA levels

C7/GC sensitive **(A)** or C1/GC resistant **(B)** cells were treated with 1μM Dex at the indicated time points and the mRNA levels of GR, c-Fos, Erg, c-Jun, p-Jun (Ser 63) and Bim (normalised to Rpl-19) were determined by qRT-PCR. Error bars represent ± standard deviation of three independent experiments. Asterisk indicates a significant difference at $p < 0.05$.

3.4.4 c-Jun and Erg occupy Bim and GR promoters respectively in GC sensitive C7 cells

We have identified a potential AP-1 response element in the Bim promoter (Suppl. Table. 3.4A) (38). Chromatin immunoprecipitation (ChIP) assays were performed to determine whether Dex affect the c-Jun, c-Fos and Erg occupancy on the Bim promoter at AP-1 site. Dex treatment induced c-Jun binding to the Bim gene after 10 h treatment (Fig. 3.4A), but did not induce c-Fos binding to Bim. As Erg has been found to interact with the AP-1 transcription factor (37), our next aim was to analyze if Erg occupies the AP-1 site on Bim. The result indicated that Erg was not recruited in a hormone dependent manner on the AP-1 binding site in Bim in sensitive cells (Fig. 3.4B).

It was previously shown that Ets family members play a role in GR auto-regulation (12). Based on the previous previous DNA footprinting results, we have identified an Ets consensus sequence near the GR binding site (39). DNA printing is a method of investigating the sequence specificity of DNA-binding proteins in vitro and that protein bound DNA regions can be identified when running on a polyacrylamide gel. This is also called the the "footprint", where the DNA has been protected from the cleavage agent. In this case, the Ets family member consensus sequence GGA(A/T) was found in footprint 12 (FP12), which is adjacent to a half GRE (FP11), and both sites are important for determining hGR1A promoter responsiveness. Here we identified an Erg consensus sequence (C/A) GGAA(G/A) (39) at the same site at footprint 12 (261bps downstream of hGR1A) (Suppl. Table 4B). Erg was efficiently and transiently recruited on the GR1A promoter in sensitive cells (Fig. 3.4C). However, AP-1 and Erg were not efficiently recruited on Bim and GR promoters in resistant cells (Fig. 3.5). Overall, we identified hormone dependent recruitment of c-Jun on the Bim promoter AP-1 site and a transient recruitment of Erg on the hGR1A only in sensitive but not resistant cells.

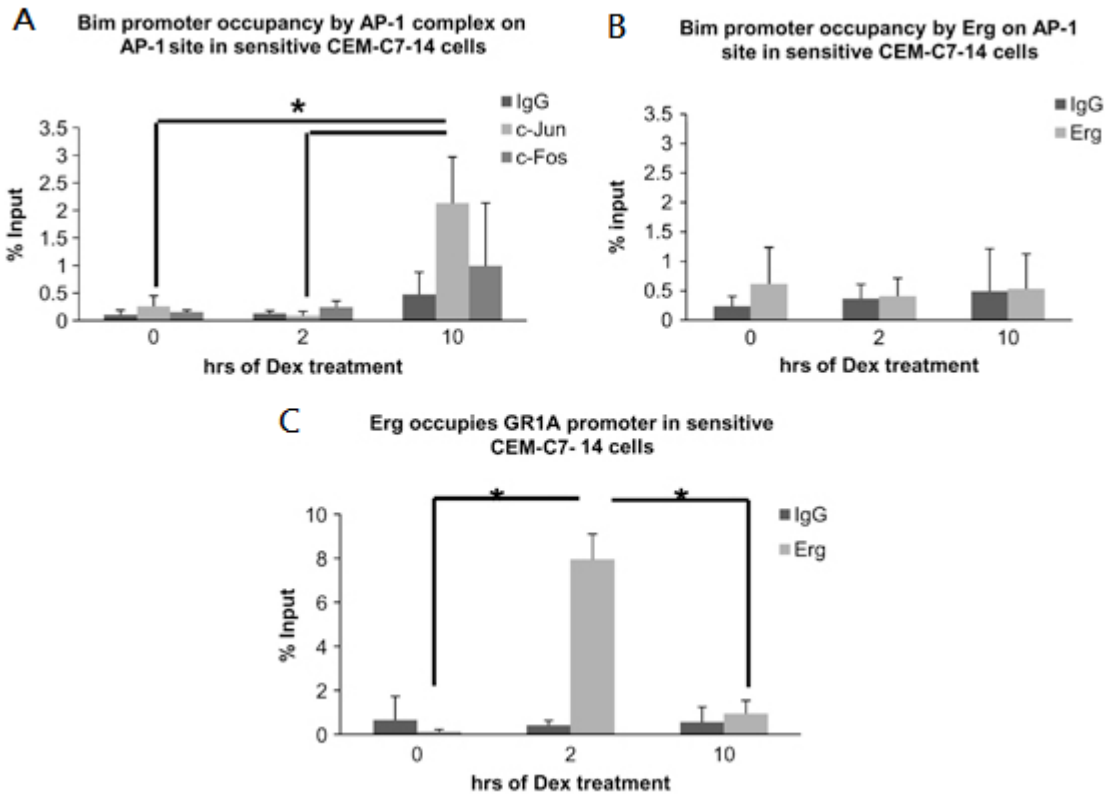

Figure 3.4 ChIP analysis of GR and Bim promoters in GC sensitive C7 cells

We identified a potential AP-1 binding site on the Bim promoter and analyzed c-Jun and c-Fos **(A)**, or Erg **(B)** occupancy on this site in C7 cells treated with 1µM Dex for the indicated times. Similar analysis was performed to determine Erg recruitment on GR1A promoter **(C)**. Error bars represent ± standard deviation of three independent qRT-PCR experiments with triplicates measurements in each experiment. Asterisk indicates a significant difference at $p < 0.05$.

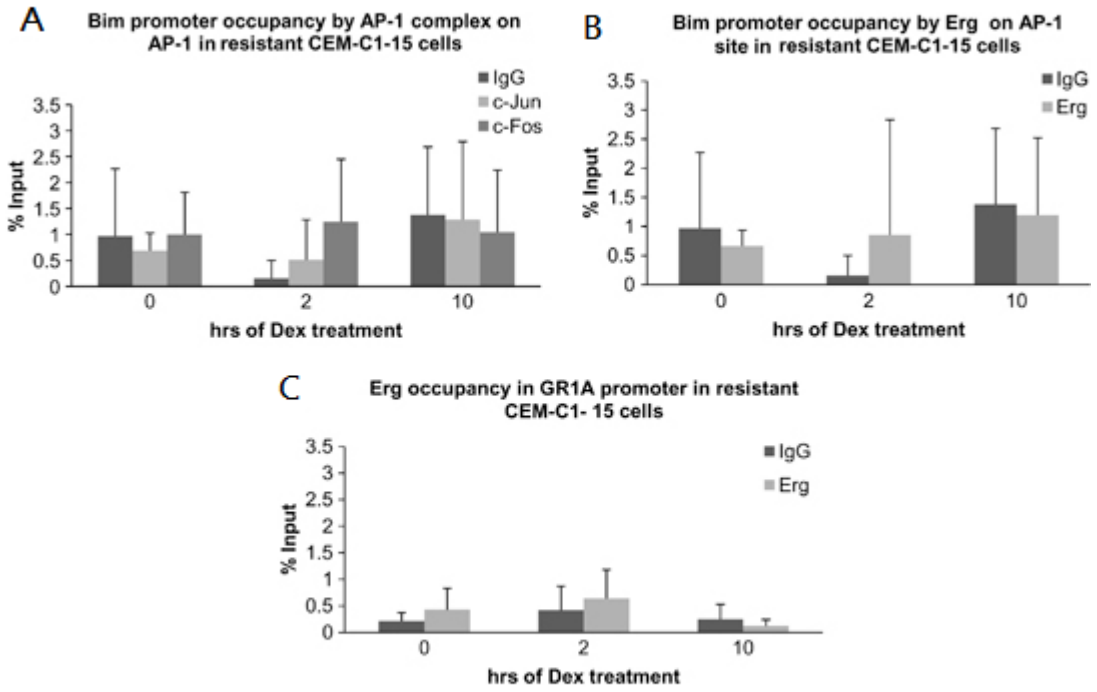

Figure 3.5 ChIP analysis of GR and Bim promoters in resistant C1 cells

ChIP analysis was carried out in resistant C1 cells as described in Fig. 3.4 to analyze c-Jun and c-Fos **(A)**, or Erg **(B)** occupancy on the potential AP-1 binding site on the Bim promoter. Analysis of Erg recruitment on the GR1A promoter **(C)**. Error bars represent ± standard deviation of three independent qRT-PCR experiments with triplicates measurements in each experiment. Asterisk indicates a significant difference at $p < 0.05$.

3.4.5 Erg inhibition increases ALL cell death

Our results indicated that Erg and c-Jun are potentially important molecules in regulating GR gene expression and GC sensitivity. Since the JNK pathway is involved in regulating activity of both GR and AP-1/Erg proteins (40; 41), the JNK inhibitor SP600125 was used to investigate its effects on cell fate. In addition, the YK-4279 compound that inhibits Erg subfamily of proteins (28) was used individually or in combination with Dex to analyze its effects on ALL cellular fate (Fig. 3.6). Dex treatment increased the percentage of apoptotic cells in C7/ GC sensitive but not in C1/GC resistant cells, whereas treatment with the Erg inhibitor caused an increase in apoptotic

cells in C1 but not C7 cells. Combination of Dex and YK-4279 treatment increased apoptotic cell death in both cell lines. Treatment of C7 and C1 lines with JNK inhibitor resulted in a minor but insignificant increase in apoptosis, whereas it significantly increased apoptosis when combined with Dex in C7 cells. These results indicated that inhibiting Erg and JNK pathways in hormone treated cells displays selective effects on apoptosis of sensitive and resistant cells. More importantly, the results showed that Erg have a potent apoptotic effect with and without Dex treatment in CEM cells and that the inhibition of Erg may have a role in restoring GR sensitivity in resistant C1 cells.

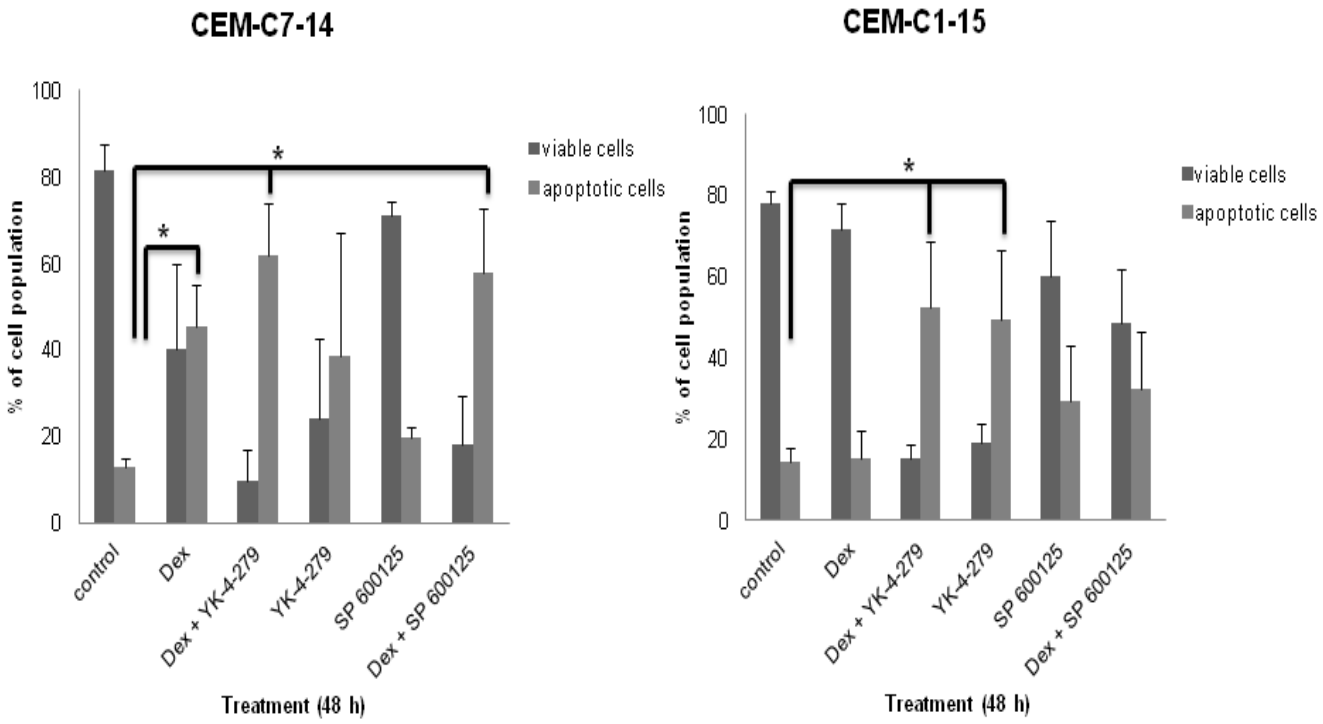

Figure 3.6 Differential effect of Erg and JNK inhibitors on cell fate in glucocorticoid sensitive versus resistant cells

The number of viable and apoptotic Dex sensitive C7 and resistant C1 cells in the presence of indicated compounds was measured by annexin V-PI staining using FACS analysis. Cells were treated individually or in combination with 1µM Dex, 10µM Erg inhibitor (YK-4279), 10µM JNK inhibitor (SP600125) for 48 h. Error bars represent ± standard deviation of three independent experiments. Asterisk indicates a significant difference at $p < 0.05$.

3.5 Discussion

The molecular basis of glucocorticoid-induced apoptosis and resistance is not fully understood. Our microarray analysis identified the association between AP-1, c-Jun and Erg in relation to GR function in leukaemia. As the pro-apoptotic Bim gene is a crucial node in GR mediated apoptosis and a known c-Jun target in neuronal cells (31), we analyzed the interplay of these factors in the control of Bim function. This was also applied to the control of GR auto-regulation (12).

15 kinetic profiles of GR regulated genes were found in GC treated C7/GC sensitive cells for 0, 2 and 10 h. 268 out of 358 genes were activated by the GR, suggesting that activation is more prevalent in leukaemia. The analysis also identified sets of early and delayed responsive genes to GCs (Fig. 3.1). These findings highlight the importance of studying the kinetics of gene expression and suggest that GR utilizes differential regulatory mechanisms to control target gene transcription. GRE containing (9) and apoptotic genes were exclusively found in GC activated clusters (Fig. 3.1), suggesting that GCs activate rather than repress most of the apoptotic genes in C7 cells.

We have identified c-Jun as a crucial target in GR and Bim regulation (Fig. 3.2 and Fig. 3.3) (30; 31). This result was supported by the observation that c-Jun is induced by GCs in leukaemia and targets Bim in neuronal cells (29, 30). We determined that c-Jun is recruited to the Bim promoter in C7 cells only (Fig. 3.4-3.5). A recent study indicated that AP-1 facilitates cell specific GR recruitment by maintaining chromatin accessibility. The complex crosstalk between GR and AP-1 transcription factors involves both mutual activation and inhibition (17), but our data indicate that the major regulatory effect occurs through GR dependent c-Jun upregulation, which then selectively activates Bim gene expression in a cell specific manner (Fig. 3.2-3.5). On the other hand, there was virtually none or very low expression of the AP-1 subunit c-Fos in CEM cells and no relevant recruitment was observed on the Bim promoter (Fig. 3.2-3.5). It is thought that the c-Jun-c-Fos heterodimer leads to GC dependent repression and that the c-Jun-c-Jun homodimer causes GC dependent stimulation in some target genes (42). We did not observe c-Fos level increase/recruitment on Bim promoter in the resistant C1 cells. It should be noted that the arrangement of GR and AP-1 binding sites is another major determinant of the regulatory factor's activities (43). For instance, when two sites are not closely juxtaposed, GR and AP-1 act synergistically regardless of the composition of AP-1, however, if the two sites are close to each other (14-18bps) then they behave as a composite GRE where activation/inhibition

occurs in a context dependent fashion (44; 45). Furthermore, the interaction of AP1 and GR with other transcription factors such as the glucocorticoid-induced leucine zipper (Gilz) can influence the GC response (46). Taken together, the interaction between GR, c-Jun and c-Fos is regulated at multiple levels including AP-1 composition, DNA binding specificity and interaction with other transcription factors. Precise details of this crosstalk and the role of c-Fos in GC response require additional research.

The activity of c-Jun is regulated by the JNK pathway. In T-ALL, the c-Jun/JNK pathway has been implicated in both pro- and anti-apoptotic effects (47; 48). However, c-Jun induction was observed in C7 cells and in T-ALL patients after GC treatment and a higher basal expression of c-Jun was detected in sensitive than in the resistant T-ALL (30; 49). A recent study indicated that c-Jun may potentially be activated through p38 MAPK as well thereby regulating Bim and inducing apoptosis (50; 51). JNK dependent c-Jun phosphorylation at Ser63 and Ser73 has been linked to c-Jun activation (52). The change in Ser63 phosphorylation in c-Jun has been shown to correlate with protection of BimEL from degradation (48). c-Jun phosphorylation at Ser63 has also been implicated in nitric oxide induced apoptosis in neural tumours (53). In addition, JNK targets GR for phosphorylation and this is proposed to inhibit GR activity at certain promoters. Therefore JNK could have a dual role in apoptosis through stimulation of c-Jun and Bim phosphorylation and inhibition of GR activity. Further investigations of the role of c-Jun phosphorylation in GC induced apoptosis of ALL cells are thus required.

Microarray analysis of patients' and cell line data, generated by this and previous studies (5, 33) (Table 3-1 & Suppl. Table 3.2) identified Erg as one of the significant differentially regulated genes between sensitive and resistant ALL. This is consistent with results found in children with Philadelphia positive (Ph+) ALL where Erg repression was found in patients with good risk (Suppl. Table 3.2B & 3.3B). This repression was however not identified in GC sensitive C7 cells, though there was a marked differential Erg expression compared to the resistant CEM cells (Fig. 3.2 & Suppl. Fig. 3.4A). As the microarray analysis was based on the phenotypes only, various subtypes or other factors may introduce noise in the analysis, which also explains why Jun was not identified.

Erg belongs to an Ets transcription factor family deregulated in prostate cancer and fused to Ewing's sarcoma (EWS) family members (54). The important role of Erg in cell proliferation in leukaemia has been found in many recent studies (24-26), where high Erg expression is an adverse prognostic factor in adult T-ALL patients (55; 56). Our results suggest that Erg is

expressed markedly in resistant cells only (Fig. 3.2 and 3.3) and that prolonged Dex treatment for 24 h differentially induces Erg protein and mRNA in resistant cells (Fig. 3.2 & 3.3; Suppl. Fig. 3.4A).

Crosstalk between Ets family and GR has been described previously (12). In GC responsive T cells, the c-Myb transcription factor increases GR auto-regulation, whereas Ets family members such as PU.1 have repressive effect in GC resistant B lymphocytes. However, Ets1-2 factors, which suppress Dex induction of the hGR1A promoter, also cause a large increase in basal promoter activity. In addition, the authors proposed that other Ets factors may be involved in earlier hGR1A transcriptional control in T cells (12). Our data identified Erg as a potential candidate for such a function, either through basal regulation or as a pioneer factor. However, we could not detect any Erg occupancy that is hormone dependent on the hGR1A promoter in C1 cells despite high Erg protein levels in these cells (Fig. 3.2, Fig. 3.5B & Suppl. Fig. 3.4). It is possible that unlike PU.1, Erg does not play a role in repressing the GR promoter in C1 cells or that it binds somewhere else on the promoter.

It seems that Erg and c-Jun have opposite expression patterns (Fig. 3.2, 3.3 & Suppl. Fig. 3.4). Crosstalk of AP-1 and Ets transcription factors has been described (57), showing that they regulate gene transcription in a sequence, position, binding affinity and stimulus dependent manner. A genome-wide analysis of Erg occupancy identified an overlap with AP-1 at prototypical Ras responsive elements, but Erg activates transcription from these elements in a Ras/MAPK independent manner (45). Thus it is possible that overexpression of Erg in C1 cells reflects disturbed feedback loops between AP-1, Erg, MAPK pathways and GR. The importance of this balance is reflected in other studies where AP-1 was found to facilitate chromatin accessibility and GR binding (44).

An anti-apoptotic effect of Erg has been identified in umbilical vein endothelial cells (58) corroborating our results where the inhibition of Erg subfamily members increases apoptosis (Fig. 3.6). Such effect is GC dependent in sensitive and GC independent in resistant cells. The anti-apoptotic role of Erg may be due to various factors. Firstly, it has been found that siRNA specific for Erg directly downregulates c-Myc in prostate epithelial cells (59). The repression of c-Myc is known to be important in initiating apoptosis in GC treated CEM cells (60), which indicates a potential role of Erg in inhibiting apoptosis via regulation of c-Myc. However, such regulatory mechanism remains questionable as Löffler *et al.* demonstrated that the repression of c-Myc is not critical for cell death (61). In leukaemia, an association between Erg and Notch1

mutations was identified. As Notch1 is important in conferring GC resistance, this suggests another possible mechanism through which Erg can control GC dependent apoptosis (24). Other roles such as fusion with Ewing's sarcoma (EWS) family protein members (62) and potential regulation of anti-apoptotic Bcl-X_L (63) may also be considered. Although our study highlights the anti-apoptotic effect of Erg (as shown in Fig. 3.6), we observed a transient Erg recruitment on the GR promoter in GC sensitive C7 cells. Since the repressive role of Ets proteins in GR regulation has been proposed (12), the effect of Erg transient recruitment on GR promoter in GC induced apoptosis of C7 cells remains to be determined.

To summarize, we propose that GC sensitivity in ALL is controlled through a series of feedback loops operating in differential temporal patterns that will at least in part determine cellular levels of GR, AP-1, Erg and Bim, ultimately contributing to cell fate. In GC treated C7 cells, GR becomes activated and alters Bim and GR transcription, potentially through AP-1 and Erg recruitment respectively. Such recruitments were not seen in C1 cells. Other factors such as MAPK signalling and c-Myb may play a role in regulating GR, AP-1 and Bim, possibly through binding to the GR promoter. These relations could be used for improvement of current therapies and provide the basis for potential differential treatment of leukaemia.

3.6 Tables

Table 3-1 List of statistically significantly expressed genes over time in both sensitive ALL and (Ph+) ALL patients with good risk**.**

STEM analysis of 68 microarrays obtained from cell lines and ALL patients. The lists of significant genes were clustered to identify the genes that showed a consistent and significant differential regulation throughout the analysis. The table indicates the mean difference (log2 scale) between sensitive and resistant ALL. (B) STEM analysis of 14 microarrays obtained from Philadelphia positive (Ph+) ALL treated according to the EsphALL protocol at Day 0 and Day 17 (36). The table shows the correlated gene expression of the candidates obtained from Table 1A. All human gene symbols indicated here are annotated according to the Gene Ontology database.

3-1A Sensitive ALL: cell lines and patients

Consistently upregulated genes (log2 fold)

Gene Symbol	0h	6-10h	24h
NCF2	0	0.69	1.42
BCL2A1	0	1.06	0.63
NFE2	0	1.21	0.52
LGALS3	0	1.04	0.47

Consistently downregulated genes (log2 fold)

Gene Symbol	0h	6-10h	24h
ERG	0	-1.06	-1.29
GBP4	0	-1.36	-1.17

3-1B: Philadelphia positive (Ph+) ALL patients showing good risk

Consistently upregulated genes (log2 fold)

Gene Symbol	Day 0	Day 17
NCF2	0	1.76
BCL2A1	0	2.33
NFE2	0	1.91
LGALS3	0	2.78

Consistently downregulated genes (log2 fold)

Gene Symbol	Day 0	Day 17
ERG	0	-2.39
GBP4	0	-2.79

3.7 Supplementary data

3.7.1 Supplementary Figures

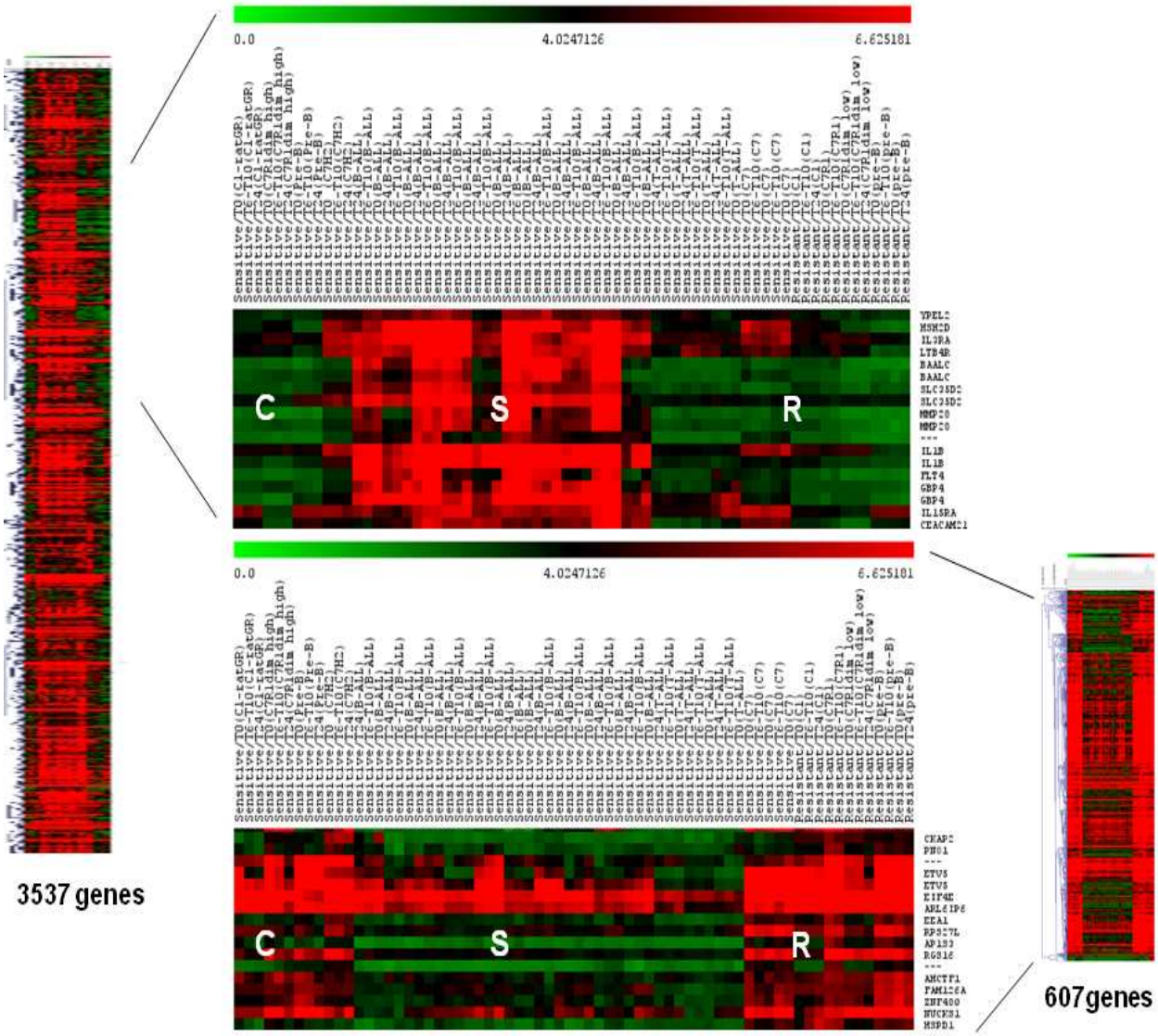

Suppl. Figure 3.1 The heatmap obtained using hierarchical clustering of genes differentially regulated in the sensitive ALL (S), sensitivity restored (C) and resistant ALL(R)

The heatmap was generated via MeV with hierarchical clustering of our own and published data (5, 33). Differential patterns were observed in sensitive versus resistant cells with surprising similarities identified in the expression patterns between sensitivity restored and resistant ALL. Comparing sensitive to resistant ALL, 3537 genes were upregulated (left panels), whereas 607 genes were downregulated (right panels). Proportion of genes displayed in the outer panels was magnified and displayed in the middle panels for clarity.

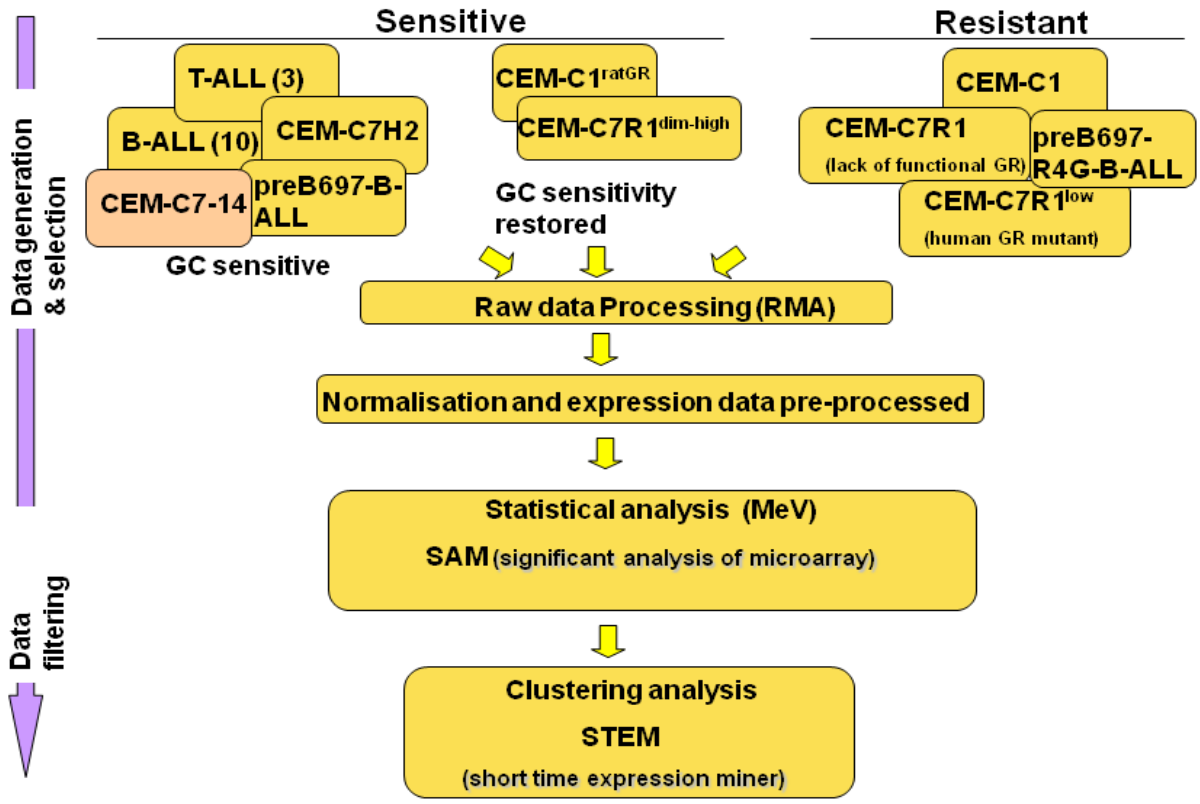

Suppl. Figure 3.2 Summary of the comparative expression profiling strategy and work flow

The details of the summary of work flow are described in the results section. A number of ALL subclones (CCRF-CEM and preB697) and patients (T- and B-ALL) microarray data were chosen from published reports (5, 33) and our data (Suppl. Table 3.1). ALL samples were categorized by phenotypic traits and further analyzed. Additional data obtained from children with Philadelphia positive (Ph+) ALL were also used for analysis (36).

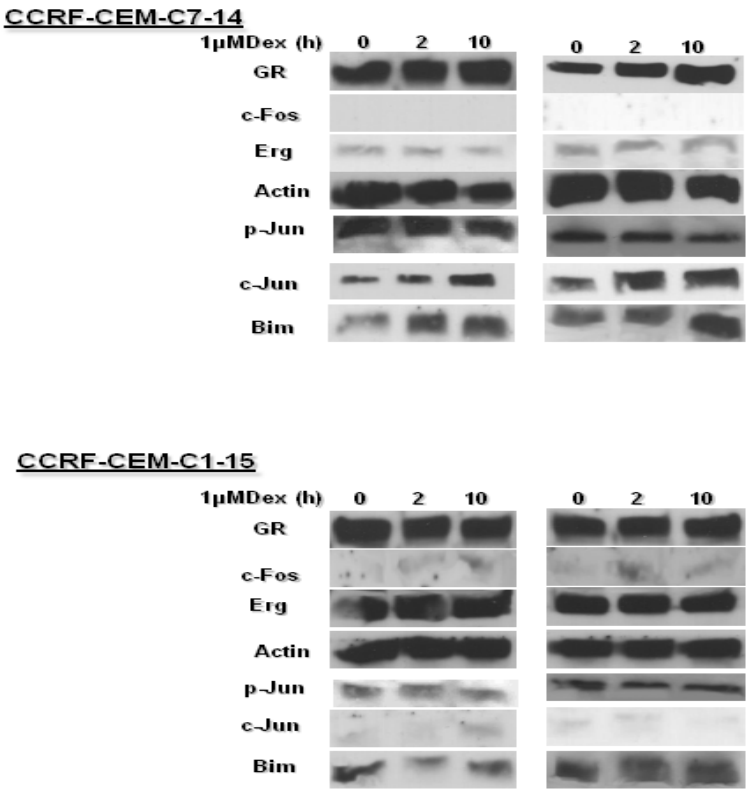

Suppl. Figure 3.3 Validation of microarray analysis in CEM-C7-14 and CEM-C1-15 cells through determination of candidate protein levels

Additional western blot analysis was performed as described in the Fig. 3.2, thus providing three independent experiments in total. Protein levels were quantified and results were included in histograms as shown in the Fig. 3.2. GR, c-Fos, Erg, c-Jun, p-Jun and Bim protein levels were normalised using actin as a control in CEM-C7-14 and CEM-C1-15 cells cultured with 1µM dexamethasone (Dex) for the indicated times.

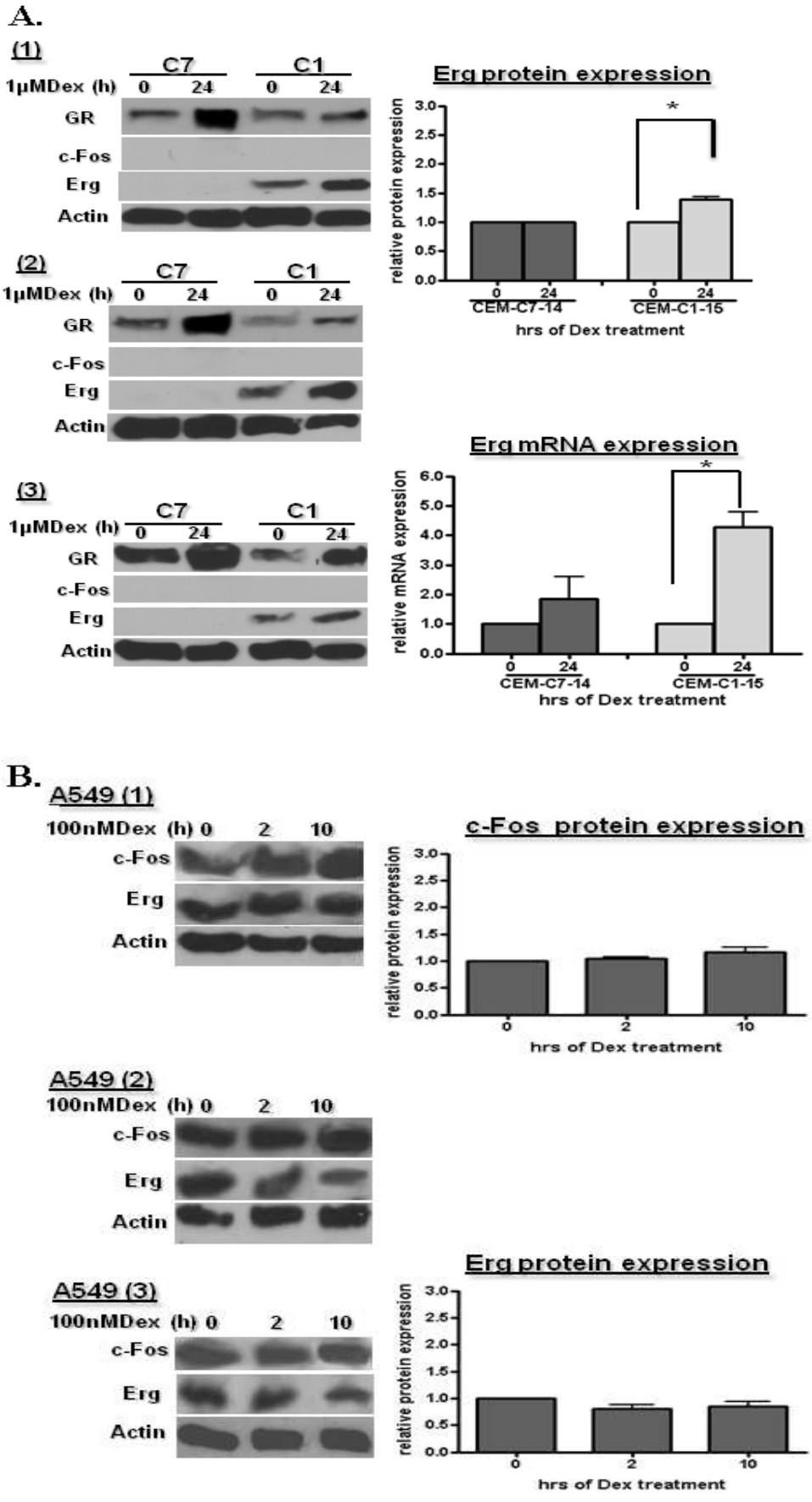

Suppl. Figure 3.4 Effect of prolonged treatment on protein and mRNA levels of candidate genes in CEM-C7-14, CEM-C1-15 and in epithelial A549 cells

(A) GR, c-Fos, Erg, c-Jun and Bim protein levels were analyzed using western blot, with actin as a control in CEM-C7-14 and CEM-C1-15 cells cultured with 1μM dexamethasone (Dex) for the 0 and 24 h. Erg mRNA level was also determined with qRT-PCR. **(B)** c-Fos, and Erg protein levels were measured using Western blot analysis, with actin as a control in A549 cells cultured with 100nM dexamethasone (Dex) for the 0, 2 and 10 h. Protein levels were quantified by ImageJ, normalised to actin and presented as a histogram. Error bars represent mean values ± standard deviation of three or more independent experiments. One representative blot is shown. Asterisk indicates a significant difference at $p < 0.05$.

3.7.2 Supplementary Tables

Suppl. Table 3.1 The table indicates all the significant GC regulated genes that were clustered using STEM in Dex treated CEM-C7-14 cells.

(A) Using TRED, regions between -2000 and 2000 bases relative from the known or predicted transcription start site (TSS), were scanned. Known GR targets were identified according to So et al., 2007 (9). Potential GREs were identified in known GR targets (green) and potential novel GR targets (red). Asterisk indicates the genes that were assigned under the GO term apoptosis. (B) The significant GC regulated gene list in CEM-C7-14 cells with their affymetrix accession numbers and the fold changes in log2 scale.

<u>Suppl. Table 3.1A</u> Description of gene expression kinetic profiles in time course Dex treated CEM-C7-14 using STEM. The table indicates all the significant GC regulated genes that were clustered using STEM in Dex treated CEM-C7-14.

Cluster ID	Gene Symbol							
Profile 13	HIPK1	---	ADAM 9	ABCA1	NINJ2	TGFB R2	*FKBP5*	TSHZ3
	BCL2L 11	ARSK	AKAP 2 /// PALM2-AKAP2	IRF9	ZFPM2	C18O RF1	ISG20	HEMGN
	ADAM TS19	VCL	PALM 2-AKAP2	USP20	CAMK1D	SLC1 A4	CD79A	CHFR
	CCDC 141	TXNIP	STIM 1	RNF144A	ELMO2	STK1 6	LY96	LMBR1
	CHD2	JUN	C10O	*ALOX5A*	HKDC1	PFKF	PRKCA	OCR1

			RF26	*P*			B2				
	ASXL2	*ITGA6*	CD93	*3*	*C7ORF2*	LBH	S3	HAU	*TNFSF8*	CDH23	
	WFS1	CPD	KIF3C		FLI1	PLXNA1	2	SYNJ	KIR3DL2 /// LOC727787	3	TMEM17
	PIK3IP 1	TRIB1	CD53	6	C9ORF1	FAIM3	*1*	*LAIR*	*IL10*	9 /// SPATA13	C1QTNF
	LEF1	DUSP6	RSAD 2		*PLXND1*	KLHL24	*M*	*MCA*	*AKAP13*		*STK11IP*
	FGFR1	NPNT	HIST1 H2BC		PIK3R1	UBE2H	*2*	*TNKS*	CCR4		RCSD1
	GABA RAPL1 /// GABARAPL3		*ELL2*	KIR3 DL3	TUBA4A	AFF3	GEF3	ARH	CLEC16A		SH3TC1
	KIR2D S2		*SFXN5*	RUNX 2	PBXIP1	PTRH1	N2	SPO	NEK1		*KLF2*
	EWSR 1 /// FLI1	/// TBC1D10A	GATSL3	CCDC 92	AIM1	GRASP	1	LZTS	B	UBASH3	*PRDM1*
	CABIN 1	18	LOC6415	C7OR F38	IPO11 /// LRRC70	PRAGMIN		JAM3	ZNF438		TAGAP
Profile 12	SEPSE CS		BTG2	SPOC K2	PITRM1	DEGS1		CD7	KATNAL1		TBCD
	APH1A		OTUB1	CLPP	UGP2	SWAP70	K	DSTY	104	C10ORF	TAF8
	KLHL1 8		*NFKBIA*	FAM1 3A	FLJ10038	SOCS1	1	PLCH	DAB2IP		SERAC1
	TBC1D 1		FAT1	CDK9	YAF2	ITK	P10	DUS	RAPH1		WDR6
	PTPR C		CLCN3	DGKA	GRAP2	NBEAL2	3D	TUBA	SMAP2		BHLHE23
	GLUL		TRAM2	SLA	GABARA PL1	NUMA1	PLD1	CRIS	66	LOC1501 196	C20ORF
Profile 15	SLFN5		BTG1	NFIL3	ATP2A3	ST3GAL6	28	MED	RSPRY1		BIVM
	FIP1L1		*NR3C1*	ARHG AP29	*CXCR4*	TAF6L	MD3	GRA	FLJ36031		SYNJ2BP
	HERP UD2		*DDIT4*	SMAR CA2	10 TRAPPC	09 C14ORF1	3	KLF1	32884	LOC1001	ZNF805
	NUCB		*TLN1*	*TSC2*	CD69	*RNASET2*		MST1	NCRNA0		PSMG4

	1			*2D3*					50		0081	
	SLC25A44											
Profile 8	SLC18A2	LOC100130872	DFNA5		SAP30	CROCC	MET TL7A		LBA1	CXORF57		
	MGC2848	FHL1	RBMS1		SNTB2	*GLRX*	RCAN1		TRAF3IP2	CORO1C		
	CUGBP2	SRGN	DNAJB4		SCRG1	FAM65B	ABCC5		KIR2DS4	ELK3		
	PTPRM	RASA1	TSNAX		IL7R	KLRC1 /// KLRC2	TFPI		PTEN /// PTENP1	C4ORF34		
	SPATA13	ANK2	LCMT2		JAK2	*CH25H*	*BIRC3*		AZI2	CAMK1D /// LOC283070		
	MACROD2	PRKAR2B	PTEN		DISC1	DLX2	*MYO1B*		SESN1	PAQR8		
	USP53	ROR1	*PAX6*	LOC389043		ZFPM1	PIGV					
Profile 2	PHTF2	MAPK6	RPL14		RPRD1A	GNAQ	LONRF1		LYSMD2	ISYNA1		
	HES1	MEF2C	NKX6-1		RGMA	C20ORF112	SPSB1		KLHL8	MBLAC2		
	LIG4	KCTD15	C5ORF30		LOC100293563	ARL6IP6	STARD4		SFRS1	TMEM65		
	CAMK4											
Profile 7	TRPV6	SOX12	LTB		RGS16	ENDOD1	NOTCH1		APLN	CCDC61		
	MXI1	SASH3	RPGR		PPAT	PCSK5	TMEM120B		LYAR	ZNF280B		
	MYC	SERPINI1	CBFA2T3		SLC19A1	C19ORF6	BATF3		SLC16A9	MIR17HG		
	SATB1	SLC16A7	PAK2		MAK16	TMEM38B	C10ORF92		NDUFAF4	NUDT19		
	LOC440900											
Profile 11	RBBP6	ZFP36L2	C6ORF108		PRKCE	HNRNPUL1	GTF2H5		CALR	HCG_1774568 /// LOC100291311		
	YOD1											

Profile 0	APOF, PSMB4, MTPAP
Profile 5	SMAD4, CEP170, C6ORF62
Profile 4	ATP2B2, MSL3, CYP3A5, POLR3K, TMEFF2
Profile 1	KRT5, FOLR1, MCOLN3, MALAT1, SLC25A30, REXO1, MUC20
Profile 14	ZNF836, *BACH1*, C12ORF35, *ALS2CR8*, STYX
Profile 9	PTPN2, C5ORF33, HPDL
Profile 6	UTRN
Profile 3	IGSF10, AHCTF1, RPL27A, RPS11, LOC100133109, YRDC, ELOVL4, CAMSAP1, ELOVL4, CAMSAP1, COL4A3BP, ZIC2, STAMBPL1, DDIT4L, C21ORF45, NEO1, ETV5, FBXO45, OSTM1

Suppl. Table 3.1B Significant GC regulated genes and the corresponding Affymetrix ID and fold changes in Dex treated CEM-C7-14 using STEM

Gene Symbol	Affyt ID	Profile ID	0h	2h (Log2-fold)	10h
HIPK1	1552516_A_AT;212293_AT	13	0	0	0.8
BCL2L11	1553096_S_AT;1555372_AT;1558143_A_AT;208536_S_AT;222343_AT;225606_AT	13	0	1	1.91
ADAMTS19	1553179_AT;1553180_AT	13	0	0	0.75
CCDC141	1553645_AT	13	0	0	0.89
CHD2	1554014_AT	13	0	0	0.62
ASXL2	1555266_A_AT;218659_AT;226251_AT	13	0	0	0.89
WFS1	1555270_A_AT;202908_AT	13	0	0	1.21
PIK3IP1	1555632_AT;221756_AT;221757_AT	13	0	0	1.62

---	1556402_AT;1556462_A_AT;1556777_A_AT;1557174_A_AT;1565105_AT;1568682_A_AT;1570439_AT;202648_AT;212952_AT;213048_S_AT;213747_AT;215147_AT;220494_S_AT;222968_AT;224989_AT;226458_AT;226725_AT;226821_AT;228443_S_AT;229359_AT;229670_AT;229733_S_AT;229934_AT;230003_AT;230053_AT;230161_AT;231083_AT;231310_AT;232125_AT;232431_AT;232576_AT;234032_AT;234111_AT;234326_AT;235207_AT;235428_AT;235735_AT;235962_AT;236395_AT;236934_AT;236999_AT;237009_AT;237018_AT;238281_AT;238826_X_AT;239105_AT;239328_AT;239571_AT;239817_AT;240015_AT;240118_AT;240195_AT;240237_AT;241617_X_AT;241925_X_AT;242406_AT;242494_AT;242568_S_AT;242929_AT;243039_AT;243495_S_AT;243509_AT;243868_AT;244665_AT	13	0	0	0.6
ARSK	1569132_S_AT;1569133_X_AT	13	0	0	0.72
VCL	200931_S_AT	13	0	0	0.64
TXNIP	201008_S_AT;201009_S_AT;201010_S_AT	13	0	0	1.32
JUN	201464_X_AT;201465_S_AT;201466_S_AT	13	0	0	1.76
ITGA6	201656_AT;215177_S_AT	13	0	0	1.85
CPD	201940_AT;201942_S_AT	13	0	0	0.96
TRIB1	202241_AT	13	0	1	3.79
ADAM9	202381_AT	13	0	0	0.89
AKAP2 /// PALM2-AKAP2	202759_S_AT;226694_AT	13	0	0	0.97
PALM2-AKAP2	202760_S_AT	13	0	0	1.09
STIM1	202764_AT	13	0	0	1.03
C10ORF26	202808_AT	13	0	0	0.78
CD93	202878_S_AT	13	0	0	0.86
KIF3C	203390_S_AT	13	0	0	0.89
CD53	203416_AT;242946_AT	13	0	0	1.21
ABCA1	203504_S_AT;203505_AT	13	0	0	1.9
IRF9	203882_AT	13	0	0	0.61
USP20	203965_AT	13	0	0	0.81
RNF144A	204040_AT	13	0	0	0.64
ALOX5AP	204174_AT	13	0	0	0.64
C7ORF23	204215_AT	13	0	0	0.67
FLI1	204236_AT;210786_S_AT	13	0	0	0.85
C9ORF16	204480_S_AT	13	0	0	0.75
FKBP5	204560_AT;224840_AT;224856_AT	13	0	1	2.48
ISG20	204698_AT;33304_AT	13	0	1	2.68

CD79A	205049_S_AT	13	0	0	0.69
LY96	206584_AT	13	0	0	1.66
PRKCA	206923_AT	13	0	0	0.82
TNFSF8	207216_AT;241819_AT	13	0	1	2.84
KIR3DL2 /// LOC727787	207313_X_AT;207314_X_AT; 211688_X_AT;216907_X_AT	13	0	0	0.77
IL10	207433_AT	13	0	1	1.72
AKAP13	208325_S_AT;209534_X_AT;221718_S_AT;222024_S_AT;224884_AT	13	0	0	1.27
CCR4	208376_AT	13	0	0	1.2
DUSP6	208893_S_AT	13	0	0	0.63
TGFBR2	208944_AT	13	0	0	1.03
C18ORF1	209573_S_AT;209574_S_AT	13	0	0	0.92
SLC1A4	209610_S_AT;209611_S_AT;212810_S_AT;212811_X_AT	13	0	0	0.68
STK16	209622_AT	13	0	0	1.02
PFKFB2	209992_AT;226733_AT	13	0	1	2.03
HAUS3	210054_AT	13	0	0	0.64
SYNJ2	210612_S_AT;212828_AT	13	0	0	0.84
LAIR1	210644_S_AT	13	0	0	0.65
MCAM	210869_S_AT	13	0	0	0.75
LEF1	210948_S_AT;221557_S_AT	13	0	0	1.21
FGFR1	210973_S_AT	13	0	0	0.7
GABARAPL1 /// GABARAPL3	211458_S_AT	13	0	0	0.97
KIR2DS2	211532_X_AT	13	0	0	0.63
EWSR1 /// FLI1	211825_S_AT	13	0	0	0.8
PLXND1	212235_AT	13	0	0	0.61
PIK3R1	212239_AT	13	0	0	0.92
TUBA4A	212242_AT	13	0	0	1.49
PBXIP1	212259_S_AT	13	0	0	0.79
AIM1	212543_AT	13	0	0	1.7
CLEC16A	212786_AT	13	0	0	0.66
NEK1	213331_S_AT	13	0	0	0.61
RSAD2	213797_AT;242625_AT	13	0	0	1.02
HIST1H2BC	214455_AT	13	0	0	0.92
KIR3DL3	216676_X_AT	13	0	0	0.65
RUNX2	216994_S_AT;232231_AT;236858_S_AT	13	0	1	2.19
CCDC92	218175_AT	13	0	0	0.9
TNKS2	218228_S_AT	13	0	0	0.86
ARHGEF3	218501_AT	13	0	0	0.93
SPON2	218638_S_AT	13	0	0	0.81
LZTS1	219042_AT;47550_AT	13	0	0	0.98
SH3TC1	219256_S_AT	13	0	0	1.07
KLF2	219371_S_AT	13	0	0	1.18

NINJ2	219594_AT	13	0	0	0.61
ZFPM2	219778_AT	13	0	0	0.95
CAMK1D	220246_AT;235626_AT	13	0	0	0.79
ELMO2	220363_S_AT;55692_AT	13	0	0	0.9
HKDC1	220585_AT	13	0	0	0.89
LBH	221011_S_AT	13	0	0	0.64
PLXNA1	221538_S_AT	13	0	0	0.62
FAIM3	221601_S_AT	13	0	0	0.7
KLHL24	221985_AT;221986_S_AT;226158_AT	13	0	0	1.01
UBE2H	222420_S_AT	13	0	0	0.75
TSHZ3	223392_S_AT;223393_S_AT	13	0	0	0.95
HEMGN	223669_AT;223670_S_AT	13	0	0	1.58
CHFR	223931_S_AT	13	0	0	0.6
LMBR1	224036_S_AT	13	0	0	0.84
OCR1	224270_AT	13	0	0	0.59
CDH23	224527_AT	13	0	0	1.19
TMEM173	224916_AT	13	0	0	0.74
C1QTNF9 /// SPATA13	225564_AT	13	0	0	1.23
STK11IP	225713_AT	13	0	0	0.63
RCSD1	225763_AT	13	0	0	0.83
NPNT	225911_AT	13	0	0	1.03
ELL2	226099_AT	13	0	0	1.14
SFXN5	226373_AT	13	0	0	0.68
GATSL3 /// TBC1D10A	226613_AT;233528_S_AT	13	0	0	1.32
AFF3	227198_AT	13	0	0	0.66
PTRH1	228014_AT	13	0	0	0.98
GRASP	228263_AT	13	0	1	1.32
UBASH3B	228353_X_AT;228359_AT;238462_AT;238587_AT	13	0	0	1.71
PRDM1	228964_AT	13	0	0	1.86
TAGAP	229723_AT	13	0	0	1.45
ZNF438	229743_AT	13	0	0	0.77
JAM3	231721_AT	13	0	0	0.92
PRAGMIN	235085_AT	13	0	0	1.36
IPO11 /// LRRC70	238488_AT	13	0	0	0.65
C7ORF38	238609_AT	13	0	0	0.61
LOC641518	243363_AT	13	0	0	1.03
CABIN1	37652_AT	13	0	0	0.61
SLC18A2	1553328_A_AT;205857_AT	8	0	0	1.68
MGC2848	1553935_AT	8	0	0	1.29
CUGBP2	1554569_A_AT;202156_S_AT;202157_S_AT;202158_S_AT;227178_AT	8	0	0	1.04
PTPRM	1555579_S_AT;203329_AT	8	0	0	1.42
SPATA13	1556601_A_AT	8	0	0	0.83

MACROD2	1563209_A_AT;235278_AT	8	0	0	2.97
LOC100130872	1569496_S_AT	8	0	0	0.88
FHL1	201539_S_AT;201540_AT;210298_X_AT;210299_S_AT;214505_S_AT	8	0	0	1.57
SRGN	201858_S_AT;201859_AT	8	0	0	1.02
RASA1	202677_AT;210621_S_AT	8	0	0	0.99
ANK2	202920_AT	8	0	0	1.42
PRKAR2B	203680_AT	8	0	0	1.22
DFNA5	203695_S_AT	8	0	0	1.93
RBMS1	203748_X_AT;207266_X_AT;209868_S_AT;225269_S_AT	8	0	0	0.67
DNAJB4	203810_AT	8	0	0	0.72
TSNAX	203983_AT	8	0	-0	0.75
LCMT2	204013_S_AT	8	0	0	0.66
PTEN	204053_X_AT;211711_S_AT	8	0	0	1.06
SAP30	204899_S_AT;204900_X_AT	8	0	0	0.79
SNTB2	205315_S_AT;226685_AT;227312_AT;238925_AT	8	0	0	0.97
SCRG1	205475_AT	8	0	0	1.51
IL7R	205798_AT;226218_AT	8	0	0	3.13
JAK2	205842_S_AT	8	0	0	1.24
DISC1	206090_S_AT	8	0	-0	1.39
CROCC	206274_S_AT	8	0	0	1.48
GLRX	206662_AT;209276_S_AT	8	0	0	1.01
FAM65B	206707_X_AT;209829_AT	8	0	0	1.29
KLRC1 /// KLRC2	206785_S_AT	8	0	-0	0.85
CH25H	206932_AT	8	0	0	2.54
DLX2	207147_AT	8	0	0	0.9
METTL7A	207761_S_AT	8	0	0	1.79
RCAN1	208370_S_AT;215253_S_AT	8	0	0	2.03
ABCC5	209380_S_AT;226363_AT	8	0	0	1.18
TFPI	209676_AT;210664_S_AT;210665_AT;213258_AT;215447_AT	8	0	0	1.06
BIRC3	210538_S_AT	8	0	0	2.35
MYO1B	212364_AT	8	0	0	1.96
LBA1	213261_AT	8	0	0	1.07
TRAF3IP2	215411_S_AT	8	0	0	0.86
KIR2DS4	216552_X_AT	8	0	0	0.63
PTEN /// PTENP1	217492_S_AT	8	0	0	1.28
AZI2	218043_S_AT;222498_AT;223846_AT;227904_AT;227905_S_AT	8	0	0	1.74
SESN1	218346_S_AT	8	0	0	0.85
CXORF57	219355_AT	8	0	0	1.57
CORO1C	221676_S_AT;222409_AT	8	0	0	1.34
ELK3	221773_AT	8	0	0	0.88
C4ORF34	224990_AT	8	0	0	0.62

CAMK1D /// LOC283070	226382_AT;226959_AT	8	0	0	0.8
PAQR8	226423_AT;227626_AT	8	0	0	1.11
USP53	230083_AT;231817_AT;237465_AT	8	0	0	1.71
ROR1	232060_AT	8	0	0	1.35
PAX6	235795_AT	8	0	0	0.71
LOC389043	240546_AT	8	0	0	3.11
ZFPM1	242282_AT	8	0	-0	0.65
PIGV	51146_AT	8	0	0	0.84
SEPSECS	1553167_A_AT	12	0	0	0.63
APH1A	1554417_S_AT	12	0	0	0.71
KLHL18	1557165_S_AT	12	0	0	0.63
TBC1D1	1568713_A_AT;1569566_AT	12	0	1	0.99
PTPRC	1569830_AT	12	0	0	0.65
GLUL	200648_S_AT;215001_S_AT;217202_S_AT	12	0	1	1.56
BTG2	201235_S_AT	12	0	0	0.81
OTUB1	201246_S_AT	12	0	0	0.61
NFKBIA	201502_S_AT	12	0	1	1.35
FAT1	201579_AT	12	0	0	0.94
CLCN3	201732_S_AT;201734_AT;201735_S_AT	12	0	0	0.83
TRAM2	202368_S_AT	12	0	0	0.62
SPOCK2	202524_S_AT	12	0	0	1.11
CLPP	202799_AT	12	0	0	0.65
FAM13A	202973_X_AT	12	0	0	0.62
CDK9	203198_AT	12	0	0	0.65
DGKA	203385_AT;211272_S_AT	12	0	0	0.67
SLA	203760_S_AT;203761_AT	12	0	1	1.38
PITRM1	205273_S_AT	12	0	0	0.77
UGP2	205480_S_AT	12	0	0	0.78
FLJ10038	205510_S_AT	12	0	0	0.96
YAF2	206238_S_AT;244783_AT	12	0	0	0.71
GRAP2	208406_S_AT	12	0	1	1.16
GABARAPL1	208869_S_AT	12	0	0	0.72
DEGS1	209250_AT	12	0	0	0.66
SWAP70	209307_AT	12	0	0	0.84
SOCS1	209999_X_AT;210001_S_AT	12	0	1	2.05
ITK	211339_S_AT	12	0	0	0.64
NBEAL2	212443_AT	12	0	1	1.09
NUMA1	214251_S_AT	12	0	0	0.59
CD7	214551_S_AT	12	0	0	0.79
DSTYK	214663_AT	12	0	0	0.63
PLCH1	214745_AT	12	0	0	0.64
DUSP10	215501_S_AT;221563_AT	12	0	1	1.06
TUBA3D	216323_X_AT	12	0	0	0.6

CRISPLD1	223475_AT	12	0	1	2.36
KATNAL1	223790_AT	12	0	1	0.87
C10ORF104	224665_AT	12	0	0	0.61
DAB2IP	225020_AT	12	0	0	0.85
RAPH1	225188_AT	12	0	0	0.77
SMAP2	225282_AT	12	0	1	1.3
LOC150166	229101_AT	12	0	0	0.66
TBCD	229192_S_AT	12	0	0	0.79
TAF8	229412_AT	12	0	0	0.59
SERAC1	232183_AT	12	0	0	0.63
WDR6	233573_S_AT	12	0	0	0.59
BHLHE23	234045_X_AT	12	0	0	0.67
C20ORF196	243507_S_AT	12	0	0	0.67
TRPV6	1559405_A_AT	7	0	0	-0.8
MXI1	202364_AT	7	0	-0	-0.6
MYC	202431_S_AT	7	0	-0	-1
SATB1	203408_S_AT	7	0	0	-0.6
SOX12	204432_AT	7	0	0	-0.6
SASH3	204923_AT	7	0	-0	-0.6
SERPINI1	205352_AT	7	0	0	-0.9
SLC16A7	207057_AT;210807_S_AT;241866_AT	7	0	-0	-0.7
LTB	207339_S_AT	7	0	0	-1
RPGR	207624_S_AT	7	0	-0	-0.7
CBFA2T3	208056_S_AT	7	0	0	-0.7
PAK2	208876_S_AT	7	0	0	-0.6
RGS16	209325_S_AT	7	0	0	-0.7
PPAT	209433_S_AT;209434_S_AT	7	0	-0	-0.7
SLC19A1	211576_S_AT	7	0	-0	-0.6
MAK16	211686_S_AT	7	0	-0	-0.6
ENDOD1	212570_AT;212573_AT	7	0	-0	-1.1
PCSK5	213652_AT	7	0	-0	-0.7
C19ORF6	213985_S_AT	7	0	-0	-0.7
TMEM38B	218772_X_AT	7	0	-0	-0.6
NOTCH1	218902_AT	7	0	-0	-0.7
TMEM120B	219154_AT	7	0	0	-0.7
BATF3	220358_AT	7	0	0	-0.6
C10ORF92	220539_AT	7	0	0	-0.7
APLN	222856_AT	7	0	-0	-1.3
LYAR	223413_S_AT;223414_S_AT	7	0	0	-0.8
SLC16A9	227506_AT	7	0	-0	-1
NDUFAF4	227559_AT	7	0	-0	-0.8
CCDC61	228475_AT	7	0	-0	-0.6
ZNF280B	230789_AT	7	0	0	-0.9
MIR17HG	232291_AT	7	0	-0	-0.7
NUDT19	235384_AT	7	0	-0	-0.7

LOC440900	243795_S_AT	7	0	-0	-0.6
SLFN5	1553055_A_AT	15	0	1	0.78
FIP1L1	1554424_AT	15	0	1	0.96
HERPUD2	1558699_A_AT	15	0	0	0.71
NUCB1	200646_S_AT	15	0	1	0.65
BTG1	200920_S_AT;200921_S_AT	15	0	2	2.5
NR3C1	201865_X_AT;201866_S_AT;211671_S_AT;216321_S_AT	15	0	1	1.63
DDIT4	202887_S_AT	15	0	1	1.2
TLN1	203254_S_AT	15	0	0	0.59
NFIL3	203574_AT	15	0	1	1.97
ARHGAP29	203910_AT	15	0	1	1.06
SMARCA2	206542_S_AT	15	0	0	0.62
TSC22D3	207001_X_AT;208763_S_AT	15	0	2	2.83
ATP2A3	207521_S_AT;213042_S_AT	15	0	0	0.67
CXCR4	209201_X_AT;211919_S_AT	15	0	1	0.9
TRAPPC10	209412_AT	15	0	0	0.59
CD69	209795_AT	15	0	1	1.87
ST3GAL6	210942_S_AT;213355_AT	15	0	1	1.74
TAF6L	213211_S_AT	15	0	0	0.6
C14ORF109	213246_AT	15	0	0	0.59
RNASET2	217983_S_AT	15	0	0	0.68
MED28	218438_S_AT	15	0	0	0.64
GRAMD3	218706_S_AT	15	0	1	1.13
KLF13	219878_S_AT;225390_S_AT	15	0	1	1.83
MST150	223276_AT	15	0	1	1.8
RSPRY1	225774_AT	15	0	1	0.9
FLJ36031	227883_AT	15	0	0	0.68
LOC100132884	228899_AT	15	0	1	0.7
NCRNA00081	232885_AT	15	0	0	0.59
BIVM	233255_S_AT	15	0	0	0.64
SYNJ2BP	235722_AT	15	0	0	0.76
ZNF805	238437_AT	15	0	1	0.76
PSMG4	242055_AT	15	0	1	0.92
SLC25A44	32091_AT	15	0	0	0.71
PHTF2	1554822_AT	2	0	-0	-0.6
HES1	203394_S_AT;203395_S_AT	2	0	-0	-1.5
LIG4	206235_AT	2	0	-0	-0.9
MAPK6	207121_S_AT	2	0	-0	-0.6
MEF2C	209199_S_AT	2	0	-0	-0.8
KCTD15	218553_S_AT	2	0	-0	-0.6
RPL14	219138_AT	2	0	-0	-0.6
NKX6-1	221366_AT	2	0	-0	-0.6
C5ORF30	221823_AT	2	0	-0	-0.7

RPRD1A	222559_S_AT	2	0	-0	-0.8
RGMA	223468_S_AT	2	0	-0	-0.8
LOC100293563	224375_AT	2	0	-0	-0.6
GNAQ	224862_AT	2	0	-0	-0.6
C20ORF112	225224_AT	2	0	-0	-0.7
ARL6IP6	225711_AT	2	0	-0	-0.7
LONRF1	226038_AT	2	0	-0	-0.8
SPSB1	226075_AT	2	0	-0	-0.8
STARD4	226390_AT	2	0	-0	-0.8
LYSMD2	226748_AT	2	0	-0	-0.7
KLHL8	226874_AT	2	0	-0	-0.6
SFRS1	227164_AT	2	0	-0	-0.8
ISYNA1	228552_S_AT	2	0	-0	-0.7
MBLAC2	230298_AT	2	0	-0	-0.7
TMEM65	241342_AT	2	0	-0	-0.7
CAMK4	241871_AT	2	0	-0	-0.8
IGSF10	1556579_S_AT	3	0	-0	-0.9
AHCTF1	1560224_AT;226115_AT	3	0	-0	-0.7
RPL27A	212044_S_AT	3	0	-0	-0.9
RPS11	213350_AT	3	0	-0	-0.7
LOC100133109	213826_S_AT	3	0	-0	-0.8
YRDC	218647_S_AT	3	0	-0	-0.7
ELOVL4	219532_AT	3	0	-0	-0.7
CAMSAP1	220409_AT	3	0	-0	-0.7
COL4A3BP	223465_AT	3	0	-0	-0.9
ZIC2	223642_AT	3	0	-0	-0.6
STAMBPL1	227606_S_AT	3	0	-0	-0.6
DDIT4L	228057_AT	3	0	-0	-0.7
C21ORF45	229671_S_AT	3	0	-0	-0.7
NEO1	229877_AT	3	0	-0	-0.6
ETV5	230102_AT	3	0	-0	-0.8
FBXO45	242294_AT	3	0	-0	-0.7
OSTM1	243287_S_AT	3	0	-0	-0.6
RBBP6	1552329_AT	11	0	1	0.64
ZFP36L2	201367_S_AT;201368_AT;201369_S_AT	11	0	1	1.39
C6ORF108	204238_S_AT	11	0	1	0.59
PRKCE	206248_AT;226101_AT	11	0	1	0.62
HNRNPUL1	209675_S_AT	11	0	1	0.62
GTF2H5	213357_AT;232905_AT	11	0	1	0.49
CALR	214315_X_AT	11	0	1	0.97
HCG_1774568 /// LOC100291311	220354_AT	11	0	1	0.62
YOD1	227309_AT	11	0	1	1.02
KRT5	201820_AT	1	0	-1	-0.4
FOLR1	211074_AT	1	0	-1	-0.5
MCOLN3	220484_AT	1	0	-1	-0.4

MALAT1	223578_X_AT	1	0	-1	-0.5
SLC25A30	226782_AT	1	0	-1	-0.3
REXO1	233939_AT	1	0	-1	-0.4
MUC20	243774_AT	1	0	-1	-0.4
ATP2B2	211586_S_AT	4	0	-1	-0.5
MSL3	214009_AT	4	0	-1	-0.6
CYP3A5	214235_AT	4	0	-1	-0.5
POLR3K	222766_AT	4	0	-1	-0.6
TMEFF2	224321_AT	4	0	-1	-0.7
ZNF836	1569076_A_AT	14	0	1	0.38
BACH1	204194_AT	14	0	1	0.35
C12ORF35	218614_AT	14	0	1	0.49
ALS2CR8	219834_AT	14	0	1	0.37
STYX	235180_AT	14	0	1	0.3
APOF	207262_AT	0	0	-0	-0.7
PSMB4	228204_AT	0	0	-1	-1.1
MTPAP	229676_AT	0	0	-1	-0.8
SMAD4	1565703_AT	5	0	-1	-0.2
CEP170	207719_X_AT	5	0	-1	-0.1
C6ORF62	213872_AT;213875_X_AT	5	0	-0	0
PTPN2	204935_AT	9	0	0	-0.6
C5ORF33	228594_AT	9	0	0	-0.6
HPDL	229332_AT	9	0	0	-0.6
UTRN	225093_AT	6	0	-0	0.69

Suppl. Table 3.2 GC regulated genes in the ALL & cell lines using STEM

GC regulated genes were identified using SAM with MeV ($p < 0.05$, fold-change $\geq$ 2-fold ($\geq$ 1 log2-fold)) followed by STEM to identify up and downregulated gene kinetics. **(A)** Statistical analysis and time course clustered GC induced genes in sensitive ALL & cell lines. **(B)** Statistical analysis and time course clustered GC induced genes in resistant ALL & cell lines.

Suppl. Table 3.2A GC regulated genes in the sensitive ALL & cell lines

Upregulated genes

Gene Symbol	Affyt ID	0h	6-10h (Log2-fold)	24h
SESN1	218346_S_AT	0	0.57	1.64
SIK1	208078_S_AT	0	1.03	1.55

FZD8	227405_S_AT;224325_AT	0	0.84	1.46
NCF2	209949_AT	0	0.69	1.42
SNX9	223028_S_AT;223027_AT	0	1.14	1.36
HBB	209116_X_AT;217232_X_AT;211696_X_AT	0	0.61	1.35
DFNA5	203695_S_AT	0	0.65	1.33
METTL7A	207761_S_AT	0	0.39	1.25
CA2	209301_AT	0	0.51	1.24
RPS6KA2	212912_AT	0	0.75	1.22
LILRB2	207697_X_AT;210146_X_AT	0	1.12	1.22
LILRA2	211102_S_AT;211101_X_AT;211100_X_AT;207857_AT	0	1.02	1.21
PRDM1	228964_AT	0	0.05	1.16
GALNT13	243779_AT	0	0.49	1.11
P2RX1	210401_AT	0	0.26	1.1
SPOCK2	202524_S_AT	0	0.7	1.09
PCLO	213558_AT	0	0.57	1.09
HBA1 /// HBA2	211699_X_AT;209458_X_AT;211745_X_AT;204018_X_AT;217414_X_AT;214414_X_AT	0	0.64	1.09
SCML4	1556472_S_AT;1563542_A_AT;1569225_A_AT;1556471_AT	0	0.87	1.05
AMY1A /// AMY1B /// AMY1C /// AMY2A /// AMY2B	208498_S_AT	0	0.43	1.05
BIRC3	210538_S_AT	0	0.37	1.05
RNASE6	213566_AT	0	0.59	1.01
BCL2A1	205681_AT	0	1.06	0.63
NFE2	209930_S_AT	0	1.21	0.52
LGALS3	208949_S_AT	0	1.04	0.47

Downregulated genes

Gene Symbol	Affyt ID	0h	6-10h (Log2-Fold)	24h
PDE4B	203708_AT;211302_S_AT	0	-2.24	-1.73
ASPM	219918_S_AT	0	-1.52	-1.66
FAM72A /// FAM72B /// FAM72C /// FAM72D	225834_AT	0	-1.13	-1.54
HMMR	209709_S_AT;207165_AT	0	-1.21	-1.53
KIF4A	218355_AT	0	-0.98	-1.51
SHCBP1	219493_AT	0	-0.9	-1.51

DTL	222680_S_AT;218585_S_AT	0	-0.62	-1.46
GINS2	221521_S_AT	0	-0.65	-1.44
TOP2A	237469_AT;201291_S_AT;201292_AT	0	-1.31	-1.35
C4ORF46	235088_AT	0	-0.38	-1.31
KIF11	204444_AT	0	-0.54	-1.31
ERG	241926_S_AT;211626_X_AT;222079_AT;213541_S_AT	0	-1.06	-1.29
CEP55	218542_AT	0	-0.3	-1.29
DLGAP5	203764_AT	0	-1.82	-1.28
OIP5	213599_AT	0	-0.92	-1.28
CCNB1	228729_AT;214710_S_AT	0	-0.93	-1.27
KIF20A	218755_AT	0	-1.09	-1.23
CDKN3	1555758_A_AT;209714_S_AT	0	-0.65	-1.22
NUSAP1	218039_AT;219978_S_AT	0	-0.75	-1.21
CENPF	207828_S_AT;209172_S_AT	0	-1.22	-1.19
IGFBP2	202718_AT	0	-0.28	-1.18
GBP4	235574_AT;235175_AT	0	-1.36	-1.17
CCNA2	203418_AT;213226_AT	0	-0.73	-1.14
KIF15	219306_AT	0	-0.28	-1.14
KIF14	206364_AT;236641_AT	0	-1.06	-1.13
CENPE	205046_AT	0	-0.88	-1.1
IL1B	205067_AT;39402_AT	0	-0.07	-1.09
CCNB2	202705_AT	0	-0.92	-1.09
TYMS	1554696_S_AT;202589_AT	0	-0.63	-1.09
SFRS12	243361_AT	0	-0.32	-1.08
UBE2T	223229_AT	0	-0.72	-1.08
MELK	204825_AT	0	-0.84	-1.08
CDC2	231534_AT;203214_X_AT;210559_S_AT;203213_AT	0	-0.45	-1.07
RAD51AP1	204146_AT	0	-0.44	-1.07
TMEM97	212281_S_AT;212282_AT;212279_AT	0	-0.48	-1.06
MND1	223700_AT	0	-0.6	-1.05
ZWINT	204026_S_AT	0	-0.3	-1.03
PBK	219148_AT	0	-0.43	-1.01

MAD2L1	1554768_A_AT;203362_S_AT	0	-0.65	-1.01

Suppl. Table 3.2B GC regulated genes in the resistant ALL & cell lines

Upregulated genes

Gene Symbol	Affyt ID	0h	6-10h (Log2-Fold)	24h
FAM49A	209683_AT	0	0.81	2.32
C4ORF34	224990_AT	0	0.45	1.1
RPS27	236621_AT	0	0.64	1.08
PLAC8	219014_AT	0	1.25	1.17
SOCS2	203373_AT;203372_S_AT	0	0.97	1.19
STAG3	219753_AT	0	1.11	1.66
RASEF	1553186_X_AT	0	0.51	1.1
METTL7A	207761_S_AT	0	0	1.06
TMEM106B	222787_S_AT	0	0.26	1.41
HIPK1	212291_AT	0	1.3	0.88
RNF125	235199_AT	0	1.92	1.44
MST150	223276_AT	0	1.1	1.18
CD69	209795_AT	0	1.21	0.4
BTG1	1559975_AT;200920_S_AT;200921_S_AT	0	1.13	1.54
C9ORF95	219147_S_AT	0	0.24	1.09
ISG20	204698_AT;33304_AT	0	1.95	2.23
SLFN5	243999_AT	0	0.97	1.98
TSC22D3	208763_S_AT;207001_X_AT	0	1.95	1.72
SLC7A11	217678_AT	0	1.24	1.51
PRSS3	213421_X_AT	0	1.51	1.75
FUS /// NR1H3	1565717_S_AT	0	1.09	0.4

Downregulated genes

Gene Symbol	Affyt ID	0h	6-10h (Log2-Fold)	24h
RIT1	239843_AT;236223_S_AT;236224_AT	0	-0.17	-1.11
GJA3	239572_AT	0	-0.39	-1.18
BBS7	219688_AT	0	-0.09	-1.23
PTPN2	204935_AT	0	-0.18	-1.27
DOCK4	205003_AT	0	-0.21	-1.11

TFDP1	242939_AT	0	-0.1	-1.27
DAB1	228329_AT	0	-0.87	-1.1
EPCAM	201839_S_AT	0	-1.14	-1.5

Suppl. Table 3.3 GC regulated genes in the Philadelphia positive (Ph+) ALL patients using STEM.

Significant GC regulated genes were identified using SAM with MeV ($p < 0.05$, fold-change ≥ 2-fold (≥ 1 log2-fold)) followed by STEM to identify up and downregulated gene kinetics. (A) Statistical analysis and clustering according to kinetic features of GC induced genes in the Philadelphia positive (Ph+) ALL patients showing good risk to the EsPHALL protocol (36). (B) Statistical analysis and clustering according to kinetic features of GC induced gene in Philadelphia positive (Ph+) ALL patients showing poor risk to the EsPHALL protocol (36).

Suppl. Table 3.3A Analysis of genes from the Philadelphia positive (Ph+) ALL patients with good risk

Upregulated genes

Gene Symbol	Affyt ID	Day0	Day17 (Log2-Fold)
CLEC12A	1552398_A_AT	0	3.24
GPBAR1	1552501_A_AT	0	1.09
COP1	1552701_A_AT	0	1.89
CD300LF	1553043_A_AT	0	1.41
CSF3R	1553297_A_AT;203591_S_AT	0	1.28
SIRPB1	1554624_A_AT	0	1.94
CLEC7A	1555756_A_AT;221698_S_AT	0	3.47
MTMR11	1556034_S_AT;205076_S_AT	0	1.79
JMJD3	1556066_AT	0	1.19
SIRPB2	1559034_AT	0	1.85
LRRC25	1559502_S_AT	0	2.04
VPS37C	1560060_S_AT;219053_S_AT	0	1.43
LOC284837	1563088_A_AT	0	2.14
CTSA	200661_AT	0	1.25

GRN	200678_X_AT;211284_S_AT;216041_X_AT	0	1.43
HK1	200697_AT	0	1.46
NPC2	200701_AT	0	1.42
CTSD	200766_AT	0	2.03
MCL1	200797_S_AT	0	1.12
ZYX	200808_S_AT;215706_X_AT	0	1.75
CTSB	200838_AT;200839_S_AT;213274_S_AT;213275_X_AT;227961_AT	0	1.02
PSAP	200871_S_AT	0	1.43
S100A10	200872_AT	0	1.35
CKAP4	200998_S_AT	0	2.28
STOM	201061_S_AT	0	1.4
PXN	201087_AT	0	1.37
ATP6V1B2	201089_AT	0	1.33
LGALS1	201105_AT	0	1.53
ATP1B1	201242_S_AT;201243_S_AT	0	2.21
APEH	201284_S_AT	0	1.06
VAMP3	201336_AT	0	1.11
CST3	201360_AT	0	3.41
IVNS1ABP	201362_AT;201363_S_AT	0	1.17
IFI30	201422_AT	0	1.64
ALDH2	201425_AT	0	1.59
SCRN1	201462_AT	0	1.59
QSOX1	201482_AT	0	1.4
PPIF	201489_AT	0	1.44
PRCP	201494_AT	0	1.11
TGFBI	201506_AT	0	3.09
OAT	201599_AT	0	1.05
MARCKS	201670_S_AT	0	1.64
SGK	201739_AT	0	1.75
CD14	201743_AT	0	4.28
CDC25B	201853_S_AT	0	1.1
EXT1	201995_AT	0	1.02
NID1	202007_AT	0	1.33
CTSL1	202087_S_AT	0	1.6
TSPO	202096_S_AT	0	1.4
BLVRB	202201_AT	0	1.66
TRIB1	202241_AT	0	2.06
CTSH	202295_S_AT	0	2.2
LEPROT	202377_AT	0	1.36
ADAM9	202381_AT	0	1.6
GNPDA1	202382_S_AT	0	1.49

RXRA	202426_S_AT	0	1.6
PRKCD	202545_AT	0	1.55
LYN	202625_AT	0	2.16
TNFSF10	202687_S_AT;202688_AT;214329_X_AT	0	2.08
LTBP1	202729_S_AT	0	1.32
ITGB2	202803_S_AT	0	1.3
SLC16A3	202856_S_AT	0	1.42
IL8	202859_X_AT	0	2.35
CD93	202878_S_AT	0	2.71
ANPEP	202888_S_AT	0	2.14
SIRPA	202896_S_AT;202897_AT	0	1.35
CTSS	202901_X_AT;232617_AT	0	1.92
FHL2	202949_S_AT	0	1.39
FAM13A1	202972_S_AT;202973_X_AT;217047_S_AT	0	1.66
PAPSS2	203058_S_AT;203060_S_AT	0	1.42
IMPA2	203126_AT	0	1.31
RHOG	203175_AT	0	1.15
S100A4	203186_S_AT	0	1.55
ATXN1	203232_S_AT;242230_AT	0	1.03
UPP1	203234_AT	0	1.86
PDLIM5	203243_S_AT;212412_AT	0	1.89
SAT1	203455_S_AT;210592_S_AT;213988_S_AT	0	1.41
PLEK	203471_S_AT	0	1.07
RTN1	203485_AT	0	2.52
CD68	203507_AT	0	1.24
CD4	203547_AT	0	1.22
FCGR2A	203561_AT	0	2.73
SULT1A1	203615_X_AT;215299_X_AT	0	1.49
CD163	203645_S_AT;215049_X_AT	0	2.28
HMOX1	203665_AT	0	2.08
SLA	203760_S_AT;203761_AT	0	1.66
BLVRA	203771_S_AT;203773_X_AT;211729_X_AT	0	1.1
CD302	203799_AT	0	3.23

WIPI1	203827_AT;213836_S_AT	0	1.74
LOC729144///MAP3K5	203837_AT	0	1.27
GCLM	203925_AT;236140_AT	0	1.57
USP20	203965_AT	0	1.13
CEBPD	203973_S_AT	0	3.29
CEBPA	204039_AT	0	1.15
PLCB2	204046_AT	0	1.05
PHACTR2	204048_S_AT	0	1.13
FRY	204072_S_AT;214318_S_AT	0	1.17
NRGN	204081_AT	0	2.66
HNMT	204112_S_AT;228772_AT	0	1.83
GNG11	204115_AT	0	1.69
TYROBP	204122_AT	0	2.82
TUBB2A	204141_AT	0	2.57
KIAA0999	204157_S_AT	0	1.33
TCIRG1	204158_S_AT	0	1.22
SLC31A2	204204_AT	0	2.43
RAB32	204214_S_AT	0	1.7
FCER1G	204232_AT	0	2.29
VDR	204254_S_AT;204255_S_AT	0	1.07
KIF21B	204411_AT	0	1.09
IFI44L	204439_AT	0	1.7
TBC1D8	204526_S_AT	0	1.53
CXCL10	204533_AT	0	1.24
KIAA0513	204546_AT	0	1.29
SLC7A7	204588_S_AT	0	2.37
VCAN	204619_S_AT;204620_S_AT;215646_S_AT;221731_X_AT	0	4.1
PARVB	204629_AT;216253_S_AT;37965_AT;37966_AT	0	1.44
IFIT3	204747_AT;229450_AT	0	1.28
PTGS2	204748_AT	0	3.14
MAL	204777_S_AT	0	1.61
ECGF1	204858_S_AT;217497_AT	0	2.01
TLR2	204924_AT	0	1.09
MX2	204994_AT	0	1.3
ARHGAP26	205068_S_AT	0	1.3
CCR1	205098_AT;205099_S_AT	0	3.41
CSF2RB	205159_AT	0	2.56

SCO2	205241_AT	0	2.28
KCNH2	205262_AT	0	1.12
SPI1	205312_AT	0	1.41
CFD	205382_S_AT	0	2.57
ISG15	205483_S_AT	0	1.03
AOAH	205639_AT	0	2.25
OASL	205660_AT	0	1.08
BCL2A1	205681_AT	0	2.33
CD86	205685_AT	0	1.05
ITGAM	205786_S_AT	0	1.74
CD1D	205789_AT	0	3.31
SLC22A4	205896_AT	0	2.06
HK3	205936_S_AT	0	2.08
IL6R	205945_AT;226333_AT	0	1.74
CD33	206120_AT	0	1.32
ASGR2	206130_S_AT	0	1.05
IL18	206295_AT	0	1.54
CFP	206380_S_AT	0	2.41
PF4	206390_X_AT	0	3.17
IGSF6	206420_AT	0	2.91
ITGA2B	206493_AT;206494_S_AT	0	1.99
APOBEC3B	206632_S_AT	0	2.78
GP1BB///SEPT5	206655_S_AT	0	2.75
CLEC10A	206682_AT	0	1.47
TFEC	206715_AT	0	2.68
LILRA3	206881_S_AT	0	1.54
CCR2///LOC729230	206978_AT	0	2.8
PLAGL1	207002_S_AT;207943_X_AT;209318_X_AT	0	2.57
SIGLEC7	207224_S_AT	0	1.08
MITF	207233_S_AT;226066_AT	0	1.12
KIAA1539	207765_S_AT;211433_X_AT	0	1.12
LILRA1	207872_S_AT;210660_AT	0	1.15
HCK	208018_S_AT	0	2.53
APLP2	208248_X_AT;208702_X_AT;208703_S_AT;208704_X_AT;211404_S_AT;214875_X_AT;228520_S_AT	0	1.66
FGR	208438_S_AT	0	2.01

LOC729659///LOC730278	208540_X_AT	0	1.42
CLU	208791_AT;208792_S_AT;222043_AT	0	2.03
NADK	208918_S_AT	0	1.06
LGALS3	208949_S_AT	0	2.78
TUBB6	209191_AT	0	1.45
ENTPD1	209473_AT	0	1.11
TNFSF12-TNFSF13///TNFSF13	209500_X_AT;210314_X_AT	0	1.49
FBP1	209696_AT	0	1.78
FRAT2	209864_AT	0	2
SELPLG	209879_AT	0	1.76
LEPR	209894_AT	0	1.39
AIF1	209901_X_AT;213095_X_AT;215051_X_AT	0	1.13
C3AR1	209906_AT	0	1.89
NFE2	209930_S_AT	0	1.91
NCF2	209949_AT	0	1.76
CASP1	209970_X_AT;211368_S_AT	0	1.27
Mar-02	210075_AT	0	1.44
TLR5	210166_AT	0	1.48
ITGAX	210184_AT	0	1.15
SLC11A1	210423_S_AT	0	1.89
VEGFA	210512_S_AT	0	2.86
SLCO3A1	210542_S_AT;219229_AT;227367_AT	0	1.41
ASAH1	210980_S_AT;213702_X_AT;213902_AT	0	1.93
TPM1	210986_S_AT;210987_X_AT	0	2.29
PSTPIP1	211178_S_AT	0	1.2
CSF2RA	211286_X_AT	0	1.26
SERPINA1	211429_S_AT	0	3.47
FCER1A	211734_S_AT	0	2.05
UBE2D1	211764_S_AT	0	1.11
FYB	211794_AT	0	2.15
RHOQ	212119_AT	0	1.15
KCTD12	212188_AT;212192_AT	0	2.61
CAMKK2	212252_AT	0	1.13
GALNT10	212256_AT	0	1.44
QKI	212263_AT;212636_AT	0	1.49
GNS	212334_AT	0	1.77
MICAL2	212472_AT;212473_S_AT	0	1.53

CEBPB	212501_AT	0	2.23
CENTD2	212516_AT	0	1.15
IL1RN	212657_S_AT	0	2.79
GM2A	212737_AT;35820_AT	0	1.12
MKL1	212748_AT	0	1.07
TLE3	212769_AT;212770_AT;228340_AT	0	1.11
DMXL2	212820_AT	0	1.85
SLC30A1	212907_AT;228181_AT	0	1.38
SLC9A8	212947_AT	0	1.43
SGMS1	212989_AT	0	2.05
SLC36A1	213119_AT	0	1.43
PLXNC1	213241_AT	0	1.67
TMEM158	213338_AT	0	1.41
MLC1	213395_AT	0	1.35
HSPA6	213418_AT	0	2.01
G0S2	213524_S_AT	0	3.18
SECTM1	213716_S_AT	0	1.49
MYO1F	213733_AT	0	1.69
DOK2	214054_AT	0	1.18
MYCL1	214058_AT	0	1.14
MTMR6	214429_AT	0	1.05
IFI44	214453_S_AT	0	1.47
RIPK5	214663_AT	0	1.14
MGC14376	214696_AT	0	1.45
FLNA	214752_X_AT	0	1.05
GLUL	215001_S_AT	0	1.84
LILRA5	215838_AT	0	2.77
KYNU	217388_S_AT	0	2.49
S100A6	217728_AT	0	1.82
TMBIM1	217730_AT	0	1.16
RAB31	217762_S_AT;217764_S_AT	0	2.05
NDFIP1	217800_S_AT;222422_S_AT;222423_AT	0	1.82
RNF130	217865_AT	0	1.01
TPCN1	217914_AT	0	1.4
FAM129A	217966_S_AT	0	1.3
SQRDL	217995_AT	0	1.04
HGSNAT	218017_S_AT	0	1.5
SCPEP1	218217_AT	0	1.36
NAGK	218231_AT	0	1
SNX10	218404_AT	0	1.97
KIAA1797	218503_AT	0	1.57
MAFB	218559_S_AT;222670_S_AT	0	2.43

FLJ11151	218610_S_AT	0	1.72
FNDC3B	218618_S_AT;225032_AT	0	1.71
PDGFC	218718_AT	0	3.03
FCGRT	218831_S_AT	0	1.19
GALNACT-2	218871_X_AT	0	1.21
GALNT11	219013_AT	0	1.58
BIN2	219191_S_AT	0	1.37
HPSE	219403_S_AT	0	1.29
TREM1	219434_AT	0	1.65
RIN3	219457_S_AT;60471_AT	0	1.41
CECR1	219505_AT	0	1.23
Mar-01	219574_AT	0	1.62
NINJ2	219594_AT	0	1.3
RAB20	219622_AT	0	1
MS4A6A	219666_AT;223280_X_AT;223922_X_AT;224356_X_AT;230550_AT	0	2.71
FAM105A	219694_AT	0	1.81
FRAT1	219889_AT	0	1.38
APOB48R	220023_AT	0	1.7
NOD2	220066_AT	0	1.98
C5AR1	220088_AT	0	3.93
CARD9	220162_S_AT	0	1.2
COTL1	221059_S_AT;224583_AT	0	2.18
NPL	221210_S_AT;223405_AT	0	1.83
TPK1	221218_S_AT	0	1.22
FFAR2	221345_AT	0	1.14
B4GALT5	221485_AT	0	2
CORO1C	221676_S_AT;222409_AT	0	1.85
EHBP1L1	221755_AT	0	1.45
JHDM1D	221778_AT;225142_AT	0	1.03
KIAA1598	221802_S_AT	0	3.03
FAM45A///FAM45B///LOC731832	221804_S_AT;222955_S_AT	0	1.02
KLF4	221841_S_AT	0	1.16
TBC1D2	222173_S_AT	0	1.46
PILRA	222218_S_AT	0	2.12
CYBRD1	222453_AT	0	1.14
EFHD2	222483_AT	0	1.16
PHCA	222687_S_AT;222688_AT	0	1.64
SDPR	222717_AT	0	3.27
TRMT6	222768_S_AT;233970_S_AT	0	1.17

OBFC2A	222872_X_AT;233085_S_AT	0	1.89
TMEM40	222892_S_AT	0	1.14
SLC40A1	223044_AT	0	2.35
EML4	223068_AT	0	1.31
FUCA2	223120_AT	0	1.67
RHOU	223168_AT	0	1.97
C4ORF18	223204_AT	0	4.54
DUSP23	223402_AT	0	1.11
TMEM120A	223482_AT	0	1.15
TNFSF13B	223501_AT;223502_S_AT	0	2.32
CCDC88B	223663_AT	0	1.03
RGS18	223809_AT	0	2.49
TLR4	224341_X_AT;232068_S_AT	0	2.53
EMILIN2	224374_S_AT	0	2.09
ARHGAP9	224451_X_AT;226906_S_AT;232543_X_AT	0	1.15
MAG1	224480_S_AT	0	2.42
RP5-1022P6.2	224826_AT	0	1.26
CPEB4	224829_AT;224831_AT	0	1.33
SLC35C2	225037_AT	0	1.18
AGTRAP	225059_AT	0	1.1
ARHGAP18	225171_AT	0	1.32
RAB11FIP1	225177_AT	0	1.18
SRXN1	225252_AT	0	1.32
RBMS1	225269_S_AT	0	1.43
FAM45A	225351_AT	0	1.11
C10ORF54	225372_AT;225373_AT	0	1.6
C1ORF85	225401_AT	0	1.09
SLC45A4	225597_AT	0	1.23
C9ORF19	225602_AT;225604_S_AT	0	1.46
JAZF1	225798_AT	0	1.52
C2ORF59///LOC541471	225799_AT	0	1.53
AADACL1	225847_AT	0	1.94
ATG16L2	225883_AT;229389_AT	0	1.11
KIAA1450	225922_AT;226460_AT	0	1.07
STEAP4	225987_AT	0	1.68
PPM1M	226074_AT	0	1.41
SUSD1	226264_AT	0	1.1
MXD1	226275_AT;228846_AT	0	2.88
LACTB	226354_AT	0	1.59

ARRDC1	226405_S_AT	0	1.32
RASSF4	226436_AT	0	1.48
MGC70857	226710_AT	0	1.1
IFIT2	226757_AT	0	1.87
STXBP5	226794_AT	0	1.03
MPEG1	226818_AT;226841_AT	0	3.86
ACPL2	226925_AT	0	1.12
SGMS2	227038_AT;242963_AT	0	1.18
AKAP13	227039_AT	0	1.07
CORO2A	227177_AT	0	1.76
FGL2	227265_AT	0	3.23
NAPSB	228055_AT;228056_S_AT	0	1.21
AMICA1	228094_AT	0	2.72
FCHO2	228220_AT	0	1.52
SLC22A15	228497_AT	0	1.55
C1ORF162	228532_AT	0	2.29
HOXA2	228642_AT	0	1.21
RAB27B	228708_AT	0	1.89
LOC150166	229295_AT	0	1.03
TLR8	229560_AT	0	3.54
LRRK2	229584_AT	0	2.76
GLT1D1	229770_AT	0	1.29
DOCK5	230206_AT;230207_S_AT;230263_S_AT	0	2.33
NFAM1	230322_AT;243099_AT	0	1.13
TUBB1	230690_AT	0	3.55
PNKD	233177_S_AT	0	1.19
LDLRAD3	234985_AT	0	1.11
SLC8A1	235518_AT	0	1.87
SCLT1	236487_AT	0	1.43
PTPN22	236539_AT	0	1.08
RBP7	238066_AT	0	1.91
TMEM71	238429_AT	0	1.7
PRRG4	238513_AT	0	1.53
MPP7	238778_AT	0	2.08
PRAM1	241742_AT	0	2.6
TFDP1	242939_AT	0	1.05
PBEF1	243296_AT	0	3.21
GAS2L1	31874_AT	0	1.58
EHBP1L1///MGC15523	91703_AT	0	1.17

Downregulated genes

Gene Symbol	Affyt ID	Day0	Day17 (Log2-Fold)
DDR1	1007_S_AT;207169_X_AT;210749_X_AT	0	-1.5
ARHGAP5	1552627_A_AT;217936_AT;233849_S_AT	0	-1.61
C5ORF22	1552660_A_AT	0	-1.26
TIGD1	1553099_AT	0	-1.07
CNOT6L	1553267_A_AT	0	-1.02
MIER3	1553336_A_AT;1554449_AT;228961_AT	0	-1.01
ZMYND11	1554159_A_AT	0	-1.21
PACSIN2	1554691_A_AT	0	-1.05
CTDSPL2	1555106_A_AT;223270_AT;223271_S_AT	0	-1.06
CD79A	1555779_A_AT;205049_S_AT	0	-3.64
LOC284952	1557267_S_AT	0	-2.23
LOC400238	1557657_A_AT	0	-1.73
LRRC8C	1558517_S_AT;228314_AT	0	-1.35
BANK1	1558662_S_AT;219667_S_AT;222915_S_AT	0	-2.97
LRRC62	1559072_A_AT;1560713_A_AT	0	-1.68
BCL11A	1559078_AT	0	-1.52
CEP68	1559159_AT;207971_S_AT;212675_S_AT	0	-1.79
PPIL4///ZC3H12D	1559263_S_AT	0	-1.52
LOC144481	1559315_S_AT	0	-3.51
DNTT	1566362_AT	0	-1.45
XBP1	200670_AT	0	-2.5
SPTBN1	200671_S_AT;200672_X_AT	0	-1.51
LAMC1	200770_S_AT;200771_AT	0	-1.23
PAFAH1B1	200813_S_AT	0	-1.19
CCND2	200951_S_AT;200952_S_AT	0	-1.64
TSPAN3	200972_AT;200973_S_AT	0	-1.2
CD9	201005_AT	0	-3.4
EIF1AX	201017_AT	0	-1.32

CD99	201028_S_AT;201029_S_AT	0	-2.05
SF3B1	201070_X_AT;214305_S_AT	0	-1.01
BTG2	201235_S_AT	0	-1.22
ETS2	201328_AT;201329_S_AT;241193_AT	0	-2.84
SOX4	201416_AT;201417_AT;201418_S_AT;213668_S_AT	0	-2.68
CNN3	201445_AT	0	-1.47
RCN2	201485_S_AT;201486_AT	0	-1.26
TSN	201504_S_AT	0	-1.12
NCBP2	201521_S_AT	0	-1.05
FHL1	201539_S_AT;201540_AT;210298_X_AT;210299_S_AT;214505_S_AT	0	-2.43
FXR1	201635_S_AT;201636_AT;201637_S_AT	0	-1.01
API5	201686_X_AT;214959_S_AT	0	-1.3
TPD52	201688_S_AT;201689_S_AT;201690_S_AT;201691_S_AT	0	-1.46
AEBP1	201792_AT	0	-1.39
FAM3C	201889_AT	0	-1.46
EFNA1	202023_AT	0	-1.34
RAI14	202052_S_AT	0	-1.89
SNX2	202113_S_AT;202114_AT	0	-1.1
ABL1	202123_S_AT	0	-1.82
BLMH	202179_AT	0	-1.02
TSPAN7	202242_AT	0	-3.73
CPSF6	202470_S_AT	0	-1.01
MLXIP	202519_AT;211789_S_AT;225157_AT	0	-1.4
ARHGEF7	202547_S_AT;202548_S_AT;235412_AT	0	-1.1
CRIM1	202551_S_AT;202552_S_AT;228496_S_AT	0	-1.97
MYLK	202555_S_AT;224823_AT	0	-2.22
S100A13	202598_AT	0	-1.45
NRIP1	202599_S_AT;202600_S_AT	0	-2.37
STK39	202786_AT	0	-1.02

DBN1	202806_AT	0	-1.17
PRDM2	203056_S_AT	0	-1.26
GALNAC4S-6ST	203066_AT	0	-2.14
RB1	203132_AT;211540_S_AT	0	-1.52
RABEP1	203223_AT;214552_S_AT;225064_AT	0	-1.25
HS2ST1	203284_S_AT	0	-1.21
LMAN1	203293_S_AT;203294_S_AT	0	-1.55
DCK	203302_AT	0	-1.14
MTF2	203346_S_AT;203347_S_AT;209704_AT	0	-1.45
PSD3	203354_S_AT;218613_AT	0	-2.08
SOCS2	203372_S_AT;203373_AT	0	-4.55
MME	203434_S_AT;203435_S_AT	0	-3.98
MAP4K5	203553_S_AT	0	-1.64
ALDH5A1	203608_AT	0	-1.65
PKD2	203688_AT	0	-1.09
PPFIBP1	203735_X_AT;203736_S_AT	0	-1.21
TCF4	203753_AT;212382_AT;212385_AT;212386_AT;212387_AT;213891_S_AT;222146_S_AT	0	-2.96
SSBP2	203787_AT;210829_S_AT	0	-3.11
NT5E	203939_AT;227486_AT	0	-1.41
SPRY2	204011_AT	0	-2.51
SCHIP1	204030_S_AT	0	-2.79
TCEAL1	204045_AT	0	-1.3
WASF1	204165_AT	0	-2.43
C7ORF23	204215_AT	0	-1.09
PIK3CA	204369_AT	0	-1.55
GAS1	204457_S_AT	0	-2.17
SLC16A2	204462_S_AT	0	-1.57
PIK3C2B	204484_AT	0	-1.15
C12ORF24	204521_AT	0	-1.41
CD22///MAG	204581_AT;217422_S_AT;38521_AT	0	-1.67
ADA	204639_AT;216705_S_AT	0	-1.21
RIMS3	204730_AT	0	-1.22
TCFL5	204849_AT	0	-1.38

PHF16	204866_AT	0	-1.83
POU2AF1	205267_AT	0	-2.64
CD79B	205297_S_AT	0	-3.22
ATF2	205446_S_AT	0	-1.07
ZNF107	205739_X_AT	0	-2.05
NOLC1	205895_S_AT	0	-1.03
DPEP1	205983_AT	0	-1
ZNF91	206059_AT	0	-1.21
ELK3	206127_AT;221773_AT	0	-1.89
SCML2	206147_X_AT	0	-1.17
BLK	206255_AT	0	-1.66
HLA-DOA	206313_AT;226878_AT	0	-1.03
PIK3CG	206369_S_AT	0	-1.07
CD19	206398_S_AT	0	-2.31
PRMT1	206445_S_AT	0	-1.28
ZNF43	206695_X_AT;222136_X_AT	0	-1.42
CSRP2	207030_S_AT;211126_S_AT	0	-3.6
MED6	207079_S_AT	0	-1.22
GAB1	207112_S_AT;225998_AT	0	-2.76
ZNF117	207117_AT;207605_X_AT;235408_X_AT;235564_AT	0	-1.19
CDK6	207143_AT;224847_AT;224848_AT;224851_AT;235287_AT;243000_AT	0	-2.07
BLNK	207655_S_AT	0	-3.82
MEF2C	207968_S_AT;209199_S_AT;209200_AT	0	-2.14
MEF2A	208328_S_AT;212535_AT;214684_AT	0	-1.05
TTC3	208661_S_AT;208664_S_AT	0	-1.14
PRDX1	208680_AT	0	-2.02
NONO	208698_S_AT;210470_X_AT	0	-1.57
PRPF6	208879_X_AT	0	-1.23
IFI16	208965_S_AT	0	-1.23
CTGF	209101_AT	0	-5.59
TCF3	209153_S_AT	0	-2.43
HBS1L	209316_S_AT	0	-1.21

FBXW11	209456_S_AT	0	-1.44
GNAI1	209576_AT;227692_AT	0	-3.07
CD200	209583_S_AT	0	-2.29
SEDLP///TRAPPC2	209751_S_AT	0	-1.4
KHDRBS3	209781_S_AT	0	-2.5
MS4A1	210356_X_AT;217418_X_AT;228599_AT	0	-3.61
GPR125	210473_S_AT	0	-1.78
NRP1	210510_S_AT;212298_AT	0	-1.31
GTF2I	210892_S_AT	0	-2.46
LEF1	210948_S_AT;221557_S_AT;221558_S_AT	0	-1.56
CLIP2	211031_S_AT	0	-2.73
MSH6	211450_S_AT	0	-2.07
LRIG1	211596_S_AT	0	-1.57
ERG	211626_X_AT;241926_S_AT	0	-2.39
TOP2B	211987_AT	0	-1.01
SMARCE1	211988_AT;211989_AT	0	-1.24
PXDN	212012_AT;212013_AT	0	-2.85
UNC84A	212074_AT	0	-1.27
DHX9	212105_S_AT;212107_S_AT	0	-2.41
ZMIZ1	212124_AT	0	-1.26
KIAA0692	212201_AT	0	-1.04
MYO1B	212364_AT;212365_AT	0	-2.66
MXRA7	212509_S_AT	0	-1.31
LSM12	212529_AT	0	-1.17
SPRY1	212558_AT	0	-1.71
ARID5B	212614_AT	0	-1.51
DENND3	212974_AT	0	-1.89
UTRN	213023_AT	0	-1.45
OLFML2A	213075_AT	0	-1.18
SLC5A3	213164_AT	0	-1.29
FLJ35348	213788_S_AT	0	-2.02
YPEL1	213996_AT;228788_AT	0	-1.12
MTMR1	214975_S_AT	0	-1.4
SEMA6A	215028_AT;220454_S_AT;223449_AT;225660_AT	0	-1.82
ITGA6	215177_S_AT	0	-2.97
TPR	215220_S_AT	0	-1.75
RCAN1	215253_S_AT	0	-1.36
TRAF3IP2	215411_S_AT	0	-1.5
CD72	215925_S_AT	0	-1.16

HHEX	215933_S_AT	0	-1.52
LOC285412///TOX4	217448_S_AT	0	-1.11
C17ORF60	217513_AT	0	-1.25
ZNF675	217547_X_AT	0	-1.03
PRMT5	217786_AT	0	-1.1
SPIN1	217813_S_AT;222431_AT	0	-1.77
SLC39A9	217859_S_AT	0	-1.33
KCTD3	217894_AT	0	-1.3
CCNB1IP1	217988_AT	0	-1.17
ZNF22	218005_AT;218006_S_AT	0	-1.66
SAV1	218276_S_AT;222573_S_AT	0	-1.4
RCBTB1	218352_AT	0	-2.12
P2RY5	218589_AT	0	-2.01
ARMCX1	218694_AT	0	-1.62
NARG2	218713_AT;235189_AT	0	-1.34
EXOC5	218748_S_AT	0	-2.31
SMC6	218781_AT	0	-1.14
LIMD1	218850_S_AT;222762_X_AT	0	-2.02
MYO5C	218966_AT	0	-2.37
SLC35E3	218988_AT	0	-2.49
OSBPL10	219073_S_AT	0	-2.12
ZBTB10	219312_S_AT;222863_AT;233899_X_AT	0	-1.4
NEIL1	219396_S_AT	0	-1.26
C14ORF139	219563_AT	0	-1.56
C1ORF165	219670_AT	0	-1.62
STK32B	219686_AT	0	-1.94
GAL3ST4	219815_AT	0	-1.05
CYTL1	219837_S_AT	0	-2.28
FCF1	219927_AT	0	-1.47
VPREB3	220068_AT	0	-2.36
FAM108B1	220285_AT;227551_AT	0	-2.01
HCG_1778643	220450_AT	0	-1.55
C17ORF48	220606_S_AT	0	-1.42
SETD2	220946_S_AT	0	-1.14
MGC29506	221286_S_AT;223565_AT	0	-1.81
VPREB1	221349_AT	0	-4.06
EGLN1	221497_X_AT;223046_AT;224314_S_AT	0	-1.19
LAT2	221581_S_AT	0	-1.52
PIGP	221689_S_AT	0	-1.3
MAN1A1	221760_AT	0	-1.1

GUCY1A3	221942_S_AT	0	-1.55
PAX5	221969_AT	0	-2.45
PNRC2	222406_S_AT	0	-2
FLJ10154	222508_S_AT;227448_AT	0	-1.49
MKRN2	222510_S_AT	0	-1.01
DHX40	222574_S_AT	0	-1.24
GALNT7	222587_S_AT	0	-1.53
TIAM2	222942_S_AT	0	-1.99
C9ORF5	223005_S_AT;223007_S_AT	0	-1
FAM60A///LOC650369///LOC728115	223038_S_AT	0	-1.94
GLS	223079_S_AT	0	-2.07
LONP2	223098_S_AT	0	-1.46
STRBP	223245_AT;223246_S_AT;233252_S_AT	0	-2.19
MST150	223276_AT	0	-2.45
KBTBD4	223765_S_AT	0	-1.2
ERGIC1	223847_S_AT;224576_AT;224577_AT	0	-1.3
DLL1	224215_S_AT	0	-1.06
RP6-213H19.1	224407_S_AT	0	-2.75
C10ORF58	224435_AT	0	-1.01
C12ORF23	224759_S_AT	0	-2.04
NAV1	224772_AT;224773_AT;224774_S_AT;233870_AT	0	-1.83
UBTD2	224834_AT	0	-1.15
SCD5	224901_AT	0	-1.22
CHD6	225026_AT	0	-1.73
C16ORF63	225088_AT	0	-1.42
MSI2	225233_AT;225237_S_AT;225240_S_AT;239232_AT;243010_AT	0	-1.78
SH3RF1	225589_AT	0	-1.16
PAG1	225622_AT;225626_AT;227354_AT	0	-1.75
UHRF1	225655_AT	0	-2.53
PRKCE	226101_AT	0	-1.59
CHML	226350_AT	0	-1.05
LOC400027	226413_AT	0	-1.15
ZCCHC7	226496_AT	0	-2.4
ANKRD10	226663_AT	0	-1.16

AFF3	227198_AT	0	-1.79
SMAD1	227798_AT	0	-2.42
STS-1	228353_X_AT;238462_AT;238587_AT	0	-2.6
UNK	228357_AT	0	-1.09
GNG7	228831_S_AT	0	-1.97
FAM69B	229002_AT	0	-1.06
FAM80B	229344_X_AT;242870_AT	0	-1.56
LOC283454	229552_AT	0	-1.14
NRXN3	229649_AT	0	-2.46
TERF2	229790_AT	0	-1.55
CIRH1A	230656_S_AT	0	-1.32
EDEM1	230659_AT	0	-2.46
FLJ20309	231152_AT	0	-1.34
LOC440345///LOC641298///LOC730099	231989_S_AT	0	-1.43
AGPAT5	232007_AT	0	-1.08
EBF1	232204_AT;233261_AT	0	-3.28
HCG_2024094	232239_AT	0	-1.14
DKFZP564O0523	232661_S_AT	0	-1.34
SUPT16H	233827_S_AT	0	-2.95
DKFZP547E087	235167_AT	0	-2.75
GBP4	235574_AT	0	-2.79
CDK9	236023_AT	0	-1.58
TMEM156	241844_X_AT	0	-1.28
LASS6	242019_AT	0	-1.63
SDK2	242064_AT	0	-2.5
LOC641518	243362_S_AT	0	-1.97
LOC651466	244042_X_AT	0	-1.26

Suppl. Table 3.3B Analysis of genes in the Philadelphia positive (Ph+) ALL patients with poor risk

Upregulated genes

Gene Symbol	Affy ID	Day0	Day17 (Log2-fold)
TACSTD2	202286_S_AT	0	1.06
PCOLCE2	219295_S_AT	0	1.65
GGTA1///LOC731515	228376_AT	0	1.54

Downregulated genes

Gene Symbol Gene Symbol	Affy ID	Day0	Day17 (Log2-fold)
ITGB2	1555349_A_AT;202803_S_AT	0	-1.1
FLNA	200859_X_AT	0	-1.11
MME	203434_S_AT	0	-2.2
NRGN	204081_AT	0	-1.42
CCL5	204655_AT	0	-1
F5	204714_S_AT	0	-1.52
DNTT	210487_AT	0	-3.62
UBE2D1	211764_S_AT	0	-1
MYO1B	212364_AT	0	-1.3
MXRA7	212509_S_AT	0	-1.15
PPBP	214146_S_AT	0	-1.64
ZNF423	214761_AT	0	-1.27
PDGFC	218718_AT	0	-1.53
BCL11B	219528_S_AT	0	-1.04
MGC29506	221286_S_AT;223565_AT	0	-1.39
RHOU	223168_AT	0	-1.14
MIRN21	224917_AT	0	-1.44
ACPL2	226925_AT	0	-1.24
MPP7	238778_AT	0	-1.34

Suppl. Table 3.4 Location and sequence of binding sites in the regulatory regions of the indicated genes

(A) Location and sequence of potential AP-1 binding sites in Bim. **(B)** Location and sequence of Erg binding sites in GR1A (12). Consensus binding sequences are taken from the following references: Erg binding site: (39); AP-1 binding site: (38)

Suppl. Table 3.4A

Transcription Factor	Binding position in Bim regulatory region	Sequence
AP-1	chr2: 111875749-111875760	CGGTGACTCACA

Suppl. Table 3.4B

Transcription Factor	Binding position in GR regulatory region	Sequence
Erg	chr5: 142657758-142657770	ACGGAAGCACTGG

Suppl. Table 3.5 List of microarray data obtained from GEO records GSE2677 (A) and GSE2842 (B) (5, 33)

Array samples were classified as three sets of time points: T0 (prior to GC treatment), T6-T10 (6-10 h of GC treatment) and T24 (24 h of GC treatment). The first column indicates the patient identifier (ID) or cell line. The second column indicates the array names used in Suppl. Fig. 3.1; the third column indicates the corresponding GEO accession number for each array sample (GSM). The detailed subject description can be obtained via GEO using the specified GSM number. (A) GSE2677 consists of 10 sets of time point arrays from 10 child-B-ALL and 3 sets from child-T-ALL. (B) GSE2842 consists of arrays obtained from GC sensitive cell-lines, GC-resistant cell lines and GC sensitivity-restored cell lines. Resistant cells are characterized by the lower expression of GR (CEM-C1), lack of functional GR (CEM-C7R1), low levels of the human GR^{dim} mutant (CEM-C7R1$^{dim\text{-}low}$) or are GC-resistant subclone of PreB697 (PreB). GC sensitivity was restored by constitutive high expression of rat GR or the human GR^{dim} mutant (labelled as CEM-C1^{ratGR}; CEM-C7R1$^{dim\text{-}high}$) (also see Suppl. Fig. 3.1 & 3.2).

Suppl. Table 3.5A

GSE2677		
Patient ID	**Array names**	**GEO accession numbers**
24	Sensitive/T24 (B-ALL) Sensitive/T6-T10 (B-ALL) Sensitive/T0 (B-ALL)	GSM51674: B-ALL-24-24h GSM51675: B-ALL-24-6h GSM51676: B-ALL-24-0h
17	Sensitive/T24 (B-ALL)	GSM51680: B-ALL-17-24h

	Sensitive/T6-T10 (B-ALL) Sensitive/T0 (B-ALL)	GSM51681: B-ALL-17-8h GSM51682: B-ALL-17-0h
13	Sensitive/T24 (B-ALL) Sensitive/T6-T10 (B-ALL) Sensitive/T0 (B-ALL)	GSM51677: B-ALL-13-24h GSM51678: B-ALL-13-8h GSM51679: B-ALL-13-0h
31	Sensitive/T24 (B-ALL) Sensitive/T6-T10 (B-ALL) Sensitive/T0 (B-ALL)	GSM51683: B-ALL-31-24h GSM51684: B-ALL-31-6h GSM51685: B-ALL-31-0h
32	Sensitive/T24 (B-ALL) Sensitive/T6-T10 (B-ALL) Sensitive/T0 (B-ALL)	GSM51686: B-ALL-32-24h GSM51687: B-ALL-32-6h GSM51688: B-ALL-32-0h
33	Sensitive/T24 (B-ALL) Sensitive/T6-T10 (B-ALL) Sensitive/T0 (B-ALL)	GSM51689: B-ALL-33-24h GSM51690: B-ALL-33-6h GSM51691: B-ALL-33-0h
37	Sensitive/T24 (B-ALL) Sensitive/T6-T10 (B-ALL) Sensitive/T0 (B-ALL)	GSM51692: B-ALL-37-24h GSM51693: B-ALL-37-6h GSM51694: B-ALL-37-0h
38	Sensitive/T24 (B-ALL) Sensitive/T6-T10 (B-ALL) Sensitive/T0 (B-ALL)	GSM51695: B-ALL-38-24h GSM51696: B-ALL-38-6h GSM51697: B-ALL-38-0h
40	Sensitive/T24 (B-ALL) Sensitive/T6-T10 (B-ALL) Sensitive/T0 (B-ALL)	GSM51698: B-ALL-40-24h GSM51699: B-ALL-40-6h GSM51700: B-ALL-40-0h

43	Sensitive/T24 (B-ALL) Sensitive/T6-T10 (B-ALL) Sensitive/T0 (B-ALL)	GSM51701: B-ALL-43-24h GSM51702: B-ALL-43-6h GSM51703: B-ALL-43-0h
25	Sensitive/T24 (T-ALL) Sensitive/T6-T10 (T-ALL) Sensitive/T0 (T-ALL)	GSM51707: T-ALL-25-24h GSM51708: T-ALL-25-6h GSM51709: T-ALL-25-0h
20	Sensitive/T24 (T-ALL) Sensitive/T6-T10 (T-ALL) Sensitive/T0 (T-ALL)	GSM51704: T-ALL-20-24h GSM51705: T-ALL-20-8h GSM51706: T-ALL-20-0h
2	Sensitive/T24 (T-ALL) Sensitive/T6-T10 (T-ALL) Sensitive/T0 (T-ALL)	GSM51710: T-ALL-2-24h GSM51711: T-ALL-2-8h GSM51712: T-ALL-2-0h

Suppl. Table 3.5B

GSE2842		
Cell line	**Array names**	**GEO accession numbers**
Pre-B ALL (GC sensitive)	Sensitive/T0 (Pre-B) Sensitive/T6-T10 (Pre-B) Sensitive/T24 (Pre-B)	GSM60545: S-Line-PreB-6h-EtOH GSM60546: S-Line-PreB-6h-GC GSM60547: S-Line-PreB-24h-GC
CEM-C7H2 (GC sensitive)	Sensitive/T0 (C7H2) Sensitive/T6-T10 (C7H2) Sensitive/T24 (C7H2)	GSM60542: S-Line-C7H2-6h-EtOH GSM60543: S-Line-C7H2-6h-GC GSM60544: S-Line-C7H2-24h-GC
CEM-C1	Resistant/T0 (C1)	GSM60560: R-Line-CEMC1-6h-EtOH

(GC resistant)	Resistant/T6-T10 (C1) Resistant/T24 (C1)	GSM60561: R-Line-CEMC1-6h-GC GSM60562: R-Line-CEMC1-24h-GC
CEM-C7R1 (GC resistant)	Resistant/T0 (C7R1) Resistant/T6-T10 (C7R1)	GSM60564: R-Line-C7R1-6h-EtOH GSM60566: R-Line-C7R1-6h-GC
CEM-C7R1$^{dim-low}$ (GC resistant)	Resistant/T0 (C7R1dim low) Resistant/T6-T10 (C7R1dim low) Resistant/T24 (C7R1dim low)	GSM60576: R-Line-C7R1dim-low-6h-EtOH GSM60578: R-Line-C7R1dim-low-6h-GC GSM60579: R-Line-C7R1dim-low-24h-GC
PreB697 ALL (GC resistant)	Resistant/T0 (pre-B) Resistant/T6-T10 (pre-B) Resistant/T0 (pre-B) Resistant/T24 (pre-B)	GSM60581: R-Line-PreB-6h-EtOH GSM60583: R-Line-PreB-6h-GC GSM60584: R-Line-PreB-24h-EtOH GSM60586: R-Line-PreB-24h-GC
CEM-C1^{ratGR} (GC sensitivity restored)	Converted/T0 (C1-ratGR) Converted//T6-T10 (C1-ratGR) Converted//T24 (C1-ratGR)	GSM60548: C-Line-CEMC1-ratGR-6h-EtOH GSM60549: C-Line-CEMC1-ratGR-6h-GC GSM60550: C-Line-CEMC1-ratGR-24h-GC
CEM-C7R1$^{dim-high}$ (GC sensitivity restored)	Converted//T0 (C7R1dim high) Converted//T6-T10 (C7R1dim high) Converted//T24 (C7R1dim high)	GSM60551: C-Line-C7R1dim-high-6h-EtOH GSM60552: C-Line-C7R1dim-high-6h-GC GSM60553: C-Line-C7R1dim-high-24h-GC

3.8 References

1. Wen LP, Madani K, Fahrni JA, Duncan SR, Rosen GD. Dexamethasone inhibits lung epithelial cell apoptosis induced by IFN-γ and Fas. *American Journal of Physiology - Lung Cellular and Molecular Physiology* 1997; **273:** L921-L929.

2. Yamamoto KR. Steroid receptor regulated transcription of specific genes and gene networks. *Annual Review of Genetics* 1985; **19:** 209-252.

3. Wang Z, Malone MH, He H, McColl KS, Distelhorst CW. Microarray analysis uncovers the induction of the proapoptotic BH3-only protein Bim in multiple models of glucocorticoid-induced apoptosis. *J Biol Chem* 2003; **278:** 23861-23867.

4. Chen DWC, Lynch JT, Demonacos C, Krstic-Demonacos M, Schwartz J-M. Quantitative analysis and modeling of glucocorticoid-controlled gene expression. *Pharmacogenomics* 2010; **11:** 1545-1560.

5. Ploner C, Rainer J, Niederegger H, Eduardoff M, Villunger A, Geley S *et al*. The Bcl2 rheostat in glucocorticoid-induced apoptosis of acute lymphoblastic leukemia. *Leukemia* 2007; **22:** 370-377.

6. Miller A, Komak S, Webb SM, Leiter E, Thompson EB. Gene expression profiling of leukemic cells and primary thymocytes predicts a signature for apoptotic sensitivity to glucocorticoids. *Cancer Cell International* 2007; **7:** 18.

7. Zong WX, Lindsten T, Ross AJ, MacGregor GR, Thompson CB. BH3-only proteins that bind pro-survival Bcl-2 family members fail to induce apoptosis in the absence of Bax and Bak. *Genes & Development* 2001; **15:** 1481-1486.

8. Erlacher M, Michalak EM, Kelly PN, Labi V, Niederegger H, Coultas L *et al*. BH3-only proteins puma and Bim are rate-limiting for gamma-radiation– and glucocorticoid-induced apoptosis of lymphoid cells in vivo. *Blood* 2005; **106:** 4131-4138.

9. So AYL, Chaivorapol C, Bolton EC, Li H, Yamamoto KR. Determinants of cell- and gene-specific transcriptional regulation by the glucocorticoid receptor. *PLoS Genet* 2007; **3:** e94.

10. Helmberg A, Auphan N, Caelles C, Karin M. Glucocorticoid-induced apoptosis of human leukemic cells is caused by the repressive function of the glucocorticoid receptor. *EMBO J.* 1995; **14:** 452–460.

11. Wallace AD, Cidlowski JA. Proteasome-mediated glucocorticoid receptor degradation restricts transcriptional signaling by glucocorticoids. *Journal of Biological Chemistry* 2001; **276:** 42714-42721.

12. Geng CD, Vedeckis WV. c-Myb and members of the c-Ets family of transcription factors act as molecular switches to mediate opposite steroid regulation of the human glucocorticoid receptor 1a promoter. *J Biol Chem* 2005; **280:** 43264-43271.

13. White RJ, Sharrocks AD. Coordinated control of the gene expression machinery. *Trends in Genetics*; **26:** 214-220.

14. Davies L, Karthikeyan N, Lynch JT, Sial E-A, Gkourtsa A, Demonacos C *et al*. Cross talk of signaling pathways in the regulation of the glucocorticoid receptor function. *Molecular Endocrinology* 2008; **22:** 1331-1344.

15. Krstic MD, Rogatsky I, Yamamoto KR, Garabedian MJ. Mitogen-activated and cyclin-dependent protein kinases selectively and differentially modulate transcriptional enhancement by the glucocorticoid receptor. *Molecular and Cellular Biology* 1997; **17:** 3947-54.

16. Diamond MI, Miner JN, Yoshinaga SK, Yamamoto KR. Transcription factor interactions: Selectors of positive or negative regulation from a single DNA element. *Science* 1990; **249:** 1266-1272.

17. De Bosscher K, Vanden Berghe W, Haegeman G. The interplay between the glucocorticoid receptor and nuclear factor-κb or activator protein-1: Molecular mechanisms for gene repression. *Endocrine Reviews* 2003; **24:** 488-522.

18. Segal E, Friedman N, Kaminski N, Regev A, Koller D. From signatures to models: Understanding cancer using microarrays. *Nat Genet.* 2005; **37:** Suppl:S38-45.

19. Yeoh EJ, Ross ME, Shurtleff SA, Williams WK, Patel D, Mahfouz R *et al*. Classification, subtype discovery, and prediction of outcome in pediatric acute lymphoblastic leukemia by gene expression profiling. *Cancer Cell* 2002; **1:** 133-143.

20. Segal E, Friedman N, Koller D, Regev A. A module map showing conditional activity of expression modules in cancer. *Nat Genet* 2004; **36:** 1090-1098.

21. Jin JY, Almon RR, DuBois DC, Jusko WJ. Modeling of corticosteroid pharmacogenomics in rat liver using gene microarrays. *J Pharmacol Exp Ther* 2003; **307:** 93-109.

22. Grice EA, Snitkin ES, Yockey LJ, Bermudez DM, Program NCS, Liechty KW *et al*. Longitudinal shift in diabetic wound microbiota correlates with prolonged skin defense response. *PNAS* 2010; **107:** 14799-14804.

23. Galon J, Franchimont D, Hiroi N, Frey G, Boettner A, Ehrhart-Bornstein M *et al*. Gene profiling reveals unknown enhancing and suppressive actions of glucocorticoids on immune cells. *FASEB J* 2002; **16:** 61-71.

24. Tsuzuki S, Taguchi O, Seto M. Promotion and maintenance of leukemia by erg. *Blood* 2011; **10:** 1182.

25. Thoms JAI, Birger Y, Foster S, Knezevic K, Kirschenbaum Y, Chandrakanthan V *et al*. Erg promotes T-acute lymphoblastic leukemia and is transcriptionally regulated in leukemic cells by a stem cell enhancer. *Blood* 2011; **117:** 7079-7089.

26. Martens J. Acute myeloid leukemia: A central role for the Ets factor Erg. *The International Journal of Biochemistry Cell Biology* 2011; **43:** 1413-1416.

27. Erkizan HV, Kong Y, Merchant M, Schlottmann S, Barber-Rotenberg JS, Yuan L *et al*. A small molecule blocking oncogenic protein Ews-Fli1 interaction with rna helicase a inhibits growth of ewing's sarcoma. *Nat Med* 2009; **15:** 750-756.

28. Rahim S, Beauchamp EM, Kong Y, Brown ML, Toretsky JA, Üren A. YK-4-279 inhibits Erg and Etv1 mediated prostate cancer cell invasion. *PLoS One* 2011; **6:** e19343.

29. Ernst J, Bar-Joseph Z. Stem: A tool for the analysis of short time series gene expression data. *BMC Bioinformatics* 2006; **7:** 191.

30. Zhou F, Thompson EB. Role of c-Jun induction in the glucocorticoid-evoked apoptotic pathway in human leukemic lymphoblasts. *Molecular Endocrinology* 1996; **10:** 306-16.

31. Biswas SC, Shi Y, Sproul A, Greene LA. Pro-apoptotic Bim induction in response to nerve growth factor deprivation requires simultaneous activation of three different death signaling pathways. *J. Biol. Chem.* 2007; **282:** 29368-29374.

32. Zhao F, Xuan Z, Liu L, Zhang MQ. TRED: A transcriptional regulatory element database and a platform for in silico gene regulation studies. *Nucleic Acids Research* 2005; **33:** D103-D107.

33. Schmidt S, Rainer J, Riml S, Ploner C, Jesacher S, Achmüller C *et al*. Identification of glucocorticoid-response genes in children with acute lymphoblastic leukemia. *Blood* 2006 **107:** 2061-9.

34. Irizarry RA, Bolstad BM, Collin F, Cope LM, Hobbs B, Speed TP. Summaries of affymetrix genechip probe level data. *Nucleic Acids Research* 2003; **31:** e15.

35. Jaiswal AK. Nrf2 signaling in coordinated activation of antioxidant gene expression. *Free Radic Biol Med.* 2004; **36:** 1199-207.

36. Mitchell CD, Richards SM, Kinsey SE, Lilleyman J, Vora A, Eden TOB *et al*. Benefit of dexamethasone compared with prednisolone for childhood acute lymphoblastic leukaemia: Results of the UK medical research council ALL97 randomized trial. *British Journal of Haematology* 2005; **129:** 734-745.

37. Verger A, Buisine E, Carrère S, Wintjens R, Flourens A, Coll J *et al*. Identification of amino acid residues in the Ets transcription factor Erg that mediate Erg-Jun/Fos-DNA ternary complex formation. *J Biol Chem* 2001; **276:** 17181-17189.

38. Carroll JS, Meyer CA, Song J, Li W, Geistlinger TR, Eeckhoute J *et al*. Genome-wide analysis of estrogen receptor binding sites. *Nat Genet* 2006; **38:** 1289-1297.

39. Cai J, Kandagatla P, Singareddy R, Kropinski A, Sheng S, Cher ML *et al*. Androgens induce functional Cxcr4 through Erg factor expression in Tmprss2-Erg fusion-positive prostate cancer cells. *Transl Oncol* 2010; **3:** 195–203.

40. Bruna A, Nicolas M, Munoz A, Kyriakis JM, Caelles C. Glucocorticoid receptor-JNK interaction mediates inhibition of the JNK pathway by glucocorticoids. *EMBO J* 2003; **22:** 6035-6044.

41. Caelles C, González-Sancho JM, Muñoz A. Nuclear hormone receptor antagonism with AP-1 by inhibition of the JNK pathway. *Genes & Development* 1997; **11:** 3351-3364.

42. Miner JN, Yamamoto KR. The basic region of AP-1 specifies glucocorticoid receptor activity at a composite response element. *Genes & Development* 1992; **6:** 2491-2501.

43. Pearce D, Matsui W, Miner JN, Yamamoto KR. Glucocorticoid receptor transcriptional activity determined by spacing of receptor and nonreceptor DNA sites. *J Biol Chem* 1998; **273:** 30081-30085.

44. Biddie SC, John S, Sabo PJ, Thurman RE, Johnson TA, Schiltz RL *et al*. Transcription factor AP1 potentiates chromatin accessibility and glucocorticoid receptor binding. *Molecular Cell* 2001; **43:** 145-155.

45. Hollenhorst PC, Ferris MW, Hull MA, Chae H, Kim S, Graves BJ. Oncogenic Ets proteins mimic activated Ras/MAPK signaling in prostate cells. *Genes & Development* 2011; **25:** 2147-2157.

46. Mittelstadt PR, Ashwell JD. Inhibition of AP-1 by the glucocorticoid-inducible protein Gilz. *J Biol Chem* 2001; **276:** 29603-29610.

47. Shaulian E, Karin M. AP-1 as a regulator of cell life and death. *Nat Cell Biol* 2002; **4:** E131-E136.

48. Leung KT, Li KKH, Sun SSM, Chan PKS, Ooi VEC, Chiu LCM. Activation of the JNK pathway promotes phosphorylation and degradation of BIMEL--a novel mechanism of chemoresistance in T-cell acute lymphoblastic leukemia. *Carcinogenesis* 2008; **29:** 544-551.

49. Barrett TJ, Vig E, Vedeckis WV. Coordinate regulation of glucocorticoid receptor and c-Jun gene expression is cell type-specific and exhibits differential hormonal sensitivity for down- and up-regulation *Biochemistry* 1996; **35:** 9746-9753.

50. Kettritz R, Choi M, Rolle S, Wellner M, Luft FC. Integrins and cytokines activate nuclear transcription factor-κb in human neutrophils. *J Biol Chem* 2004; **279:** 2657-2665.

51. Qi X, Pramanik R, Wang J, Schultz RM, Maitra RK, Han J *et al*. The p38 and JNK pathways cooperate to trans-activate vitamin d receptor via c-Jun/AP-1 and sensitize human breast cancer cells to vitamin D3-induced growth inhibition. *Journal of Biological Chemistry* 2002; **277:** 25884-25892.

52. Hibi M, Lin A, Smeal T, Minden A, Karin M. Identification of an oncoprotein- and UV-responsive protein kinase that binds and potentiates the c-Jun activation domain. *Genes & Development* 1993; **7:** 2135-2148.

53. Li L, Feng Z, Porter AG. JNK-dependent phosphorylation of c-Jun on serine 63 mediates nitric oxide-induced apoptosis of neuroblastoma cells. *Journal of Biological Chemistry* 2004; **279:** 4058-4065.

54. Seth A, Watson DK. Ets transcription factors and their emerging roles in human cancer. *European Journal of Cancer* 2005; **41:** 2462-2478.

55. Baldus CD, Burmeister T, Martus P, Schwartz S, Gökbuget N, Bloomfield CD *et al*. High expression of the Ets transcription factor Erg predicts adverse outcome in acute T-lymphoblastic leukemia in adults. *JCO* 2006; **24:** 4714-4720.

56. Baldus CD, Martus P, Burmeister T, Schwartz S, Gökbuget N, Bloomfield CD *et al*. Low Erg and Baalc expression identifies a new subgroup of adult acute T-lymphoblastic leukemia with a highly favorable outcome. *JCO* 2007; **25:** 3739-3745.

57. Basuyaux JP, Ferreira E, Stéhelin D, Buttice G. The Ets transcription factors interact with each other and with the c-Fos/c-Jun complex via distinct protein domains in a DNA-dependent and -independent manner. *J. Biol. Chem.* 1997; **272:** 26188-26195.

58. Birdsey GM, Dryden NH, Amsellem V, Gebhardt F, Sahnan K, Haskard DO *et al*. Transcription factor Erg regulates angiogenesis and endothelial apoptosis through VE-cadherin. *Blood* 2008; **111:** 3498-3506.

59. Sun C, Dobi A, Mohamed A, Li H, Thangapazham RL, Furusato B *et al*. Tmprss2-Erg fusion, a common genomic alteration in prostate cancer activates c-Myc and abrogates prostate epithelial differentiation. *Oncogene* 2008; **27:** 5348-5353.

60. Medh RD, Wang A, Zhou F, Thompson EB. Constitutive expression of ectopic c-Myc delays glucocorticoid-evoked apoptosis of human leukemic CEM-C7 cells. *Oncogene.* 2001; **20:** 4269-4639.

61. Löffler M, Ausserlechner MJ, Tonko M, Hartmann BL, Bernhard D, Geley S *et al*. c-Myc does not prevent glucocorticoid-induced apoptosis of human leukemic lymphoblasts. . *Oncogene* 1999; **18:** 4646-4631.

62. Yi HK, Fujimura Y, Ouchida M, Prasad DDK, Rao VN, Reddy ESP. Inhibition of apoptosis by normal and aberrant Fli-1 and Erg proteins involved in human solid tumors and leukemias. *Oncogene* 1997; **14:** 1259-1268.

63. Sevilla L, Aperlo C, Dulic V, Chambard JC, Boutonnet C, Pasquier O *et al*. The Ets2 transcription factor inhibits apoptosis induced by colony-stimulating factor 1 deprivation of macrophages through a Bcl-XL-dependent mechanism. *Mol. Cell. Biol.* 1999; **19:** 2624-2634.

64. Medh RD, Saeed MF, Johnson BH, Thompson EB. Resistance of human leukemic CEM-C1 cells is overcome by synergism between glucocorticoid and protein kinase A pathways: Correlation with c-Myc suppression. *Cancer Research* 1998; **58:** 3684-3693.

65. Li C, Wong W. Model-based analysis of oligonucleotide arrays: Expression index computation and outlier detection. *Proc Natl Acad Sci U S A* 2001; **98:** 31–6.

66. Bolstad B, Irizarry R, Astrand M, Speed T. A comparison of normalization methods for high density oligonucleotide array data based on variance and bias. *Bioinformatics* 2003; **19:** 185-93.

67. Smyth G. Linear models and empirical bayes methods for assessing differential expression in microarray experiments. *Stat Appl Genet Mol Biol* 2004; **3:** article 3.

68. Saeed AI, Sharov V, White J, Li J, Liang W, Bhagabati N *et al*. TM4: A free, open-source system for microarray data management and analysis. *Biotechniques* 2003; **34:** 374-378.

69. Ernst J, Nau GJ, Bar-Joseph Z. Clustering short time series gene expression data. *Bioinformatics* 2005; **21:** i159-i168.

70. Xenaki G, Ontikatze T, Rajendran R, Stratford IJ, Dive C, Krstic-Demonacos M *et al*. Pcaf is an Hif-1alpha cofactor that regulates p53 transcriptional activity in hypoxia. *Oncogene* 2008; **27:** 5785-5796.

71. Lynch J, Rajendran R, Xenaki G, Berrou I, Demonacos C, Krstic-Demonacos M. The role of glucocorticoid receptor phosphorylation in Mcl-1 and Noxa gene expression. *Molecular Cancer* 2010; **9:** 38.

72. Schmidt D, Wilson MD, Spyrou C, Brown GD, Hadfield J, Odom DT. Chip-seq: Using high-throughput sequencing to discover protein-DNA interactions. *Methods* 2009; **48:** 240-248.

73. Al-Shahrour F, Díaz-Uriarte R, Dopazo J. Fatigo: A web tool for finding significant associations of gene ontology terms with groups of genes. *Bioinformatics* 2004; **20:** 578-580.

4 CHAPTER 4: Modelling the mechanism of GR/c-Jun/Erg crosstalk of acute lymphoblastic leukaemia

By taking the models and the findings from Chapter 2 and 3, in **Chapter 4** we are able to further extend the models and make new predictions. This Chapter has appeared in "Chen DW-C, Krstic-Demonacos M and Schwartz J-M, Modeling the mechanism of GR/c-Jun/Erg crosstalk of acute lymphoblastic leukemia, Frontiers in Physiology, doi: 10.3389/fphys.2012.00410", with modifications. All authors contributed equally to this work. D.W.C. built the model, performed the experiments and wrote the manuscript. M.K-D. and J-M.S. supervised this project.

4.1 Abstract

Acute lymphoblastic leukaemia (ALL) is one of the most common forms of malignancy that occurs in lymphoid progenitor cells, particularly in children. Synthetic steroid hormones glucocorticoids (GCs) are widely used as part of the ALL treatment regimens due to their apoptotic function, but their use also brings about various side effects and drug resistance. The identification of the molecular differences between the GCs responsive and resistant cells therefore are essential to decipher such complexity and can be used to improve therapy. However, the emerging picture is complicated as the activities of genes and proteins involved are controlled by multiple factors. By adapting the systems biology framework to address this issue, we here integrated the available knowledge together with experimental data via the building of a series of mathematical models. This rationale enabled us to successfully unravel molecular interactions involving c-Jun in GC induced apoptosis and to identify Erg as determinant for GC resistance. Furthermore we demonstrated the importance of using a systematic approach to translate human disease processes into computational models in order to derive information-driven new hypotheses.

4.2 Introduction

Acute lymphoblastic leukaemia (ALL) refers to a neoplasm of T- or B- lymphoid progenitor cells, which is found to be the most common childhood malignancy (1). Despite the 85%-90% cure rate in children (2), a quarter of the cases suffer relapse, with drug resistance being a major cause (3). Glucocorticoids (GC) have been used as part of the treatment of many diseases including ALL, owing to their anti-inflammatory and anti-cancerous actions (4). One of the main

causes for resistance to GC is the defective signalling of GC to target genes in relation to apoptosis.

The principle of GC therapy in ALL is GC induced apoptosis, whereby GC activates the glucocorticoid receptor (GR) that upon hormone binding translocates to the nucleus and targets the apoptosis mediating family, the B-cell lymphoma 2 (Bcl-2). The Bcl-2 member Bim is known to be an essential initiator of apoptosis (5-8) and an indirect GR target (8). The GR regulation of Bim in ALL is however not fully defined; it was reported that c-Jun may be a potential candidate for targeting Bim activation (9-12). Apart from the Bcl-2 family members, we and other recently reported that the Ets protein, Erg is induced by GC in the resistant ALL CEM-C1-15 cells and may be a crucial GR target for determining GC resistance (13-16).

Although recent high through-put technologies have advanced the understanding of complex gene regulatory mechanisms, it is important to note that complex molecular mechanisms cannot be deciphered using experimental data alone. Considering the wide range and large volume of presented data and information about GR, Bim and Erg, computational modelling can be considered as an effective strategy for the interpretation of such data from various sources (17-19). In addition, modelling using timecourse data not only raises the prospect of inferring the existence of causal relationships between genes, but also of identifying the direction of causality from the regulated genes (20). Among various modelling approaches, ordinary differential equations (ODE) have been widely used for studying the dynamics of gene networks. They offer the advantages of maintaining the quantitativeness and causality inherent in dynamical systems equations while being computationally manageable for small systems.

Recently we have proposed a series of ODE kinetic models for GR regulation by integrating time series of gene and protein expression data with kinetic modelling through information theory (17). We identified crucial time points that distinguish early GC and delayed GC response genes. To develop a more global understanding of GR action, we have extended this investigation to new time points and examined time-dependent GR regulated genes with gene expression microarray. Timecourse gene expression clustering led to further identification of crucial genes c-Jun and Erg (Ets-related gene) as potential biomarkers for GC resistance (9).

Here we present extended models of GR regulation of c-Jun, Bim and Erg based on a set of ordinary differential equations (ODE) (17). Several possibilities for interactions between GR and the selected genes were analysed and the models that led to the best agreement with the experimental response were identified. We sought to show how our models can be further

adapted to integrate and study the analysis of GC regulated gene expression time series and obtain better understanding towards the regulatory mechanisms between GR, c-Jun, Bim and Erg in leukaemia.

4.3 Material and Methods

4.3.1 Protein and mRNA expression measurements

Timecourse protein and mRNA measurements were performed according to the methods as described previously (17). In brief, CCRF-CEM cells were plated in six-well plates in RPMI-1640 supplemented with 10% DCC-FBS and incubated overnight. 1µM of dexamethasone (Sigma, MO, USA), 10µM YK-4-279 or 10 µM JNK inhibitor II (SP600125) were added to the medium and cells were incubated for 0, 2, 10 and 48 hours accordingly. The relative protein expressions were then measured and calculated via immuno-blotting and ImageJ software, with actin as a control. GR (H-300), c-Jun (H79) and Erg (D-3) were purchased from Santa Cruz Biotechnology (Santa Cruz, CA, USA.); Actin and Bim antibodies were purchased from Abcam (Cambridge, UK). The relative mRNA levels were measured using quantitative real time PCR analysis with Bio-Rad Chromo4 system (Opticon monitor 3 software version 3.1) using the standard curve method with RPL-19 as the control (list of primer sequence can be found in (9). All results are reported as mean ± standard deviation unless otherwise noted. The Tukey's multiple comparison test was carried out to analyze western, qRT-PCR using SPSS 16.0 (SPSS Statistics).

4.3.2 Signalling network representation

To construct the GR/c-Jun/Bim and GR/Erg pathways, literature information was used to assemble the signalling topologies. As described previously and in (12), GR activates Bim through an indirect mechanism in C7 cells, potentially through either direct or indirect c-Jun activation. Two models were built to represent GR/c-Jun/Bim in C7 cells, which differ by the involvement of an extra set of unknown protein X synthesis (Models 1-2). We have previously identified an increase in Erg expression in GC-resistant C1 cells in response to GC treatment, and this was not found in GC-sensitive C7 cells. In C1 cells, GR/Erg models were defined as Erg being either a direct or an indirect GR target (Models 3-4); a potential glucocorticoid response element was identified via the champion ChiP transcription factor search portal which is a text mining tool based on SABiosciencs' database Decipherment of DNA element (DECODE). In C7 cells, although there were no significant changes with Erg expression, we did find a transient Erg recruitment on the GR promoter after 2 h of GC treatment. This highlights the potential role of

Erg in regulating GR transcription. For this reason we constructed two models, one includes only GR autoregulation in C7 cells (21; 22), the other includes both GR autoregulation and Erg regulation of GR transcription (Models 5-6). Therefore, we present six models, including two models representing GR regulation on c-Jun and Bim in C7 cells, two models for the control of Erg on GR autoregulation in C7 cells and two models showing Erg being either a direct or indirect GR target in C1 cells. The network models were implemented using the CellDesigner software (www.celldesigner.org) (23; 24). Protein and mRNA degradation and basal synthesis rates were included in all models using mass action kinetics, without taking cellular translocation into consideration.

4.3.3 Parameter estimation and simulation

All parameter estimations were performed using the Systems Biology Markup Language-based parameter estimation tool (SBML-PET) (25), which relies on the sets of ordinary differential equations (ODE) associated to model reactions and on the obtained experimental data. As shown in (26), GR has a relatively slow half-life between 27-42 h in the absence or presence of Dex, with a kinetic parameter of 0.0165 h^{-1} to 0.0257 h^{-1}. For this reason, parameters were constrained between 0.01 and 1 for the estimation process. Once the estimated parameters were obtained, model simulations were then carried out using the CellDesigner software. Least-square residual values (ε) were calculated as seen in (17) in order to determine the quality of the fit between simulations and experimental data.

$$\varepsilon = \sqrt{\frac{1}{n}\sum_{i=1}^{n}\left(\frac{y_i - Y_i}{Y_i}\right)^2}$$

where ε is the residual, n is the number of experimental data points, y_i are the experimental values and Y_i are the simulated values of the variable under consideration.

4.4 Results

4.4.1 Modelling GR regulation of Bim via c-Jun activation in GC sensitive C7 cells

GR induced apoptosis occurs through an intrinsic mitochondria dependent pathway via regulation of BCL-2 family proteins. In particular, the pro-apoptotic member Bim (BCL-2 interacting mediator of cell death) is known to be upregulated in sensitive ALL cells upon treatment with Dex through an indirect mechanism and plays a crucial role in apoptosis (6; 8; 17). However, the molecular mechanism for Bim induction by GR is unclear. We and other have

previously identified that c-Jun may be involved in the upregulation of Bim by GR (17; 27). Compared to the known direct GR target Bcl-X_L, both c-Jun and Bim were induced by GR much later, as a dramatic induction was observed between 6-10 hours (h), suggesting a potential delayed and indirect GR induced activation mechanism (17). However, we cannot rule out the possibility that GR may induce c-Jun directly, as a putative glucocorticoid response element was found at -1.6 kilo-basepairs from the c-Jun promoter (28). We also found two potential GR binding sites with the use of DECODE (Suppl. Table 4.1). A schematic diagram of GR inducing c-Jun is presented in Suppl. Fig. 4.1.

To model GR induced Bim activation, we considered two scenarios, involving either c-Jun being directly activated by GR before activating Bim, (Model 1), or c-Jun being indirectly activated through *de novo* protein synthesis of an unknown protein X (Model 2) (Fig. 4.1A & B). The experimental data used for parameter simulation were taken from previous results (9), where protein and mRNA expression series were obtained after treatment with 1μM Dex for 2 and 10 h in addition to the control (0 h). Model topologies were constructed via CellDesigner, with the inclusion of basal synthesis, protein and mRNA degradation which were described by mass action kinetics; the equations used in the model are presented in Table 4-1. Cellular translocation and compartmental levels were not taken into account in the models. The unknown parameters were estimated from the defined topologies and the experimental data in combination with the use of SBML-PET. Due to the absence of quantitative data of most signalling components, we carried out the parameter estimation procedure in two parts: GR basal synthesis, protein and mRNA degradation were estimated firstly, followed by the rest of unknown parameters. Fig. 4.2 shows experimental and simulated time courses using Models 1-2 of GR, c-Jun and Bim protein and mRNA levels. All mRNA and proteins show induction but the simulation with Model 2 exhibited a more similar trend to our previous results (9; 17), where a logarithmic tendency was seen. This observation is crucial since we have previously shown that direct and indirect GR targets can be distinguished based on the simulation trend, where direct GR targets exhibit a linear trend and indirect GR targets behave closer to a logarithmic function, due to the time delay required for the upstream pathway to be activated. At the protein level, Bim simulation seemed to fit better with Model 2, with an increase of up to 7.4-fold at 24 h and a smaller least-square residual value ($\varepsilon = 0.2605$) compared to Model 1 (17.18-fold at 24 h, $\varepsilon = 0.6969$) (Fig. 4.2A). In contrast, c-Jun protein simulation with Model 1 fits better (13.9-fold at 24 h, $\varepsilon = 0.4997$) than Model 2 (28.1-fold at 24 h, $\varepsilon = 0.8338$), particularly after 10 h of treatment (Model 1: 4.5-fold at 10 h; Model 2: 6.2-fold at 10 h). Compared to the simulations of protein levels, mRNA simulations with both Model 1 and Model 2 seemed to fit better with the experimental data (Fig.

4.2B). A logarithmic shaped mRNA simulation of both Bim and c-Jun was seen with Model 2 only, in contrast an almost linear increase of Bim mRNA simulation was observed with Model 1. Least square residual values in both models were much closer to each other for mRNA than proteins (Model 1: c-Jun (ε=0.3241), Bim (ε=0.1471); Model 2: c-Jun (ε=0.2276), Bim (ε=0.1891)).

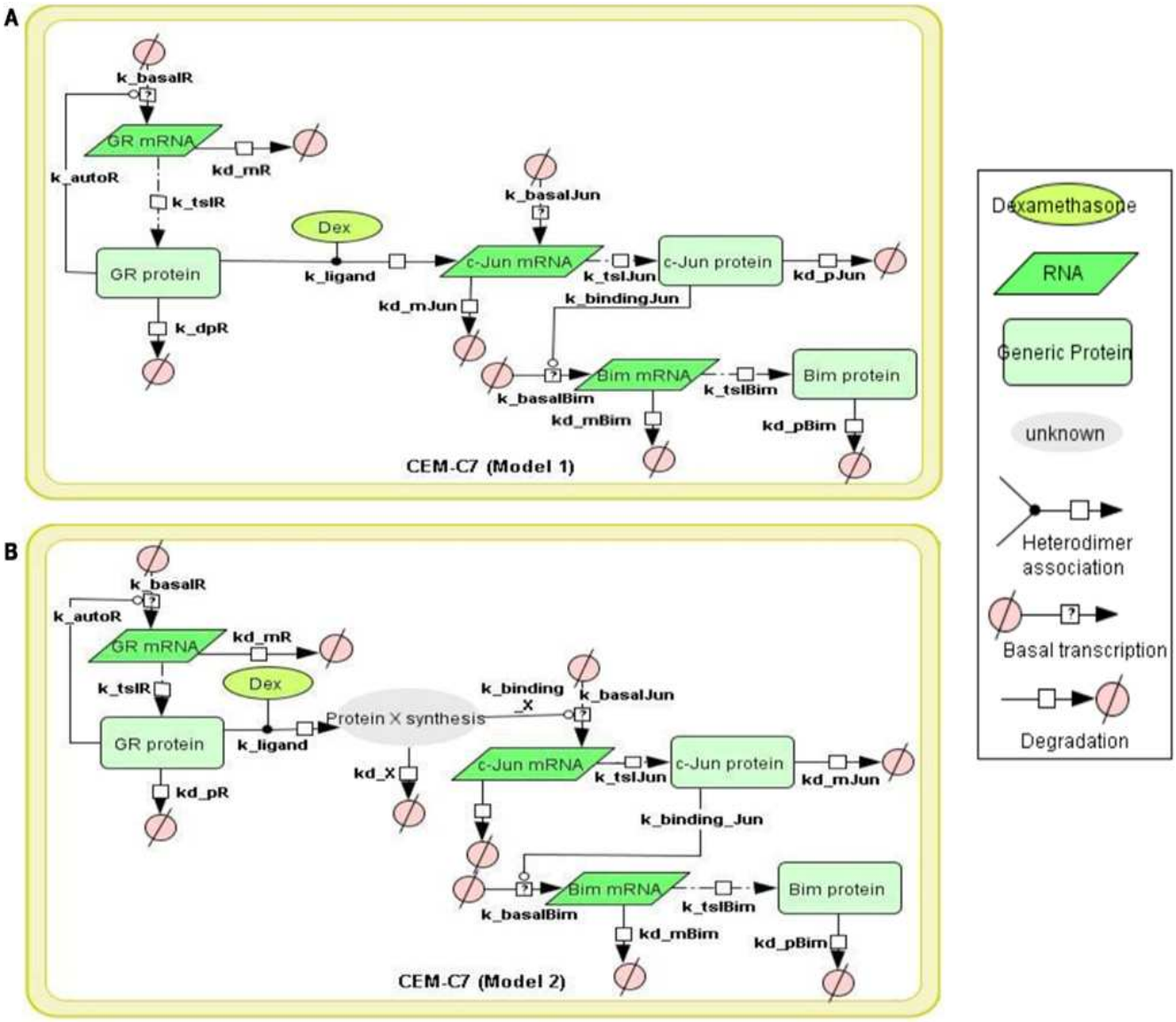

Figure 4.1 Topology of GR/Jun/Bim models in CEM-C7-14 cells

Schematic representation of GR inducing Bim via c-Jun. The figure summarizes the basic mechanism of Bim regulation controlled by GR. The model topology was based on (9; 17), where glucocorticoid passes through the cell membrane, causes GR activation by dissociating GR from the cytoplasmic heat shock protein (HSP) complex. The bound GR dimerises, either activates or represses its target genes through binding to GREs in the target

genes or via the recruitment of other transcription factors. All models were constructed by CellDesigner, based on the known or potential molecular mechanisms but without taking the cytoplasmic-nuclear compartmentalization into account. Basal transcription, GR auto-regulation, mRNA degradation, protein degradation and binding dynamics were included in the models and the reactions were described using first order mass action kinetics. The details of the kinetic equations in all models are described in Table 4-1. **(A)** Model 1 represents GR induces Bim activation via direct binding to c-Jun **(B)** Model 2 is similar to Model 1 but differs by the nature of the interaction between the GR and c-Jun. An extra step of protein synthesis was introduced for targeting down-stream target gene c-Jun in Model 2.

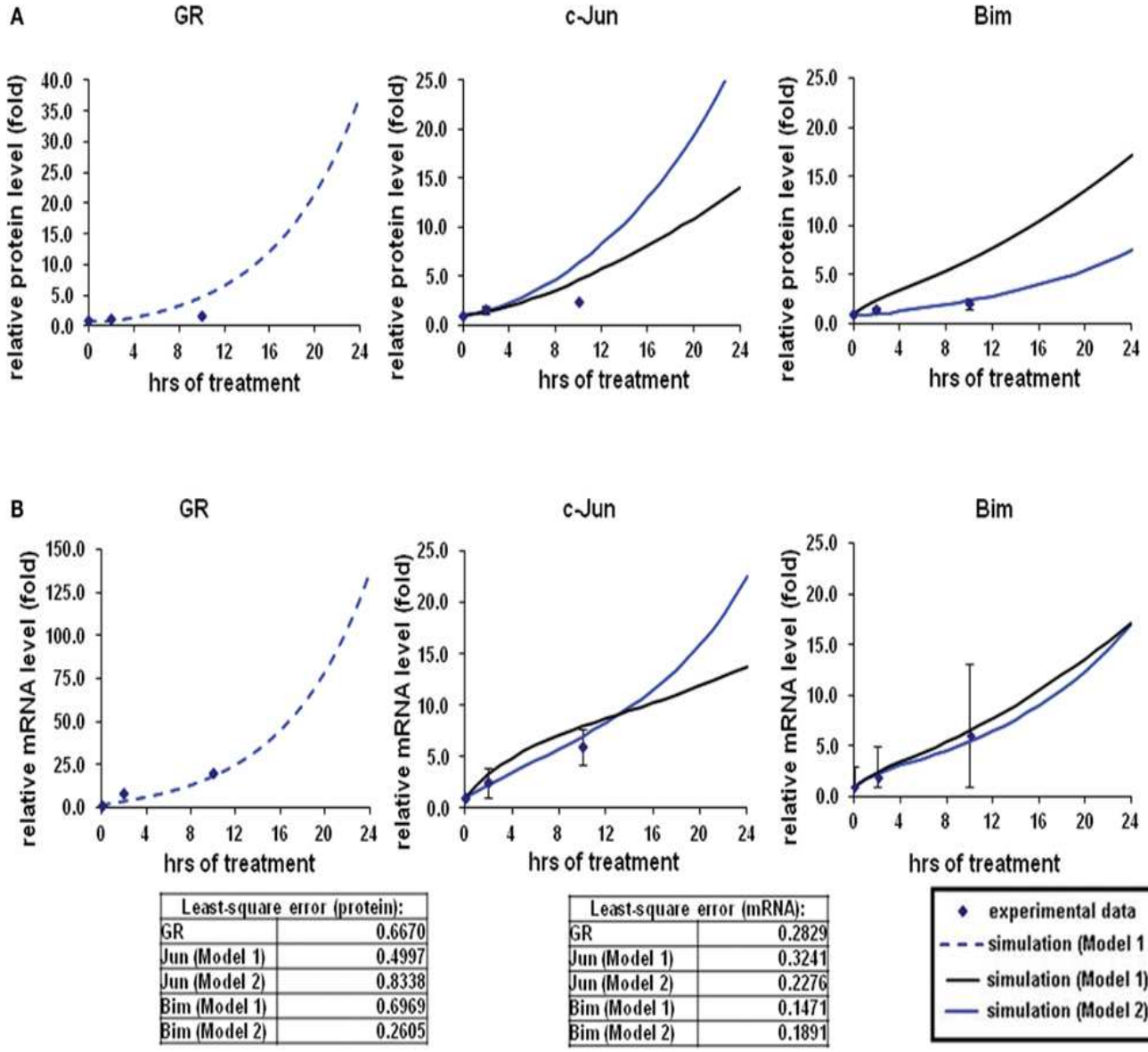

Least-square error (protein):	
GR	0.6670
Jun (Model 1)	0.4997
Jun (Model 2)	0.8338
Bim (Model 1)	0.6969
Bim (Model 2)	0.2605

Least-square error (mRNA):	
GR	0.2829
Jun (Model 1)	0.3241
Jun (Model 2)	0.2276
Bim (Model 1)	0.1471
Bim (Model 2)	0.1891

Figure 4.2 Simulations of GR/Jun/Bim induction in CEM-C7-14 cells

The simulations process and the experimental data were described in our previous work (9; 17). In brief, the expression dynamics were simulated with the use of CellDesigner and SBML-PET parameter estimation tool based on the experimental data obtained at 0, 2 and 10 hours after 1μM dexamethasone (Dex) treatment (9) Solid squares are the mean of the normalised experimental data and bars are the standard deviations for three sets of experiments. The simulation process is divided to two steps, the parameters for GR activation alone were first obtained (dotted line), and then the rest of the parameters were estimated based on the individual model topologies. The black solid line represents the simulation by Model 1 and the blue line is the simulation of Model 2 **(A)** Protein timecourse simulations of GR, c-Jun and Bim in CEM-C7-14 cells. **(B)** The simulations for GR, c-Jun and Bim mRNA dynamics. The models as shown revealed the characteristic kinetics of GR, c-Jun and Bim in response with Dex in CEM-C7-14 cells. The residual value was calculated to assess the quality of the fit between the simulations and the experimental data.

4.4.2 Modelling the role of Erg in GR gene expression in GC sensitive C7 cells

We have previously characterised the kinetic response to GR in ALL through time course clustering of gene expression microarray (9). Results from the experiments and analyses identified Erg as one of the crucial genes that determine GC resistance. In addition, chromatin immunoprecipitation results showed that Erg was transiently recruited on the GR1A promoter in sensitive C7 cells only. Erg is a member of the Ets transcription factor family which has been linked to growth of adult haematopoietic cells and fusion with genes that are involved in cancer, such as the EWS gene in Ewing's sarcoma (13; 29). It has recently been identified as a prognosis factor in T-ALL and prostate cancer (13; 15; 30). Ets subfamily members have also been linked to GR regulation in ALL (14; 16) (Suppl. Fig. 4.1).

To systematically assess the factors of resistance to GC therapy in CEM cells, we developed kinetic models of GR/Erg signalling. As GR was found to recruit on the GR promoter in C7 cells, we sought to build a model that can capture the effect of Erg on GR expression and verify our experimental results. We here constructed two models, with Model 3 and Model 4 differing by Erg regulation on GR (Fig. 4.3A & B). Both models captured GR and Erg transcription, translation and degradation and each reaction was described by mass action kinetics (Table 4-1). The regulation between Erg and GR expression is not only an important component of GR homeostasis, but also a potential factor provoking GC resistance in relation to the level of GR. The simulations showed that Model 4 overall fits better to our experimental results, where

microarray, western and qRT-PCR analysis identified a low level of Erg (≤1-fold) and an increase of GR (protein simulation increased up to 4.4-fold and mRNA up to 27.5-fold), although GR induction was smaller compared to GR simulations in Model 3 (with both protein and mRNA simulation exceeding 140 fold-change at 24 h). This is particularly apparent at the Erg mRNA level, in comparison with the low level of Erg mRNA simulation in Model 4, an increase was observed in Model 3 (4.3-fold at 24 h) (Fig. 4.4A & B). In addition, in Model 4 the simulation of both Erg protein and mRNA level decreased after 4 h of Dex treatment before gradually reaching a steady state (protein simulation: 0.9-fold, mRNA simulation 0.2-fold). At the protein level, least square residual values for GR (ε=1.1880) and Erg (ε=0.4218) were both higher in Model 3 than in Model 4 (GR: ε=0.2758; Erg: ε=0.1874), with GR showing a greater discrepancy in comparison with the other components. The residual values of GR and Erg mRNA simulations were lower than their protein simulations in both Model 3 and Model 4, ranging between 0.3-0.5 (Model 3: GR: ε=0.4058; Erg: ε=0.3665; Model 4: GR: ε=0.3896; Erg: ε=0.5852). Altogether it seemed that Model 4 simulations and analysis corroborated earlier findings (9), which further confirms that this model is more appropriate. These results also highlight the importance of the role of Erg expression on GR regulation.

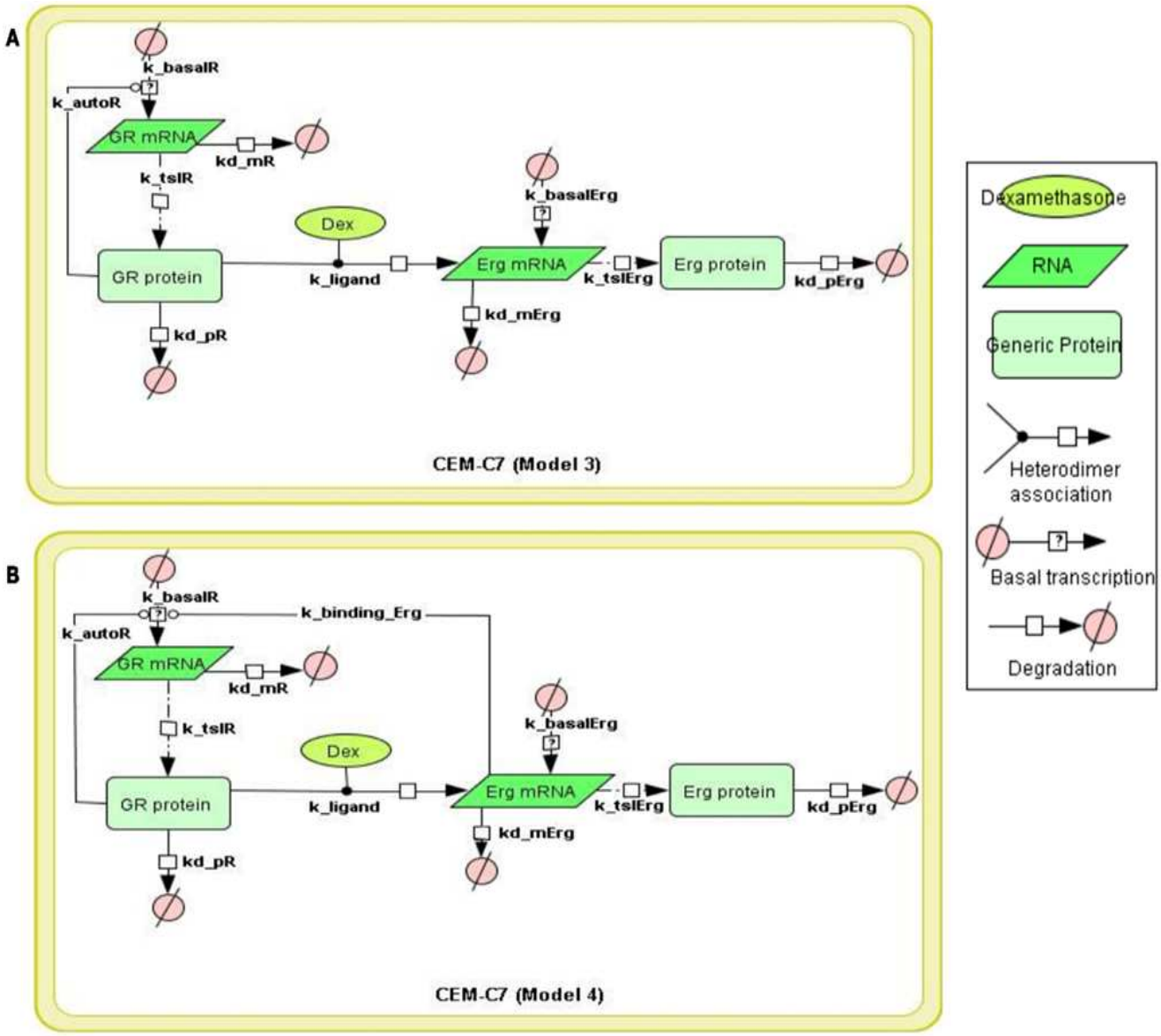

Figure 4.3 Topology of GR/Erg models in CEM-C7-14 cells

Schematic representation of GR/Erg pathway. The nature of the topologies was based on previously established direct GR target model (17). Model 3 and Model 4 are similar and only differ by the regulation of GR, in Model 3 GR regulation is controlled by GR itself **(A)** whereas in Model 4 GR regulation is controlled by both GR itself and Erg direct interaction to GR gene **(B)**.

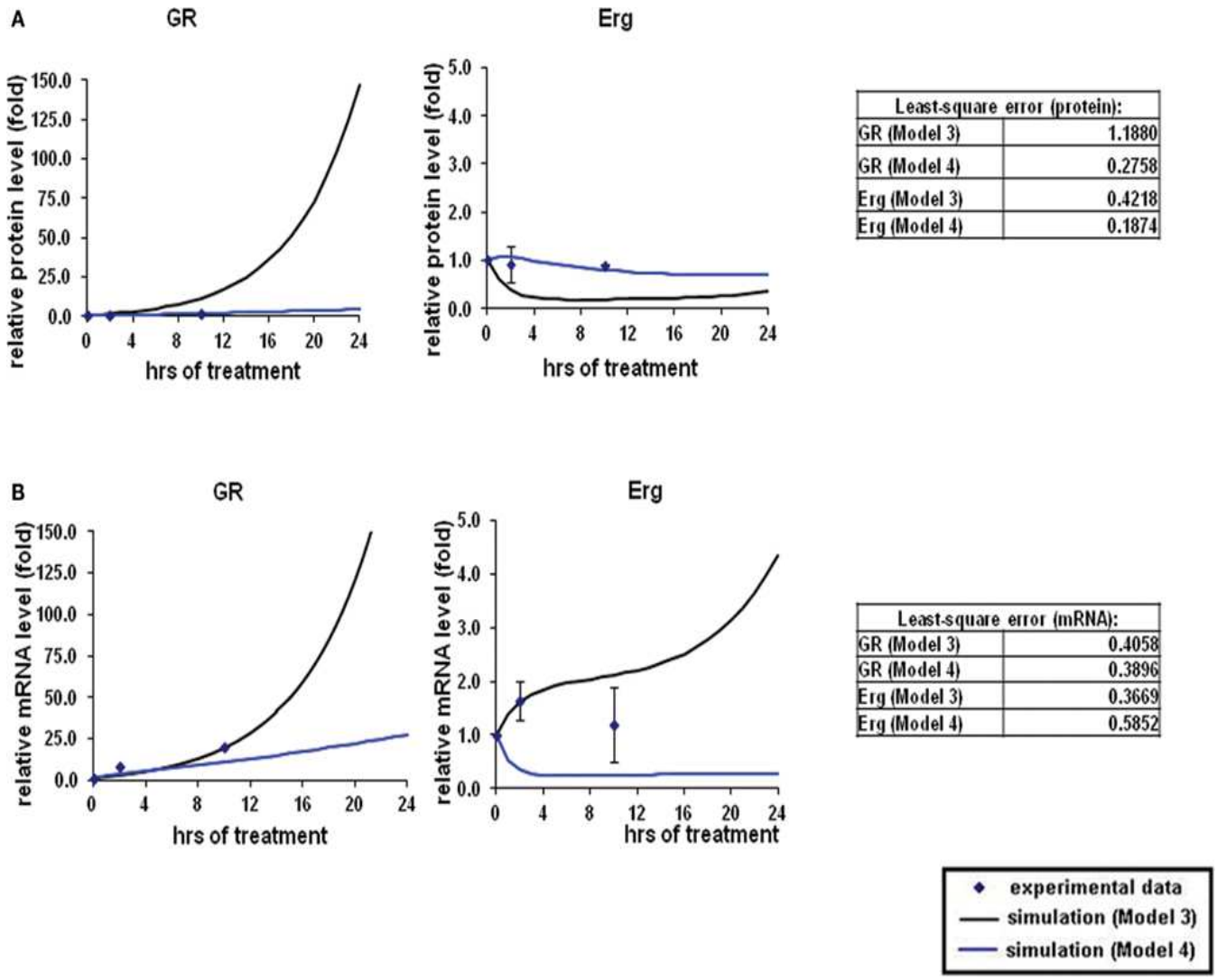

Figure 4.4 Simulations of GR/Erg pathway in CEM-C7-14 cells

Protein timecourse simulation of GR/Erg pathway in CEM-C7-14 cells. The same process of simulation was carried out in Model 3 and Model 4 as described in Figure 2. Solid squares are the experimental data and the error bars are means ± standard deviation for three sets of experiments. The black solid line represents the simulation by Model 3 and the blue line is the simulation of Model 4. The residual value was calculated to assess the quality of the fit between the simulations and the experimental data. **(B)** GR and Erg mRNA timecourse simulations in CEM-C7-14 cells.

4.4.3 Modelling the role of Erg in GR gene expression in GC resistant C1 cells

In the next step, we sought to investigate the GR dependent Erg induction that was previously found in resistant C1 cells only. Treatment with Dex was found to induce Erg expression in C1 cells and an increase of apoptosis was observed when treated with Erg inhibitor

(9). GR may be able to directly activate Erg, as a potential GRE was identified on the Erg promoter (Suppl. Table 4.1B). Based on the experimental data obtained and strategy outlined above, we created two models for the GR induced Erg expression (Fig. 4.5). Similar to the direct and indirect models as established in (17), the two models differed by an extra step of *de novo* protein synthesis (Fig. 4.5A & B); the positive GR autoregulation feedback loop was not included in C1 cells (17; 21; 22).

The overall simulations with both direct (Model 5) and indirect models (Model 6) showed an induction in both GR and Erg protein and mRNA levels (Fig. 4.6A & B). At the protein level, GR protein simulations showed an increase of ≥15-fold with both models whereas protein simulation with Model 6 increased at a much lower rate in comparison (2.3-fold at 24 h) with Model 5. Erg protein simulation with Model 5 seemed to fit better than Model 6, with the simulation clearly showing a better fit to the experimental data. Despite the consistent upregulating simulation trends compared with the experimental results, least square analysis showed that apart from Erg with Model 5 (ε=0.6486), the residual values were all greater than 1 (Model 5: GR (ε=1.5566) & Model 6: GR (ε=1.0605), Erg (ε=1.3059)). In contrast to protein simulations, mRNA simulations were found to have a good fit to the experimental data with both models, where GR and Erg mRNA were both induced. The mRNA simulations with both models appeared to increase at a slower rate in comparison with the protein simulations; in Model 5 GR mRNA increased up to 13.6-fold and Erg mRNA up to 2.3-fold at 24 h, whereas Model 6 showed a lower increase rate with GR mRNA (5.4-fold) but a higher and more linear induction in Erg mRNA (17.9-fold). Much smaller residual values were calculated at the mRNA levels, with Model 5 (GR: ε=0.2346, Erg: ε=0.3856) having a better fit than Model 6 (GR: ε=0.4034, Erg: ε=0.6590). These findings support the hypothesis that GR may activate Erg expression by directly targeting the GRE on the Erg promoter.

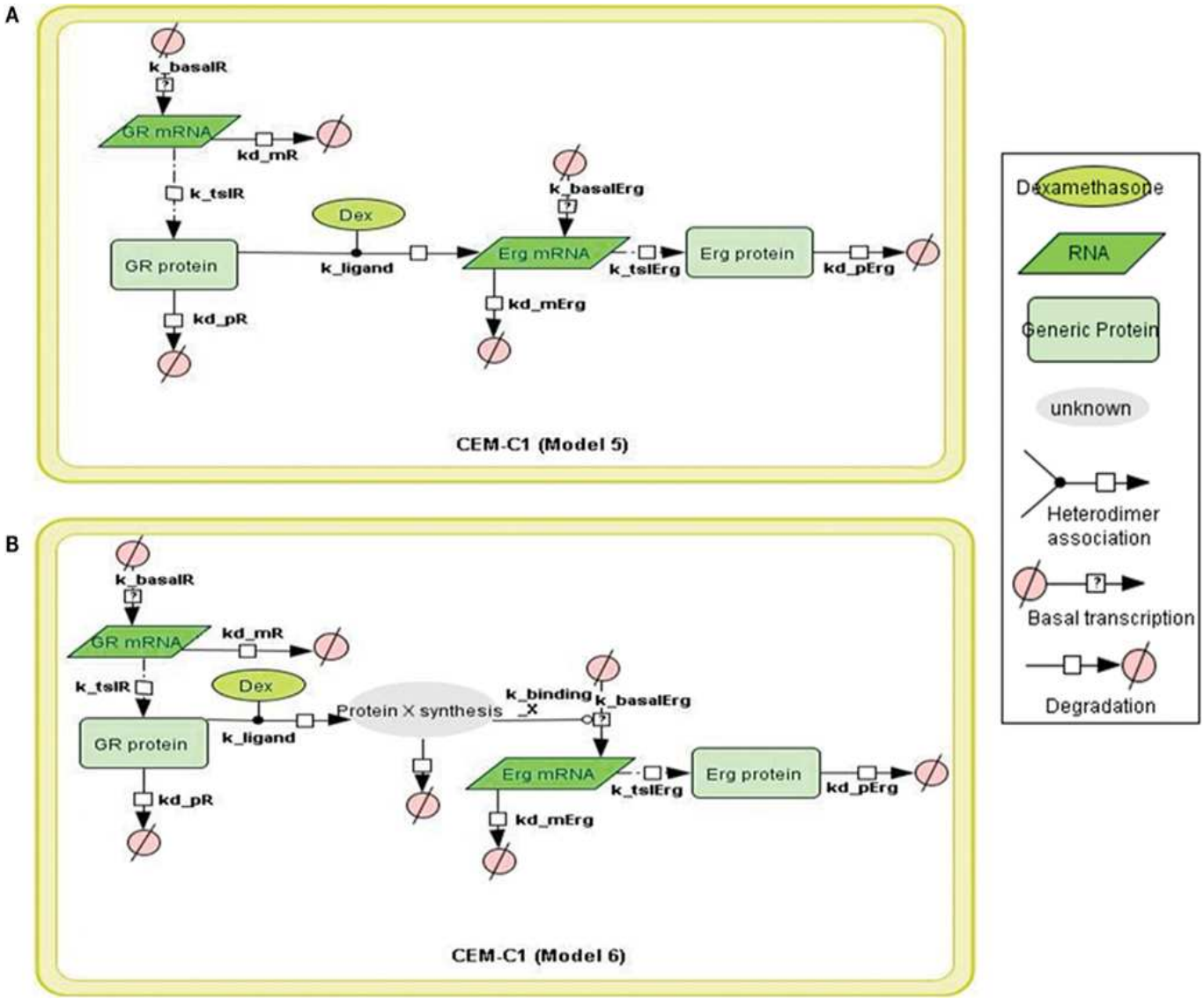

Figure 4.5 Topology of GR/Erg models in CEM-C1-15 cells

Schematic representation of GR/Erg pathway in CEM-C1-15 cells. The nature of the topologies was based on previously established direct and indirect GR target models in CEM-C1-15 cells (17). GR auto-regulation was not included in CEM-C1-15, Model 5 and Model 6 differ by the GR regulation on Erg induction, with Model 5 indicating Erg as a direct GR target **(A)** and Model 6 showing Erg as an indirect GR target where *de novo* protein synthesis is required for Erg induction **(B)**.

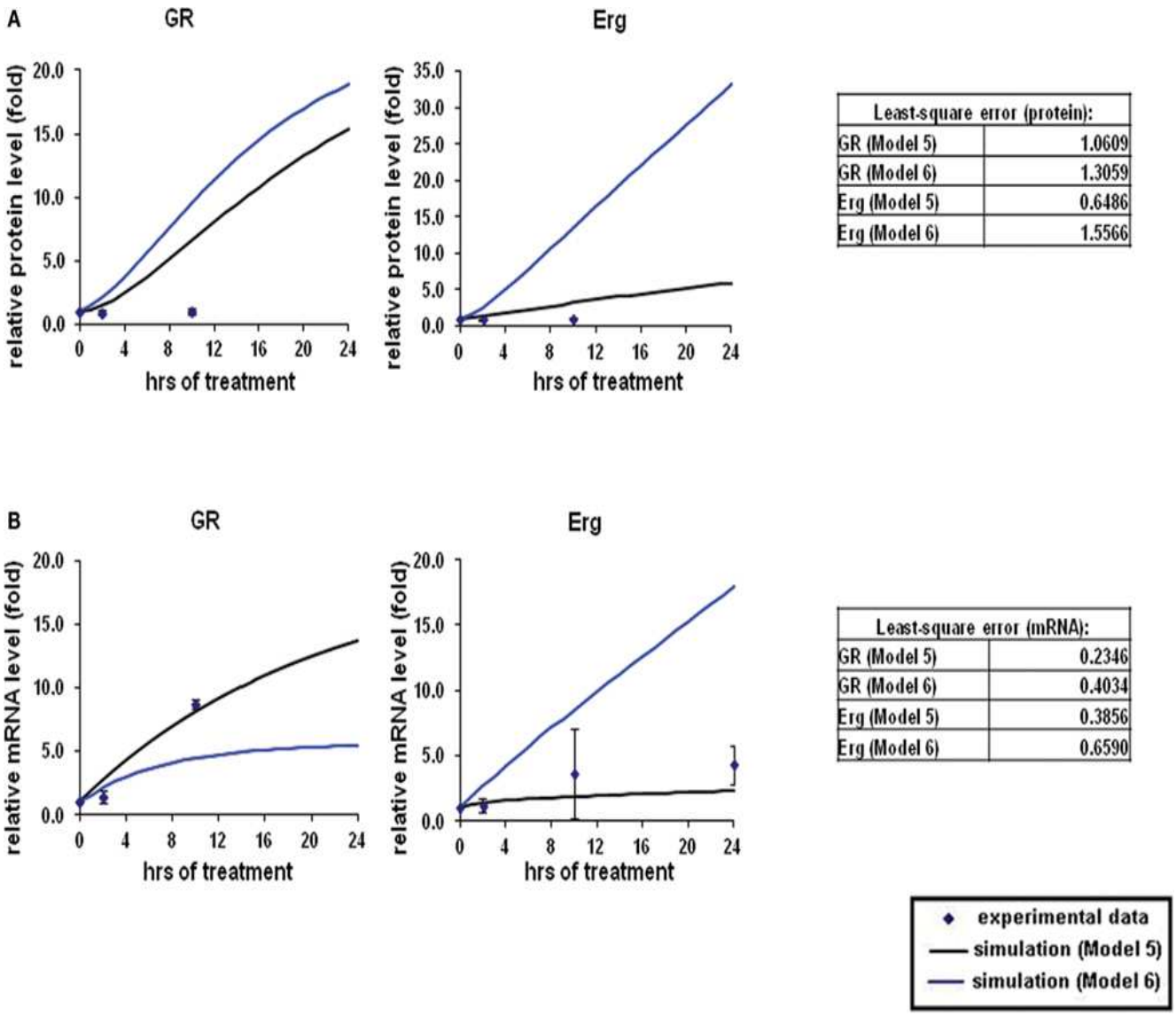

Figure 4.6 Simulations of GR/Erg pathway in CEM-C1-15 cells

The same process of simulation was carried out in Model 5 and Model 6 as described in Fig. 4.2. Solid squares are the experimental data and the error bars are means ± standard deviation for three sets of experiments. The black solid line represents the simulation by Model 5 and the blue line is the simulation of Model 6. **(A)** Protein timecourse simulation of GR/Erg pathway in CEM-C1-15 cells. **(B)** GR and Erg mRNA timecourse simulations in CEM-C1-15 cells.

4.5 Discussion

Glucocorticoids (GC) have a pivotal role in the treatment of acute lymphoblastic leukaemia (ALL) through initiating apoptosis. Despite the relatively high cure rate, GC resistance still remains a therapeutic problem due to its unknown molecular mechanism. Thanks to advances in

"omics" technologies, there is a growing amount of literature and molecular models dealing with GC induced signalling. Bim, a well known pro-apoptotic Bcl-2 member, has been identified as a crucial player in apoptosis and is able to trigger cell death (6). It is known that Bim is activated by GR via an indirect mechanism where *de novo* protein synthesis is required (8). Nevertheless, the exact mechanism of Bim induction by GR is poorly understood. Foxo3a (Forkhead box subgroup O3a) has been suggested as a potential candidate for targeting and activating Bim, thereby initiating apoptosis in chronic myeloid leukaemia (31). This however may not be the case in ALL as we identified upregulation of GILZ in C7 cells (9; 17), which can protect ALL cells by provoking nuclear exclusion of Foxo3 (32). In the case of ALL, we observed an induction of both GILZ and Bim but not Foxo3 in C7 cells (17), suggesting that the exclusion of nuclear Foxo3 may also occur in ALL under the influence of GILZ and further supporting the idea that an alternative protein is involved in Bim induction (12). Timecourse microarrays in ALL (9) and a study of Bim in neuronal cells (11) had led us to believe that c-Jun may be a crucial player in Bim activation. On the other hand, Erg has recently been identified as a crucial prognosis factor for determining GC resistance (13). We have verified these results and found that Erg signalling may be involved in GR regulation with a cell specific mechanism (9).

Our ODE models of GR induced apoptosis capture the dynamics of GR regulation of Bim via c-Jun and the crosstalk between GR and Erg independently. For GR/c-Jun/Bim regulation, two possible topologies were constructed, where the two models differed by the nature of *de novo* protein synthesis (Fig. 4.1A &B). Simulation outcomes of GR interaction with c-Jun and Bim were consistent with the few biological data available, where GR induced c-Jun and Bim over time (7; 10). Least square analysis showed that c-Jun mRNA and Bim protein with Model 2 fitted better with the experimental data whereas c-Jun protein and Bim mRNA fitted better with Model 1 (Fig. 4.2A & B). These results may be explained by a possible involvement of alternative mechanisms, as treatment with the protein synthesis inhibitor cycloheximide has shown that c-Jun expression was not affected and the induction became more prominent comparing with the pre-treatment. Further nuclear run on tests have indicated that c-Jun induction requires at least 6 h Dex treatment. Such process takes much longer than the time required for GR translocation and binding to the promoter of the target gene, as previous green fluorescent protein experiment indicated that a full GR translocation takes only 2 hours to complete (33). Taken together, the author suggested that the mechanism for the delayed c-Jun induction may be secondary, potentially through the relief from a protein repressor of transcription (27). Our previous chromatin immunoprecipitation results had shown c-Jun recruitment on Bim promoter and that inhibition of c-Jun N-terminal kinases (JNKs) with

SP600125 did not repress, but in fact enhanced apoptosis in C7 cells despite Bim expression being reduced (Suppl. Fig. 4.2A) (9; 12), suggesting an alternative signalling pathway for c-Jun induction. Lu *et al.* have demonstrated that the p38 MAPK pathway is linked to the promotion of Dex induced apoptosis and that the inhibition of p38 reduced Bim induction (12). Furthermore, Dex did not affect the total level of p38 protein but induced p38 phosphorylation (12), and inhibition of p38 was shown to result in a significant increase in c-Jun mRNA level in monocytes (34). On the contrary, a study of p38 inhibitor and MEK/ERK inhibitor in the bacterial lipopolysaccharides (35) induced murine macrophages, indicated that both inhibitors were essential to suppress c-Jun induction. Hence it is possible that such repression of c-Jun may be acting in conjunction with other signalling pathways (36).

Another subject of special interest to this study was to investigate the role of Erg in determining GC resistance, since we have identified Erg recruitment on GR promoter in C7 cells only but a substantial Erg expression was found in resistant C1 cells (9). Since the relation between GR and Erg remains obscure, we aimed to evaluate the role of Erg in the GR signalling pathway, which could be modulated in a cell dependent manner. Our GR/Erg models were devised into four sets, with two potential mechanisms each in C7 and C1 cells.

To place Erg in the GR induction model in C7 cells, we considered the regulatory influence of Erg on GR autoregulation. Based on previous literature and the finding of Erg recruitment on GR promoter, we hypothesised that Model 4 with direct Erg regulation on GR expression would have a better fit with the experimental data than Model 3 (Fig. 4.3A & B) (9; 16). Indeed, simulations with Model 4 showed an increase in GR mRNA and protein level, and more importantly a low level of Erg protein and mRNA, despite that a more dramatic increase of GR protein and mRNA levels were identified in Model 3 simulations (Fig. 4.4A & B). The residual values calculated indicated that the Erg protein and GR mRNA simulations fit better with Model 4, suggesting the need of extending the number of time points of experimental data. Preliminary western blotting based on two sets of independent experiments confirmed the potential role of Erg in GR regulation when treated with a functional inhibitor of Erg, YK-4-279. In this case, a much lower GR protein expression was identified in the presence and absence of Dex (Suppl. Fig. 4.2A). The results showed that despite limited data, Model 4 was still able to reflect the expected experimental observations to a good extent, where the inclusion of Erg regulating GR directly generates a low level of Erg. It should be noted that we also identified a depletion of Bim protein expression when treated with YK-4-279, which suggested a possible role for Erg in the regulation of Bim (Suppl. Fig. 4.2). The correlated apoptosis assay with annexin V, however

still showed an increase in apoptosis, indicating a potential switch to an alternative apoptotic signalling pathway. More investigation is required to clarify these results (9). Yu *et al.* has conducted a detailed study on Erg in the GR subfamily- androgen receptor (AR) signalling, where they have shown an inhibitory role of Erg on the AR gene (37), which reinforces the importance of Erg in GR regulation. In addition, it has been suggested that the balance of Erg and AR may be controlled by two possible mechanisms: Erg may inhibit AR by a negative autoregulatory loop, or by Erg affecting the AR target gene selectivity (38), which may both have an impact on AR regulation. Since AR and GR share high homology in the DNA binding domain and recognize similar hormone response elements, it is possible that Erg also directly regulates GR expression or forms another level of control over GR target genes. The abovementioned mechanism should be considered in the GR/Erg model (39; 40).

As the positive regulation of Erg by GR was only observed in the resistant C1 cells and a consensus GRE was identified in Erg, in the next step we aimed to determine whether Erg acts as a direct GR target. By adapting the direct GR and indirect GR model in C1 cells as indicated in (17), two models were described (Fig. 4.5). GR autoregulation was not considered in resistant C1 cells and the two models differed by a step of *de novo* protein X synthesis. The simulation results showed an induction of GR and Erg protein and mRNA levels with both Model 5 and Model 6, with GR protein and Erg mRNA and protein showing a more dramatic increase in Model 6 (Fig. 4.6A & B). By observing the trend and evaluating the residual values, which appeared to fit better with Model 5 in all cases, we hypothesise that Erg is likely to be a direct GR target. Further experimental results are required to test this prediction. Western blotting of Dex in combination with YK-4-279 treatment showed a lower Bim expression than the control in C1 cells (Suppl. Fig. 4.2B), even though a significant increase in apoptosis was identified previously (9). This suggests that Erg may either be acting as an activator upstream of anti-apoptotic target genes, or as a repressor of pro-apoptotic signalling but not via Bim activation.

We have successfully built quantitative models to study c-Jun, Bim and Erg signalling and their interaction with GR. The models account for established as well as novel experimental observations, demonstrated the interplay between GR, c-Jun and Bim, and enabled us to clarify how Erg is regulated as a cell specific modulator. Taking the experimental observations into account, this systems biology approach allowed us to distinguish between alternative mechanisms and determine the role of c-Jun and Erg in the network. Our models can serve as a basis to study GR/c-Jun/Bim and GR/Erg signalling in ALL and can be continuously extended as more data becomes available. Overall, this study shows that systems biology approach

combining mechanistic modelling with experimental analysis is of invaluable help to dissect complex signalling pathways and improve our understanding towards disease and drug action.

4.6 Tables

Table 4-1 Kinetic equations describing GR mediated induction of Bim, c-Jun and Erg

The set of ordinary differential equations describes the GR regulatory kinetics implemented in our models. Here, the kinetics is essentially the same but with different protein or mRNA names. *kd_X* represents the overall degradation of factor X; *k_binding_X* is the regulation between the unknown *proteinX* and the target gene; *k_binding_Erg* is the regulation between Erg and GR; *k_ligand* is the rate of complex association of dexamethasone and GR; *kd_m* and *kd_p* represent the first order rate constants of the degradation of mRNA and protein respectively. The term *Tsl* denotes translation, *basal* denotes basal transcription, *proteinX* the unknown protein and *R* the glucocorticoid receptor.

Model 1 & 2

GR

$$\frac{d[R\_mRNA]}{dt} = k\_basalR + [R] \cdot k\_\_autoR - [R\_mRNA] \cdot kd\_mR$$

$$\frac{d[R]}{dt} = [R\_mRNA] \cdot k\_tslR - [R] \cdot kd\_pR$$

Model 1

Bim

$$\frac{d[Bim\_mRNA]}{dt} = k\_basalBim + [Jun] \cdot k\_binding\_Jun - [Bim\_mRNA] \cdot k\_dmBim$$

$$\frac{d[Bim]}{dt} = [Bim\_mRNA] \cdot k\_tslBim - [Bim] \cdot kd\_pBim$$

Jun

$$\frac{d[Jun\_mRNA]}{dt} = k\_basalJun - [Jun\_mRNA] \cdot kd\_mJun + [Dex] \cdot [R] \cdot k\_ligand$$

$$\frac{d[Jun]}{dt} = [Jun\_mRNA] \cdot k\_tslJun - [Jun] \cdot kd\_pJun$$

Model 2

Bim

$$\frac{d[Bim\_mRNA]}{dt} = k\_basalBim + [Jun] \cdot k\_binding\_Jun - [Bim\_mRNA] \cdot k\_dmBim$$

$$\frac{d[Bim]}{dt} = [Bim\_mRNA] \cdot k\_tslBim - [Bim] \cdot kd\_pBim$$

Jun

$$\frac{d[Jun\_mRNA]}{dt} = k\_basalJun + [\mathrm{Pr}oteinX\_synthesis] \cdot k\_binding\_X - [Jun\_mRNA] \cdot kd\_mJun$$

$$\frac{d[Jun]}{dt} = [Jun\_mRNA] \cdot k\_tslJun - [Jun] \cdot kd\_pJun$$

Protein X synthesis

$$\frac{d[proteinX\_synthesis]}{dt} = [Dex] \cdot [R] \cdot k\_ligand - [proteinX\_synthesis] \cdot kd\_X$$

Model 3

GR

$$\frac{d[R\_mRNA]}{dt} = k\_basalR + [R] \cdot k\_\_autoR - [R\_mRNA] \cdot kd\_mR$$

$$\frac{d[R]}{dt} = [R\_mRNA] \cdot k\_tslR - [R] \cdot kd\_pR$$

Erg

$$\frac{d[Erg\_mRNA]}{dt} = k\_basalErg - [Erg\_mRNA] \cdot k\_dmErg + [R] \cdot [Dex] \cdot k\_ligand$$

$$\frac{d[Erg]}{dt} = [Erg\_mRNA] \cdot k\_tslErg - [Erg] \cdot kd\_pErg$$

Model 4

GR

$$\frac{d[R\_mRNA]}{dt} = k\_basalR + [R] \cdot k\_\_autoR - [R\_mRNA] \cdot kd\_mR + [Erg\_mRNA] \cdot k\_binding\_Erg$$

$$\frac{d[R]}{dt} = [R\_mRNA] \cdot k\_tslR - [R] \cdot kd\_pR$$

Erg

$$\frac{d[Erg\_mRNA]}{dt} = k\_basalErg - [Erg\_mRNA] \cdot k\_dmErg + [R] \cdot [Dex] \cdot k\_ligand$$

$$\frac{d[Erg]}{dt} = [Erg\_mRNA] \cdot k\_tslErg - [Erg] \cdot kd\_pErg$$

Model 5

GR

$$\frac{d[R\_mRNA]}{dt} = k\_basalR - [R\_mRNA] \cdot kd\_mR$$

$$\frac{d[R]}{dt} = [R\_mRNA] \cdot k\_tslR - [R] \cdot kd\_pR$$

Erg

$$\frac{d[Erg\_mRNA]}{dt} = k\_basalErg - [Erg\_mRNA] \cdot k\_dmErg + [R] \cdot [Dex] \cdot k\_ligand$$

$$\frac{d[Erg]}{dt} = [Erg\_mRNA] \cdot k\_tslErg - [Erg] \cdot kd\_pErg$$

Model 6

GR

$$\frac{d[R\_mRNA]}{dt} = k\_basalR - [R\_mRNA] \cdot kd\_mR$$

$$\frac{d[R]}{dt} = [R\_mRNA] \cdot k\_tslR - [R] \cdot kd\_pR$$

Erg

$$\frac{d[Erg\_mRNA]}{dt} = k\_basalErg - [Erg\_mRNA] \cdot k\_dmErg + [proteinX\_synthesis] \cdot k\_binding\_X$$

$$\frac{d[Erg]}{dt} = [Erg\_mRNA] \cdot k\_tslErg - [Erg] \cdot kd\_pErg$$

Protein X synthesis

$$\frac{d[proteinX\_synthesis]}{dt} = [Dex] \cdot [R] \cdot k\_ligand - [proteinX\_synthesis] \cdot kd\_X$$

4.7 Supplementary data

4.7.1 Supplementary Figures

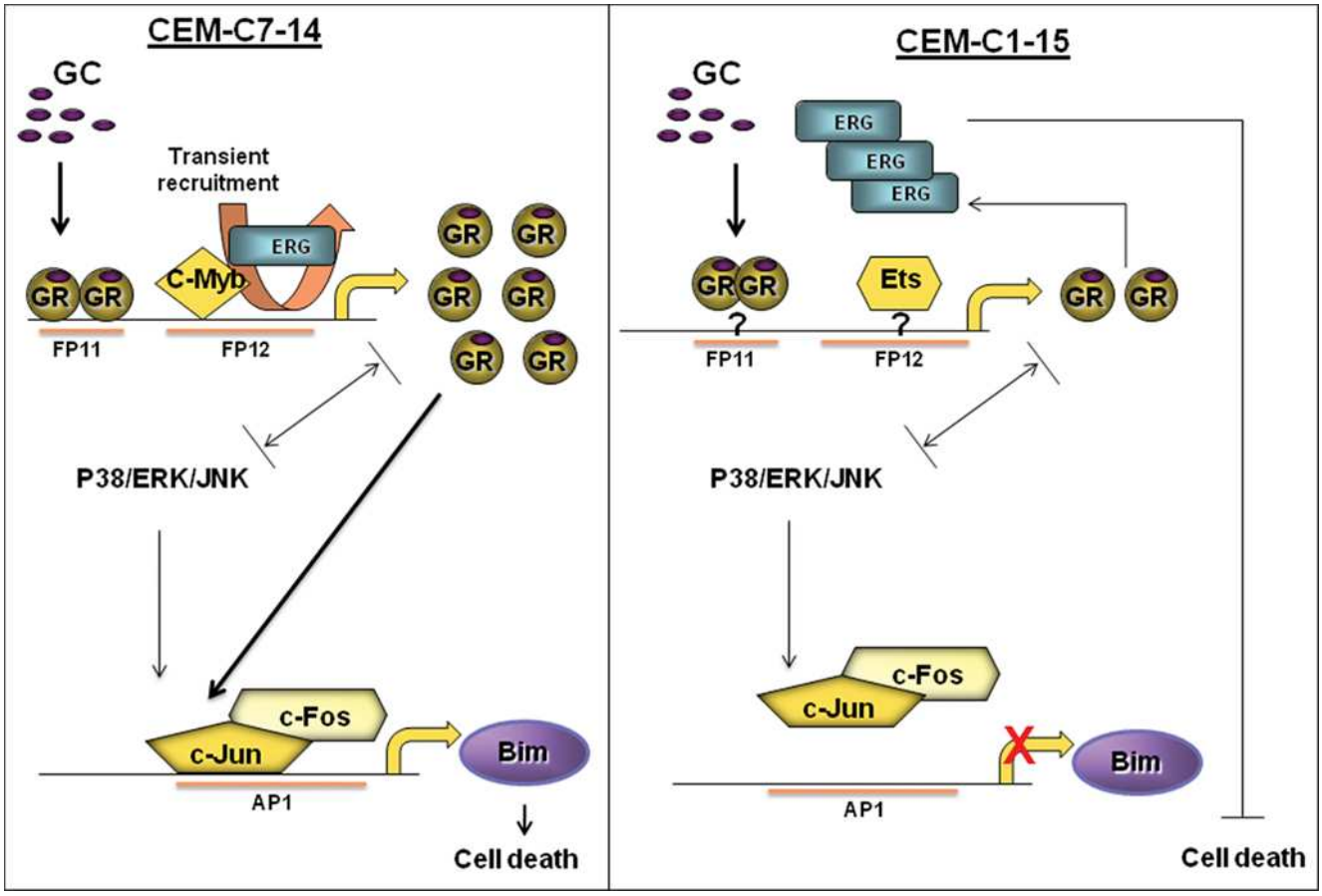

Suppl. Figure 4.1 Proposed regulation of cell death in leukaemia

In CEM-C7 cells, upon GC treatment, GR becomes activated and alters Bim and GR transcription, potentially through AP-1 and Erg recruitment respectively. This may be cell specific as such recruitments were not seen in CEM-C1 cells. Other factors such as MAPK signalling (i.e. JNK or P38) and c-Myb may play a role in regulating GR, AP-1 and Bim.

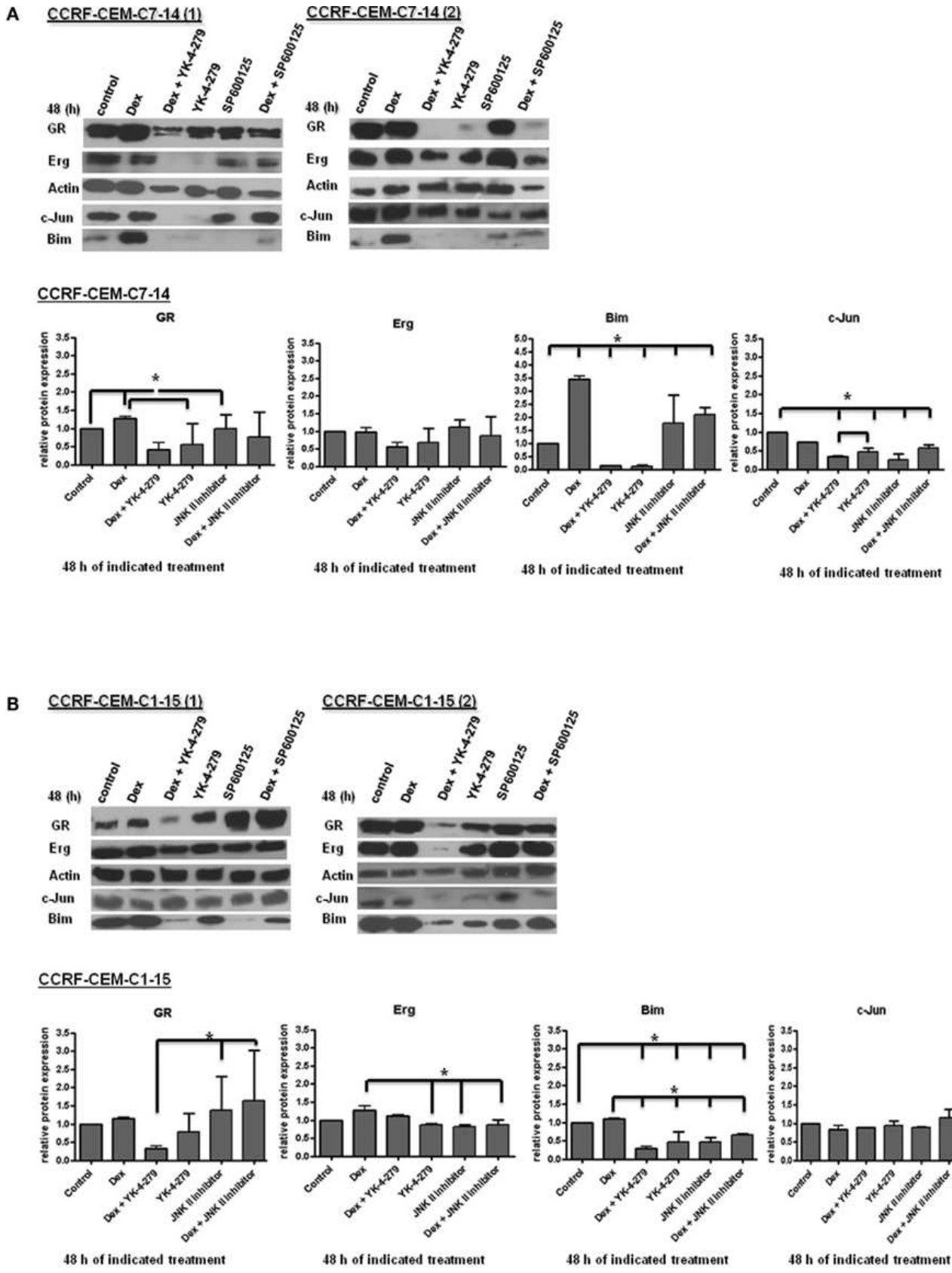

Suppl. Figure 4.2 GR target gene protein expression in CEM cells

Western blot analysis of GR, Erg, c-Jun and Bim protein levels, with actin as a control in C7 **(A)** and C1 **(B)** cells cultured with a combination of 1μM Dex, 10μM YK-4-279, 10μM JNK inhibitor (SP600125) for the indicated times. Protein levels were quantified by ImageJ, normalised to actin and presented as a histogram. Error bars represent ± standard deviation of two independent experiments. Asterisk indicates a significant difference at $p < 0.05$ using the ANOVA Tukey's test.

4.7.2 Supplementary Tables

Transcription factor	Binding protein	Strand	Sequence
A. LOCATION AND SEQUENCE OF POTENTIAL GR BINDING SITES IN C-JUN			
GR	Chr1:59247433–59247449	+	AGGTCCATGCAGTTCTT
GR	Chr1:59247576–59247595	–	TCGTGCACACTGGGGGCGCC
B. LOCATION AND SEQUENCE OF POTENTIAL GR BINDING SITES IN ERG			
GR	Chr1:40036930–40036946	–	CAATAACACGTGGTGAC

Suppl. Table 4.1 Location and sequence of binding sites in the regulatory regions of the indicated genes

Potential GRE sites were identified using the text mining tool - The Champion ChiP Transcription Factor Search Portal (CCTSF) from Qiagen SABiosciences's database. **(A)** Location and sequence of potential GR-1 binding sites in c-Jun. **(B)** Location and sequence of GR binding sites in Erg.

4.8 References

1. Pui C-H, Robison LL, Look AT. Acute lymphoblastic leukaemia. *The Lancet* 2008; **371:** 1030-1043.

2. Onciu M. Acute lymphoblastic leukemia. *Hematology/Oncology Clinics of North America* 2009; **23:** 655-674.

3. Mullighan CG, Zhang J, Kasper LH, Lerach S, Payne-Turner D, Phillips LA *et al*. CREBBP mutations in relapsed acute lymphoblastic leukaemia. *Nature* 2011; **471:** 235-239.

4. Schaaf MJM, Cidlowski JA. Molecular mechanisms of glucocorticoid action and resistance. *The Journal of Steroid Biochemistry and Molecular Biology* 2002; **83:** 37-48.

5. Abrams MT, Robertson NM, Yoon K, Wickstrom E. Inhibition of glucocorticoid-induced apoptosis by targeting the major splice variants of Bim mRNA with small interfering RNA and short hairpin RNA. *Journal of Biological Chemistry* 2004; **279:** 55809-55817.

6. Ploner C, Rainer J, Niederegger H, Eduardoff M, Villunger A, Geley S *et al*. The Bcl2 rheostat in glucocorticoid-induced apoptosis of acute lymphoblastic leukemia. *Leukemia* 2007; **22:** 370-377.

7. Zhao Y-n, Guo X, Ma Z-g, Gu L, Ge J, Li Q. Pro-apoptotic protein Bim in apoptosis of glucocorticoid-sensitive and -resistant acute lymphoblastic leukemia CEM cells. *Medical Oncology* 2011; **28:** 1609-1617.

8. Wang Z, Malone MH, He H, McColl KS, Distelhorst CW. Microarray analysis uncovers the induction of the proapoptotic BH3-only protein Bim in multiple models of glucocorticoid-induced apoptosis. *Journal of Biological Chemistry* 2003; **278:** 23861-23867.

9. Chen DW, Saha V, Liu JZ, Schwartz J-M, Krstic-Demonacos M. Erg and AP-1 as determinants of glucocorticoid response in acute lymphoblastic leukemia. *Oncogene* 2012.

10. Zhou F, Thompson EB. Role of c-Jun induction in the glucocorticoid-evoked apoptotic pathway in human leukemic lymphoblasts. *Molecular Endocrinology* 1996; **10:** 306-16.

11. Biswas SC, Shi Y, Sproul A, Greene LA. Pro-apoptotic Bim induction in response to nerve growth factor deprivation requires simultaneous activation of three different death signaling pathways. *Journal of Biological Chemistry* 2007; **282:** 29368-29374.

12. Lu J, Quearry B, Harada H. p38-MAP kinase activation followed by Bim induction is essential for glucocorticoid-induced apoptosis in lymphoblastic leukemia cells. *FEBS Letters* 2006; **580:** 3539-3544.

13. Tsuzuki S, Taguchi O, Seto M. Promotion and maintenance of leukemia by Erg. *Blood* 2011; **117:** 3858-3868.

14. Baldus CD, Burmeister T, Martus P, Schwartz S, Gökbuget N, Bloomfield CD *et al*. High expression of the Ets transcription factor Erg predicts adverse outcome in acute T-lymphoblastic leukemia in adults. *Journal of Clinical Oncology* 2006; **24:** 4714-4720.

15. Thoms JAI, Birger Y, Foster S, Knezevic K, Kirschenbaum Y, Chandrakanthan V *et al*. Erg promotes T-acute lymphoblastic leukemia and is transcriptionally regulated in leukemic cells by a stem cell enhancer. *Blood* 2011; **117:** 7079-7089.

16. Geng C-D, Vedeckis WV. c-Myb and members of the c-Ets family of transcription factors act as molecular switches to mediate opposite steroid regulation of the human glucocorticoid receptor 1A promoter. *Journal of Biological Chemistry* 2005; **280:** 43264-43271.

17. Chen DW-C, Lynch JT, Demonacos C, Krstic-Demonacos M, Schwartz J-M. Quantitative analysis and modeling of glucocorticoid-controlled gene expression. *Pharmacogenomics* 2010; **11:** 1545-1560.

18. Hoffmann A, Levchenko A, Scott ML, Baltimore D. The IκB–NF-κB signaling module: Temporal control and selective gene activation. *Science* 2002; **298:** 1241-1245

19. Faratian D, Goltsov A, Lebedeva G, Sorokin A, Moodie S, Mullen P *et al*. Systems biology reveals new strategies for personalizing cancer medicine and confirms the role of PTEN in resistance to trastuzumab. *Cancer Research* 2009; **69:** 6713-6720.

20. Sayyed-Ahmad A, Tuncay K, Ortoleva P. Transcriptional regulatory network refinement and quantification through kinetic modeling, gene expression microarray data and information theory. *BMC Bioinformatics* 2007; **8:** 20.

21. Ramdas J, Liu W, Harmon JM. Glucocorticoid-induced cell death requires autoinduction of glucocorticoid receptor expression in human leukemic T cells. *Cancer Research* 1999; **59:** 1378-1385.

22. Schmidt S, Irving JAE, Minto L, Matheson E, Nicholson L, Ploner A *et al*. Glucocorticoid resistance in two key models of acute lymphoblastic leukemia occurs at the level of the glucocorticoid receptor. *The FASEB Journal* 2006; **20:** 2600-2602.

23. Funahashi A, Matsuoka Y, Jouraku A, Morohashi M, Kikuchi N, Kitano H. Celldesigner 3.5: A versatile modeling tool for biochemical networks. *Proceedings of the IEEE* 2008; **96:** 1254-1265.

24. Funahashi A, Morohashi M, Kitano H, Tanimura N. Celldesigner: A process diagram editor for gene-regulatory and biochemical networks. *BIOSILICO* 2003; **1:** 159-162.

25. Zi Z, Klipp E. Sbml-pet: A systems biology markup language-based parameter estimation tool. *Bioinformatics* 2006; **22:** 2704-2705.

26. Pedersen KB, Geng C-D, Vedeckis WV. Three mechanisms are involved in glucocorticoid receptor autoregulation in a human T-lymphoblast cell line. *Biochemistry* 2004; **43:** 10851-10858.

27. Zhou F, Medh RD, Zhang W, Ansari NH, Thompson EB. The delayed induction of c-Jun in apoptotic human leukemic lymphoblasts is primarily transcriptional. *The Journal of Steroid Biochemistry and Molecular Biology* 2000; **75:** 91-99.

28. Jonat C, Rahmsdorf HJ, Park KK, Cato ACB, Gebel S, Ponta H *et al*. Antitumor promotion and antiinflammation: Down-modulation of AP-1 (Fos/Jun) activity by glucocorticoid hormone. *Cell* 1990; **62:** 1189-1204.

29. Sorensen PH, Lessnick SL, Lopez-Terrada D, Liu XF, Triche TJ, Denny CT. A second Ewing's sarcoma translocation, t(21;22), fuses the Ews gene to another Ets−family transcription factor, Erg. *Nature Genetics* 1994; **6:** 146 - 151.

30. Nam RK, Sugar L, Wang Z, Yang W, Kitching R, Klotz LH *et al*. Expression of Tmprss2:Erg gene fusion in prostate cancer cells is an important prognostic factor for cancer progression. *Cancer Biology & Therapy* 2007; **6:** 40-45.

31. Essafi A, Fernandez de Mattos S, Hassen YAM, Soeiro I, Mufti GJ, Thomas NSB *et al*. Direct transcriptional regulation of Bim by Foxo3a mediates sti571-induced apoptosis in BCR-ABL-expressing cells. *Oncogene* 2005; **24:** 2317-2329.

32. Latré de Laté P, Pépin A, Assaf-Vandecasteele H, Espinasse C, Nicolas V, Asselin-Labat M-L *et al*. Glucocorticoid-induced leucine zipper (Gilz) promotes the nuclear exclusion of Foxo3 in a Crm1-dependent manner. *Journal of Biological Chemistry* 2010; **285:** 5594-5605.

33. Htun H, Barsony J, Renyi I, Gould DL, Hager GL. Visualization of glucocorticoid receptor translocation and intranuclear organization in living cells with a green fluorescent protein chimera. *93* 1996; **10:** 4845–4850.

34. Dobreva ZG, Miteva LD, Stanilova SA. The inhibition of JNK and p38 MAPKs downregulates IL-10 and differentially affects c-Jun gene expression in human monocytes. *Immunopharmacology and Immunotoxicology* 2009; **31:** 195-201.

35. Rahim S, Beauchamp EM, Kong Y, Brown ML, Toretsky JA, Ãœren A. YK-4-279 inhibits Erg and Etv1 mediated prostate cancer cell invasion. *PLoS ONE* 2011; **6:** e19343.

36. Morton S, Davis RJ, McLaren A, Cohen P. A reinvestigation of the multisite phosphorylation of the transcription factor c-Jun. *EMBO J* 2003; **22:** 3876-3886.

37. Yu J, Yu J, Mani R-S, Cao Q, Brenner CJ, Cao X *et al*. An integrated network of androgen receptor, polycomb, and Tmprss2-Erg gene fusions in prostate cancer progression. *Cancer Cell* 2010; **17:** 443-454.

38. Chen Y, Sawyers CL. Coordinate transcriptional regulation by Erg and androgen receptor in fusion-positive prostate cancers. *Cancer cell* 2010; **17:** 415-6.

39. Forman BM, Samuels HH. Minireview: Interactions among a subfamily of nuclear hormone receptors: The regulatory zipper model. *Molecular Endocrinology* 1990; **4:** 1293-1301.

40. Laudet V, Hänni C, Coll J, Catzeflis F, Stéhelin D. Evolution of the nuclear receptor gene superfamily. *EMBO J* 1992; **11:** 1003-1013.

5 CHAPTER 5: General Discussion and Conclusions

After an overview of the results from **Chapter 2-4**, in this chapter we discuss the adopted analytical framework, the findings and the interpretations that were made. This chapter also summarizes the aims and issues addressed in this study and how it is correlated with work published by other groups.

5.1 Overall Discussion: Placing the model in GC induced apoptosis

This thesis demonstrates the importance of adopting systems biology concepts to study the GR transduction in acute lymphoblastic leukaemia. In Chapter 2, we presented models that were able to capture the kinetics of direct and indirect GR targets in apoptosis in an ALL dependent manner, using Bcl-X_L and Bim as examples. In addition, we have included several other known GR targets such as GR itself and GILZ as comparisons. We also used our models to test the interaction between GR and one of its target genes, the Bcl-2 member Bmf. The generated simulations corresponded well with the experimental data showing the model's suitability for the study. Models also made a prediction in which Bmf is likely to be directly regulated by GR; this was validated by our results with the use of the protein synthesis inhibitor cycloheximide. We also identified specific kinetic characteristics and crucial time points for distinguishing between early and late response gene regulations by GR. This allowed us to design the Dex timecourse treatment for the study of Bim regulation by GR in the sensitive ALL CEM-C7-14 cells. In resistant ALL CEM-C1-15 cells, we identified an initial increase followed by decrease of the GR protein levels but not the GR mRNA levels, suggesting that GR degradation may play a role in GC resistance. Unlike in CEM-C7-14 cells, it is unclear if GR regulates its own expression in CEM-C1-15 cells, however, other mechanisms such as GR translation and potential involvement with microRNA should also be taken into consideration. GILZ expression was also found to be induced in both sensitive and resistant CEM cells, with C1-15 cells displaying a more dramatic GILZ induction. It was shown that GILZ may be associated with Bcl-X_L regulation (1), and GILZ may influence Bim regulation by potentially inducing FOXO3a nuclear exclusion (2). This highlights the significance of GILZ function in GC sensitivity in ALL and also suggests alternative factors other than FOXO3a are regulating Bim.

To investigate the underlying mechanism of GC resistance, particularly the regulation of Bim in ALL, we conducted a series of timecourse microarray analyses by taking results from Chapter

2 into consideration. In Chapter 3, we focused on the study of GR response to Dex treatment in time on a genome-wide scale. Timecourse microarrays were conducted in various ALLs treated with GCs and grouped based on their phenotype to GC response. The microarray study was divided into two parts, one focused on timecourse of gene expression in relation to Bim in GC-sensitive C7-14 cells, the other part focused on identifying potential biomarkers for determining GC sensitivity. In the first part of Chapter 3, we adapted timecourse clustering and determined that c-Jun was a potential player in upregulating Bim under GC treatment. Experimental results showed that such mechanism is cell-type specific as c-Jun recruitment on the Bim promoter was only identified in sensitive C7-14 cells. Such recruitment may be a crucial factor in determining the execution of apoptosis in C7-14 cells. In addition, an apoptosis assay revealed that c-Jun upregulation was not affected when inhibiting the JNK pathway with the use of the SP600125 JNK inhibitor, suggesting the involvement of alternative c-Jun regulations such as via the p38 MAPK pathway. In the second part of the same study, we conducted timecourse microarray analysis of various ALL cell lines and patients based on their phenotypic response to GC treatment. Additional clinical microarray data obtained from Philadelphia positive (Ph+) ALL patients were also analysed and used to correlate with our results. We observed Erg as one of the significant differentially regulated genes when compared with sensitive and resistant ALL, suggesting Erg being a potential biomarker for GC resistance. Further experimental results confirmed that Erg was upregulated in GC treated resistant C1-15 cells only and that Erg was specifically recruited on the GR promoter in sensitive C7-14 cells but not in C-15 cells. On the other hand, there were reports showing an interaction between Erg and the Jun-Fos complex (3), raising the possibility that Erg may form a complex with AP-1 on the Bim promoter. This was however not identified in either resistant or sensitive CEM cells, suggesting that either Erg does not affect Bim regulation through interaction with AP-1 or that Erg may potentially interact with AP-1 elsewhere in the Bim gene. Taken together, we hypothesised that Erg may have a role in dictating GC resistance by influencing GR regulatory activities, and that siRNA of Erg will be required to confirm such hypothesis. Our results have further confirmed the role of Erg in GC resistance, where we showed that treatment with the Erg functional inhibitor YK-4279 was able to reverse GC sensitivity in C1-15 cells. The exact mechanism remains to be studied as Erg is involved in many biological processes including gene fusion and has been shown to form crosstalk with AP-1 and potentially regulates GR activity in a MAPK dependent manner (4). Taken together, in Chapter 3 we indicated an association with c-Jun in Bim upregulation in GC sensitive ALL, identified the role of Erg in GC resistance and more importantly we also illustrated the successfulness of our approach.

With the conclusion and findings drawn from Chapter 2-3, in Chapter 4 we aimed to model the relationship between GR, c-Jun, Bim and Erg in both sensitive and resistant ALL. The building of the models was adapted from Chapter 2 with modifications. We sought to investigate several aspects. The first aspect was the relationship between GR, c-Jun and Bim, as potential GR binding regions in the Jun promoter were identified, hence it would be important to see whether GR directly activates c-Jun induced Bim expression in C7-14 cells or not. The second aspect was that after identifying Erg recruitment on GR promoter in C7-14 cells, it would be interesting to see how well the simulations fit with the experimental data. This would also provide evidence for the robustness of the models that we constructed. Finally, as it was shown that a specific Erg upregulation existed in C1-15 cells only and that a potential GR binding region was identified on the Erg gene, we therefore built models to test the likelihood of Erg being a direct GR target in C1-15 cells. With regards to modelling GR/c-Jun/Bim, two models were constructed which differed by a step of *de novo* protein synthesis prior to c-Jun transcription. The models indicated that the GR/c-Jun/Bim simulation trend in general fits better when there was a step of *de novo* protein synthesis involved. We did observe that a minor part of the simulations, such as c-Jun protein expression, seemed to fit better in the model with no new protein synthesis when compared with the experimental data. A possible reason for this observation may be the limitation of the data which affects the parameter estimating process. Another possible explanation is the set up of the topology. As discussed in Chapter 4, GR may activate c-Jun through the relief of a protein repressor transcription (5), hence introducing such repression may help to improve the model predictions.

Another subject of interest was the specificity of Erg regulation in sensitive and resistant ALL. The overall Erg simulations in C7-14 cells showed that the inclusion of Erg regulating GR expression corroborated better with the experimental results. When treated with the Erg inhibitor YK-4279 we observed a depletion of Bim protein expression, suggesting a potential role of Erg in Bim regulation. The preliminary ChIP results showed that Erg was not recruited to the Bim promoter by forming contact with the AP-1 complex (Chapter 3); we thus concluded that Erg may regulate Bim activity by causing an impact on the GR autoregulation. In the case of C1-15 cells, we aimed to see if Erg acts as a direct GR target due to its high expression when treated with GC and the presence of a GR binding site in the Erg promoter with the use of the Champion ChiP Transcription Factor Search Portal from SABiosciences. Again, despite the lack of kinetic data, the simulations were still able to capture the experimental observation. The kinetic simulations indicated that Erg is likely to be directly regulated by GR. Although previous results in Chapter 3 have shown that the treatment with YK-4279 is able to enhance apoptosis, this may

not be down to the Bim regulation, as we found a low Bim protein expression in C1-15 cells when under YK-4279 treatment. This suggests that Erg may control potential alternative pathways to trigger apoptosis in C1-15 cells.

Based on the study described in Chapter 2-5, we conclude that there is a crosstalk between GR, AP-1, Erg and Bim regulation in inducing apoptosis in acute lymphoblastic leukaemia. We also demonstrated a successful example of using kinetic models to mimic GR induced apoptosis and showed that such approach fits well with the principle of systems biology. In conclusion, we established a series of models that were able to help us generate hypotheses to better understand GR function and this in turn allowed us to refine the models in an iterative process for making more useful predictions. Furthermore, our findings may lead to the use of Erg as a potential biomarker of GR resistance for ALL therapies and stratification of patients. We also envisage that these finding can be used for many other diseases treated with glucocorticoids including different types of leukaemia, inflammatory and immunological disorders.

5.2 References

1. Ayroldi E, Riccardi C. Glucocorticoid-induced leucine zipper (Gilz): A new important mediator of glucocorticoid action. *FASEB J.* 2009; **23:** 3649-58.

2. Latré de Laté P, Pépin A, Assaf-Vandecasteele H, Espinasse C, Nicolas V, Asselin-Labat M-L *et al*. Glucocorticoid-induced leucine zipper (Gilz) promotes the nuclear exclusion of Foxo3 in a Crm1-dependent manner. *Journal of Biological Chemistry* 2010; **285:** 5594-5605.

3. Verger A, Buisine E, Carrère S, Wintjens R, Flourens A, Coll J *et al*. Identification of amino acid residues in the Ets transcription factor Erg that mediate Erg-Jun/Fos-DNA ternary complex formation. *Journal of Biological Chemistry* 2001; **276:** 17181-17189.

4. Hollenhorst PC, Ferris MW, Hull MA, Chae H, Kim S, Graves BJ. Oncogenic Ets proteins mimic activated Ras/MAPK signaling in prostate cells. *Genes & Development* 2011; **25:** 2147-2157.

5. Zhou F, Medh RD, Zhang W, Ansari NH, Thompson EB. The delayed induction of c-Jun in apoptotic human leukemic lymphoblasts is primarily transcriptional. *J Steroid Biochem Mol Biol.* 2000; **15:** 91-99.

6. Klipp E, Herwig R, Kowald A, Wierling C, Lehrach H. Systems biology in practice. Concepts, implementation, and application, 1st edn. WILEY-VCH Verlag GmbH & Co. KGaA: Berlin, 2005.

6 CHAPTER 6: Future work

Following the discussion and conclusions, in this chapter we identified limitations of the study and make possible suggestions for future improvements.

6.1 Future directions

The presented models have shown that it is possible to gain more understanding towards GR functions and provide a logical explanation to the experimental data with the use of a systems biology approach, combined with known mechanisms of GR induced gene expression from the literature. The results obtained from this study provide a strong foundation for future work to gain more understanding towards GR induced apoptosis and sensitivity to glucocorticoids. As mentioned by Klipp and co-workers (2005), the initial model rarely provides a full explanation for the studied objects and usually leads to more open questions and answers, hence an iterative process of model refinement is essential (1). For this reason, we hope to improve our models on several aspects in order to gain more insights.

Firstly, more details of molecular interactions will need to be included. For instance, different cellular compartments need to be introduced into the model to discriminate the expression of cytoplasmic and nuclear GR. Secondly, the role of transcriptional cofactors in relation to selected gene transcription should be modelled. For example, the GR coactivator P300/CBP induces chromatin remodelling to allow access of the transcription factors and also recruits other coactivators by acting as a scaffold protein, which suggests a possible alternative mechanism for delayed primary induction (2, 3). Post translational modifications are another crucial process for proper GR function, particularly phosphorylation is thought to be important in regulation of nuclear localization, transcriptional activities and stability of GR (4-6).

In addition, extending simulation time and incorporating the half-life of dexamethasone may allow us to observe any potential feedback mechanism. The regulation of GR protein stability is poorly understood, and it is hypothesised that it may be regulated via the ubiquitin-proteasome pathway (7). Longer simulation may allow us to test the relationship between the GR half-life and the ubiquitin-proteasome pathway and elucidate the mode of GR regulation.

To further improve the model, more sophisticated equations can be used to represent the established reactions. For example, Hill functions may be used to represent the binding parameters between the transcription factor and the promoter. It would probably require ChIP-seq data to obtain more accurate number of binding sites for the use of Hill function. Also, with the use of single delay differential equations, the time for individual processes to be completed can be incorporated within the model.

Experimentally, to analyse the unknown proteins that targets c-Jun and Bim, we will test a few potential candidates such as p38 to determine their relation to Bim induction, potentially with the use of a p38 inhibitor (SB203580). Further investigations will be carried out to test the interaction of GR and Bmf, and GR and Erg. This includes identifying potential GRE within the Bmf and Erg genes using bioinformatics sequence analysis, site directed mutagenesis of potential GREs, luciferase assay to assess transcriptional activity in the cells, and chromatin immunoprecipitation (ChIP) to determine the GR location on Erg; silencing RNA may also be used. In addition, GR actions are target gene, cell type and stimulus specific; the investigation of GR effects in other cell types and directly from patients will be useful towards better understanding of the GR related gene network in specific ALL phenotypes. Eventually we would like to construct more robust models to investigate the physiological role of GR, Bim and Erg, the c-Jun-c-Fos complex and other possible compositions of AP-1 and other Ets family members in GR sensitivity.

The ultimate goal is to apply our findings clinically. As mentioned in Chapter 1, treatment with ALL typically consists of administration of a cocktail of drugs alongside with dexamethasone and chemotherapy is commonly used a part of the treatment. Chemotherapeutic drugs are known to cause DNA damage and such process could also form another level of crosstalk with the GR pathway. Further work is needed to understand GR action when combined with various ALL treatments. In addition, ALL patient subtypes should also be taken into consideration during the research as the results are likely to vary according to the individuals.

6.2 References

1. Klipp E, Herwig R, Kowald A, Wierling C, Lehrach H *Systems biology in practice. Concepts, implementation, and application*, 1st edn. WILEY-VCH Verlag GmbH & Co. KGaA: Berlin, 2005.

2. Lee JW, Lee YC, Na SY, Jung DJ, Lee SK. Transcriptional coregulators of the nuclear receptor superfamily: Coactivators and corepressors. *Cell. Mol. Life Sci.* 2001; **58:** 289-297.

3. Glass CK, Rosenfeld MG. The coregulator exchange in transcriptional functions of nuclear receptors. *Genes & Dev.* 2000; **14:** 121-141.

4. Wang Z, Frederick J, Garabedian MJ. Deciphering the phosphorylation "Code" Of the glucocorticoid receptor in vivo. *J. Biol. Chem.* 2002; **277:** 26573-26580.

5. Davies L, Karthikeyan N, Lynch JT, Sial E-A, Gkourtsa A, Demonacos C *et al*. Cross talk of signaling pathways in the regulation of the glucocorticoid receptor function. *Mol. Endocrinol.* 2008; **22:** 1331-1344.

6. Wallace AD, Cidlowski JA. Proteasome-mediated glucocorticoid receptor degradation restricts transcriptional signaling by glucocorticoids. *J. Biol. Chem.* 2001; **276:** 42714-42721.

7. Kinyamu HK, Chen J, Archer TK. Linking the ubiquitin-proteasome pathway to chromatin remodeling/modification by nuclear receptors. *Mol. Endocrinol.* 2005; **34:** 281-297.

7 CHAPTER 7: Appendices

Appendices contain a list of chemical compounds buffers, PCR protocols, antibodies and primers that were used throughout the thesis.

7.1 List of compounds used for cytotoxic stress

Compound	Final concentration	Company
Dexamethasone (Dex)	100nm /1µM	Sigma
Cycloheximide (CHX)	1µM	Sigma
SP600125	10µM	Sigma
YK-4279	10µM	Sigma

7.2 Western Blotting

7.2.1 High Salt lysis buffer (A) with poteinase inhibitor cocktails (B) for cell lysis

A

High salt lysis buffer	Stock	Final	For 10ml
HEPES pH 7.5	1M	45mM	450µl
NaCl	5M	400mM	800µl
EDTA	0.5M	1mM	20µl
Glycerol	100%	10%	1ml
NP-40	100%	0.50%	500µl
DTT	1M	1mM	10µl
PMSF	100mM	1mM	100µl
PI	1000x	1x	10µl
NaOV	1M	2mM	20µl
β-Glycerol phosphate	500mM	20mM	400µl
NaPPi	200mM	5mM	250µl
H_20			6.44ml

B

PI 1000x	Concentration
Aprotinin	1µg/ml
Leupeptin	1µg/ml
Pepstatin A	1µg/ml

7.2.2 SDS gels

SDS gels were prepared using:

	7.5%		10%	
Solutions (Makes 3 gels)	Resolving	Stacking	Resolving	Stacking
Water	13.3ml	6.73ml	10.94ml	6.73ml
Acrylamide	7ml	1.67ml	9.33ml	1.67ml
Tris pH 8.95 (1.5M)	7ml		7ml	
Tris pH 6.95 (1M)		1.25ml		1.25ml
EDTA (0.2M)	0.28ml	100µl	0.28ml	100µl
SDS (10%)	0.28ml	100µl	0.28ml	100µl
APS (10%)	157µl	157µl	157µl	157µl
TEMED	17µl	17µl	17µl	17µl

7.2.3 Bradford assay

Bradford assay for determining protein concentration:

Bradford Assay	Volume
Bradford reagent (Bio-Rad)	200µl
Sterile water	800µl
Protein extract	2µl

7.2.4 3xSDS sample loading buffer

3x SDS sample buffer	Stock	Final (1x)	Per 10ml (3x)
Tris pH 6.95	1M	62.5mM	1.87ml

Glycerol	100%	10%	3ml
β-Mercapthoethanol	100%	5%	1.5ml
SDS	10%	2%	0.6g
H_20			3.64ml

7.2.5 1xSDS running buffer

1x SDS running buffer	Final	For 1Litre
Tris	25mM	3g
Glycine	190mM	14.4g
SDS	35mM	1g

7.2.6 1xWestern transfer buffer

1x Western transfer buffer	Final	For 1Litre
Tris	22mM	3.3g
Glycine	75mM	11.3g
Methanol	20%	200ml

7.3 RNA extraction and qRT-PCR

7.3.1 Reverse transcription assay

Component	Volume
RNA template	1µg
Anchored Oligo-dT (500ng/µl)	1µl
1st strand synthesis buffer (5x)	4µl
Reverse-iT RTase blend	1µl
dNTP mix (10mM)	1µl
H_20	Up to 20µl

7.3.2 qRT-PCR master mixture

Component	Company	Volume for 1x Reaction (16µl total)
Thermopol buffer	New England	2µl

(10x)	Biolabs	
dNTP (10mM)	Bioline	0.4µl
MgCl2	Bioline	0.6µl
SYBR-green (1/2000)	Sigma	0.75µl
Taq DNA polymerase	New England Biolabs	0.2µl
Forward primer (50µM)	Eurogentec	0.06µl
Reverse primer (50µM)	Eurogentec	0.06µl
H_20	Sigma	11.93µl

7.3.3 qRT-PCR set up for amplification of gene of interest

Segment	Temperature	Duration	No. of Cycles
Initial denaturation	95°C	10min	1
Denaturation	95°C	30sec	35
Annealing	50°C	30sec	35
Extension	72°C	1min	35
Final Extention	72°C	5min	1
Melting curves	60-90°C, read every 1°C	15sec	1

7.4 Polymerase chain reaction (PCR)

7.4.1 PCR mixture

Component	Company	Volume for 1x Reaction (49µl total)
Phusion HF buffer (5x)	New England Biolabs	10µl
dNTP (10mM)	Bioline	1µl
Phusion DNA polymerase	New England Biolabs	0.5µl
Forward primer (20µM)	Eurogentec	1µl

Reverse primer (20µM)	Eurogentec	1µl
H_20	Sigma	35.5µl

7.4.2 PCR set up for amplification of protein-DNA bound region

Segment	Temperature	Duration	No. of Cycles
Initial denaturation	95°C	5min	1
Denaturation	95°C	1min	35
Annealing	50°C	1min	35
Extension	72°C	1min	35
Final Extention	72°C	10min	1
Melting curves	60-90°C, read every 1°C	15sec	1

7.5 Chromatin immuneprecipitation (ChIP) assay

7.5.1 ChIP-qPCR procedure

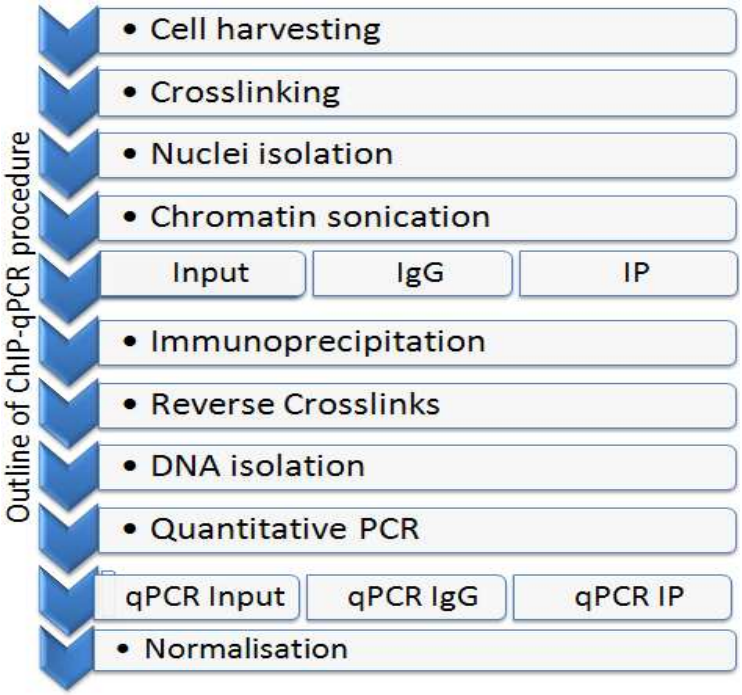

Figure 7.1 The principle of ChIP assay

The diagram represents the principle of ChIP assay. In brief, chromatin is extracted from the cells. The DNA and binding proteins are crosslinked followed by cell lysis and sonication

and the subjected chromatin-DNA complex is immunoprecipitated with specific primary antibody for the protein of interest. The protein-DNA complex crosslinks are then reversed and magnetic beads are used to isolate the bound chromatins, which are then ready to be quantified using qPCR. Detailed protocol can be found in Material and Methods, section 6.9 in (1).

7.5.2 ChIP Buffer

Buffer	Chemical ingredients
Formaldehyde solution	50mM Hepes-KOH, 100mM NaCl, 1mM EDTA, 0.5mM EGTA, 11% formaldehyde
Lysis Buffer I	50mM Hepes-KOH; pH:7.5, 140mM NaCl, 1mM EDTA, 10% glycerol, 0.5% Igepal CA-630, 0.25% Triton X-100
Lysis Buffer II	10mM Tris-HCl; pH:8.0, 200mM NaCl, 1mM EDTA, 0.5mM EGTA
Lysis Buffer III	10mM Tris-HCl; pH:8.0, 100mM NaCl, 1mM EDTA, 0.5mM EGTA, 0.1% Na-Deoxycholate, 0.5% N-lauroylsarcosine
Blocking solution	0.5% BSA w/v in PBS
RIPA buffer	50mM Hepes-KOH; pH:7.5, 500mM LiCl, 1mM EDTA, 1% Igepal CA-630, 0.7% Na-Deoxycholate
Tris buffered saline (TBS)	20mM Tris-HCl; pH:7.6, 150mM NaCl
Elution Buffer	50mM Tris-HCl; pH:8, 100mM EDTA and 1% SDS w/v
Rnase A	1mg/ml Rnase A
Poteinase K	20mg/ml Poteinase K
NaCl solution	5M NaCl
Glycogen	20µg/µl glycogen

7.5.3 Sonicated chromatin for ChIP

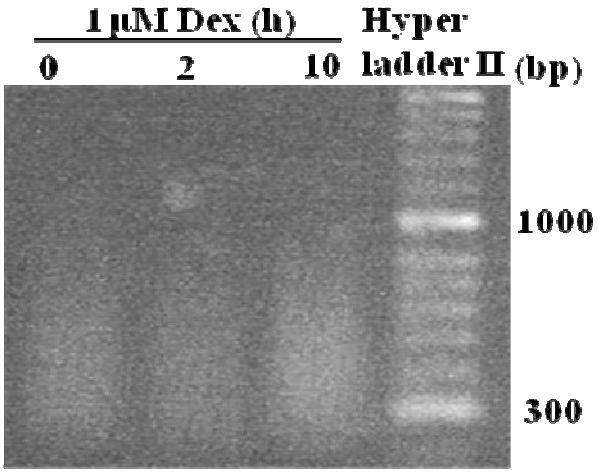

Figure 7.2 ChIP shearing efficiency

The figure represents a typical sheared chromatin agarose gel that was sonicated for ChIP (as described in Chapter 4) and has been visualised using 2% agarose gel electrophoresis. Lane 1-3 (0, 2 and 10 h) showed equal shearing of DNA of all samples. A DNA hyperladder was used to determine the molecular weight of the DNA fragments.

7.6 List of Antibodies

Antibody	Code	Company	Concentration (µl)
Actin	Ab8227	Abcam	1 in 5000
Bcl-X_L	2762	Cell Signalling	1 in 1000
Bim	Ab15184	Abcam	1 in 3000
c-Jun	Sc-1694	Santa Cruz	1 in 300
P-c-Jun	9164	Cell Signalling	1 in 1000
GR	sc-1004	Santa Cruz	1 in 5000
GR	2f8	M. Alexis (Hellenic research foundation)	5 in 1000
GR (H300)	sc-8992	Santa Cruz	1 in 1000
Bmf	AHP732	AbD Serotec	1 in 300
Gilz	sc-33780	Santa Cruz	1 in 1000
Erg	sc-271048	Santa Cruz	1 in 300

c-Fos	sc-7202	Santa Cruz	1 in 300

7.7 List of primers

A

qRT-PCR	F/R	Sequence
Bmf	F	ATGGAGCCATCTCAGTGTGTG
Bmf	R	CCCCGTTCCTGTTCTCTTCT
Bcl-X_L	F	GGAGCTGGTGGTTGACTTTC
Bcl-X_L	R	TCACTGAATGCCCGCCGGTAC
Bim	F	GAGAAGGTAGACAATTGCAG
Bim	R	GACAATGTAACGTAACAGTCG
GILZ	F	GGACTTCACGTTTCAGTGGACA
GILZ	R	AATGCGGCCACGGATG
c-Jun	F	ACTGCAAAGATGGAAACGAC
c-Jun	R	AAAATGTTTGCAACTGCTGC
c-Fos	F	TCTCTTACTACCACTCACCC
c-Fos	R	TGGAGTGTATCAGTCAGCTC
Erg	F	CAATCTCGAGCTATGGCCAGCACTATTAAGGAAGC
Erg	R	CAATCTCGAGCTATGGCCAGCACTATTAAGGAAGC
GR	F	GTTGCTCCCTCTCGCCCTCATTC
GR	R	CTCTTACCCTCTTTCTGTTTCTA
Rpl19	F	ATGTATCACAGCCTGTACCTG
Rpl19	R	TTCTTGGTCTCTTCCTCCTTG

B

ChIP	F/R	Sequence
Bim TRE	F	GCAACCTCTCCCAACTTCAG
Bim TRE	R	GCATCACTTGCTGAACCAAA
GR ErgRE	F	CTTGCTCCCTCTCGCCCTCATTC
GR ErgE	R	CTCTTACCCTCTTTCTGTTTCTA

7.8 References

1. Rajendran R. The transcriptional cofactor pcaf as mediator of the interplay between p53 and HIF-1 alpha and its role in the regulation of cellular energy metabolism. University of Manchester, *School of Pharmacy and Pharmaceutical Sciences*. 2011; eScholarID**:**151843.